The role of reactive oxygen species in zebrafish caudal fin regeneration

A thesis submitted to the University of Manchester for the degree of Doctor of Philosophy in the Faculty of Biology, Medicine and Health

2019

Kunal Chopra

School of Biological Sciences

List of Contents

Abbreviations

A-CGD- autosomal CGD	APO- apocynin
BMP/bmp- bone morphogenetic protein	CGD- chronic granulomatous disease
CFP- caerulean fluorescent protein	CH- congenital hypothyroidism
CRISPR- clustered regularly interspaced short palindromic repeats	
CYBA- Cytochrome b-245, α polypeptide	CYBB- cytochrome b(558) subunit ß
DPA- days post amputation	dpi- days post injection
DPI- diphenyleneiodonium	DUOX- dual oxidase
ENU- N-ethyl-N-nitrosourea	FGF/fgf- fibroblast growth factor
HBV- hindbrain ventricle	HH/Hh- hedgehog
MMI- methimazole	MS-222- tricaine methanesulfonate
NOX- NADPH oxidase	ROI- reactive oxygen intermediates
ROS- reactive oxygen species	sgRNA- single guide RNA
SOD- superoxide dismutase	TH- thyroid hormone
WPA- weeks post amputation	WT- wild type
X-CGD- X-linked CGD	YFP- yellow fluorescent protein

Word count, excluding references: 34,448

Abstract

A sustained increase in ROS is essential for regeneration to occur in various models systems ranging from the fin in zebrafish, to the tail in frogs, salamanders and geckos. This effect of ROS has been, so far, demonstrated using pharmacological inhibition to target various sources of ROS including the transmembrane NADPH oxidases (NOXes). To focus on the role of NOXes in regeneration, we generated *nox* mutants by targeting *duox*, *nox5* and *cyba* (a key subunit of NOXes 1-4). We confirmed that mutations led to *Aspergillus* susceptibility in *cyba* mutants, congenital hypothyroidism in *duox* mutants, and anaesthesia tolerance in *nox5* mutants. These individual commentaries on the various Noxes, while not immediately related to regeneration, authenticate the strains as functional mutants. To estimate their individual contribution to ROS production these mutants were generated in a transgenic background, *HyPer*, which specifically helps visualise H_2O_2 flux. We found that ROS levels remain elevated for up to two weeks post-amputation in wild type animals, but only a week among *nox* mutants. A consequence of this reduced ROS flux was a significantly reduced rate of caudal fin regeneration among *cyba* and *duox* mutants. We also provide clues into the possible temporal distribution of Nox activity post-amputation. Finally, we show that ROS levels, both in the amputated and unamputated state, oscillate during the day.

Declaration

No portion of the work referred to in this thesis has been submitted in support of an application for another degree or qualification of this or any other university or other institute of learning.

Copyright Statement

Acknowledgements

The PhD has been one of the most beautiful chapters in my life. My work here, at Manchester, is the synthesis of a lifelong fascination for the natural world, the guidance and supervision of some very inspiring teachers, the enthusiasm I have for developmental biology, the support of some fabulous friends and the love of my parents!

I was born with ß thalassaemia and it wasn't easy bringing me up. This was in the 80s when the condition was known but management options were restricted to big cities. Upon my diagnosis, my parents made the choice to live apart, a choice that saw my mum, my younger brother, my granddad and me permanently settle in Delhi so I could get treatment at the Army hospital, while my dad would be posted all over the country. They spent their best years living apart, with us seeing each other only during the summer and winter holidays. I cannot even begin to fathom how they did it. In 2007, my brother saved my life as he donated his bone marrow and I underwent a stem cell transplant. Shailendra, Jagral, Kewal and Reshma took care of us. Salice and Mithril were always present to comfort me. When I returned to Delhi after the transplant, Anuradha would often take me to the Army Hospital for my follow-ups. This work is dedicated to family.

My first encounter with an animal was at the age of 2 as I attempted to ride, and fell off a sheep. Growing up, I was endlessly fascinated by plants and animals. My fascination was amplified under the instruction of my high school biology teacher, Mrs. Filomina Jose, as I undertook botanical dissections, studying zoological specimens and field trips. I went on to read Zoology for my Bachelor's where I was taught comparative anatomy and evolution by Mrs. Ramaa Sinha. Her enthusiasm for these became the reason I came to love evolution. Mrs. Sinha would lecture from National Geographic and a host of up-to-date science magazines, ensuring that we stayed in touch with the latest in the field. I am very grateful for their instruction and guidance.

My pursuit for a PhD really began in Sheffield, my home for my first six years in England. Here, I met Kalin, who was starting his PhD at the time. I remain in awe of his enthusiasm for the length and breadth of the biological sciences. We would have endless conversations about development, larval forms, gymnosperms, whales and prehistoric creatures, while night would turn to dawn. Kalin has inspired me constantly, and is the main reason I steered into developmental biology.

After finishing my course at Sheffield, I had hoped to get accepted into PhD immediately. Instead, it was a struggle that lasted nearly two years. At this point in time I met George and Christine Rees, at St. Mary's, whom I now consider to be my family in the UK. We have shared Christmas dinners, Easter sunrises and many other happy memories. I have also been able to turn to them during some of the most difficult times, and for all of this, I am very grateful.

Given the popularity of PhDs, and the flawed standard of determining candidates' worth on grades, it is an incredible challenge to get across one's motivation and enthusiasm. In such circumstances, my supervisor at Sheffield University, Dr. Henry Roehl, gave me the opportunity to be a research assistant, immediately ending my period of struggle. In his lab I realised how much I love being an experimental researcher. I made my foray into zebrafish research and there was no looking back. I am unassessibly grateful to Henry. I also thank Dr. Gordon Cooper, Dr. Louise Robson and Dr. Stephen Brown for giving me volunteering opportunities in their labs, to gather experience.

At Manchester, after a rough start, I found my footing in the lab, and a huge part of this was owed to my colleagues Javier and Chloe for their all-round company and encouragement. I am also very grateful to Shoko for being patient with my queries and dedicating time to help me learn the ropes. I also thank Rob for the confidence he had in my being able to do ISH protocols and for always being cheerful! And of course, I am so glad to have David, Claire, Lauren, Kirsty and Nat who always indulge my silliness and offer great advice. From the Papalopulu lab, I thank Ximena, Parnian, Veronica and Eamon. I also want to thank my advisor Adam Hurlstone- his composed demeanour and encouragement have always made me feel good about my work. Recently, I also came under the supervision of Jorge Elias, and it has been really exciting working on a field completely new to me. I also thank Federica, Riba and Raghavendra for helping with protocols. I thrive when I work as part of a team, and it has been an incredible experience working alongside all of you.

I have had the pleasure to supervise several students in the course of this project! I would like to acknowledge the singular talents and the collective contributions of Milda, Vishali, Rachel, Ram and Syafiq. Brainstorming and reflecting on results is one of the pleasures of scientific investigation and I am very glad that our interactions gave way to some really exciting ideas. During the last year, I also became very close friends with Lindsey. Lindsey has always looked out for me, helped me with fin clipping and her arrival in the lab was very timely as she injected a new dose of enthusiasm! Thank you!

Gratitude is also due to the BSF, Histology and Bioimaging. Thank you David and Vicky, for taking such great care of my fish, for dealing with all the confusing strain names and for being patient with my mistakes. Thank you Pete, Grace and Natalie for teaching how to section and stain effectively, and thank you Peter, for teaching me how to use the widefield microscope a million times over!

It's not all about lab work though! I am very grateful to the International Office Relations staff including Anthony Morris, Samantha Franks and Christine Burns for making me feel welcome at Manchester. I convey my sincerest gratitude to the Scar Free Foundation for choosing to support my studies, putting aside the stiff rules that usually accompany funding considerations for international students. I also thank the lovely reception staff at the Michael Smith building! Rachel, Shevonne, Tom, Jason, Adrian and Darren, thanks for always greeting all of us with a smile and for the chats after long hours in the lab.

In my final year, I have had the chance to work at Manchester Student Homes! What a fantastic experience it has been! I am very pleased to have worked as part of the team and I thank Cooper, Penny, Poppy, Luke, Niamh, Ayesha, Shirley, Paul and Tom! There hasn't been a single dull day!

On the way here, I cannot forget my friends who have always propped me up. To Parivesh, Anuradha, Anushree, Pallabi, Athoni, Neike, Lima, Jaspreet, Gaurav, Rahul, Jose, Paula, Dongwook, Bhagyashree, Teresa, Mallika, Addie, Paweł, Nids, Magda, Maria, Gabriela, Rosalina, Mukti, Emily and Anna.

And finally, to you Enrique! My deepest gratitude goes out to you for making me part of your team! I have learned an immense deal and I have really enjoyed working under your supervision. Your excitement and enthusiasm at my results, your praise for our first zebrafish publication, and your unending patience with my questions have all driven me to put in my best efforts and keep my thinking cap always on! Thank you very much.

A note on the alternative thesis format

This PhD thesis is formatted in the alternative style, such that experiments, methodology, analysis and citations are presented as stand-alone manuscripts intended for publication in peer-reviewed journals. While manuscript #2 was published earlier this year, manuscripts #1 and #4 are in various stages of preparation for such.

The manuscripts are preceded by a broad introduction/background that covers a concise overview of appendage regeneration, followed by the aims. Each segment has its own pagination. The manuscripts give way to a section on concluding remarks and future directions.

The more you see them up close, the more mesmerising they appear. Common laboratory strains of zebrafish.

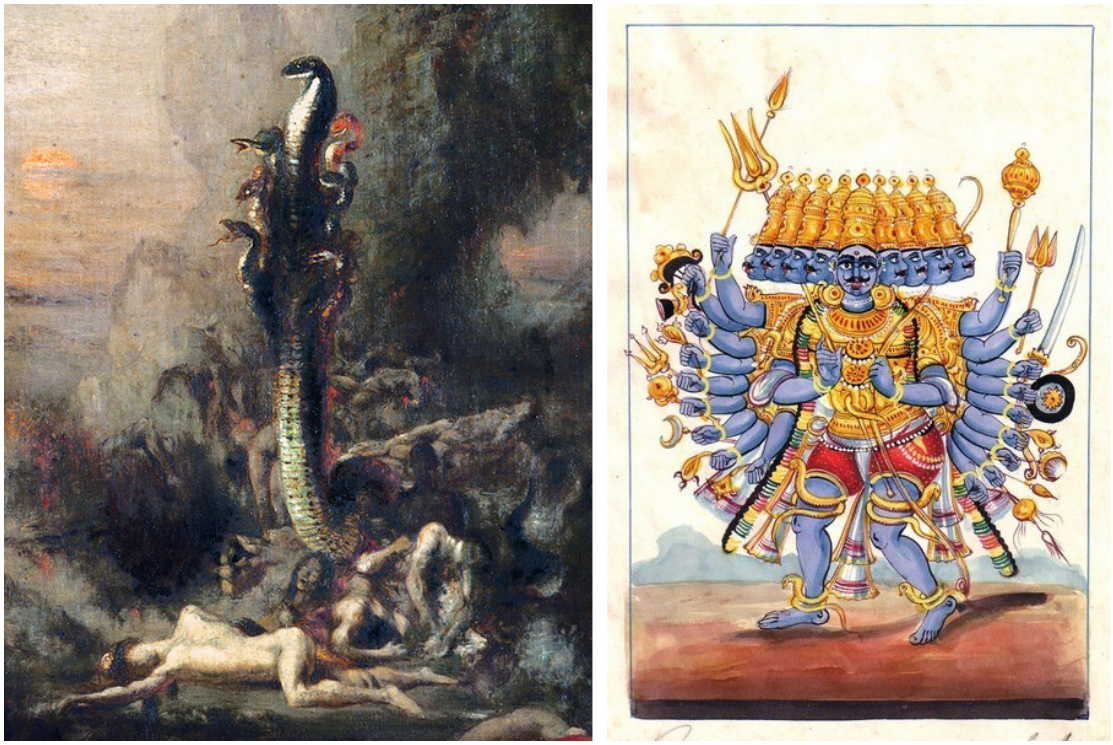

The Hydra (left) and Ravana (right). Mythological champions of regeneration

INTRODUCTION

The Lernaîa Hýdra, a terrible serpentine gatekeeper to the Underworld, is undoubtedly the most popular preamble to scientific conferences on regeneration. Accounts from as early as 500BCE describe the ability of the Hydra to regenerate two heads for every decapitation. In Greek mythology, Heracles and Iolaus best the beast by decapitating and cauterising the neck. Meanwhile, in Hindu mythology, the Ramayana (7-4CE) describes the great King of Lanka, Ravana. Immune to death by decapitation, the ten-headed Ravana is able to replace lost heads.

While it may not feature in mythology, the zebrafish's regenerative capabilities are legendary. Zebrafish have also independently helped attest the roles of genes in modelling human disease. Coming back to regeneration though, many teleosts can regenerate complex structures. Specifically in relation to fin regeneration, a sampling is tabulated below.

Species	Appendage	Citation
Astronotus ocellatus (Oscar)	Pectoral fin	(Darnet et al. 2019)
Caraussius auratus (goldfish)	Caudal fin	(Santamaría et al. 1996)
Cyprinus carpio (carp)	Caudal fin epidermis	(Böckelmann, Ochandio, and Bechara 2010)
Danio rerio (zebrafish)	Caudal fin	(Lee et al. 2005)
Eigenmannia virescens (glass knifefish)	Anal fin	(Srivastava 1978)
Gambusia schoelleri (mosquito fish)	Caudal and pectoral fins	(Khalil and Aziz 1989)
Lepisosteus oculatus (spotted gar)	Pelvic fin	(Darnet et al. 2019)
Nothobranchius furzeri (killifish)	Caudal fin	(Wendler et al. 2015)
Onchorhynchus mykiss (rainbow trout)	Caudal fin	(Alonso et al. 2000)
Oryzias latipes (medaka)	Caudal fin	(Sekimizu, Tagawa, and Takeda 2007)
Polyodon spathulus (American paddlefish)	Pelvic fin	(Darnet et al. 2019)
Polypterus senegalus (bichir)	Pectoral fin	(Cuervo et al. 2012)
Salaria pavo (peacock blenny)	Pectoral fin	(Misof and Wagner 1992)
Tilapia mossambica (tilapia)	Caudal fin	(Kemp and Park 1970)

Defining regeneration

Regeneration can proceed via 1) morphallaxis, a redeployment of existing cells in the absence of active cell proliferation or 2) epimorphosis, which incurs cellular proliferation and the construction of a blastema (Tanaka and Reddien 2011). Typically, morphallaxis gives two identical individuals that are smaller than the original animal. Epimorphic regeneration refers to the re-formation of morphologically complex tissue via blastema formation, and a key event in this type of regeneration is high levels of cellular proliferation. Defined as a collection of heterogeneous, lineage-restricted mesenchymal progenitor cells, a blastema may form via (i) resident stem cells (Weissman, Anderson, and Gage 2001; Stocum 2017), (ii) dedifferentiation of a cell type (Knopf et al. 2011) and (iii) transdifferentiation (Jopling, Boue, and Belmonte 2011).

In the last decade or so similarities have emerged in cellular and molecular dynamics between adult and larval regeneration (A. Kawakami, Fukazawa, and Takeda 2004). Thus, regeneration has acquired a more comprehensive definition of a process that permits organisms to regain the functionality of organs or structures following injury or disease (Stoick-Cooper, Moon, and Weidinger 2007), a process that likely involves common mechanistic principles operating regardless of the extent of damage, tissue, age, and maybe conserved across species (Yoshinari et al. 2009).

Why the zebrafish?

Among vertebrates, bony fish and amphibians retain remarkable regenerative potential, an attribute that diminishes steeply as one ascends the tetrapod clade. Excitingly, traditional views suggest that fishes collectively do not form a monophyletic group (Volff 2005). This has been recently affirmed via a detailed phylogeny that spans across representatives of all major bony fish lineages (Betancur-r et al. 2013). Simply stated, even though bony fish are very basal compared to other derived tetrapods, they share a common ancestor with humans. This common ancestry makes fish, such as the zebrafish, a coveted model for human disease and regenerative medicine.

With the zebrafish genome project in 2001, the zebrafish made its debut in the post-genomic era. The project laid out a direct comparison of human and zebrafish genomes. It emerged that 71.4% of human genes have at least one zebrafish orthologue. 47% of these have a one-to-one relationship with a zebrafish orthologue. In reciprocal, 69% of zebrafish genes have at least one human orthologue (Howe et al. 2013). Over 26,000 protein-coding genes have been reported in the zebrafish (Collins et al. 2012), and with the arrival of the zebrafish mutation project (Kettleborough et al. 2013) mutant alleles for many of these are available from resources including ZFIN (Zebrafish Information Network) (Howe et al. 2013) and KIT (Karlsruhe Institute of Technology) (Geisler et al. 2016). As described later, driving mutations into homozygosity not only reveals their roles in regenerative mechanisms but may also highlight their involvement in pathologies. Genome browsers such as Ensemble serve as a comprehensive, readily accessible catalogue of this genomic data, and they work well with online utilities such as CRISPRscan (Moreno-mateos et al. 2015), which are targeted towards genome editing.

Larva or adult?

Many fish, including zebrafish, retain lifelong regenerative capacity. The choice of developmental stage then becomes dependent on the investigation. Larval forms achieve regenerational milestones with ease as is exemplified in zebrafish (A. Kawakami, Fukazawa, and Takeda 2004; Yoshinari and Kawakami 2011; Roehl 2018), *Xenopus* and the paedomorphic Axolotl (Wang et al. 2014; Joven, Elewa, and Simon 2019). However, larval forms are in a state of incredible developmental unrest. The abundance of precursor pools and stem cells in larvae may go as far as to make regeneration an extension of the developmental processes themselves (Roehl 2018). Indeed, RNAseq profiling of the axolotl regenerating limb has revealed how the blastema takes on a limb-bud-like transcriptional profile (Gerber et al. 2018). Then, there have been suggestions that larval regeneration is the outcome of processes that are quite different from those in adult forms (A. Kawakami, Fukazawa, and Takeda 2004; Yoshinari and Kawakami 2011). In the larval zebrafish (**Fig. 1**), and equally, other larval teleosts, there is also something to be said about the minute

scale of the organs, their comparative simplicity to adult organs, and the remodelling of internal anatomy. In total, these considerations make larval regeneration a system rife with interpretative and technical challenges.

Post-metamorphic or adult animals present the opportunity to examine regeneration in complex and completely differentiated tissues. It does come with the challenge of age-related decline of regenerative capacity. For example, the killifish (*Nothobranchius furzeri*) displays an age-dependent decline in caudal fin regeneration (Wendler et al. 2015). This is not surprising though when this is considered within the context of evolution as it highlights interspecific differences. Finally, while focussing on adults may offload the uncertainty of developmental processes, it must be remembered that fish grow throughout their lives (Dutta 1994; Topczewska et al. 2016). The sum total of these challenges makes the adults an exciting as well as stringent model system.

Fig. 1. The adult (top) and larval (bottom) zebrafish. Choice of model depends on the investigation. Scale bar=5mm (top), 1.25mm (bottom).

The adult caudal fin

Taxonomically speaking, zebrafish fall into the Class Actinopterygii. Etymologically, this derives from Latin actino- ("having rays") + Ancient Greek πτέρυξ (pteruks, "wing, fins"). This is so because teleost fins consist of bony lepidotrichia (bony fin rays). Each lepidotrichium comprises two symmetrical hemirays encasing blood vessels, nerve fibres and connective tissue (Becerra et al. 1983), and follows a specific pattern of bifurcations. Interestingly, fin growth in juvenile zebrafish is continuous, asynchronous, and allometric. In the adult, this transitions into episodic, synchronous and isometric growth i.e., growth is in proportion to body size (Goldsmith et al. 2006). This growth is via the distal addition of segments to each ray (Haas 1962), rather than by an increase in the length and width of a fixed number of skeletal elements as in tetrapods. The distal tips of the rays encase a tuft of unmineralised actinotrichia (Akimenko et al. 2003). All fins in zebrafish are able to regenerate, with a special clause for pectoral fins, which exhibit a sexual dimorphism in their regeneration (Nachtrab, Czerwinski, and Poss 2011).

The adult caudal fin (**Fig. 2**) is easily accessible unlike the paired fins that are very close to the body, and the other unpaired fins that are trickier to amputate. It has unlimited regeneration potential (Azevedo et al. 2011), and while original structures are fully regenerated, there is a degree of heteromorphy because the position of the first bifurcation in the regenerated bony ray undergoes distalisation (Akimenko et al. 2003). This is somewhat akin to the *Xenopus* tadpole tail, which upon regeneration loses the original configurational arrangement of muscle fibres and neurons (Love et al. 2011). Importantly, regeneration is achieved without any scar formation (**Fig. 3**).

Event	Time (days post amputation)
Amputation	T0
Wound closure	>1dpa
Disorganisation, dedifferentiation	>1dpa
Blastema formation	1-2dpa
Blastema outgrowth	1-3dpa
Blastema maintenance, rapid growth, progressive redifferentiation, morphogenesis	5-10dpa
Termination of regeneration, homeostasis	20dpa onwards

Table 2. Consequences of caudal fin amputation (Gauron et al. 2013; Pfefferli and Jaźwińska 2015).

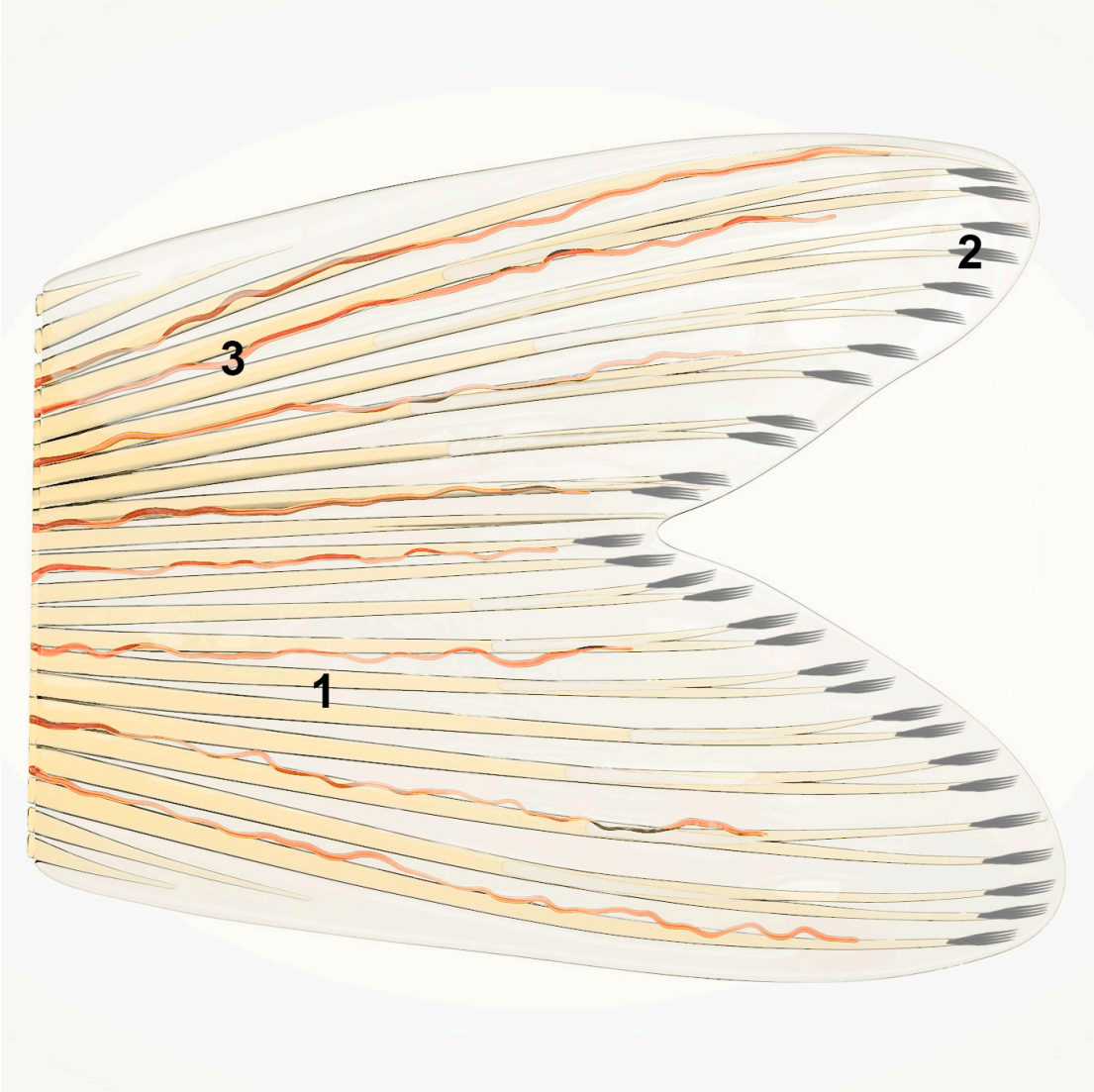

Fig. 2 Schematic of zebrafish caudal fin. 1- Lepidotrichia, 2- Actinotrichia (exaggerated representation), 3- Blood vessel. Credits to Kalin Narov (www.embryosafari.com)

Fig. 3 The amputated caudal fin the adult achieves complete, scar-free, regeneration by 4weeks post amputation (wpa). Scale bar=5mm

A note on endoskeletal appendage regeneration

The endoskeletal elements of paired fins share a deep homology with tetrapod limbs (Schneider and Shubin 2013; Davis 2013). It is thus very exciting to mention a recent study that examined endoskeletal regeneration across diverse actinopterygian taxa. Models included the American paddlefish (*Polyodon spathula*), spotted gar (*Lepisosteus oculatus*), bichir (*Polypterus ocellatus*), oscar (*Astronotus ocellatus*), goldfish (*Carassius auratus*), and blue gourami (*Trichogaster trichopterus*). Transcriptomic data of the bichir's blastema showed components of ROS signalling, among others (Darnet et al. 2019). An interesting point of contrast emerges when one compares the goldfish and the zebrafish, both phylogenetically related memers of the family Cyprinidae, While the goldfish is able to regenerate if amputated endoskeletally (Darnet et al. 2019), this is not always the case with zebrafish where caudal amputation, as an example of endoskeletal amputation, has variable outcomes (Shao et al. 2009; Pápai et al. 2019). Importantly, this study may be considered as an example of why cross-species examination is increasingly indicated in regeneration.

The blastema- cellular and molecular attributes

Following its amputation, the caudal fin completely regenerates through the formation of blastemae. These form distally to the fin rays. The first step towards blastema formation is the rapid migration and rearrangement of epithelial cells from the stump to cover the surface of the cut, thus forming a wound epidermis (Santos-Ruiz et al. 2002). The wound epidermis is crucial since in its absence regeneration does not ensue. Regeneration in the zebrafish fin occurs unidirectionally, in a proximo-distal manner, suggesting that blastema-building conditions are only met proximally (Akimenko et al. 2003). This observation is in association with the importance of the nervous system in the initiation of regeneration. As early as 1952, Singer proposed that nerves have a "neurotrophic" influence on the cells of the blastema. Denervation post-blastema formation stops further growth of the blastema (Akimenko et al. 2003).

The structural organisation of the blastema (**Fig. 4**), in the teleost fin consists of four domains: (i) the distal-most tip comprises a small group of cells that are largely non-proliferative during regenerative growth (Nechiporuk and Keating 2002), (ii) the lateral regions comprise highly proliferative osteoblast progenitors (Brown, Fisher, and Iovine 2009), (iii) directly medial to the osteoblast progenitors is another population of proliferative cells thought to give rise to actinotrichia (J. Zhang et al. 2010) and (iv) the remainder are thought to be fibroblasts, distributed medially (Tu and Johnson 2011).

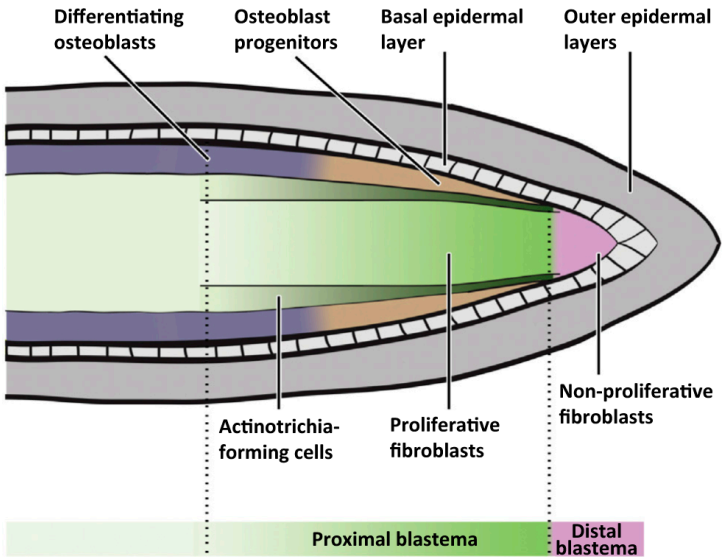

Fig. 4 Compartments in the blastema of a single fin ray in the zebrafish. Various tissue domains can be identified by 2dpa (Wehner and Weidinger 2015)

Tissue interactions at the vicinity of wounds are critical for blastema establishment. An array of genes is induced in the basal wound epidermis, including *β-catenin*, *lef1*, wnt ligands, *bmp2b*, *shh*, *ptch1*, and the homeobox transcription factors, msxA and msxD. Additionally, blastema cells are characterised by the expression of *msx* genes (*msxB* and *msxC*), which are suggested to maintain them in the dedifferentiated state. Furthermore, a number of molecules such as fibroblast growth factor 24 (fgf24), bmp4, hoxA11B hoxA13B, retinoic acid receptor gamma, and stromal cell-derived factor-1 (sdf-1) have also been suggested to be involved in regeneration (Yoshinari et al. 2009).

Hh signalling and the transcription factor lef1 are implicated in epidermal patterning. Positioning of the *lef1/shh* domain is achieved by the opposing action of two distinct FGF signalling branches (Lee et al. 2009). *lef1* and *shh* expression in the epidermis are also dependent on Wnt/β-catenin signalling (Y. Kawakami et al. 2006; Stoick-Cooper, Moon, and Weidinger 2007).

Blastemal cell proliferation is regulated by FGF signalling (Poss et al. 2000) and BMP signalling (Smith et al. 2006). Blastemal proliferation is also dependent on Hh, activin, IGF, and Notch signalling. The expression of ligands and pathways components for all of these pathways is, in turn, regulated by or dependent upon Wnt/β-catenin signalling.

Regeneration requires a strict coordination between progenitor cell proliferation and differentiation. Notch signalling is vital for maintaining blastemal progenitor cells in a proliferative state and to prevent their differentiation along the skeletogenic lineage (Grotek, Wehner, and Weidinger 2013). Regenerative growth is blocked by the knockdown of Notch pathway components. Additionally, Wnt/β-catenin signalling is active in distally located osteoblast progenitors and promotes the maintenance of runx2^{+} osteoblast progenitors in an immature state. In contrast, BMP signalling is active further proximally, where osteoblasts mature (Stewart et al. 2014).

Wnt/β-catenin signalling may also partially modulate inflammatory processes including scar formation, fibrosis, wound healing and tissue remodelling in mammals (Koch et al. 2011). In a transcriptional reporter line of Wnt/β-catenin signalling it was found that resected caudal fin had a large number of cells with active Wnt/β-catenin signalling. Also, crossing a transgenic line expressing heat shock-inducible Dkk1 (an inhibitor of Wnt/β-catenin signalling) with neutrophil or macrophage tracking lines led to an almost complete inhibition of macrophage accumulation as well as delayed neutrophil resolution within the injured area. Thus, active Wnt signalling might mitigate early stage inflammation and serve as a molecular switch to progress to later stages of the immune response (Petrie et al. 2014).

Taken together, it appears that Wnt/β-catenin signalling regulates epidermal patterning, blastemal proliferation, and osteoblast maturation indirectly, while directly promoting osteoblast progenitor maintenance. Qualifying as an orchestrator of regeneration, Wnt/β-catenin signalling sets up signalling centres that emanate secondary signals that control these processes (Wehner and Weidinger 2015).

Reactive oxygen species (ROS): sources and redox biology

ROS include reactive oxygen intermediates (ROI) along with ozone (O_3) and singlet oxygen ($^1O_2$). ROI are successive 1-electron reduction products of O_2, including the radical superoxide anion ($O_2^{\bullet -}$) and the non-radical hydrogen peroxide (H_2O_2) en route the production of water (Nathan and Ding 2010) (**Fig. 5**). The term reactive species has been expanded to include reactive nitrogen, chlorine, and bromine species. **Table 3** lists a collective of ROS. The mitochondrial electron transport chain leaks about 1%–2% of its electrons as $O_2^{\bullet -}$, a process that is further increased by hypoxia, which acts to deregulate the mitochondrial electron transport chain. The focus of this work, however, are the transmembrane NADPH oxidases (NOXes), which generate ROS in a variety of tissues to serve normal physiological functions as varied as innate immunity, signal transduction, and biochemical reactions, e.g., to produce thyroid hormone (Bedard and Krause 2007; Lambeth 2007).

Free radicals (indicated by •)	**Non-radicals**
Superoxide $O_2^{\bullet -}$	Hydrogen peroxide H_2O_2
Hydroxyl $OH^{\bullet}$	Hypobromous acid HOBr
Hydroperoxyl $HO_2^{\bullet}$	Hypochlorous acid HOCl
Carbonate $CO_3^{-\bullet}$	Ozone O_3
Alkoxyl $RO^{\bullet}$	Singlet oxygen $O_2{}^1\Delta g$
Peroxyl $RO_2^{\bullet}$	Organic peroxides ROOH
Carbon dioxide radical $CO_2^{-\bullet}$	Peroxynitrite $ONOO^-$
Singlet oxygen $O_2{}^1\sum g^+$	Peroxynitrate O_2NOO^-
	Peroxynitrous acid ONOOH
	Peroxomonocarbonate $HOOCO_2^-$

Table 3. Some ROS. All oxygen radicals are ROS, but not all ROS are oxygen radicals.

Redox biology began as oxygen became prominent in the Earth's atmosphere over 2.2 billion years ago, largely due to the evolution of photosynthesis by cyanobacteria. In evolving to use solar energy to split water, they gained reducing power to drive metabolism, but the byproduct, tonnes of O_2, was discarded into the atmosphere (Lane 2002). Interestingly, this has been described as an early case of air pollution (Halliwell 2006). Metallic ore deposits consumed the initial excess of this O_2, and following that, the rise in atmospheric O_2 led to formation of the protective ozone (O_3) layer. This may have helped organisms to colonise land. Elevated atmospheric O_2 also precipitated ferrous iron (Fe^{2+}) from aqueous environments by forming insoluble ferric complexes, leaving water bodies with only trace amounts of soluble iron (Lane 2002). This was an advantage because Fe^{2+} reacts rapidly with H_2O_2 to yield the highly toxic hydroxyl radical, via the Fenton reaction.

$$Fe^{2+} + H_2O_2 \rightarrow Fe\ (III) + OH^{\bullet}\ (\text{free radical}) + OH^{-}\ (\text{hydroxide ion})$$

Fenton chemistry occurs *in vivo*, but is carefully modulated by limiting the availability of both Fe^{2+} and H_2O_2 (Halliwell and Gutteridge 2006). It would have been difficult to evolve aerobic life in a world awash with Fe^{2+}. As atmospheric O_2 rose, many anaerobes must have died out, with present day ones presumably the descendants of those that adapted to anoxic microenvironments. In the majority of organisms antioxidant defenses arose, and the earliest of these may have been mechanisms to shield DNA from Fenton chemistry (Wiedenheft et al. 2005).

Production of the highly toxic $OH^{\bullet}$ during Fenton's reaction is an essential consideration in relation to the secondary reactions of such free radicals. A free radical is any species capable of independent existence, and one that contains one or more unpaired electrons in an atomic or molecular orbital. As molecular O_2 has two unpaired electrons in its π^* orbitals, it is a free radical. However, both these electrons have the same spin quantum number. This is the most stable state (ground state) of O_2, and is the form that exists in the air around us. For O_2 to oxidise a non-radical by accepting a pair of electrons from it, both these electrons must have the same spin to fit into the vacant spaces in the π^* orbitals. A pair of electrons in an atomic or molecular orbital cannot meet this criterion, since they have opposite spins (+1/2 and -1/2). This spin restriction makes O_2 accept electrons one at a time,

explaining why O_2 reacts sluggishly with most non-radicals. In contrast, O_2 often reacts rapidly with other radicals by single electron transfers.

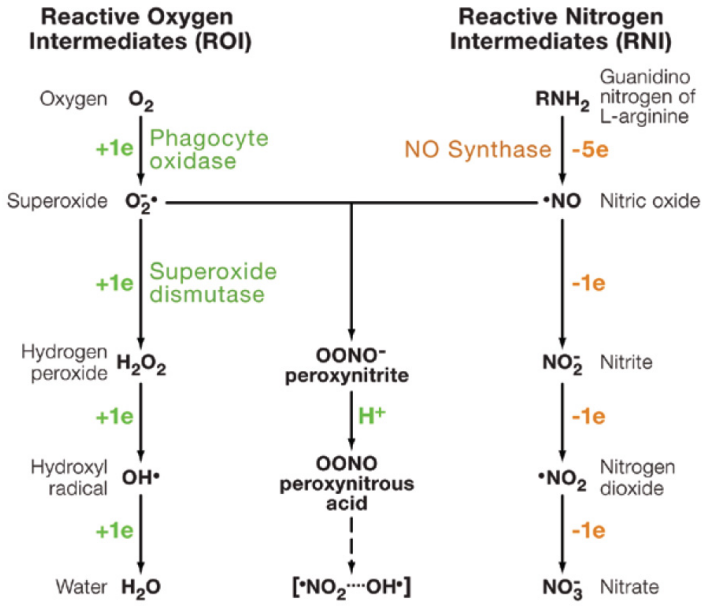

Fig. 5 Manufacture of reactive oxygen and reactive nitrogen intermediates, and their interactions (Nathan and Ding 2010).

More reactive forms of O_2, the singlet oxygen $^1O_2$, can be generated by an input of energy that rearranges the electrons, thus removing the spin restriction and greatly increasing the oxidising ability. $^1O_2$ can directly oxidize proteins, DNA, and lipids (Foote et al., 1985). Sunbathing provides energy input that photosensitises $^1O_2$, which causes skin damage (Halliwell and Gutteridge 2006). When a single electron is supplied to O_2, the product is superoxide radical, $O_2^{\bullet-}$. Addition of another electron to $O_2^{\bullet-}$ gives the peroxide ion O_2^{2-}, a non-radical (no unpaired electrons left) featuring a weaker oxygen-oxygen bond. Addition of two more electrons to O_2^{2-} disbands the molecule, giving two O^{2-} (oxide ions). The two-electron reduction product of O_2 is H_2O_2, and the four-electron product, water.

Damaging effects of ROS

The universal requirement of O_2 for energy production via mitochondria obscures the fact that it is a toxic mutagenic gas, capable of causing oxidative stress. A brief glimpse into the chemical interactions of oxygen free radicals helps understand why. 1) Two free radicals can join their unpaired electrons to form a covalent bond. Thus,

nitric oxide ($NO^{\bullet}$) and superoxide ($O_2^{\bullet -}$) rapidly react fast to form the non-radical peroxynitrite (Beckman and Koppenol 1996) (**Fig. 5**).

$$NO^{\bullet} + O_2^{\bullet -} \rightarrow ONOO_2 \text{ (peroxynitrite)}$$

Peroxynitrite rapidly protonates, at physiological pH, to peroxynitrous acid (ONOOH). Peroxynitrite also reacts with CO_2, to give nitrogen dioxide and carbonate radical, both of which are powerful oxidising agents.

$$ONOO_2 + CO_2 \rightarrow ONOOCOO^- \rightarrow NO_2^{\bullet} \text{ (nitrogen dioxide)} + CO_3^{-\bullet} \text{ (carbonate radical)}$$

2) A radical may adduct to another molecule resulting in an unpaired electron. For example, OH adds to position 8 in the ring structure of guanine in DNA forming 8-oxo -2'- deoxyguanosine. This lesion is mutagenic (Evans, Dizdaroglu, and Cooke 2004), and may also cause loss of epigenetic information (Pizzino et al. 2017).

3) A reactive radical (e.g. $OH^{\bullet}$ or $NO_2^{\bullet}$) may remove a hydrogen atom from a C–H bond, e.g. from a hydrocarbon side chain of a polyunsaturated fatty acid (PUFA) residue in a membrane, leaving an unpaired electron on the carbon. Carbon-centered radicals react fast with O_2 to generate peroxyl radicals. These are reactive enough to both oxidise membrane proteins and attack adjacent PUFA side chains, propagating a chain reaction. A new C radical is formed to continue the chain, and a lipid hydroperoxide forms. In long PUFA chains the peroxyl radicals can whip around and abstract H from the same PUFA, giving cyclic peroxides (Morrow 2003).

$$CH + OH^{\bullet} \text{ (or } NO_2^{\bullet}) \rightarrow C + H_2O \text{ (or } HNO_2)$$

$$C + O2 \rightarrow C\text{-}OO \text{ (peroxyl)}$$

$$CH + C\text{-}OO \rightarrow C + COOH$$

An introduction to NADPH oxidases (NOXes)

Seven NOX isoforms are presently recognised. These are NOX1, NOX2, NOX3, NOX4, NOX5, DUOX1 and DUOX2 (Bedard and Krause 2007). In line with their preserved function, the NOXes feature common structural attributes. These include 1) an NADPH-binding site at the COOH terminus, 2) a FAD-binding region in the proximity of the most COOH-terminal transmembrane domain, 3) six conserved

transmembrane domains, and 4) four highly conserved heme-binding histidines (Lambeth 2004; Bedard and Krause 2007; Brandes, Weissmann, and Schröder 2014). NOXes also feature additional subunits, regulatory proteins and ions for their biochemical function. These include GP91^{phox}, P22^{phox}, the organiser subunit P47^{phox}, the activator subunit P67^{phox}, and Rac proteins. These are not present in every NOX eg. NOXes 1-4 require P22^{phox} for their activation and stabilisation, but NOX5 and DUOX 1and2 do not, requiring calcium instead (**Fig. 6**) (Lambeth 2004; Bedard and Krause 2007). **Table 4** summarises a tissue-wide expression of the various isoforms.

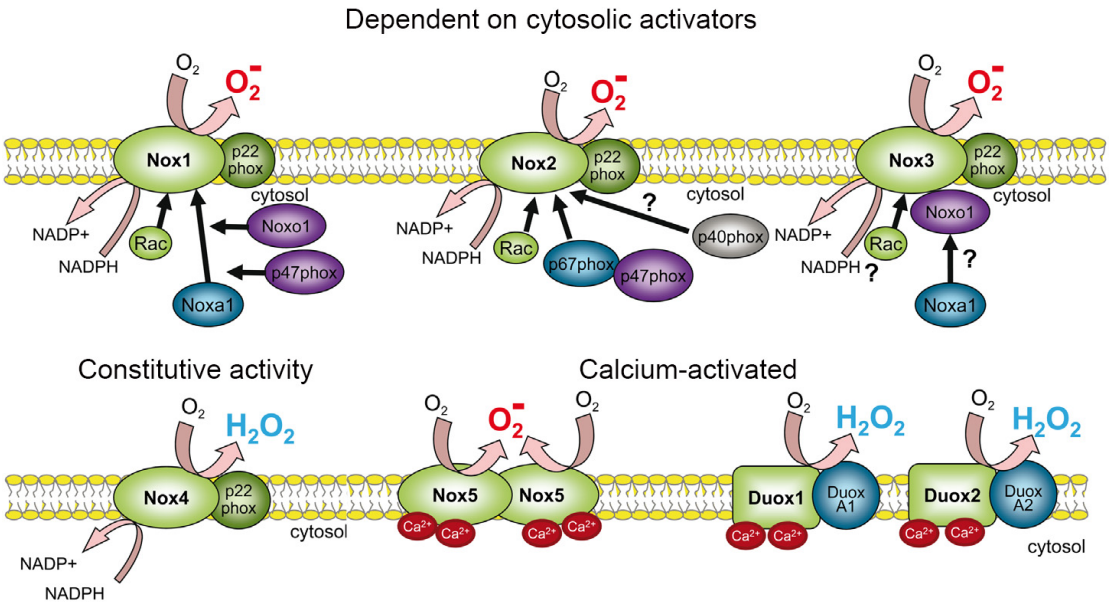

Fig. 6. Composition and activation of NOX enzymes (adapted from Brandes, Weissmann, and Schröder 2014)

Isoform	High level expression	Medium to low level expression
NOX1	Colon	Smooth muscle, endothelium, uterus, placenta, prostate, osteoclasts, retinal pericytes
NOX2	Phagocytes	B lymphocytes, neurons, cardiomyocytes, skeletal muscle, hepatocytes, endothelium, hematopoietic stem cells, smooth muscle
NOX3	Inner ear	Foetal kidney, foetal spleen, skull bone, brain
NOX4	Kidney, blood vessels	Osteoclasts, endothelium, smooth muscle, hematopoietic stem cells, fibroblasts, keratinocytes, melanoma cells, neurons
NOX5	Lymphoid tissue, testis	Endothelium, smooth muscle, pancreas, placenta, ovary, uterus, stomach, various foetal tissues
DUOX1	Thyroid	Airway epithelia, tongue epithelium, cerebellum, testis
DUOX2	Thyroid	Salivary and rectal glands, gastrointestinal epithelia, airway epithelia, uterus, gall bladder, pancreatic islets

Table 4. Tissue distribution of NOX isoforms (Adapted from Bedard and Krause 2007)

In relation to Nox-derived ROS, most pathologies (**Table 5**) are associated with overproduction of ROS by Nox enzymes, as a result of the oxidative stress that damages tissues over time. Three conditions are known to arise from underproduction of Nox-mediated ROS (Lambeth 2007). Two of these, chronic granulomatous disease and congenital hypothyroidism, are covered in this work, and alongside the proposed role of ROS in regeneration, these highlight the essential role of ROS.

Disease	Tissue	Candidate
Diseases of decreased Nox activity		
Chronic granulomatous disease	Phagocytes	Nox2
Defective gravity perception	Inner ear	Nox3
Congenital hypothyroidism	Thyroid gland	Duox2
Diseases of increased Nox activity		
Arthritis	Phagocytes	Nox2
Inflammatory bowel disease	Phagocytes, intestinal epithelium	Nox1, Nox2
Shock lung	Lung	Nox2
Emphysema	Lung	Nox1, Nox3
Asthma	Lung	Nox2, Nox4
Pulmonary hypertension	Lung	Nox4
Cardiac hypertrophy	Heart	Nox2, Nox4
Hypertension	Vascular smooth muscle	Nox1, Nox2
Atherosclerosis	Vascular	Nox1, Nox2
Diabetic vascular disease	Vascular endothelium	Nox1, Nox2
Diabetic nephropathy	Kidney	Nox2, Nox4
Renal hypertension	Kidney	Nox2
Glomerulonephritis	Kidney	Nox2, Nox4
Melanoma	Skin	Nox4
Barrett's adenocarcinoma	Oesophagus	Nox5
Prostate cancer	Prostate	Nox1, Nox5
Parkinson's disease	Brain	Nox2
Amyotrophic lateral sclerosis	Spinal motor neurons	Nox2

Table 5. Known and proposed roles of Nox-derived ROS in pathologies (Adapted from Lambeth 2007).

The discovery of ROS in appendage regeneration

The role of ROS in appendage regeneration has been demonstrated in an assemblage of organisms. This was first revealed during tail regeneration in *Xenopus* tadpoles. Using a transgenic reporter, HyPer, for estimating ROS, it was found that elevated ROS levels sustained until regeneration was complete (Love et al. 2013) (**Fig. 7**). Also, microarray data suggested an increase in NADPH levels during regeneration (Love et al. 2011). This informed the pharmacological targeting of NADPH oxidases, thus revealing a block on regeneration (Gauron et al. 2013; Love et al. 2013). Eventually, using pharmacological inhibition Nox2 was shown to be implicit in gecko tail regeneration (Qing Zhang et al. 2016). Most recently, the requirement for ROS has been demonstrated during axolotl tail regeneration, once again, via chemical inhibition (Al Haj Baddar, Chithrala, and Voss 2019). The role of NOX-mediated ROS as an early injury signal is thus indicated. While the role of downstream players is beyond the scope of this project, the following is a description of the various processes that ROS regulates post-injury.

H_2O_2 and leukocyte chemotaxis

The inflammatory phase of wound healing is characterised by the release of large amounts of superoxide radical by neutrophils, which is later converted to H_2O_2 by SOD. However, this H_2O_2 burst is predated by H_2O_2 release from resident non-inflammatory cells at the wound site (Love et al. 2013) (**Fig. 7**). Duox-mediated H_2O_2 has been shown to be vital for attracting neutrophils to a wound, likening it to be a chemoattractant (Niethammer et al. 2009). With the help of Duox morphants it was demonstrated how *duox* knockdown translates into a significant decrease of neutrophils recruitment. Specific oxidation of a cysteine residue (C466) in the neutrophil SFK, Lyn, has been described to cause such oxidant-dependent neutrophil chemotaxis. Complementing the postulated role of H_2O_2 as a chemotactic signal is the epithelial production of another neutrophil chemoattractant IL-8 (CXCL8). IL-8 production is promoted by injurious and microbial stimuli and mediated by DUOX-dependent cell signalling pathways. The role of IL-8 homologs in wound-induced neutrophil recruitment has been highlighted in zebrafish tail fin injury models. Zebrafish have two CXCL8 homologs namely Cxcl8-l1 and Cxcl8-l2. Both these

homologs had variable effects on neutrophil recruitment and migration speed (Van Der Vliet and Janssen-Heininger 2014).

H_2O_2 and signalling pathways

As described above, cellular proliferation during regeneration is strongly linked with Fgf and Wnt signalling. Wound sites exhibit an absence of Wnt/β-catenin immediately post-amputation followed by its sustained activation from 24hpa. This has been shown in *X. tropicalis* tadpoles, using a Wnt/β-catenin reporter line, which uses multimerized TCF optimal promoter (TOP) sites to drive the expression of destabilized GFP. Pharmacological inhibition of ROS production via DPI, APO and MCI-86 led to a marked decrease in Wnt/β-catenin, when treatment was administered from 0hpa to 36hpa. In a Wnt reporter line this translated into a decreased Wnt/β-catenin-directed dsGFP fluorescence signal (Love *et al.*, 2013). *In vitro*, H_2O_2 has been shown to modulate Wnt/β-catenin signalling via nucleoredoxin, a small redox-sensitive protein from the thioredoxin family (Funato *et al*., 2006). ISH showed nucleoredoxin to be expressed during tail regeneration (Love *et al.*, 2013). *fgf20* is a direct transcriptional target of Wnt/β-catenin signalling (Chamorro *et al*., 2005) and has been shown to be markedly upregulated during tail regeneration in *X. laevis* (Lin and Slack, 2008). *fgf20* also emerged as the most highly upregulated *fgf* gene during tail regeneration in *X. tropicalis*, as revealed by a microarray analysis (Love *et al.*, 2011). This was corroborated using *in situ* hybridisation, whereby high expression levels of *fgf20* were detected in the regenerative bud tissue from 12hpa onwards. Being a direct target of Wnt/β-catenin, the expression levels of *fgf20* were decreased in tadpoles treated with the ROS inhibitors DPI, APO or MCI-186. The individual role of *fgf20* during tail regeneration was also examined using antisense morpholinos targeting two separate splice junctions in the *X. tropicalis fgf20*. Although *fgf20* morphants were able to heal the wound epidermis, in contrast to control morphants, the regeneration of the axial tissues expressing *fgf20*, and overall tail regrowth were significantly reduced. Thus, *fgf20* function is required for regeneration of the axial tissues of the tail, but not for healing the epidermal tissues (Love *et al.*, 2013).

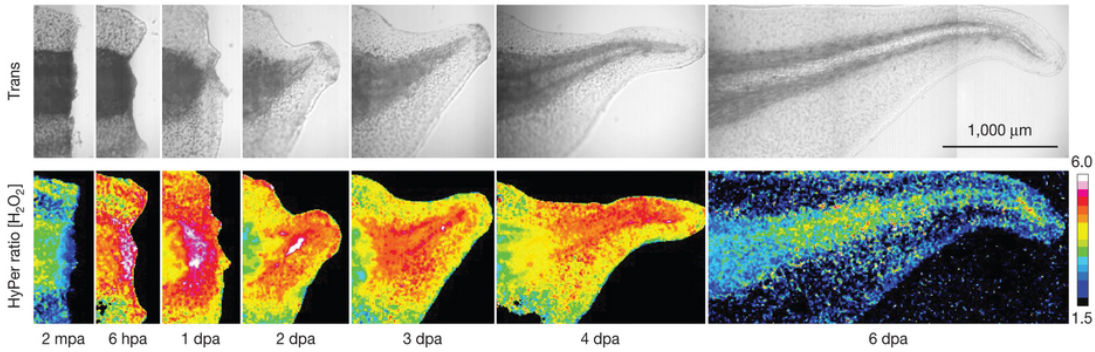

Fig. 7. ROS production following tail amputation in the *Xenopus* tadpole. A F_1 transgenic tadpole expressing HyPerYFP demonstrates the burst of H2O2 that follows injury (Love et al. 2013). HyPerYFP is a ratiometric reporter fluorophore. A YFP variant, it possesses an oxidative sensitive OxyR domain that responds to oxidation, causing a reversible conformational change and a marked change in fluorescence excitation. It is particularly sensitive to H_2O_2 over other ROS (Belousov et al. 2006), thus allowing the visualization of H_2O_2 dynamics post-injury.

H_2O_2, re-epithelialisation and wound healing

The amount of oxygen dissolved in blood increases greatly when patients breathe pure oxygen in a pressurized chamber as part of hyperbaric oxygen therapy (HBOT). At normal atmospheric pressure, the saturation of haemoglobin with oxygen is 97%. It can reach 100% in a hyperbaric chamber. Large amounts of ROS are then generated (Gill and Bell 2004). HBOT is reported to improve wound healing and reduce ulcer size in diabetic patients (Kessler et al. 2003), enhance keratinocyte migration and maturation (Kairuz et al. 2007) and improve healing of ischemic wounds (Qixu Zhang et al. 2008). Topically applied hyperbaric oxygen improved wound healing in both diabetic and non-diabetic patients and this action appears to be correlated with *vegf* expression(Gordillo et al. 2008). H_2O_2 cream containing 1.5% H_2O_2 was reported to improve blood flow in the skin of guinea pigs (Tur, Bolton, and Constantine 1995). This is just a sampling of examples that state the importance of H_2O_2 in wound healing.

With this background, we hypothesised that a reduction in ROS production would lead to a reduction in the rate of caudal fin regeneration in the adult zebrafish.

The questions we asked were:

- Are NADPH oxidases an essential source of ROS following injury?

- Is ROS production sustained during caudal fin regeneration in the adult zebrafish?
- Is there a critical NOX?

To address these questions, the aims of this project were:

- To generate *nox* mutants in zebrafish
- Establish a protocol for estimating *in vivo* ROS levels using a transgenic reporter line, *Tg(HyPer)*
- Drive homozygosity of *nox* mutations in a *Tg(HyPer)* background to estimate ROS levels *in vivo*
- To assess the effect of the various *nox* mutants on fin regeneration.

In this body of work, I address caudal fin regeneration in the adult zebrafish. For the first time, it is shown how reactive oxygen species (ROS) oscillate as the amputated caudal fin reconstitutes. Serendipitously, I also demonstrate how mutations in ROS production align with two commonly known medical conditions, indicating the suitability of this tropical wonder as a model of human disease. All findings culminate as we report that *cyba* and *duox* mutations influence the rate of regeneration, and that mutating the *noxes* is reflected in the reduction of post-amputation ROS flux.

References

1. Akimenko, Marie-Andrée Andrée, Manuel Marí-Beffa, José Becerra, and Jacqueline Géraudie. 2003. "Old Questions, New Tools, and Some Answers to the Mystery of Fin Regeneration." *Developmental Dynamics* 226 (2): 190–201. https://doi.org/10.1002/dvdy.10248.
2. Alonso, Mônica, Yara A Tabata, Marcos G Rigolino, and Ricardo Y Tsukamoto. 2000. "Effect of Induced Triploidy on Fin Regeneration of Juvenile Rainbow Trout, Oncorhynchus Mykiss." *Journal of Experimental Zoology* 287 (7): 493–502. https://doi.org/10.1002/1097-010X(20001201)287:7<493::AID-JEZ5>3.0.CO;2-8.
3. Azevedo, Ana Sofia, Bartholomäus Grotek, António Jacinto, Gilbert Weidinger, and Leonor Saúde. 2011. "The Regenerative Capacity of the Zebrafish Caudal Fin Is Not Affected by Repeated Amputations." *PLOS ONE* 6 (7): e22820. https://doi.org/10.1371/journal.pone.0022820.
4. Becerra, J, G S Montes, S R R Bexiga, and L C U Junqueira. 1983. "Structure of the Tail Fin in Teleosts." *Cell and Tissue Research* 230 (1): 127–37. https://doi.org/10.1007/BF00216033.
5. Beckman, J S, and W H Koppenol. 1996. "Nitric Oxide, Superoxide, and Peroxynitrite: The Good, the Bad, and Ugly." *American Journal of Physiology-Cell Physiology* 271 (5): C1424–37. https://doi.org/10.1152/ajpcell.1996.271.5.C1424.
6. Bedard, Karen, and Karl-Heinz Heinz Krause. 2007. "The NOX Family of ROS-Generating NADPH Oxidases: Physiology and Pathophysiology." *Physiological Reviews* 87 (1): 245–313. https://doi.org/10.1152/physrev.00044.2005.
7. Belousov, Vsevolod V., Arkady F. Fradkov, Konstantin A. Lukyanov, Dmitry B. Staroverov, Konstantin S. Shakhbazov, Alexey V. Terskikh, and Sergey Lukyanov. 2006. "Genetically Encoded Fluorescent Indicator for Intracellular Hydrogen Peroxide." *Nature Methods* 3 (4): 281–86. https://doi.org/10.1038/nmeth866.
8. Betancur-r, Ricardo, Richard E Broughton, Edward O Wiley, Kent Carpenter, J Andrés López, Chenhong Li, Nancy I

Holcroft, et al. 2013. “The Tree of Life and a New Classification of Bony Fishes” 0732988. https://doi.org/10.1371/currents.tol.53ba26640df0ccaee75bb165c8c26288.Abstract.
9. Böckelmann, P K, B S Ochandio, and I J Bechara. 2010. “Histological Study of the Dynamics in Epidermis Regeneration of the Carp Tail Fin (Cyprinus Carpio, Linnaeus, 1758) .” *Brazilian Journal of Biology* . scielo .
10. Brandes, Ralf P., Norbert Weissmann, and Katrin Schröder. 2014. “Nox Family NADPH Oxidases: Molecular Mechanisms of Activation.” *Free Radical Biology and Medicine* 76: 208–26. https://doi.org/10.1016/j.freeradbiomed.2014.07.046.
11. Brown, Andrew M, Shannon Fisher, and M Kathryn Iovine. 2009. “Osteoblast Maturation Occurs in Overlapping Proximal-Distal Compartments during Fin Regeneration in Zebrafish.” *Developmental Dynamics : An Official Publication of the American Association of Anatomists* 238 (11): 2922–28. https://doi.org/10.1002/dvdy.22114.
12. Collins, John E, Simon White, Stephen M J Searle, and Derek L Stemple. 2012. “Incorporating RNA-Seq Data into the Zebrafish Ensembl Genebuild.” *Genome Research* 22 (10): 2067–78. https://doi.org/10.1101/gr.137901.112.
13. Cuervo, Rodrigo, Rocío Hernández-Martínez, Jesús Chimal-Monroy, Horacio Merchant-Larios, and Luis Covarrubias. 2012. “Full Regeneration of the Tribasal <Em>Polypterus</Em> Fin.” *Proceedings of the National Academy of Sciences* 109 (10): 3838 LP – 3843. https://doi.org/10.1073/pnas.1006619109.
14. Darnet, Sylvain, Aline C Dragalzew, Danielson B Amaral, Josane F Sousa, and Andrew W Thompson. 2019. “Deep Evolutionary Origin of Limb and Fin Regeneration” 116 (30). https://doi.org/10.1073/pnas.1900475116.
15. Davis, Marcus C. 2013. “The Deep Homology of the Autopod: Insights from Hox Gene Regulation.” *Integrative and Comparative Biology* 53 (2): 224–32. https://doi.org/10.1093/icb/ict029.
16. Dutta, H. 1994. “Growth in Fishes.” *Gerontology* 40 (2–4): 97–112. https://doi.org/10.1159/000213581.
17. Evans, Mark D, Miral Dizdaroglu, and Marcus S Cooke. 2004. “Oxidative DNA Damage and Disease: Induction, Repair and Significance.” *Mutation Research/Reviews in Mutation Research* 567 (1): 1–61. https://doi.org/https://doi.org/10.1016/j.mrrev.2003.11.001.
18. Foote, C S, Valentine, J S, Greenberg A, Liebman, J F, editors. 1985. Active Oxygen in Chemistry. Chapman and Hall,
19. New York
20. Gauron, Carole, Christine Rampon, Mohamed Bouzaffour, Eliane Ipendey, Jeremie Teillon, Michel Volovitch, and Sophie Vriz. 2013. “Sustained Production of ROS Triggers Compensatory Proliferation and Is Required for Regeneration to Proceed.” *Scientific Reports* 3: 1–9. https://doi.org/10.1038/srep02084.
21. Geisler, Robert, Nadine Borel, Marco Ferg, Jana Viktoria Maier, and Uwe Strähle. 2016. “Maintenance of Zebrafish Lines at the European Zebrafish Resource Center.” *Zebrafish* 13 (S1): S-19-S-23. https://doi.org/10.1089/zeb.2015.1205.
22. Gerber, Tobias, Prayag Murawala, Dunja Knapp, Wouter Masselink, Maritta Schuez, Sarah Hermann, Malgorzata Gac-santel, et al. 2018. “Single-Cell Analysis Uncovers Convergence of Cell Identities during Axolotl Limb Regeneration” 0681 (October). https://doi.org/10.1126/science.aaq0681.
23. Gill, A L, and C N A Bell. 2004. “Hyperbaric Oxygen: Its Uses, Mechanisms of Action and Outcomes.” *QJM: An International Journal of Medicine* 97 (7): 385–95. https://doi.org/10.1093/qjmed/hch074.
24. Goldsmith, Matthew I, M Kathryn Iovine, Thomas O’Reilly-Pol, and Stephen L Johnson. 2006. “A Developmental Transition in Growth Control during Zebrafish Caudal Fin Development.” *Developmental Biology* 296 (2): 450–57. https://doi.org/https://doi.org/10.1016/j.ydbio.2006.06.010.
25. Gordillo, Gayle M, Sashwati Roy, Savita Khanna, Richard Schlanger, Sorabh Khandelwal, Gary Phillips, and Chandan K Sen. 2008. “TOPICAL OXYGEN THERAPY INDUCES VASCULAR ENDOTHELIAL GROWTH FACTOR EXPRESSION AND IMPROVES CLOSURE OF CLINICALLY PRESENTED CHRONIC WOUNDS.” *Clinical and Experimental Pharmacology and Physiology* 35 (8): 957–64. https://doi.org/10.1111/j.1440-1681.2008.04934.x.
26. Grotek, Bartholomäus, Daniel Wehner, and Gilbert Weidinger. 2013. “Notch Signaling Coordinates Cellular Proliferation with Differentiation during Zebrafish Fin Regeneration.” *Development* 140 (7): 1412 LP – 1423. https://doi.org/10.1242/dev.087452.
27. Haas, Hermann J. 1962. “Studies on Mechanisms of Joint and Bone Formation in the Skeleton Rays of Fish Fins.” *Developmental Biology* 5 (1): 1–34. https://doi.org/https://doi.org/10.1016/0012-1606(62)90002-7.
28. Haj Baddar, Nour W Al, Adarsh Chithrala, and S Randal Voss. 2019. “Amputation-Induced Reactive Oxygen Species Signaling Is Required for Axolotl Tail Regeneration.” *Developmental Dynamics* 248 (2): 189–96. https://doi.org/10.1002/dvdy.5.
29. Halliwell, Barry. 2006. “Reactive Species and Antioxidants. Redox Biology Is a Fundamental Theme of Aerobic Life.” *Plant Physiology* 141 (2): 312–22. https://doi.org/10.1104/pp.106.077073.
30. Halliwell, B, and Gutteridge J M C. 2006. Free Radicals in Biology and Medicine, Ed 4. Clarendon Press, Oxford
31. Howe, Kerstin, Matthew D. Clark, Carlos F. Torroja, James Torrance, Camille Berthelot, Matthieu Muffato, John E. Collins, et al. 2013. “The Zebrafish Reference Genome Sequence and Its Relationship to the Human Genome.” *Nature* 496 (7446): 498–503. https://doi.org/10.1038/nature12111.
32. Jopling, Chris, Stephanie Boue, and Juan Carlos Izpisua Belmonte. 2011. “Dedifferentiation, Transdifferentiation and Reprogramming: Three Routes to Regeneration.” *Nature Reviews Molecular Cell Biology* 12 (2): 79–89. https://doi.org/10.1038/nrm3043.
33. Joven, Alberto, Ahmed Elewa, and Andra Simon. 2019. “Model Systems for Regeneration : Salamanders,” no. January: 0–2. https://doi.org/10.1242/dev.167700.
34. Kairuz, Evette, Zee Upton, Rebecca A Dawson, and Jos Malda. 2007. “Hyperbaric Oxygen Stimulates Epidermal Reconstruction in Human Skin Equivalents.” *Wound Repair and Regeneration* 15 (2): 266–74. https://doi.org/10.1111/j.1524-475X.2007.00215.x.
35. Kawakami, Atsushi, Taro Fukazawa, and Hiroyuki Takeda. 2004. “Early Fin Primordia of Zebrafish Larvae Regenerate by a Similar Growth Control Mechanism with Adult Regeneration.” *Developmental Dynamics* 231 (4): 693–99. https://doi.org/10.1002/dvdy.20181.
36. Kawakami, Yasuhiko, Concepción Rodriguez Esteban, Marina Raya, Hiroko Kawakami, Mercè Martí, Ilir Dubova, and Juan Carlos Izpisúa Belmonte. 2006. “Wnt/Beta-Catenin Signaling Regulates Vertebrate Limb Regeneration.” *Genes & Development* 20 (23): 3232–37. https://doi.org/10.1101/gad.1475106.

37. Kemp, Norman E, and Jae Ho Park. 1970. “Regeneration of Lepidotrichia and Actinotrichia in the Tailfin of the TeleostTilapia Mossambica.” *Developmental Biology* 22 (2): 321–42. https://doi.org/https://doi.org/10.1016/0012-1606(70)90157-0.
38. Kessler, Laurence, Pascal Bilbault, Francoise Ortéga, Claire Grasso, Raphael Passemard, Dominique Stephan, Michel Pinget, and Francis Schneider. 2003. “Hyperbaric Oxygenation Accelerates the Healing Rate of Nonischemic Chronic Diabetic Foot Ulcers.” *Diabetes Care* 26 (8): 2378 LP – 2382. https://doi.org/10.2337/diacare.26.8.2378.
39. Kettleborough, Ross N.W., Elisabeth M. Busch-Nentwich, Steven A. Harvey, Christopher M. Dooley, Ewart De Bruijn, Freek Van Eeden, Ian Sealy, et al. 2013. “A Systematic Genome-Wide Analysis of Zebrafish Protein-Coding Gene Function.” *Nature* 496 (7446): 494–97. https://doi.org/10.1038/nature11992.
40. Knopf, Franziska, Christina Hammond, Avinash Chekuru, Thomas Kurth, Stefan Hans, Christopher W. Weber, Gina Mahatma, et al. 2011. “Bone Regenerates via Dedifferentiation of Osteoblasts in the Zebrafish Fin.” *Developmental Cell* 20 (5): 713–24. https://doi.org/https://doi.org/10.1016/j.devcel.2011.04.014.
41. Koch, Stefan, Porfirio Nava, Caroline Addis, Wooki Kim, Timothy L Denning, Linheng Li, Charles A Parkos, and Asma Nusrat. 2011. “The Wnt Antagonist Dkk1 Regulates Intestinal Epithelial Homeostasis and Wound Repair.” *Gastroenterology* 141 (1): 259-268.e2688. https://doi.org/10.1053/j.gastro.2011.03.043.
42. Lambeth, J. David. 2004. “NOX Enzymes and the Biology of Reactive Oxygen.” *Nature Reviews Immunology* 4 (3): 181–89. https://doi.org/10.1038/nri1312.
43. Lambeth, J David. 2007. “Nox Enzymes, ROS, and Chronic Disease: An Example of Antagonistic Pleiotropy.” *Free Radical Biology & Medicine* 43 (3): 332–47. https://doi.org/10.1016/j.freeradbiomed.2007.03.027.
44. Lane N. 2002. Oxygen, the Molecule That Made the World. Oxford University Press, Oxford
45. Lee, Yoonsung, Sara Grill, Angela Sanchez, Maureen Murphy-Ryan, and Kenneth D Poss. 2005. “Fgf Signaling Instructs Position-Dependent Growth Rate during Zebrafish Fin Regeneration.” *Development* 132 (23): 5173 LP – 5183. https://doi.org/10.1242/dev.02101.
46. Lee, Yoonsung, Danyal Hami, Sarah De Val, Birgit Kagermeier-Schenk, Airon A Wills, Brian L Black, Gilbert Weidinger, and Kenneth D Poss. 2009. “Maintenance of Blastemal Proliferation by Functionally Diverse Epidermis in Regenerating Zebrafish Fins.” *Developmental Biology* 331 (2): 270–80. https://doi.org/https://doi.org/10.1016/j.ydbio.2009.05.545.
47. Love, Nick R., Yaoyao Chen, Boyan Bonev, Michael J. Gilchrist, Lynne Fairclough, Robert Lea, Timothy J. Mohun, Roberto Paredes, Leo Ah Zeef, and Enrique Amaya. 2011. “Genome-Wide Analysis of Gene Expression during Xenopus Tropicalis Tadpole Tail Regeneration.” *BMC Developmental Biology* 11 (1): 70. https://doi.org/10.1186/1471-213X-11-70.
48. Love, Nick R., Yaoyao Chen, Shoko Ishibashi, Paraskevi Kritsiligkou, Robert Lea, Yvette Koh, Jennifer L. Gallop, Karel Dorey, and Enrique Amaya. 2013. “Amputation-Induced Reactive Oxygen Species Are Required for Successful Xenopus Tadpole Tail Regeneration.” *Nature Cell Biology* 15 (2): 222–28. https://doi.org/10.1038/ncb2659.
49. Misof, Bernhard Y, and Günter P Wagner. 1992. “Regeneration in Salaria Pavo (Blenniidae, Teleostei).” *Anatomy and Embryology* 186 (2): 153–65. https://doi.org/10.1007/BF00174953.
50. Moreno-mateos, Miguel A, Charles E Vejnar, Jean-denis Beaudoin, Juan P Fernandez, Emily K Mis, Mustafa K Khokha, and Antonio J Giraldez. 2015. “CRISPRscan : Designing Highly Efficient SgRNAs for CRISPR-Cas9 Targeting in Vivo” 12 (10). https://doi.org/10.1038/nmeth.3543.
51. Morrow, Samuel S Fam and Jason D. 2003. “The Isoprostanes: Unique Products of Arachidonic Acid Oxidation-A Review.” *Current Medicinal Chemistry*. https://doi.org/http://dx.doi.org/10.2174/0929867033457115.
52. Nachtrab, Gregory, Michael Czerwinski, and Kenneth D. Poss. 2011. “Sexually Dimorphic Fin Regeneration in Zebrafish Controlled by Androgen/GSK3 Signaling.” *Current Biology : CB* 21 (22): 1912–17. https://doi.org/10.1016/j.cub.2011.09.050.
53. Nathan, Carl, and Aihao Ding. 2010. “SnapShot : Reactive Oxygen Intermediates (ROI),” 8–10. https://doi.org/10.1016/j.cell.2010.03.008.
54. Nechiporuk, Alex, and Mark T Keating. 2002. “A Proliferation Gradient between Proximal and <Em>Msxb</Em>-Expressing Distal Blastema Directs Zebrafish Fin Regeneration.” *Development* 129 (11): 2607 LP – 2617. http://dev.biologists.org/content/129/11/2607.abstract.
55. Niethammer, Philipp, Clemens Grabher, A. Thomas Look, and Timothy J. Mitchison. 2009. “A Tissue-Scale Gradient of Hydrogen Peroxide Mediates Rapid Wound Detection in Zebrafish.” *Nature* 459 (7249): 996–99. https://doi.org/10.1038/nature08119.
56. Pápai, Nóra, Ferenc Kagan, György Csikós, Mónika Kosztelnik, Tibor Vellai, and Máté Varga. 2019. “No Correlation between Endo- and Exoskeletal Regenerative Capacities in Teleost Species.” *Fishes* . https://doi.org/10.3390/fishes4040051.
57. Petrie, Timothy A, Nicholas S Strand, Chao Tsung-Yang, Jeremy S Rabinowitz, and Randall T Moon. 2014. “Macrophages Modulate Adult Zebrafish Tail Fin Regeneration.” *Development* 141 (13): 2581 LP – 2591. https://doi.org/10.1242/dev.098459.
58. Pfefferli, Catherine, and Anna Jaźwińska. 2015. “The Art of Fin Regeneration in Zebrafish.” *Regeneration (Oxford, England)* 2 (2): 72–83. https://doi.org/10.1002/reg2.33.
59. Pizzino, Gabriele, Natasha Irrera, Mariapaola Cucinotta, Giovanni Pallio, Federica Mannino, Vincenzo Arcoraci, Francesco Squadrito, Domenica Altavilla, and Alessandra Bitto. 2017. “Oxidative Stress: Harms and Benefits for Human Health.” Edited by Victor M Victor. *Oxidative Medicine and Cellular Longevity* 2017: 8416763. https://doi.org/10.1155/2017/8416763.
60. Poss, Kenneth D, Jiaxiang Shen, Alex Nechiporuk, Gerald McMahon, Bernard Thisse, Christine Thisse, and Mark T Keating. 2000. “Roles for Fgf Signaling during Zebrafish Fin Regeneration.” *Developmental Biology* 222 (2): 347–58. https://doi.org/https://doi.org/10.1006/dbio.2000.9722.
61. Roehl, Henry Hamilton. 2018. “Linking Wound Response and Inflammation to Regeneration in the Zebrafish Larval Fin” 477: 473–77.
62. Santamaría, J A, M Marí-Beffa, L Santos-Ruiz, and J Becerra. 1996. “Incorporation of Bromodeoxyuridine in Regenerating Fin Tissue of the Goldfish Carassius Auratus.” *Journal of Experimental Zoology* 275 (4): 300–307.

https://doi.org/10.1002/(SICI)1097-010X(19960701)275:4<300::AID-JEZ8>3.0.CO;2-T.
63. Santos-Ruiz, Leonor, Jesús A Santamaría, Josefa Ruiz-Sánchez, and José Becerra. 2002. "Cell Proliferation during Blastema Formation in the Regenerating Teleost Fin." *Developmental Dynamics* 223 (2): 262–72. https://doi.org/10.1002/dvdy.10055.
64. Schneider, Igor, and Neil H Shubin. 2013. "The Origin of the Tetrapod Limb: From Expeditions to Enhancers." *Trends in Genetics* 29 (7): 419–26. https://doi.org/https://doi.org/10.1016/j.tig.2013.01.012.
65. Sekimizu, Koshin, Masatomo Tagawa, and Hiroyuki Takeda. 2007. "Defective Fin Regeneration in Medaka Fish (Oryzias Latipes) with Hypothyroidism." *Zoological Science* 24 (7): 693–99. https://doi.org/10.2108/zsj.24.693.
66. Shao, Jinhui, Xiaojing Qian, Chengxia Zhang, and Zenglu Xu. 2009. "Fin Regeneration from Tail Segment with Musculature, Endoskeleton, and Scales." *Journal of Experimental Zoology Part B: Molecular and Developmental Evolution* 312B (7): 762–69. https://doi.org/10.1002/jez.b.21295.
67. Smith, A, F Avaron, D Guay, B K Padhi, and M A Akimenko. 2006. "Inhibition of BMP Signaling during Zebrafish Fin Regeneration Disrupts Fin Growth and Scleroblast Differentiation and Function." *Developmental Biology* 299 (2): 438–54. https://doi.org/https://doi.org/10.1016/j.ydbio.2006.08.016.
68. Stewart, Scott, Alan W. Gomez, Benjamin E. Armstrong, Astra Henner, and Kryn Stankunas. 2014. "Sequential and Opposing Activities of Wnt and BMP Coordinate Zebrafish Bone Regeneration." *Cell Reports* 6 (3): 482–98. https://doi.org/https://doi.org/10.1016/j.celrep.2014.01.010.
69. Stocum, David L. 2017. "Mechanisms of Urodele Limb Regeneration." *Regeneration (Oxford, England)* 4 (4): 159–200. https://doi.org/10.1002/reg2.92.
70. Stoick-Cooper, Cristi L, Randall T Moon, and Gilbert Weidinger. 2007. "Advances in Signaling in Vertebrate Regeneration as a Prelude to Regenerative Medicine." *Genes & Development* 21 (11): 1292–1315. https://doi.org/10.1101/gad.1540507.
71. Tanaka, Elly M., and Peter W. Reddien. 2011. "The Cellular Basis for Animal Regeneration." *Developmental Cell* 21 (1): 172–85. https://doi.org/10.1016/j.devcel.2011.06.016.
72. Topczewska, Jolanta M., Ramy A. Shoela, Joanna P. Tomaszewski, Rupa B. Mirmira, and Arun K. Gosain. 2016. "The Morphogenesis of Cranial Sutures in Zebrafish." *PLoS ONE* 11 (11): 1–23. https://doi.org/10.1371/journal.pone.0165775.
73. Tu, Shu, and Stephen L. Johnson. 2011. "Fate Restriction in the Growing and Regenerating Zebrafish Fin." *Developmental Cell* 20 (5): 725–32. https://doi.org/10.1016/j.devcel.2011.04.013.
74. Tur, Ethel, Laura Bolton, and Barry E Constantine. 1995. "Topical Hydrogen Peroxide Treatment of Ischemic Ulcers in the Guinea Pig: Blood Recruitment in Multiple Skin Sites." *Journal of the American Academy of Dermatology* 33 (2, Part 1): 217–21. https://doi.org/https://doi.org/10.1016/0190-9622(95)90238-4.
75. Vliet, Albert Van Der, and Yvonne M.W. Janssen-Heininger. 2014. "Hydrogen Peroxide as a Damage Signal in Tissue Injury and Inflammation: Murderer, Mediator, or Messenger?" *Journal of Cellular Biochemistry* 115 (3): 427–35. https://doi.org/10.1002/jcb.24683.
76. Volff, J. N. 2005. "Genome Evolution and Biodiversity in Teleost Fish." *Heredity* 94 (3): 280–94. https://doi.org/10.1038/sj.hdy.6800635.
77. Wang, Heng, Shahryar Khattak, Maritta Schuez, Kathleen Roensch, Tatiana Sandoval-guzma, Eugeniu Nacu, Akira Tazaki, Alberto Joven, and Elly M Tanaka. 2014. "Fundamental Differences in Dedifferentiation and Stem Cell Recruitment during Skeletal Muscle Regeneration in Two Salamander Species," 174–87. https://doi.org/10.1016/j.stem.2013.11.007.
78. Wehner, Daniel, and Gilbert Weidinger. 2015. "Signaling Networks Organizing Regenerative Growth of the Zebrafish Fin." *Trends in Genetics* 31 (6): 336–43. https://doi.org/10.1016/j.tig.2015.03.012.
79. Weissman, Irving L, David J Anderson, and Fred Gage. 2001. "S TEM AND P ROGENITOR C ELLS : Origins , and Transdifferentiations." *Cell and Develeopmental Biology*, 387–403. https://doi.org/10.1146/annurev.med.54.101601.152334.
80. Wendler, Sebastian, Nils Hartmann, Beate Hoppe, and Christoph Englert. 2015. "Age-Dependent Decline in Fin Regenerative Capacity in the Short-Lived Fish Nothobranchius Furzeri." *Aging Cell* 14 (5): 857–66. https://doi.org/10.1111/acel.12367.
81. Wiedenheft, Blake, Jesse Mosolf, Deborah Willits, Mark Yeager, Kelly A Dryden, Mark Young, and Trevor Douglas. 2005. "An Archaeal Antioxidant: Characterization of a Dps-like Protein from Sulfolobus Solfataricus." *Proceedings of the National Academy of Sciences of the United States of America* 102 (30): 10551–56. https://doi.org/10.1073/pnas.0501497102.
82. Yoshinari, Nozomi, Takashi Ishida, Akira Kudo, and Atsushi Kawakami. 2009. "Gene Expression and Functional Analysis of Zebrafish Larval Fin Fold Regeneration." *Developmental Biology* 325 (1): 71–81. https://doi.org/https://doi.org/10.1016/j.ydbio.2008.09.028.
83. Yoshinari, Nozomi, and Atsushi Kawakami. 2011. "Mature and Juvenile Tissue Models of Regeneration in Small Fish Species," no. August: 62–78.
84. Zhang, Jing, Purva Wagh, Danielle Guay, Luis Sanchez-Pulido, Bhaja K Padhi, Vladimir Korzh, Miguel A Andrade-Navarro, and Marie-Andrée Akimenko. 2010. "Loss of Fish Actinotrichia Proteins and the Fin-to-Limb Transition." *Nature* 466 (7303): 234–37. https://doi.org/10.1038/nature09137.
85. Zhang, Qing, Yongjun Yingjie Wang, Lili Man, Ziwen Zhu, Xue Bai, Sumei Wei, Yan Liu, et al. 2016. "Reactive Oxygen Species Generated from Skeletal Muscles Are Required for Gecko Tail Regeneration." *Scientific Reports* 6 (February): 20752. https://doi.org/10.1038/srep20752.
86. Zhang, Qixu, Qing Chang, Robert A Cox, Xuemei Gong, and Lisa J Gould. 2008. "Hyperbaric Oxygen Attenuates Apoptosis and Decreases Inflammation in an Ischemic Wound Model." *Journal of Investigative Dermatology* 128 (8): 2102–12. https://doi.org/https://doi.org/10.1038/jid.2008.53.

Manuscript #1

Zebrafish *cyba* mutations provide a model for human chronic granulomatous disease

Zebrafish *cyba* mutations provide a model for human chronic granulomatous disease

Kunal Chopra[1], Vishali Shathish[2], Enrique Amaya[1], Jorge Amich Elias[2∫∫]

[1]Division of Cell Matrix Biology & Regenerative Medicine, Michael Smith Building, School of Biological Sciences, Faculty of Biology, Medicine and Health, University of Manchester, Oxford Road, Manchester, United Kingdom

[2]Manchester Fungal infection Group, Core Technology Facility, School of Biological Sciences, Faculty of Biology, Medicine and Health, University of Manchester, Oxford Road, Manchester, United Kingdom

[∫∫]Corresponding author

Email addresses:

KC: kunal.chopra@postgrad.manchester.ac.uk

EA: Enrique.amaya@manchester.ac.uk

JAE: jorge.amichelias@manchester.ac.uk

Zebrafish *cyba* mutations provide a model for human chronic granulomatous disease

Abstract

Chronic Granulomatous disease (CGD) is an inherited primary immunodeficiency, and is the outcome of defects in any of the subunits of the NAPDH oxidases (NOXes). This impairs the respiratory burst in phagocytic leukocytes, leaving patients prone to life-threatening infections and inflammatory complications. Of the several structural NOX subunits we focus on $p22^{phox}$ (cyba). While *cyba* mutations are rare, patient survival is strongly associated with the production of reactive oxygen species (ROS), and hence, the clinical outcomes remain significant. We generated a zebrafish mutant for *cyba* via CRISPR/Cas9. Using the fungus *Aspergillus fumigatus* as a pathogen, we describe the susceptibility of *cyba* mutant larvae, when conidia are injected in the yolk sac. An increasing trend in mortality was identified among mutants indicating its efficacy an *in vivo* model. Future *in vitro* assays involving neutrophil-conidia contact would be essential in further characterising these mutants as suitable models.

INTRODUCTION

Chronic granulomatous disease (CGD) is an inherited primary immunodeficiency caused by functional impairment of the NOX complex expressed on phagocytes, and characterised by recurrent and severe bacterial and fungal infections, and dysregulated inflammation (Arnold and Heimall 2017). The NOX complex is comprised of membrane-bound and cytosolic proteins that function in concert to produce a burst of microbicidal ROS when professional phagocytes, including neutrophils and macrophages, encounter microbial intruders. This burst has been demonstrated in humans (Dahlgren and Karlsson 1999) and amphioxus (Yang, Huang, and Xu 2016), among others. The earliest cases of CGD were all reported in males and the first publication to describe the condition is known from 1954. It wasn't until another decade though that sex-linked inheritance of CGD was confirmed (Windhorst, Holmes, and Good 1967). Eventual discovery of female patients then lined up the constituent causes to both sex-linked and autosomal mutations. X-linked CGD (XCGD) is an outcome of mutations in *$GP91^{phox}$* (*CYBB*), and accounts for the majority of diagnoses in the US and Europe (Buvelot et al. 2016). Autosomal CGD (ACGD) derives from mutations in any of the various subunits that partner with $GP91^{phox}$ for it to acquire a stable and functional configuration, including $P22^{phox}$ (encoded by *CYBA*). ACGD is predominant in Tunisia, Iran

(Movahedi et al. 2004) and Israel (Wolach et al. 2008), and at least one study attributes this to consanguineous marriages (Fattahi et al. 2011). *Staphylococcus aureus* and *Aspergillus fumigatus* are the most frequent pathogens inflicting CGD patients (Marciano et al. 2014; Buvelot et al. 2016). Here, we present a new vertebrate model for CGD - the zebrafish. We describe its generation via CRISPR/Cas9 and provide evidence supporting the effect of the mutation on ROS production. Our observations are in sync with those published in WT animals, and offer the potential to develop this into a full-fledged piscine model of CGD, the first of its kind.

NADPH oxidases, Reactive oxygen intermediates (ROIs), and ROS – a synopsis

Reactive oxygen intermediates (ROI) comprise successive 1-electron reduction products of O_2 en route to the production of water. These include superoxide anion ($O_2^{\bullet -}$), hydroxyl radical ($OH^{\bullet}$), peroxyl ($RO_2^{\bullet}$), alkoxyl (RO^{-}), and non-radicals such as hydrogen peroxide (H_2O_2) (Nathan and Ding 2010; Mailloux 2015). Reactive oxygen species (ROS) include ROI plus ozone (O_3) and singlet oxyradical ($^1O_2$). Both terms are sometimes used interchangeably and may also be extended to include hypochlorous (HOCl), hypobromous (HOBr), and hypoiodous acids (HOI), which arise by peroxidase-catalysed oxidation of halides (Nathan and Ding 2010). While the mitochondrion is the major production centre of ROS (Moldovan and Moldovan 2004), physiological production of H_2O_2 is mainly mediated by the transmembrane NOXes (Bedard and Krause 2007; Brandes, Weissmann, and Schröder 2014), a crucial enzymatic source of ROS.

Seven NOX isoforms are presently recognised. These are NOX1, NOX2, NOX3, NOX4, NOX5, DUOX1 and DUOX2 (Bedard and Krause 2007). The zebrafish lacks Nox3 and has a single Duox instead of DUOX1 and DUOX2 (B. T. Kawahara, Quinn, and Lambeth 2007). In line with their preserved function, the NOXes feature common structural attributes. These include 1) an NADPH-binding site at the COOH terminus, 2) a FAD-binding region in the proximity of the most COOH-terminal transmembrane domain, 3) six conserved transmembrane domains, and 4) four highly conserved heme-binding histidines (Lambeth 2004; Bedard and Krause 2007; Brandes, Weissmann, and Schröder 2014). NOX2 is the prototype NOX and was uncovered in CGD patients whose phagocytes either bore an abnormal variant or lacked

the NOX altogether. NOX2 has been synonymous with GP91^{phox} (CYBB) (Royer-Pokora *et al.*, 1986; Segal and Shatwell, 1997). Since later onwards though CYBB has precisely referred to the heme-binding transmembrane portion of the protein (Yu et al. 1998) (**Fig. 1**). The closest structural homologs of NOX2 are NOX1, 3 and 4. NOXes also feature additional subunits, regulatory proteins and ions for their biochemical function (Lambeth 2004; Bedard and Krause 2007). GP91^{phox} (CYBB) and P22^{phox} (CYBA) form a heterodimer called cytochrome b_{558} (Arnold and Heimall 2017). This association is reported to be a prerequisite for the maturation and stabilisation of the heterodimer, and localisation of the heterodimer to specific membrane compartments. Likewise, CYBA is essential to NOX1, 3 and 4 (Bedard and Krause 2007). During phagocyte activation two cytosolic subunits are crucial as well. These are the organiser subunit P47^{phox} (NCF1) and the activator subunit P67^{phox} (NCF2). Briefly, using NOX2 as an example (**Fig. 1**), P67^{phox} must interact with NOX2 in the presence of Rac, to activate it, but on its own the interaction between the two is weak. It is reinforced by P47^{phox}, which in turn interacts with the C terminus of CYBA (Brandes, Weissmann, and Schröder 2014; Stasia 2016). The resulting conformational change enables the cytosolic NADPH to donate an electron, thus kickstarting ROS production. In transfected cell lines, NOXes 1, 3 and 4 only produce ROS when co-expressed with CYBA (T. Kawahara et al. 2005), once again demonstrating the importance of this association.

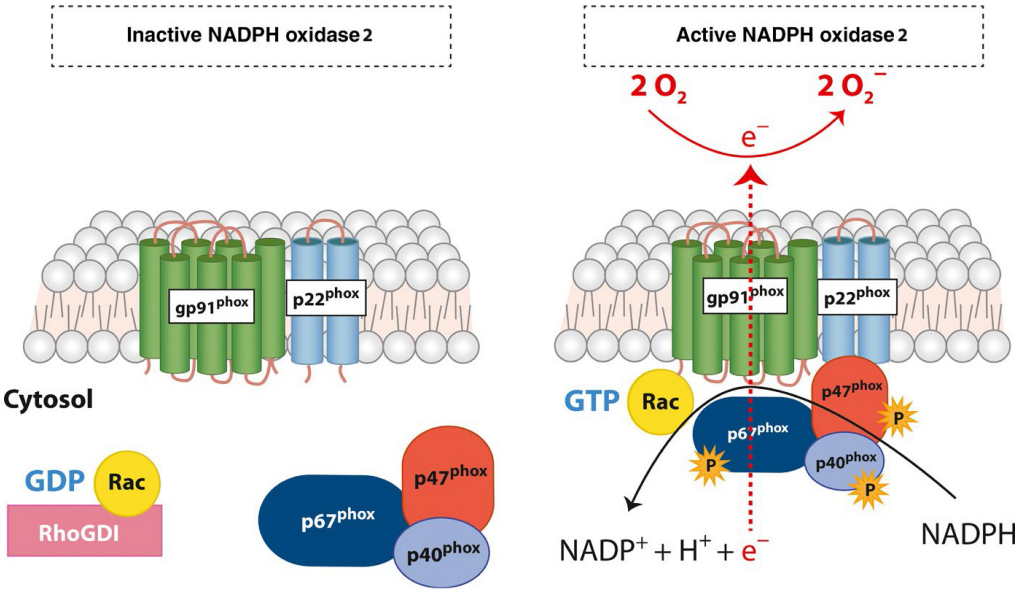

Fig. 1. Activation of NOX2. As single electron transporters, NOX enzymes pass electrons from NADPH to the electron acceptor oxygen, on the other side of the membrane. P22^{phox} (CYBA) is an essential component for stabilisation and activation of NOX2 (Zeng et al. 2019).

The route of ROS production includes the oxidation of the cytosolic NADPH followed by the reduction of oxygen across the membrane to generate superoxide. While Nox1–5 generate superoxide that requires dismutation into H_2O_2 by a separate SOD, DUOXes generate H_2O_2 without requiring a separate SOD (Ameziane-el-hassani et al. 2005). Superoxide itself is weak, membrane impermeable and remains localised. H_2O_2 reacts rapidly, is membrane permeable, and owing to greater stability it can diffuse away from the site of production (Rada and Leto 2008). As neutrophils encounter microorganisms or inflammatory mediators, there is a burst in oxygen consumption and ROS generation. The first report of this respiratory burst from NOXes dates back to over five decades (Rossi and Zatti 1964).

In terms of clinical relevance, only *cybb*, *ncf1*, *ncf2*, and *cyba* are implicit in CGD, and account for 33% (*cybb*), 20% (*ncf1*), 5% (*ncf2*) and 5% (*cyba*) cases (Rada and Leto 2008; Arnold and Heimall 2017). With CYBB being a distinct component of NOX2, NOXes 1, 3 and 4 are not implicated in CGD. Being independent of CYBA and cytosolic subunits for stabilisation or activation, NOX5 (Bánfi et al. 2001; T. Kawahara et al. 2005) and the DUOXes (Wang et al. 2005) are not implicated in CGD either.

Infections and inflammatory complications in CGD

NOX2 expression has been regarded as being phagocyte-specific (Sumimoto, Miyano, and Takeya 2005). While studies on neutrophils from CGD patients have shown that NOX2 is dispensable for the killing of many types of bacteria (Winkelstein et al. 2000), catalase-positive organisms can only be combated by NOX2-expressing neutrophils (Bedard and Krause 2007). To this end, individuals with CGD experience recurrent infections, most frequently brought on by *Aspergillus* spp*., Burkholderia cepacia, Staphylococcus aureus, Serratia marescens*, *Nocardia* spp., *Salmonella* (Winkelstein et al. 2000; Jones et al. 2008; Martire et al. 2008; Marciano et al. 2015) as well as Bacille Calmette-Guerin and *Mycobacterium tuberculosis* (Lee et al. 2008; Conti et al. 2016; Wolach et al. 2017). Invasive infections by filamentous fungi are especially important contributors to morbidity and mortality in CGD (Blumental et al. 2011; Beauté et al. 2011; Falcone and Holland 2012). In fact, microbiologic analyses restricted to *Aspergillus, Burkholderia, Nocardia, Serratia* and *Staphylococcus* revealed *Aspergillus* to have the highest incidence, ranging from between

41-55%. Further, *Aspergillus fumigatus* is the most prevalent *Aspergillus* species (Marciano et al. 2014). Pneumonia is the commonest outcome of invasive aspergillosis in CGD (Winkelstein et al. 2000; B. H. Segal et al. 2011). Inflammatory complications often accompany infections in CGD patients, affecting various organs (Alimchandani et al. 2013; Damen et al. 2010; Magnani et al. 2014). Exclusively occurring in CGD, mulch pneumonitis is a hyperinflammatory condition that can be aggressive if not treated early (Siddiqui et al. 2007).

A. fumigatus is an opportunistic fungal pathogen (Buchwalow 1995), and exposure typically occurs via inhalation of conidia into the respiratory tract. Alveolar macrophages resident in the pulmonary tract ingest and kill conidia, while neutrophils use oxygen-dependent mechanisms to attack hyphae germinating from conidia that escape macrophage surveillance. The importance of the phagocyte respiratory burst in combating aspergillosis is evidenced by the frequent occurrence of infection in patients with CGD, which appears to result from a failure to kill hyphae by monocytic (Espinosa et al. 2014) and neutrophilic oxidative mechanisms. H_2O_2 has potent antihyphal activity *in vitro*, while neutrophil-mediated hyphal damage is strongly blocked by myeloperoxidase inhibitors, the hydrogen peroxide scavenger, catalase, and to a lesser extent, superoxide dismutase (Morgenstern et al. 1997; B. H. R. R. Segal 2010).

Current models of CGD

Three laboratory models of CGD have been reported to date. All are murine models, and include two X-linked *gp91^{phox}* (*CYBB*) mutants (Pollock et al. 1995; Sweeney et al. 2017) and the autosomal recessive *p22phox* (*CYBA*) mutant (Nakano et al. 2008). Both *CYBB* mutants closely resemble patients with CGD in that the males lack a respiratory burst, thus exhibiting enhanced susceptibility to infection with *A. fumigatus*, *S. aureus*, and *Candida albicans*, among others (Pollock et al. 1995; Sweeney et al. 2017). Similarly, *CYBA* mutants lack detectable superoxide production in their neutrophils, and are highly susceptible to necrotising pneumonia (Nakano et al. 2008).

In following up the reported role of ROS in regeneration (Love et al. 2013; Gauron et al. 2013), we sought a candidate that would directly affect the NOXes it binds to. Overall, since CYBA is implicit in both, structural integrity and activation of NOXes1-4, it indicates that any

mutations will likely cripple its membrane partner NOXes. Recently, morpholinos for *cyba* were reported to model infection in zebrafish larvae (Wiemann et al. 2017). Here, we targeted zebrafish *cyba* using CRISPR/Cas9, taking the modelling of CGD to a stable non-mammalian mutant strain for the first time. We present a hitherto unexplored route of infection for *Aspergillus* and show that *cyba* mutants are sensitive to infection compared to wild type (WT) peers.

We have chosen the zebrafish larva based on its amenability to microinjection. The spores (conidia) of *A. fumigatus* WT A1163 and RAG 29 (constitutively expressing fluorescent protein TurboFP635) are injected into the yolk sac of the larvae. The *A. fumigatus* RAG 29 is tagged with TURBOFP 635, a far-red protein from the sea anemone *Entacmaea quardicolor.* TURBOFP 635 is characterised by fast maturation, a high pH-stability and photostability (Evrogen 2007). Confocal microscopy is employed to visualise fungal growth.

Materials and methods

Zebrafish husbandry

Zebrafish (*Danio rerio*) husbandry was undertaken in a re-circulating system maintained at 28.5°C, with a 14h photoperiod. Conditions were uniform for WT and all GM strains. Embryos are obtained by marbling tanks, or by isolating pairs in breeding chambers. Larvae were staged as previously described (Kimmel *et al*., 1995).

sgRNA design and production of CRISPR mutants

Single guide RNAs (sgRNAs) were designed for targeting exon 1 of zebrafish *cyba*, using the online tool CRISPRscan (Moreno-mateos et al. 2015). Entering the Ensemble ID for *cyba* in the CRISPRscan tool automatically listed multiple gRNAs against coding exons of the genes, displaying them by rank. gRNAs were then chosen based on rank, location within the first 50% of the ORF and distance from the initiation codon. A sgRNA template requires a 52nt oligo (sgRNA primer) 5' TAATACGACTCACTATAGG(N=18)GTTTTAGAGCTAGAA, containing the T7 promoter, the 20nt specific DNA-binding sequence [GG(N=18)] and a constant 15nt tail. This was used in combination with an 80nt reverse oligo AAAAGCACCGACTCGGTGCCACTTTTTCAAGTTGATAACGGACTAGCCTTATTT TAACTTGCTATTTCTAGCTCTAAAAC invariant 3' end (tail primer) to generate a 117bp PCR product. Oligos were obtained from Sigma-Aldrich®. The PCR cycler settings for this primer extension were 3 min at 95°C; 30 cycles of 30s at 95°C, 30s at 45°C and 30s at 72°C; and a final step at 72°C for 7 min. PCR products were purified using Qiaquick (Qiagen) columns, and approximately 120–150ng of DNA were used as a template for a T7 *in vitro* transcription reaction. *In vitro* transcribed sgRNAs were treated with DNase and precipitated with sodium acetate and ethanol (Moreno-mateos et al. 2015). Purified sgRNA and Cas9-NLS protein (New England Biolabs® Inc.) were diluted to 300ng/ul. Equal volumes of Cas9-NLS protein, sgRNA and Phenol Red (Sigma-Aldrich®)

were mixed to obtain the final injection mix. Injection drop size was adjusted to 1nl using a graticule scale. All embryos were injected at the one-cell stage.

Genomic Extraction

Individual larvae were added to individual PCR tubes containing lysis Buffer (10mM Tris-HCL, pH 8.0, 1mM EDTA, 0.3% Tween-20, 0.3% NP40), proteinase K stock (20-25mg/ml), 1ul/50ul lysis buffer. This was incubated in a thermal cycler programmed to 55°C (2hours), 95°C (10 minutes) and a 12°C hold.

Polymerase Chain Reaction

PCR was undertaken for genomic DNA using ExTaq DNA Polymerase (TaKaRa). For CRISPR mutants, Initial identification of indels was undertaken following Sanger sequencing. Subsequent identification of established CRISPR mutants was undertaken using restriction digest with HindIII. Genotyping and identification of *sa1179*8 mutants was undertaken via Sanger sequencing (GATC Biotech). Primers used are listed in **Table 1.** T_M for the Cyba F1 and Cyba R1 pair was 51.1°C.

Cyba F1	AGTTTATTTGCCAGTGACAGCA	Genomic PCR for CRISPR mutants
Cyba R1	CTCAAGCAGCCTACCAAACC	Genomic PCR for CRISPR mutants
M13 Reverse	GTAAAACGACGGCCAGTG	For identifying indels

Table 1. List of primers

***Aspergillus fumigatus* strains and Spore Harvesting**

Aspergillus fumigatus WT A1160 and RAG29 were used to inject the larvae. Strains were cultured in *Aspergillus* complete media (ACM) in a 20ml flask and incubated at 37°C for at least 2 days prior to spore harvesting. ACM (1L) was prepared using the following reagents: Adenine (0.075g), Glucose (10g), Yeast Extract (1g), Bacteriological peptone (2g), Casamino acids (1g), Vitamin solution (10ml), Salt solution (20ml), Ammonium Tartrate (10ml from 500mM stock), pH 6.5 with 10M NaOH and finally 1.5% of agar to solidify it (G.PontecorvoJ.A.RoperL.M.ChemmonsK.D.MacdonaldA.W.J.Bufton 1953). For spore harvesting, a 1X NaCl-Tween (0.9 mg/ml NaCl + 0.002% Tween-20) was prepared using MiliQ water and 10X NaCl Tween. 10ml of the 1X Tween was added per flask and flasks were agitated to detach spores. This suspension was filtered using a Mira cloth (Merck Milipore) followed by centrifugation at 4000RPM, for 5minutes. Pellet was resuspended in 10ml of 1X Tween, followed again by centrifugation at 400RPM for 5minutes. Pellet was resuspended 5ml of the 1X Tween to make a master solution. To count the spores, 1/10 and 1/100 dilutions were made from the master solution and 1X Tween. Spores were counted using a Neubauer counting chamber (haematocytometer) (Marinfeld,Germany) on a Nikon Optiphot at a 40x magnification. The final concentration of the spores was found using the following formula:

Concentration of spores = number of spores/7 (sections counted) x 25 x 10^4 x 100 (dilution factor).

Microinjection

From the spore concentration, various dilutions were prepared. These were 50 conidia/5nl, 50 conidia/2nl, 20 conidia/2nl, and 10 conidia/2nl. Freshly harvested spores were used for each trial. Prior to injection, larvae were anaesthetised in MS-222, and positioned laterally on injection plates made of 3% agarose in E3 pre-treated with 1ml filter-sterilised 2% bovine serum albumin (BSA) to prevent larval abrasion against the agarose surface and facilitate handling (Brothers, Newman, and Wheeler 2011; Knox et al. 2014; E. E. Rosowski et al. 2018). Spore suspensions were directly injected into the yolk sac of 2dpf larvae, using a microinjection setup consisting of a Picospritzer II (General Valve Corporation) and a Leica MZ6 stereomicroscope. The injected volume was 1nl, unless specified otherwise.

Survival Analysis

Viability of larvae was checked twice per day to monitor survival. Dead larvae were plated on Potato Dextrose Agar (PDA). Plates were incubated at 37°C and appearance of hyphal masses was used as confirmation for aspergillosis-led mortality. Survival was statistically assessed using the Log Rank Test, in Prism 8.1 (GraphPad Software, Inc.)

Fluorescence microscopy

The 96 well glass bottom plate with cells/conidia were viewed using Nikon TE-2000 Workstation (Fluorescence microscope. The plates were viewed under 10x, 20x and 40x and using the MetaMorph software the cells/conidia were viewed under brightfield and using RFP laser.

Confocal Microscopy

Zebrafish Larvae were placed horizontally with the yolk sac facing up on an 8-well ibidi. Mounted larvae were viewed using a Confocal Laser Scanning Microscope (Leica Microsystems), under 10x, 25x (wet) and 40x, running LasX software. The lasers used were Argon (green to yellow) (GFP) and White (red to far red) (TURBO FP635).

Results

Generation and description of *cyba* mutant zebrafish

Zebrafish *cyba* is mapped to chromosome 18: 31,094,846-31,097,287. It has 4 splice variants, only one of which codes protein (Ensemble 84 Mar 2016). Similar to murine *CYBA* (Nakano et al. 2008) the protein coding variant in zebrafish *cyba* also contains 6 exons and 5 introns. The proline-rich C-terminus of cyba renders its functional capability to bind to the SH3 domains of ncf1 (T. Kawahara et al. 2005). In anticipation of early protein truncation, we targeted two sequences on exon 1. We obtained F_1 heterozygotes by crossing F_0 adults

to WTs. *cyba*$^{+/-}$ animals were identified via restriction digest with HindIII. These were then sequenced. We found a 12bp deletion leading to an in-frame mutation, and a 5bp deletion, leading to a frameshift mutation. Incrossing F_1 heterozygotes carrying the latter led to the establishment of a stable mutant line harbouring a 5bp deletion (**Fig. 2A**) hereafter referred to as *cyba*$^{ex1.5bp-/-}$. Mutants are viable, fertile and do not require antibiotic supplementation. Outwardly, they appear healthy, and with the exception of their pigment patterns, there were no other apparent differences between these and WT animals (**Fig. 3**). The different pigment patterns themselves were not an outcome of the mutation. The F_0 founder animal for the *cyba*$^{ex1.5bp-/-}$ mutation was a *nacre*$^{-/-}$ individual. The *nacre*$^{-/-}$ mutation affects pigment cell fate in the zebrafish neural crest. Mutants lack melanophores throughout development but have increased numbers of iridophores (Lister et al. 1999). This was crossed to an animal with WT pigmentation pattern. The resulting progeny was a mixture of various pigment patterns, including the regular WT, leopard (mutants develop melanophore spots instead of stripes) (Watanabe et al. 2006) and *roy orbison* (mutants lack iridiophores) (Ren et al. 2002; D'Agati et al. 2017). Now, many labs have the latter two strains, among others, in the background of various, supposedly WT stocks. This would explain why we obtained a variety of pigment patterns. Fortuitously though, these pigment backgrounds are very effective at assisting in experiments related to regeneration. While those experiments are outside the scope of this piece of work, briefly, the lack of solid stripes help visualise the flux of ROS via fluorescent reporter proteins such as HyPer (Belousov et al. 2006).

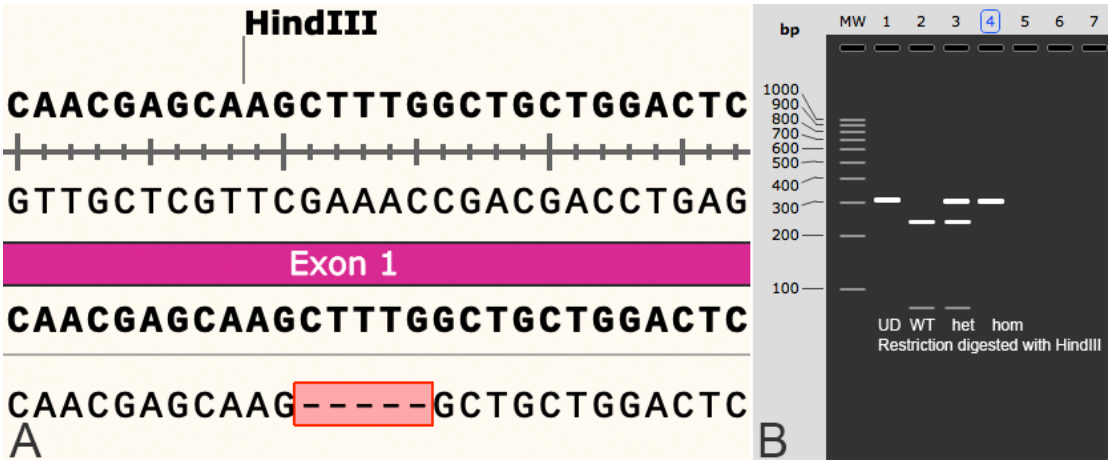

Fig. 2. Confirmation of *cyba* mutations in zebrafish. **A.** CRISPR-meditated mutagenesis led to a 5bp deletion in exon 1. **B.** The 5bp deletion removes the diagnostic HindIII restriction enzyme site, enabling easy identification of genotype. CRISPR mutants were F_4 generation.

***Aspergillus fumigatus* causes lethal infection in *cyba* mutant zebrafish larvae**

We trialled several routes for infecting larvae. A simple immersion of zebrafish larvae in a suspension containing high concentration of fungal conidia yielded no mortality among WTs and mutants. Further, amputating the caudal fin fold followed by immersion had no effect either. Next, we tried injecting conidia in the hindbrain ventricle (HBV), following a widely used protocol (Knox et al. 2014). Given the transparent nature of the ventricle, spores were co-injected with the dye phenol red, to confirm delivery. This revealed the disadvantage of "kickback" of the injected volume. While accessing the HBV is straightforward, some injected volume was always ejected out of the animal, thus leading to inconsistencies in doses between individual larvae. Meanwhile, the yolk sac in zebrafish larvae is easily accessible, large and actively used by the animals for sustenance. Injecting into the yolk can be undertaken without any visual aid since delivery is easily observed in its fatty environment. It has been used as a route of infection in modelling tuberculosis (Veneman et al. 2014), *Cronobacter turicensis* (Fehr et al. 2015), *Candida albicans* (Seman et al. 2018) but never for *Aspergillus*. Thus, the next step was to trial yolk injections.

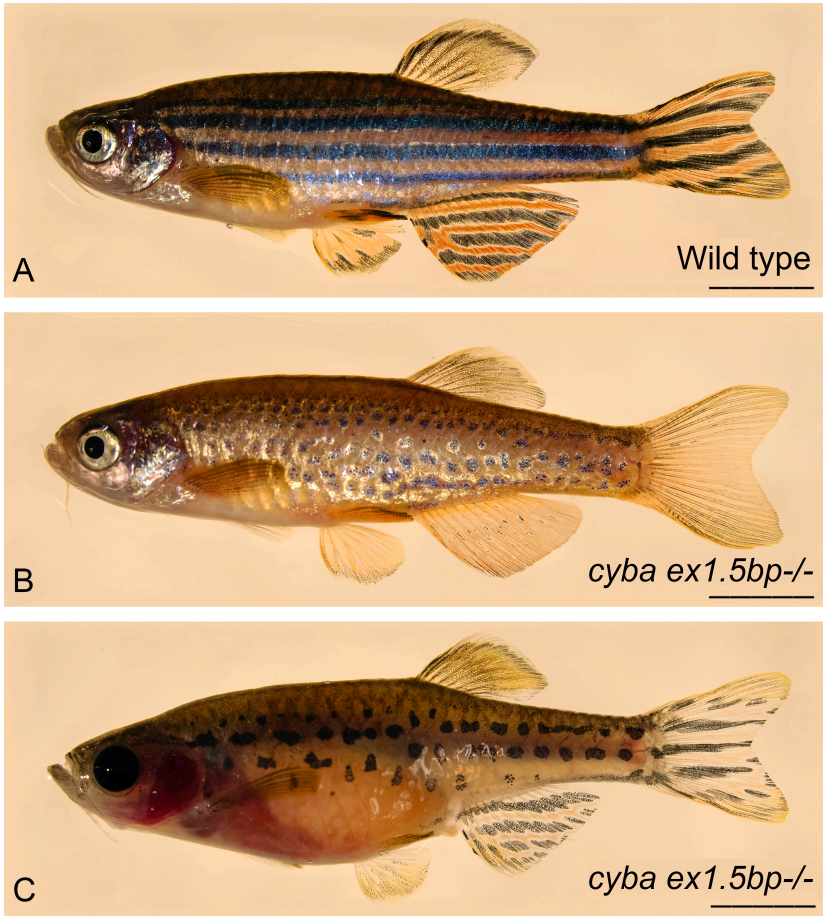

Fig. 3. General comparison of *cyba* mutants and WT zebrafish siblings. Mutant animals are healthy, grow into fertile adults and do not require any antibiotics for maintenance. A. The native WT pigment pattern consists of dark stripes alternating with lighter interstripes. B and C. Aside from the WT, laboratory strains of zebrafish come in a variety of pigment patterns such as *leopard* where animals have clusters of melanophores instead of stripes (B), and *roy orbison* where iridiophores are missing (C). These pigment patterns are recessive and may often be in the background of 'WT looking' strains. As a result, they will emerge during incrossing. Scale bar = 5mm.

Trial 1: A 10 conidia/nl concentration of *A. fumigatus* was used, to introduce the previously described dose of 50 conidia (Knox et al. 2014) per animal. We used WT, *cyba*$^{ex1.5b+-/-}$, and *cyba*$^{ex1.5bp-/-}$ animals at 2dpf. However, 5nl was found to be a significantly high volume as it exceeded the yolk sac volume, leading to bursting of the sac and rapid mortality. The injected volume was therefore adjusted to 2nl. 12 of each type were injected, out of which 6 WT, 4 *cyba*$^{ex1.5bp+/-}$, and 7 *cyba*$^{ex1.5bp-/-}$ larvae died by 3day post injection (dpi). Dead larvae were plated on PDA plates. Most of the mortalities were due to fungal infection but some appeared to have died due to bacterial infection. This trial confirmed the efficacy of the yolk sac as suitable route for infection. Importantly, no "kickback" was observed, guaranteeing consistency of dose delivery.

Trial 2: A second trial was run, using WT (n=15) and *cyba*$^{ex1.5bp-/-}$ (n=16) animals, using 25 conidia/nl of *A. fumigatus* RAG29 (**Table 2**). The next day 2 of each type were found to be immobile. By 3dpi all the animals except one WT were found to be dead. Survival curves for both, mutants and WTs ran very close to each other (**Fig. 6**) and the difference between the two was not significant (Log Rank test, P value 0.7537). The dead animals were plated on PDA to confirm they indeed died due to fungal infection (**Fig. 5**). Compared to WT siblings of X-CGD mice, who are resilient to *A. fumigatus* infection (Pollock et al. 1995; Morgenstern et al. 1997), this was surprising. Since we were using a novel route of infection, we considered the possibility that this concentration may have been too high, or the route too efficient, and therefore adjusted the infection dose for the next experiment.

Trial 3: This trial employed WT larvae (n=31) and *cyba*$^{ex1.5bp-/-}$ larvae (n=8). At 2dpf larvae were injected with 10 conidia/nl of *A. fumigatus* RAG29 (**Table 2**). After 2 days 15 of the 31 larvae died and were plated on PDA plates. After 3 days, 7 more larvae had died and were plated on PDA plates. All of the *cyba*$^{ex1.5bp-/-}$ died by 2 days after injection. In this trial, only 2 of the 31 WT larvae survived (**Fig. 6**). Difference in survivability between the groups was significant this time (Log Rank test, ** P value 0.0026).

Trial 4: For this trial, WT (n =6) and *cyba*$^{ex1.5bp-/-}$ (n =20) were used. It was intended to include heterozygote animals as well but the matings of homozygous to WT animals were unsuccessful and did not yield any offspring. Two concentrations were used, 10 conidia/nl and 5 conidia/nl of *A. fumigatus* RAG29 (**Table 2**). For the first concentration, *cyba*$^{ex1.5bp-/-}$ larvae (n =10) were injected. For the second, WT (n =6) and *cyba*$^{ex1.5bp-/-}$ (n =10) were

injected. By 3 dpi 4 of 10 *cyba*$^{ex1.5bp-/-}$ larvae that were injected with 10 conidia/nl had perished. From the lower concentration group, the mortality was WT = 1 and *cyba*$^{ex1.5bp-/-}$ = 4 (**Fig. 6**). Dead animals were plated on PDA to confirm fungal invasion. Difference in survivability following the lower dose was significant (Log Rank test, ** P value 0.0052).

Trial 5: We repeated injection of WT (n=11) and *cyba*$^{ex1.5bp-/-}$ (n=15) larvae with a 5 conidia/nl concentration (**Table 2**). By 3dpi, 3 of 11 WT and 13 of 15 *cyba*$^{ex1.5bp-/-}$ had succumbed. This trial successfully reproduced the results of the previous trial, indicating that 5 conidia/nl is the optimum concentration. Once again, difference in survivability was significant (Log Rank test, ** P value 0.0019), thus confirming the result of the previous trial.

Regardless of the concentration of conidia injected, all larvae that developed infection showed similar symptoms. During the initial stages of infection the swimming ability of the larvae was affected wherein they could be seen moving their pectoral fins, but not achieving any movement. As infection advances, it appears to affect the swim bladder (Fig. 5) and the larvae are no longer able to remain upright. Terminal infection is characterised by extensive necroses and feebly moving gill arches and heartbeat.

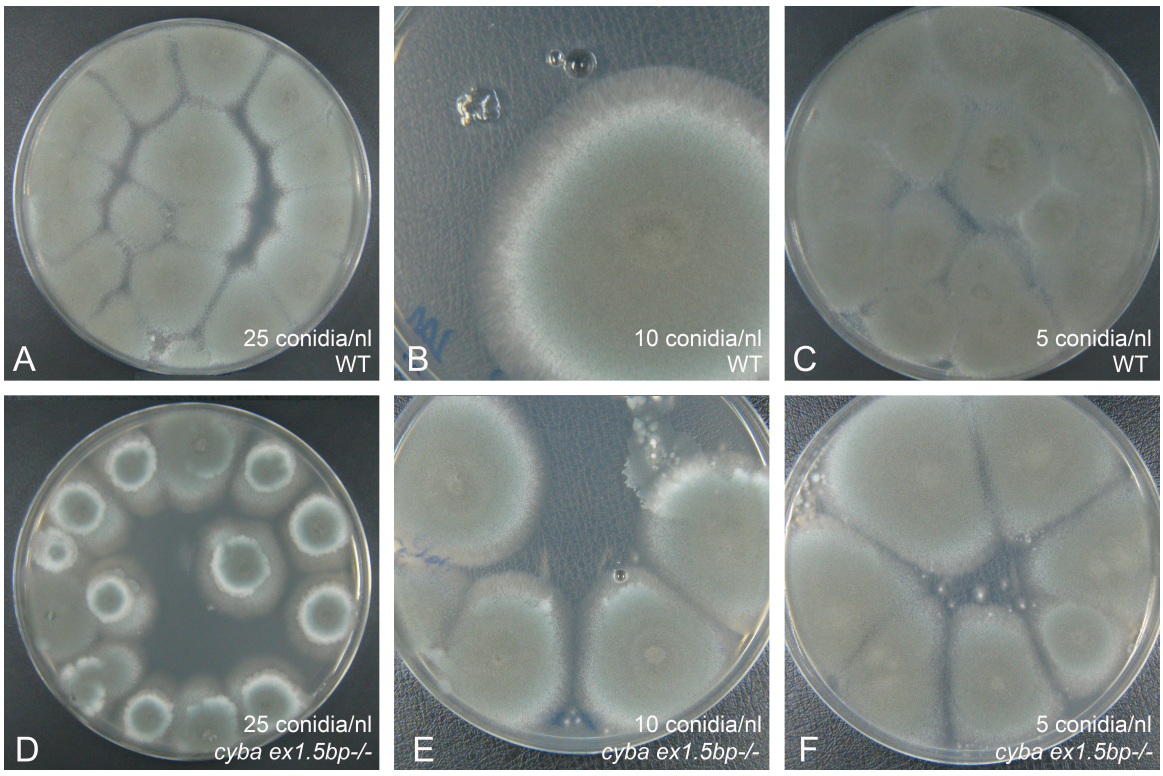

Fig. 5. Diagnostic test for fungus-associated mortality. Conidia were injected at indicated concentrations, and dead larvae were plated on PDA plates. Plates were then incubated at 37°C, and hyphal projections from plated larvae were used for confirming aspergillosis. Experimental end point was 3dpi, i.e. any larvae found dead beyond this were not plated.

Trial	No. of conidia injected	WT		*cyba*$^{ex1.5bp+/-}$		*cyba*$^{ex1.5bp-/-}$	
		Total	Mortality at 3dpi	Total	Mortality at 3dpi	Total	Mortality at 3dpi
1	50 conidia/nl	12	6	12	4	12	7
2	25 conidia/nl	15	14	-	-	16	16
3	10 conidia/nl	31	22	-	-	8	8
4	5 conidia/nl	6	1	-	-	10	4
5	5 conidia/nl	11	3	-	-	15	13

Table 2. Outcomes of various conidial injection trials in zebrafish larvae, injected at 2dpf.

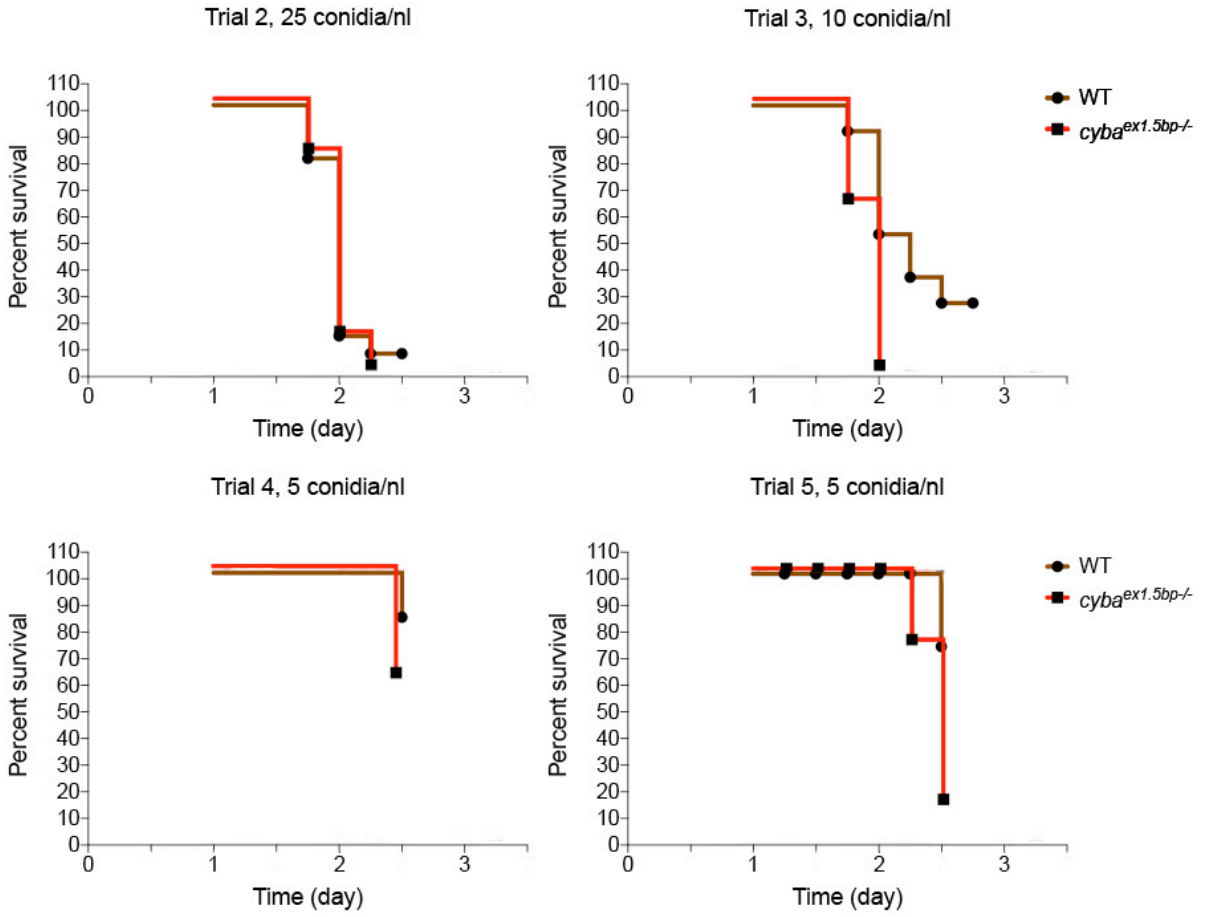

Fig. 6. Survivability curves for WT and *cyba* mutant siblings. Higher doses overwhelm both, WT and mutants. However, WTs are able to tolerate lower concentrations, while mutants succumb to these as well (Log Rank Test, ** P< 0.005)

DISCUSSION

Similarity to humans notwithstanding, traditional mammalian models only allow limited visual access *in vivo*, are unsuitable for high-throughput studies, and come with a different set of ethical considerations. In sharp contrast is the zebrafish with its high fecundity, transparent larvae, and hardy keep. By 36hpf, they have functional circulation that includes

an innate immune system that shows conservation with mammalian innate immune systems (Van Der Vaart, Spaink, and Meijer 2012) and a fully functional complement system (Boshra, Li, and Sunyer 2006). Also, larvae do not have an adaptive immune system, thus providing the chance to study innate immunity in isolation (E. Rosowski et al. 2018). An interesting observation on both murine models of X-CGD (Pollock et al. 1995; Sweeney et al. 2017) is that they only appear to offer a sex-specific investigation of CGD. Meanwhile, zebrafish demonstrate complex polygenic sex determination, with further understanding still required (Liew and Orbán 2013). This may very well mean that *cybb* might as well be autosomal, thus allowing a broader pan-sex investigation. Within the realm of infectious diseases, larval and adult zebrafish have effectively modelled for bacterial, viral, fungal and parasitic infections, some of which are tabulated in **Table 3**.

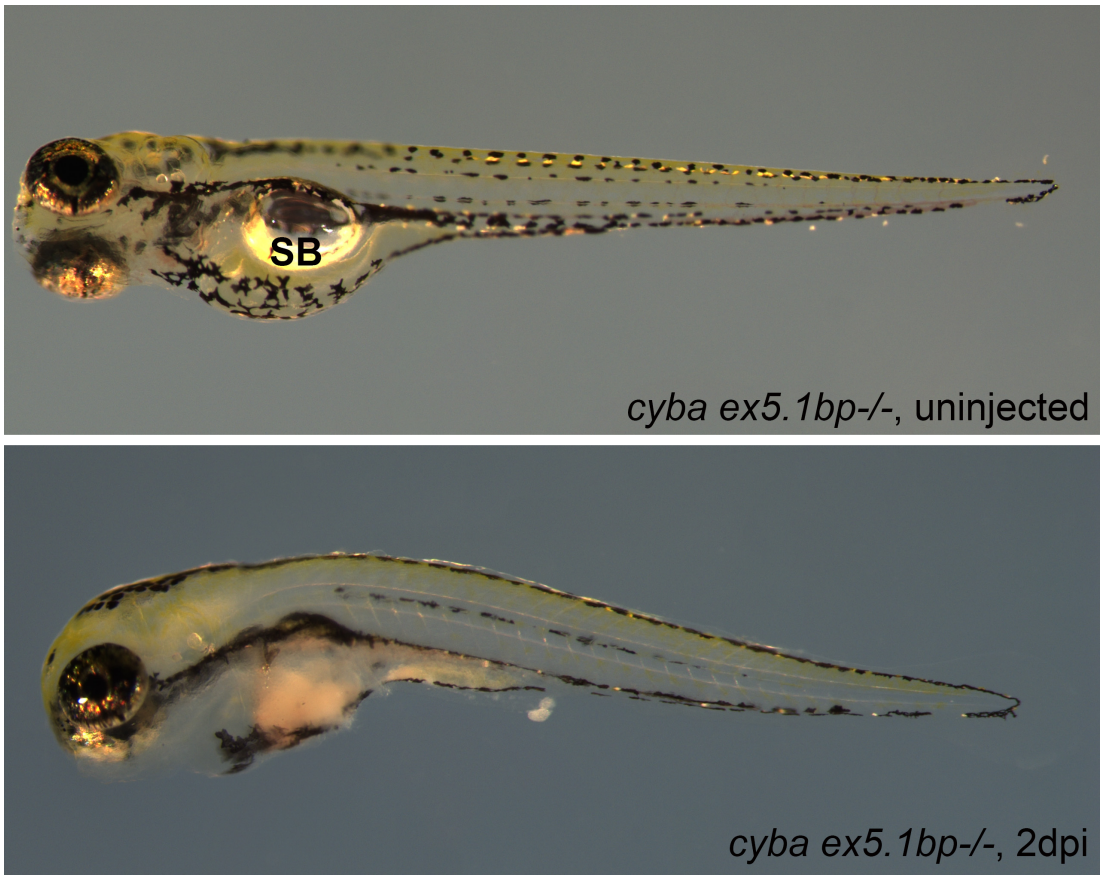

Fig. 7. *cyba* mutants show systemic infection following *Aspergillus* injection. Comparison of *cyba*$^{ex1.5bp-/-}$ mutants - uninjected animal (top) and injected (below). Injected animals show necroses and the swim bladder (SB) is no longer distinguishable by 3dpi.

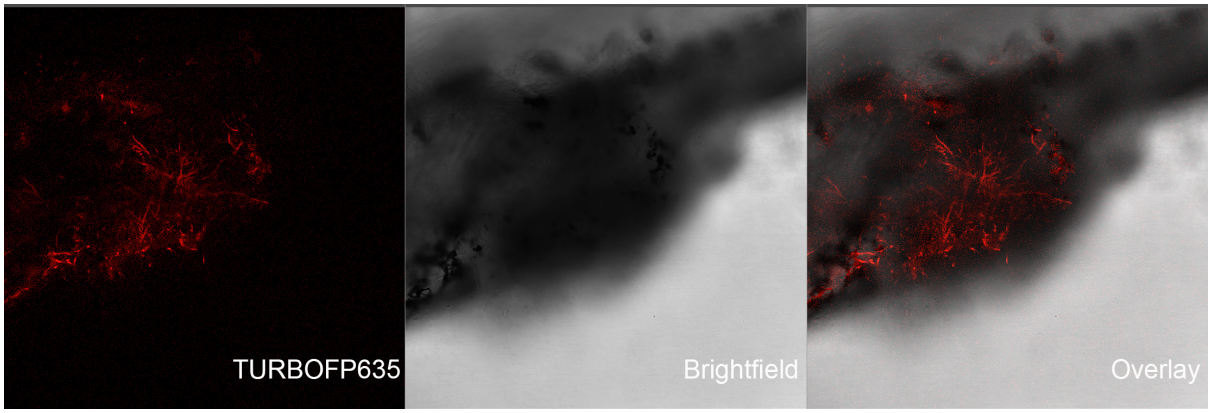

Fig. 8. Confocal image of hyphal projections seen around the yolk sac. At 2dpi, *cyba*$^{ex1.5bp-/-}$ larvae injected with 10 conidia/nl show extensive hyphal projections, which results in mortality. Image credits to CAM (Phenotyping Centre at Manchester) / MFIG

Infection	Pathogen	Reference
Bacterial	*Staphylococcus aureus*	(Prajsnar et al. 2008)
Viral	Herpes Simplex virus Type 1	(Burgos et al. 2008)
Bacterial	*Pseudomonas aeruginosa*	(Brannon et al. 2009)
Fungal	*Candida albicans*	(Brothers, Newman, and Wheeler 2011)
Bacterial	*Streptococcus agalactiae*	(Patterson et al. 2012)
Viral	Chikungunya virus	(Palha et al. 2013)
Bacterial	*Mycobacterium marinum*	(Oksanen et al. 2013)
Viral	Influenza A virus	(Gabor et al. 2014)
Bacterial	*Escherichia coli*	(Nguyen-Chi et al. 2014)
Bacterial	*Streptococcus pneumoniae*	(Saralahti et al. 2014)
Fungal	*Aspergillus fumigatus*	(Knox et al. 2014)
Fungal	*Mucor circinelloides*	(Voelz, Gratacap, and Wheeler 2015)
Viral	Hepatitis C virus	(Ding et al. 2015)
Fungal	*Cryptococcus neoformans*	(Bojarczuk et al. 2016)
Protozoan	*Trypanosoma cruzi*	(Akle et al. 2017)

Table 2. List of zebrafish models of pathogenic agents.

Some consider it unlikely that a comprehensive functional understanding of all human protein-coding genes will be available in the near future (Kettleborough et al. 2013). An advantage of modelling human disease in the zebrafish is the possibility of addressing specific phenotypes resulting from gene disruption, in a short span of time and on a large number of animals. In this regard, phenotypic screens can be performed for genes involved

in different human pathologies. As an externally fertilising species, the zebrafish genome can be altered easily by injecting fertilised eggs at the one-cell stage. The advent of newer CRISPR tools such as CRISPRSCAN (Moreno-mateos et al. 2015) has enhanced the chances of obtaining bi-allelic mutations as early as in F_0 animals while minimising off-target effects. This coupled with easy accessibility to genomic resources makes the process straightforward. The decision to target *cyba* was informed by its role in the sustained increase in ROS following caudal amputation in *Xenopus* tadpoles. Specifically, morpholinos targeting *cyba* have been shown to reduce regeneration in the *Xenopus* tadpole tail by ~33%. This increase in ROS is essential for regeneration to occur, and in the *Xenopus* tadpole continues until regeneration is complete. (Love et al. 2013). This makes *cyba* a promising candidate for investigating ROS and regeneration.

While CRISPR-mediated mutants are now easy to generate, another consideration has become relevant in relation to the mutants themselves, that of transcriptional adaptation. Transcriptional adaptation occurs when a mutation leads to the increased expression of related genes that are able to assume the function of the mutated gene. Latest evidence suggests that transcriptional adaptation is encouraged by nonsense-mediated decay of mutant mRNA, with increased expression of mRNA from paralogues buffering against the effects of the mutation. Both, CRISPR and ENU mutations may lead to premature stops, and thus to nonsense-mediated decay (El-Brolosy et al. 2019). Also, the common ancestor of zebrafish and 22,000 other ray-finned fish likely underwent a complete genome duplication (Taylor et al. 2003), thus making a case for possible paralogues to act as adapting genes. Thus, we BLASTed PCR primers for *cyba*, as well as the protein sequence to check for identity with any paralogues but did not find any. This coupled with the CGD phenotype gave reasonable confidence to assume that the severity of the phenotype was not diluted.

Successful targeting of *cyba* would impair the function of Nox2. While NOX2 function is impaired in CGD, the production of ROIs, which can be quantified (Kuhns et al. 2010), varies from 0.1% to 27% of the normal range. This in turn is dependent on the type of mutation i.e. nonsense, missense, deletion etc., and not necessarily on pattern of inheritance. Even so,

rate of survival among CGD patients is lower among X-CGD cohorts than in A-CGD cohorts (Kuhns et al. 2010; Marciano et al. 2014). Both, the X-CGD mouse model (Sweeney et al. 2017) and our *cyba* model result from a deletion. Yet, we found that *cyba*$^{ex1.5b-/-}$ animals thrive, even though they are maintained without any antibiotic assistance. This is in sharp contrast to X-CGD mice that show increased morbidity in spite of receiving the antibiotic Sulfatrim for maintenance (Sweeney et al. 2017). This raised concerns as to whether these fish had any functional mutation. A recent analysis on ENU and CRISPR mutant zebrafish lines revealed altered processing of mRNA transcripts that enable escaping nonsense-mediated decay (Anderson et al. 2017). Additionally, a recent report has emerged that discusses benign *CYBA* variants (Sun et al. 2017). Therefore, our concern was whether these genetic mutants were functional mutants as well.

To test this, we tried to recapitulate the human scenario to check susceptibility. *A. fumigatus* is pervasive but practically harmless in immunocompetent individuals. In CGD though it insidiously leads to invasive aspergillosis. To achieve invasive infection, *Aspergillus* conidia must sprout filamentous hyphae, a milestone considered to be vital to its pathology (Fischer et al. 2017). *Aspergillus* models of infection have recently been developed in zebrafish larvae (Knox et al. 2014; Herbst et al. 2015) and the transparency of the larva affords observing sprouting hyphae over a multi-day infection progression. The preferred site of injection for fungal infection has been the larval HBV via the otic vesicle (Brothers, Newman, and Wheeler 2011; Knox et al. 2014; E. E. Rosowski et al. 2018). We attempted direct injection into the HBV but the ejection of injected suspension rendered delivery as inconsistent. Also, this method required some expertise, given the dimensions of the ventricle. By contrast, yolk sac injection required minimal handling of the larvae and was rapid, indicating high-throughput. Indeed, this route has been used for injecting *Salmonella typhimurium* and *Mycobacterium marinum* (Benard et al. 2012), *Staphylococcus epidermis* and *Staphylococcus aureus* (Veneman et al. 2013) and *Candida albicans* (Chao et al. 2010; Seman et al. 2018). Besides technical considerations, both routes of infection have their advantages and limitations. The HBV is devoid of phagocytes but these can migrate here, allowing visualisation of microbe-phagocyte interactions, and herein lies the strength of this route. However, HBV injections must be undertaken between 36-48hpf as after this window

its volume decreases. The yolk sac too is an excellent location for imaging phagocyte-microbe encounters (E. Rosowski et al. 2018), and remains amenable to injection for its lifetime. Also, blood vessels in the vicinity of the yolk (Fishelson 1995) may be potential routes for dissemination of infection. However, the yolk may be too efficient at delivering systemic infection, as was evident by our initial trials where both, mutants and WTs were decimated. We were able to overcome this limitation by adjusting the infection dose.

Relative susceptibility to *A. fumigatus* has been demonstrated in mice models of CGD. Following intratracheal or intransal inoculation, WT littermates showed ~500-fold reduction in the mean number of viable conidia cultured from lung tissue by 72 hours post-inoculation. Phenotypically, only mild peribronchial pneumonia was observed, and by seven days, fewer than 100 viable conidia remained in lung tissue. No mortality was observed. In contrast, male X-CGD mice developed necrotising peribronchiolar and alveolar pneumonia, and 70 times as many viable conidia were cultured. This led to a ~48% mortality (Pollock et al. 1995). These observations were successfully reproduced when these X-CGD mice were challenged with different conidial concentrations. The highest concentration resulted in ~87% mortality among mutants but none among the WTs. Phenotypically, higher doses produced rapidly fatal bronchopneumonia in X-CGD mice, whereas the progression of disease was slower at lower doses, with development of chronic inflammatory lesions (Morgenstern et al. 1997). Of course, inoculum doses in mice are significantly large, and so, a direct comparison for our *cyba* model can instead be made with previous studies on zebrafish models of infection. WT larvae injected with morpholino for the transcription factor pu.1 were highly susceptible to *A. fumigatus*, leading to 100% mortality brought on by extensive hyphal growth. pu.1 mediates differentiation of myelo-erythroid progenitors into the myeloid lineage, thus highlighting the importance of macrophages and neutrophils in resisting infection. Morphants exposed to heat-inactivated conidia escaped unscathed (Knox et al. 2014). In a separate study, larvae with defective neutrophil migration succumbed to *A. fumigatus*, with a mortality rate of 80%. Taken together, we have observed comparable rates of mortality in our *cyba* mutants and previously published models. This also serves as verification of the consistency that can be achieved when using a stable mutant model. Furthermore, we have established the yolk sac as a convenient and efficient route of

infection for *Aspergillus*. While time constraints only afforded five trials for survivability assays (three of these being for optimisation) reproducibility was achieved. This highlights yet another advantage of zebrafish over mice in that adult zebrafish breed readily and prolifically, allowing repeats. Mice, on the other hand, generally produce litters of 1 to 10 pups and can only bear approximately three litters in their lifetime.

The global burden of fungal disease remains of high concern in the wake of increasing immunosuppression brought on by HIV and other post-operative medication regimes (Vallabhaneni et al. 2016). This is further emphasised when contrasting the wide spectrum of therapeutic options for treating bacterial infections with those for treating invasive fungal infections (Roemer and Krysan 2014). Compounding this further still are the variable prognoses for fungal infections, which are dependent on the patient's underlying condition, species of pathogen as well as drug availability (Sloan, Dedicoat, and Lalloo 2009; Pfaller et al. 2012). Specifically, in the case of *A. fumigatus*, ≥ 50% mortality (Gregg and Kauffman 2015) coupled with growing resistance to antifungals (Perlin, Shor, and Zhao 2015) calls for *in vivo* approaches to better understand immune interactions. In conclusion, we have demonstrated that *cyba* mutant zebrafish offer a suitable high-throughput approach to model CGD. Pairing this *in vivo* approach with *in vitro* protocols, such as isolation of phagocytes and their interactions with *A. fumigatus*, will further provide a more comprehensive understanding.

References:

1. Akle, Veronica, Nathalie Agudelo-Dueñas, Maria A Molina-Rodriguez, Laurel Brianne Kartchner, Annette Marie Ruth, John M González, and Manu Forero-Shelton. 2017. "Establishment of Larval Zebrafish as an Animal Model to Investigate Trypanosoma Cruzi Motility In Vivo." *JoVE*, no. 127: e56238. https://doi.org/doi:10.3791/56238.
2. Alimchandani, Meghna, Jin-Ping Lai, Phyu Phyu Aung, Sajneet Khangura, Natasha Kamal, John I Gallin, Steven M Holland, et al. 2013. "Gastrointestinal Histopathology in Chronic Granulomatous Disease: A Study of 87 Patients." *The American Journal of Surgical Pathology* 37 (9): 1365–72. https://doi.org/10.1097/PAS.0b013e318297427d.
3. Ameziane-el-hassani, Rabii, Stanislas Morand, Jean-luc Boucher, Yves-michel Frapart, Diane Agnandji, Marie-sophie Noe, Jacques Francon, Khalid Lalaoui, Alain Virion, and Corinne Dupuy. 2005. "Dual Oxidase-2 Has an Intrinsic Ca 2 -Dependent H 2 O 2 -Generating Activity *" 280 (34): 30046–54. https://doi.org/10.1074/jbc.M500516200.
4. Anderson, Jennifer L, Timothy S Mulligan, Meng-Chieh Shen, Hui Wang, Catherine M Scahill, Frederick J Tan, Shao J Du, Elisabeth M Busch-Nentwich, and Steven A Farber. 2017. "MRNA Processing in Mutant Zebrafish Lines Generated by Chemical and CRISPR-Mediated Mutagenesis Produces Unexpected Transcripts That Escape Nonsense-Mediated Decay." *PLoS Genetics* 13 (11): e1007105. https://doi.org/10.1371/journal.pgen.1007105.
5. Arnold, Danielle E, and Jennifer R Heimall. 2017. "A Review of Chronic Granulomatous Disease." *Advances in Therapy* 34 (12): 2543–57. https://doi.org/10.1007/s12325-017-0636-2.
6. Bánfi, Botond, Gergely Molnár, Andres Maturana, Klaus Steger, Balázs Hegedûs, Nicolas Demaurex, and Karl-Heinz Krause. 2001. "A Ca2+-Activated NADPH Oxidase in Testis, Spleen, and Lymph Nodes ." *Journal of Biological Chemistry* 276 (40): 37594–601. https://doi.org/10.1074/jbc.M103034200.
7. Beauté, Julien, Gaëlle Obenga, Loïc Le Mignot, Nizar Mahlaoui, Marie-Elisabeth Bougnoux, Richard Mouy, Marie-Anne

Gougerot-Pocidalo, et al. 2011. “Epidemiology and Outcome of Invasive Fungal Diseases in Patients With Chronic Granulomatous Disease: A Multicenter Study in France.” *The Pediatric Infectious Disease Journal* 30 (1). https://journals.lww.com/pidj/Fulltext/2011/01000/Epidemiology_and_Outcome_of_Invasive_Fungal.14.aspx.
8. Bedard, Karen, and Karl-Heinz Heinz Krause. 2007. “The NOX Family of ROS-Generating NADPH Oxidases: Physiology and Pathophysiology.” *Physiological Reviews* 87 (1): 245–313. https://doi.org/10.1152/physrev.00044.2005.
9. Belousov, Vsevolod V., Arkady F. Fradkov, Konstantin A. Lukyanov, Dmitry B. Staroverov, Konstantin S. Shakhbazov, Alexey V. Terskikh, and Sergey Lukyanov. 2006. “Genetically Encoded Fluorescent Indicator for Intracellular Hydrogen Peroxide.” *Nature Methods* 3 (4): 281–86. https://doi.org/10.1038/nmeth866.
10. Benard, Erica L., Astrid M. van der Sar, Felix Ellett, Graham J. Lieschke, Herman P. Spaink, and Annemarie H. Meijer. 2012. “Infection of Zebrafish Embryos with Intracellular Bacterial Pathogens.” *Journal of Visualized Experiments*, no. 61: 1–8. https://doi.org/10.3791/3781.
11. Blumental, Sophie, Richard Mouy, Nizar Mahlaoui, Marie-Elisabeth Bougnoux, Marianne Debré, Julien Beauté, Olivier Lortholary, Stéphane Blanche, and Alain Fischer. 2011. “Invasive Mold Infections in Chronic Granulomatous Disease: A 25-Year Retrospective Survey.” *Clinical Infectious Diseases* 53 (12): e159–69. https://doi.org/10.1093/cid/cir731.
12. Bojarczuk, Aleksandra, Katie A Miller, Richard Hotham, Amy Lewis, Nikolay V Ogryzko, Alfred A Kamuyango, Helen Frost, et al. 2016. “Cryptococcus Neoformans Intracellular Proliferation and Capsule Size Determines Early Macrophage Control of Infection.” *Scientific Reports* 6 (1): 21489. https://doi.org/10.1038/srep21489.
13. Boshra, H, J Li, and J O Sunyer. 2006. “Recent Advances on the Complement System of Teleost Fish.” *Fish & Shellfish Immunology* 20 (2): 239–62. https://doi.org/https://doi.org/10.1016/j.fsi.2005.04.004.
14. Brandes, Ralf P., Norbert Weissmann, and Katrin Schröder. 2014. “Nox Family NADPH Oxidases: Molecular Mechanisms of Activation.” *Free Radical Biology and Medicine* 76: 208–26. https://doi.org/10.1016/j.freeradbiomed.2014.07.046.
15. Brannon, Mark K, J Muse Davis, Jonathan R Mathias, Chris J Hall, Julia C Emerson, Philip S Crosier, Anna Huttenlocher, Lalita Ramakrishnan, and Samuel M Moskowitz. 2009. “Pseudomonas Aeruginosa Type III Secretion System Interacts with Phagocytes to Modulate Systemic Infection of Zebrafish Embryos.” *Cellular Microbiology* 11 (5): 755–68. https://doi.org/10.1111/j.1462-5822.2009.01288.x.
16. Brothers, Kimberly M., Zachary R. Newman, and Robert T. Wheeler. 2011. “Live Imaging of Disseminated Candidiasis in Zebrafish Reveals Role of Phagocyte Oxidase in Limiting Filamentous Growth.” *Eukaryotic Cell* 10 (7): 932–44. https://doi.org/10.1128/EC.05005-11.
17. Buchwalow, Igor B. 1995. “Bruce S. Zwilling, Toby K. Eisenstein (Editors) Macrophage-Pathogen Interactions (Immunology Series Volume 60). XX + 634 S., 30 Abb., 19 Tab. New York-Basel-Hong Kong 1994. Marcel Dekker Inc. $ 185.00. ISBN: 0–8247-9124-X.” *Journal of Basic Microbiology* 35 (3): 194. https://doi.org/10.1002/jobm.3620350313.
18. Burgos, Javier S., Jorge Ripoll-Gomez, Juan M. Alfaro, Isabel Sastre, and Fernando Valdivieso. 2008. “Zebrafish as a New Model for Herpes Simplex Virus Type 1 Infection.” *Zebrafish* 5 (4): 323–33. https://doi.org/10.1089/zeb.2008.0552.
19. Buvelot, Helene, Klara M Posfay-Barbe, Patrick Linder, Jacques Schrenzel, and Karl-Heinz Krause. 2016. “Staphylococcus Aureus, Phagocyte NADPH Oxidase and Chronic Granulomatous Disease.” *FEMS Microbiology Reviews* 41 (2): 139–57. https://doi.org/10.1093/femsre/fuw042.
20. Chao, Chun-Cheih, Po-Chen Hsu, Chung-Feng Jen, I-Hui Chen, Chieh-Huei Wang, Hau-Chien Chan, Pei-Wen Tsai, et al. 2010. “Zebrafish as a Model Host for <Em>Candida Albicans</Em> Infection.” *Infection and Immunity* 78 (6): 2512 LP – 2521. https://doi.org/10.1128/IAI.01293-09.
21. Conti, Francesca, Saul Oswaldo Lugo-Reyes, Lizbeth Blancas Galicia, Jianxin He, Güzide Aksu, Edgar Borges de Oliveira Jr., Caroline Deswarte, et al. 2016. “Mycobacterial Disease in Patients with Chronic Granulomatous Disease: A Retrospective Analysis of 71 Cases.” *Journal of Allergy and Clinical Immunology* 138 (1): 241-248.e3. https://doi.org/10.1016/j.jaci.2015.11.041.
22. D’Agati, Gianluca, Rosanna Beltre, Anna Sessa, Alexa Burger, Yi Zhou, Christian Mosimann, and Richard M White. 2017. “A Defect in the Mitochondrial Protein Mpv17 Underlies the Transparent Casper Zebrafish.” *Developmental Biology* 430 (1): 11–17. https://doi.org/https://doi.org/10.1016/j.ydbio.2017.07.017.
23. Dahlgren, Claes, and Anna Karlsson. 1999. “Respiratory Burst in Human Neutrophils.”
24. Damen, Gerard M, J Han van Krieken, Esther Hoppenreijs, Erim van Os, Jules J M Tolboom, Adillia Warris, Jan-Bart Yntema, Edward E S Nieuwenhuis, and Johanna C Escher. 2010. “Overlap, Common Features, and Essential Differences in Pediatric Granulomatous Inflammatory Bowel Disease.” *Journal of Pediatric Gastroenterology and Nutrition* 51 (6). https://journals.lww.com/jpgn/Fulltext/2010/12000/Overlap,_Common_Features,_and_Essential.2.aspx.
25. Ding, Cun Bao, Ye Zhao, Jing Pu Zhang, Zong Gen Peng, Dan Qing Song, and Jian Dong Jiang. 2015. “A Zebrafish Model for Subgenomic Hepatitis C Virus Replication.” *International Journal of Molecular Medicine* 35 (3): 791–97. https://doi.org/10.3892/ijmm.2015.2063.
26. El-Brolosy, Mohamed A, Zacharias Kontarakis, Andrea Rossi, Carsten Kuenne, Stefan Günther, Nana Fukuda, Khrievono Kikhi, et al. 2019. “Genetic Compensation Triggered by Mutant MRNA Degradation.” *Nature* 568 (7751): 193–97. https://doi.org/10.1038/s41586-019-1064-z.
27. Espinosa, Vanessa, Anupam Jhingran, Orchi Dutta, Shinji Kasahara, Robert Donnelly, Peicheng Du, Jeffrey Rosenfeld, et al. 2014. “Inflammatory Monocytes Orchestrate Innate Antifungal Immunity in the Lung.” *PLOS Pathogens* 10 (2): e1003940. https://doi.org/10.1371/journal.ppat.1003940.
28. Evrogen. 2007. “Far-Red Fluorescent Protein TurboFP635,” no. C.
29. Falcone, E Liana, and Steven M Holland. 2012. “Invasive Fungal Infection in Chronic Granulomatous Disease: Insights into Pathogenesis and Management.” *Current Opinion in Infectious Diseases* 25 (6). https://journals.lww.com/co-infectiousdiseases/Fulltext/2012/12000/Invasive_fungal_infection_in_chronic_granulomatous.8.aspx.
30. Fattahi, Fatemeh, Mohsen Badalzadeh, Leyla Sedighipour, Masoud Movahedi, Mohammad Reza Fazlollahi, Seyed Davood Mansouri, Ghamar Taj Khotaei, et al. 2011. “Inheritance Pattern and Clinical Aspects of 93 Iranian Patients with Chronic Granulomatous Disease.” *Journal of Clinical Immunology* 31 (5): 792. https://doi.org/10.1007/s10875-011-9567-x.
31. Fehr, Alexander, Athmanya K. Eshwar, Stephan C.F. Neuhauss, Maja Ruetten, Angelika Lehner, and Lloyd Vaughan. 2015. “Evaluation of Zebrafish as a Model to Study the Pathogenesis of the Opportunistic Pathogen Cronobacter Turicensis.” *Emerging Microbes and Infections* 4 (5). https://doi.org/10.1038/emi.2015.29.
32. Fischer, Gregory J, William Bacon, Jun Yang, Jonathan M Palmer, Taylor Dagenais, Bruce D Hammock, and Nancy P Keller. 2017.

"Lipoxygenase Activity Accelerates Programmed Spore Germination in Aspergillus Fumigatus ." *Frontiers in Microbiology* . https://www.frontiersin.org/article/10.3389/fmicb.2017.00831.
33. Fishelson, L. 1995. "Ontogenesis of Cytological Structures around the Yolk Sac during Embryologic and Early Larval Development of Some Cichlid Fishes." *Journal of Fish Biology* 47 (3): 479–91. https://doi.org/10.1111/j.1095-8649.1995.tb01916.x.
34. G.PontecorvoJ.A.RoperL.M.ChemmonsK.D.MacdonaldA.W.J.Bufton. 1953. "144. The Genetics of Aspergillus Nidulans." *Advances in Genetics* 5 (7): 141–238.
35. Gabor, Kristin A, Michelle F Goody, Walter K Mowel, Meghan E Breitbach, Remi L Gratacap, P Eckhard Witten, and Carol H Kim. 2014. "Influenza A Virus Infection in Zebrafish Recapitulates Mammalian Infection and Sensitivity to Anti-Influenza Drug Treatment." *Disease Models &Amp; Mechanisms* 7 (11): 1227 LP – 1237. https://doi.org/10.1242/dmm.014746.
36. Gauron, Carole, Christine Rampon, Mohamed Bouzaffour, Eliane Ipendey, Jeremie Teillon, Michel Volovitch, and Sophie Vriz. 2013. "Sustained Production of ROS Triggers Compensatory Proliferation and Is Required for Regeneration to Proceed." *Scientific Reports* 3: 1–9. https://doi.org/10.1038/srep02084.
37. Gregg, Kevin S, and Carol A Kauffman. 2015. "Invasive Aspergillosis: Epidemiology, Clinical Aspects, and Treatment." *Semin Respir Crit Care Med* 36 (05): 662–72. https://doi.org/10.1055/s-0035-1562893.
38. Herbst, Susanne, Anand Shah, Maria Mazon Moya, Vanessa Marzola, Barbara Jensen, Anna Reed, Mark A Birrell, et al. 2015. "Phagocytosis-Dependent Activation of a TLR9–BTK–Calcineurin–NFAT Pathway Co-Ordinates Innate Immunity to Aspergillus Fumigatus." *EMBO Molecular Medicine* 7 (3): 240–58. https://doi.org/10.15252/emmm.201404556.
39. Jones, L B K R, P McGrogan, T J Flood, A R Gennery, L Morton, A Thrasher, D Goldblatt, L Parker, and A J Cant. 2008. "Special Article: Chronic Granulomatous Disease in the United Kingdom and Ireland: A Comprehensive National Patient-Based Registry." *Clinical & Experimental Immunology* 152 (2): 211–18. https://doi.org/10.1111/j.1365-2249.2008.03644.x.
40. Kawahara, By Tsukasa, Mark T. Quinn, and J. David Lambeth. 2007. "Molecular Evolution of the Reactive Oxygen-Generating NADPH Oxidase (Nox/Duox) Family of Enzymes." *BMC Evolutionary Biology* 7: 1–21. https://doi.org/10.1186/1471-2148-7-109.
41. Kawahara, Tsukasa, Darren Ritsick, Guangjie Cheng, and J David Lambeth. 2005. "Point Mutations in the Proline-Rich Region of P22 Phox Are Dominant Inhibitors of Nox1- and Nox2-Dependent Reactive Oxygen Generation * □" 280 (36): 31859–69. https://doi.org/10.1074/jbc.M501882200.
42. Kettleborough, Ross N.W., Elisabeth M. Busch-Nentwich, Steven A. Harvey, Christopher M. Dooley, Ewart De Bruijn, Freek Van Eeden, Ian Sealy, et al. 2013. "A Systematic Genome-Wide Analysis of Zebrafish Protein-Coding Gene Function." *Nature* 496 (7446): 494–97. https://doi.org/10.1038/nature11992.
43. Knox, Benjamin P, Qing Deng, Mary Rood, Jens C Eickhoff, and Nancy P Keller. 2014. "Distinct Innate Immune Phagocyte Responses to Aspergillus Fumigatus Conidia and Hyphae in Zebrafish Larvae" 13 (10): 1266–77. https://doi.org/10.1128/EC.00080-14.
44. Kuhns, Douglas B, W Gregory Alvord, Theo Heller, Jordan J Feld, Kristen M Pike, Beatriz E Marciano, Gulbu Uzel, et al. 2010. "Residual NADPH Oxidase and Survival in Chronic Granulomatous Disease." *New England Journal of Medicine* 363 (27): 2600–2610. https://doi.org/10.1056/NEJMoa1007097.
45. Lambeth, J. David. 2004. "NOX Enzymes and the Biology of Reactive Oxygen." *Nature Reviews Immunology* 4 (3): 181–89. https://doi.org/10.1038/nri1312.
46. Lee, Pamela P W, Koon-Wing Chan, Liping Jiang, Tongxin Chen, Chengrong Li, Tsz-Leung Lee, Priscilla H S Mak, Susanna F S Fok, Xiqiang Yang, and Yu-Lung Lau. 2008. "Susceptibility to Mycobacterial Infections in Children With X-Linked Chronic Granulomatous Disease: A Review of 17 Patients Living in a Region Endemic For Tuberculosis." *The Pediatric Infectious Disease Journal* 27 (3). https://journals.lww.com/pidj/Fulltext/2008/03000/Susceptibility_to_Mycobacterial_Infections_in.6.aspx.
47. Liew, Woei Chang, and László Orbán. 2013. "Zebrafish Sex: A Complicated Affair." *Briefings in Functional Genomics* 13 (2): 172–87. https://doi.org/10.1093/bfgp/elt041.
48. Lister, J A, C P Robertson, T Lepage, S L Johnson, and D W Raible. 1999. "Nacre Encodes a Zebrafish Microphthalmia-Related Protein That Regulates Neural-Crest-Derived Pigment Cell Fate." *Development (Cambridge, England)* 126 (17): 3757–67. http://www.ncbi.nlm.nih.gov/pubmed/10433906.
49. Love, Nick R., Yaoyao Chen, Shoko Ishibashi, Paraskevi Kritsiligkou, Robert Lea, Yvette Koh, Jennifer L. Gallop, Karel Dorey, and Enrique Amaya. 2013. "Amputation-Induced Reactive Oxygen Species Are Required for Successful Xenopus Tadpole Tail Regeneration." *Nature Cell Biology* 15 (2): 222–28. https://doi.org/10.1038/ncb2659.
50. Magnani, Alessandra, Pauline Brosselin, Julien Beauté, Nathalie de Vergnes, Richard Mouy, Marianne Debré, Felipe Suarez, et al. 2014. "Inflammatory Manifestations in a Single-Center Cohort of Patients with Chronic Granulomatous Disease." *Journal of Allergy and Clinical Immunology* 134 (3): 655-662.e8. https://doi.org/10.1016/j.jaci.2014.04.014.
51. Mailloux, Ryan J. 2015. "Teaching the Fundamentals of Electron Transfer Reactions in Mitochondria and the Production and Detection of Reactive Oxygen Species." *Redox Biology* 4: 381–98. https://doi.org/10.1016/j.redox.2015.02.001.
52. Marciano, Beatriz E., Christine Spalding, Alan Fitzgerald, Daphne Mann, Thomas Brown, Sharon Osgood, Lynne Yockey, et al. 2014. "Common Severe Infections in Chronic Granulomatous Disease." *Clinical Infectious Diseases* 60 (8): 1176–83. https://doi.org/10.1093/cid/ciu1154.
53. ———. 2015. "Common Severe Infections in Chronic Granulomatous Disease." *Clinical Infectious Diseases* 60 (8): 1176–83. https://doi.org/10.1093/cid/ciu1154.
54. Martire, Baldassarre, Roberto Rondelli, Annarosa Soresina, Claudio Pignata, Teresa Broccoletti, Andrea Finocchi, Paolo Rossi, et al. 2008. "Clinical Features, Long-Term Follow-up and Outcome of a Large Cohort of Patients with Chronic Granulomatous Disease: An Italian Multicenter Study." *Clinical Immunology* 126 (2): 155–64. https://doi.org/https://doi.org/10.1016/j.clim.2007.09.008.
55. Moldovan, Leni, and Nicanor I. Moldovan. 2004. "Oxygen Free Radicals and Redox Biology of Organelles." *Histochemistry and Cell Biology* 122 (4): 395–412. https://doi.org/10.1007/s00418-004-0676-y.
56. Moreno-mateos, Miguel A, Charles E Vejnar, Jean-denis Beaudoin, Juan P Fernandez, Emily K Mis, Mustafa K Khokha, and Antonio J Giraldez. 2015. "CRISPRscan : Designing Highly Efficient SgRNAs for CRISPR-Cas9 Targeting in Vivo" 12 (10). https://doi.org/10.1038/nmeth.3543.
57. Morgenstern, David E., Mary A.C. Gifford, Ling Lin Li, Claire M. Doerschuk, and Mary C. Dinauer. 1997. "Absence of Respiratory Burst in X-Linked Chronic Granulomatous Disease Mice Leads to Abnormalities in Both Host Defense and Inflammatory Response to Aspergillus Fumigatus." *Journal of Experimental Medicine* 185 (2): 207–18. https://doi.org/10.1084/jem.185.2.207.

58. Movahedi, M, A Aghamohammadi, N Rezaei, N Shahnavaz, A Babaei Jandaghi, A Farhoudi, Z Pourpak, M Moin, M Gharagozlou, and D Mansouri. 2004. “Chronic Granulomatous Disease: A Clinical Survey of 41 Patients from the Iranian Primary Immunodeficiency Registry.” *International Archives of Allergy and Immunology* 134 (3): 253–59. https://doi.org/10.1159/000078774.
59. Nakano, Yoko, Chantal M Longo-guess, David E Bergstrom, William M Nauseef, Sherri M Jones, and Botond Bánfi. 2008. “Mutation of the CYBA Gene Encoding P22 Phox Causes Vestibular and Immune Defects in Mice.” *The Journal of Clinical Investigation* 118 (3): 1176–85. https://doi.org/10.1172/JCI33835.1176.
60. Nathan, Carl, and Aihao Ding. 2010. “SnapShot : Reactive Oxygen Intermediates (ROI),” 8–10. https://doi.org/10.1016/j.cell.2010.03.008.
61. Nguyen-Chi, Mai, Quang Tien Phan, Catherine Gonzalez, Jean-François Dubremetz, Jean-Pierre Levraud, and Georges Lutfalla. 2014. “Transient Infection of the Zebrafish Notochord with <Em>E. Coli</Em> Induces Chronic Inflammation.” *Disease Models &Amp; Mechanisms* 7 (7): 871 LP – 882. https://doi.org/10.1242/dmm.014498.
62. Oksanen, Kaisa E, Nicholas J A Halfpenny, Eleanor Sherwood, Sanna-Kaisa E Harjula, Milka M Hammarén, Maarit J Ahava, Elina T Pajula, Marika J Lahtinen, Mataleena Parikka, and Mika Rämet. 2013. “An Adult Zebrafish Model for Preclinical Tuberculosis Vaccine Development.” *Vaccine* 31 (45): 5202–9. https://doi.org/https://doi.org/10.1016/j.vaccine.2013.08.093.
63. Palha, Nuno, Florence Guivel-Benhassine, Valérie Briolat, Georges Lutfalla, Marion Sourisseau, Felix Ellett, Chieh-Huei Wang, et al. 2013. “Real-Time Whole-Body Visualization of Chikungunya Virus Infection and Host Interferon Response in Zebrafish.” *PLOS Pathogens* 9 (9): e1003619. https://doi.org/10.1371/journal.ppat.1003619.
64. Patterson, Hayley, Anni Saralahti, Mataleena Parikka, Shaynoor Dramsi, Patrick Trieu-Cuot, Claire Poyart, Samuli Rounioja, and Mika Rämet. 2012. “Adult Zebrafish Model of Bacterial Meningitis in Streptococcus Agalactiae Infection.” *Developmental and Comparative Immunology* 38 (3): 447–55. https://doi.org/10.1016/j.dci.2012.07.007.
65. Perlin, David S, Erika Shor, and Yanan Zhao. 2015. “Update on Antifungal Drug Resistance.” *Current Clinical Microbiology Reports* 2 (2): 84–95. https://doi.org/10.1007/s40588-015-0015-1.
66. Pfaller, Michael A, Shawn A Messer, Mary R Motyl, Ronald N Jones, and Mariana Castanheira. 2012. “Activity of MK-3118, a New Oral Glucan Synthase Inhibitor, Tested against Candida Spp. by Two International Methods (CLSI and EUCAST).” *Journal of Antimicrobial Chemotherapy* 68 (4): 858–63. https://doi.org/10.1093/jac/dks466.
67. Pollock, Jonathan D, David A Williams, Mary A C Gifford, Ling Lin Lp, Xunxiang Du, Jason Fisherman, Stuart H Orkin, Claire M Doerschuk, Mary C Dinauer, and James Whitcomb. 1995. “Mouse Model of X-Linked Chronic Granulomatous Disease, an Inherited Defect in Phagocyte Superoxide Production.” *Nature Genetics* 9 (february): 202–9.
68. Prajsnar, Tomasz K, Vincent T Cunliffe, Simon J Foster, and Stephen A Renshaw. 2008. “A Novel Vertebrate Model of Staphylococcus Aureus Infection Reveals Phagocyte-Dependent Resistance of Zebrafish to Non-Host Specialized Pathogens.” *Cellular Microbiology* 10 (11): 2312–25. https://doi.org/10.1111/j.1462-5822.2008.01213.x.
69. Rada, B., and T. Leto. 2008. “Oxidative Innate Immune Defenses by Nox/Duox Family NADPH Oxidases.” *Contributions to Microbiology* 15: 164–87. https://doi.org/10.1159/000136357.
70. Ren, Jason Q, William R McCarthy, Hongwei Zhang, Alan R Adolph, and Lei Li. 2002. “Behavioral Visual Responses of Wild-Type and Hypopigmented Zebrafish.” *Vision Research* 42 (3): 293–99. https://doi.org/https://doi.org/10.1016/S0042-6989(01)00284-X.
71. Roemer, Terry, and Damian J Krysan. 2014. “Antifungal Drug Development: Challenges, Unmet Clinical Needs, and New Approaches.” *Cold Spring Harbor Perspectives in Medicine* 4 (5). https://doi.org/10.1101/cshperspect.a019703.
72. Rosowski, Emily E., Nicholas Raffa, Benjamin P. Knox, Netta Golenberg, Nancy P. Keller, and Anna Huttenlocher. 2018. “Macrophages Inhibit Aspergillus Fumigatus Germination and Neutrophil-Mediated Fungal Killing.” *PLoS Pathogens* 14 (8): 1–28. https://doi.org/10.1371/journal.ppat.1007229.
73. Rosowski, Emily, Benjamin Knox, Linda Archambault, Anna Huttenlocher, Nancy Keller, Robert Wheeler, and J. Davis. 2018. “The Zebrafish as a Model Host for Invasive Fungal Infections.” *Journal of Fungi* 4 (4): 136. https://doi.org/10.3390/jof4040136.
74. Rossi, F, and M Zatti. 1964. “Biochemical Aspects of Phagocytosis in Poly-Morphonuclear Leucocytes. NADH and NADPH Oxidation by the Granules of Resting and Phagocytizing Cells.” *Experientia* 20 (1): 21–23. https://doi.org/10.1007/BF02146019.
75. Royer-pokora, Brigitte, Louis M Kunkelt, Anthony P Monacot, Sabra C Goff, Peter E Newburger, Robert L Baehner, F Sessions Cole, John T Curnutte, and Stuart H Orkin. 1986. “Disease on the Basis of Its Chromosomal Location.”
76. Saralahti, Anni, Hannaleena Piippo, Mataleena Parikka, Birgitta Henriques-Normark, Mika Rämet, and Samuli Rounioja. 2014. “Adult Zebrafish Model for Pneumococcal Pathogenesis.” *Developmental & Comparative Immunology* 42 (2): 345–53. https://doi.org/https://doi.org/10.1016/j.dci.2013.09.009.
77. SEGAL, ANTHONY W, and KAROLYN P SHATWELL. 1997. “The NADPH Oxidase of Phagocytic Leukocytesa.” *Annals of the New York Academy of Sciences* 832 (1): 215–22. https://doi.org/10.1111/j.1749-6632.1997.tb46249.x.
78. Segal, Brahm H., Paul Veys, Harry Malech, and Morton J. Cowan. 2011. “Chronic Granulomatous Disease: Lessons from a Rare Disorder.” *Biology of Blood and Marrow Transplantation* 17 (1 SUPPL): S123–31. https://doi.org/10.1016/j.bbmt.2010.09.008.
79. Segal, Brahm H.R. ROMANI. 2010. “Invasive Aspergillosis in Chronic Granulomatous Disease.” *Aspergillosis: From Diagnosis to Prevention* 47 (Supplement I): 527–43. https://doi.org/10.1007/978-90-481-2408-4_31.
80. Seman, Brittany G., Jessica L. Moore, Allison K. Scherer, Bailey A. Blair, Sony Manandhar, Joshua M. Jones, and Robert T Wheeler. 2018. “Yeast and Filaments Have Specialized, Independent Activities in a Zebrafish Model of Candida Albicans Infection.” *Infection and Immunity* 86 (10): 1–16. https://doi.org/10.1128/IAI.00415-18.
81. Siddiqui, Sophia, Victoria L Anderson, Diane M Hilligoss, Mario Abinun, Taco W Kuijpers, Henry Masur, Frank G Witebsky, et al. 2007. “Fulminant Mulch Pneumonitis: An Emergency Presentation of Chronic Granulomatous Disease.” *Clinical Infectious Diseases* 45 (6): 673–81. https://doi.org/10.1086/520985.
82. Sloan, Derek J, Martin J Dedicoat, and David G Lalloo. 2009. “Treatment of Cryptococcal Meningitis in Resource Limited Settings.” *Current Opinion in Infectious Diseases* 22 (5). https://journals.lww.com/co-infectiousdiseases/Fulltext/2009/10000/Treatment_of_cryptococcal_meningitis_in_resource.7.aspx.
83. Stasia, Marie José. 2016. “CYBA Encoding P22phox, the Cytochrome B558 Alpha Polypeptide: Gene Structure, Expression, Role and Physiopathology.” *Gene* 586 (1): 27–35. https://doi.org/10.1016/j.gene.2016.03.050.
84. Sumimoto, Hideki, Kei Miyano, and Ryu Takeya. 2005. “Molecular Composition and Regulation of the Nox Family NAD(P)H Oxidases.” *Biochemical and Biophysical Research Communications* 338 (1): 677–86. https://doi.org/https://doi.org/10.1016/j.bbrc.2005.08.210.

85. Sun, Jinqiao, Min Wen, Ying Wang, Danru Liu, Wenjing Ying, and Xiaochuan Wang. 2017. “The Three CYBA Variants (Rs4673, Rs1049254 and Rs1049255) Are Benign: New Evidence from a Patient with CGD.” *BMC Medical Genetics* 18 (1): 127. https://doi.org/10.1186/s12881-017-0492-6.
86. Sweeney, Colin L, Uimook Choi, Chengyu Liu, Sherry Koontz, Seung-kwon Ha, and Harry L Malech. 2017. “CRISPR-Mediated Knockout of Cybb in NSG Mice Establishes a Model of Chronic Granulomatous Disease for Human Stem-Cell Gene Therapy Transplants” 28 (7): 565–75. https://doi.org/10.1089/hum.2017.005.
87. Taylor, Js, Ingo Braasch, Tancred Frickey, and Axel Meyer. 2003. “Genome Duplication, a Trait Shared by 22 000 Species of Ray-FInned FIsh.” *Genome Research*, 382–90. https://doi.org/10.1101/gr.640303.1.
88. Vaart, Michiel Van Der, Herman P. Spaink, and Annemarie H. Meijer. 2012. “Pathogen Recognition and Activation of the Innate Immune Response in Zebrafish.” *Advances in Hematology* 2012. https://doi.org/10.1155/2012/159807.
89. Vallabhaneni, Snigdha, Rajal K Mody, Tiffany Walker, and Tom Chiller. 2016. “The Global Burden of Fungal Diseases.” *Infectious Disease Clinics of North America* 30 (1): 1–11. https://doi.org/https://doi.org/10.1016/j.idc.2015.10.004.
90. Veneman, Wouter J., Rubén Marín-Juez, Jan de Sonneville, Anita Ordas, Susanne Jong-Raadsen, Annemarie H. Meijer, and Herman P. Spaink. 2014. “Establishment and Optimization of a High Throughput Setup to Study Staphylococcus Epidermidis and Mycobacterium Marinum Infection as a Model for Drug Discovery.” *Journal of Visualized Experiments*, no. 88: 1–9. https://doi.org/10.3791/51649.
91. Veneman, Wouter J., Oliver W. Stockhammer, Leonie de Boer, Sebastian A.J. Zaat, Annemarie H. Meijer, and Herman P. Spaink. 2013. “A Zebrafish High Throughput Screening System Used for Staphylococcus Epidermidis Infection Marker Discovery.” *BMC Genomics* 14 (1): 1–15. https://doi.org/10.1186/1471-2164-14-255.
92. Voelz, Kerstin, Remi L Gratacap, and Robert T Wheeler. 2015. “A Zebrafish Larval Model Reveals Early Tissue-Specific Innate Immune Responses to <Em>Mucor Circinelloides</Em>” *Disease Models &Amp; Mechanisms* 8 (11): 1375 LP – 1388. https://doi.org/10.1242/dmm.019992.
93. Wang, Dantong, Xavier De Deken, Milutin Milenkovic, Yue Song, Isabelle Pirson, Jacques E Dumont, and Françoise Miot. 2005. “Identification of a Novel Partner of Duox: EFP1, A THIOREDOXIN-RELATED PROTEIN .” *Journal of Biological Chemistry* 280 (4): 3096–3103. https://doi.org/10.1074/jbc.M407709200.
94. Watanabe, Masakatsu, Motoko Iwashita, Masaru Ishii, Yoshihisa Kurachi, Atsushi Kawakami, Shigeru Kondo, and Norihiro Okada. 2006. “Spot Pattern of Leopard Danio Is Caused by Mutation in the Zebrafish Connexin41.8 Gene.” *EMBO Reports* 7 (9): 893–97. https://doi.org/10.1038/sj.embor.7400757.
95. Wiemann, Philipp, Adi Perevitsky, Fang Yun Lim, Yana Shadkchan, Benjamin P Knox, Julio A Landero Figueora, Tsokyi Choera, et al. 2017. “Aspergillus Fumigatus Copper Export Machinery and Reactive Oxygen Intermediate Defense Counter Host Copper-Mediated Oxidative Antimicrobial Offense.” *Cell Reports* 19 (5): 1008–21. https://doi.org/10.1016/j.celrep.2017.04.019.
96. Windhorst, DorothyB., Beulah Holmes, and RobertA. Good. 1967. “A NEWLY DEFINED X-LINKED TRAIT IN MAN WITH DEMONSTRATION OF THE LYON EFFECT IN CARRIER FEMALES.” *The Lancet* 289 (7493): 737–39. https://doi.org/https://doi.org/10.1016/S0140-6736(67)91360-8.
97. Winkelstein, Jerry A, Mary C Marino, Richard B Jr. Johnston, John Boyle, John Curnutte, John I Gallin, Harry L Malech, et al. 2000. “Chronic Granulomatous Disease: Report on a National Registry of 368 Patients.” *Medicine* 79 (3). https://journals.lww.com/md-journal/Fulltext/2000/05000/Chronic_Granulomatous_Disease__Report_on_a.3.aspx.
98. Wolach, Baruch, Ronit Gavrieli, Martin de Boer, Giora Gottesman, Josef Ben-Ari, Menachem Rottem, Yechiel Schlesinger, Galia Grisaru-Soen, Amos Etzioni, and Dirk Roos. 2008. “Chronic Granulomatous Disease in Israel: Clinical, Functional and Molecular Studies of 38 Patients.” *Clinical Immunology* 129 (1): 103–14. https://doi.org/https://doi.org/10.1016/j.clim.2008.06.012.
99. Wolach, Baruch, Ronit Gavrieli, Martin de Boer, Karin van Leeuwen, Sivan Berger-Achituv, Tal Stauber, Josef Ben Ari, et al. 2017. “Chronic Granulomatous Disease: Clinical, Functional, Molecular, and Genetic Studies. The Israeli Experience with 84 Patients.” *American Journal of Hematology* 92 (1): 28–36. https://doi.org/10.1002/ajh.24573.
100. Yang, Ping, Shengfeng Huang, and Anlong Xu. 2016. *The Oxidative Burst System in Amphioxus*. *Amphioxus Immunity*. China Science Publishing & Media Ltd. https://doi.org/10.1016/B978-0-12-849903-0/00008-7.
101. Yu, Lixin, Mark T Quinn, Andrew R Cross, and Mary C Dinauer. 1998. “Gp91phox Is the Heme Binding Subunit of the Superoxide-Generating NADPH Oxidase.” *Proceedings of the National Academy of Sciences* 95 (14): 7993 LP – 7998. https://doi.org/10.1073/pnas.95.14.7993.
102. Zeng, Melody Y, Irina Miralda, Cortney L Armstrong, Silvia M Uriarte, and Juhi Bagaitkar. 2019. “The Roles of NADPH Oxidase in Modulating Neutrophil Effector Responses.” *Molecular Oral Microbiology* 34 (2): 27–38. https://doi.org/10.1111/omi.12252.

Manuscript #2

Zebrafish *duox* mutations provide a model for human congenital hypothyroidism

© 2019. Published by The Company of Biologists Ltd | Biology Open (2019) 8, bio037655. doi:10.1242/bio.037655

RESEARCH ARTICLE

Zebrafish *duox* mutations provide a model for human congenital hypothyroidism

Kunal Chopra, Shoko Ishibashi and Enrique Amaya*

ABSTRACT

Thyroid dyshormonogenesis is a leading cause of congenital hypothyroidism, a highly prevalent but treatable condition. Thyroid hormone (TH) synthesis is dependent on the formation of reactive oxygen species (ROS). In humans, the primary sources for ROS production during thyroid hormone synthesis are the NADPH oxidases DUOX1 and DUOX2. Indeed, mutations in *DUOX1* and *DUOX2* have been linked with congenital hypothyroidism. Unlike humans, zebrafish has a single orthologue for *DUOX1* and *DUOX2*. In this study, we investigated the phenotypes associated with two nonsense mutant alleles, *sa9892* and *sa13017*, of the single *duox* gene in zebrafish. Both alleles gave rise to readily observable phenotypes reminiscent of congenital hypothyroidism, from the larval stages through to adulthood. By using various methods to examine external and internal phenotypes, we discovered a strong correlation between TH synthesis and *duox* function, beginning from an early larval stage, when T_4 levels are already noticeably absent in the mutants. Loss of T_4 production resulted in growth retardation, pigmentation defects, ragged fins, thyroid hyperplasia/external goiter and infertility. Remarkably, all of these defects associated with chronic congenital hypothyroidism could be rescued with T_4 treatment, even when initiated when the fish had already reached adulthood. Our work suggests that these zebrafish *duox* mutants may provide a powerful model to understand the aetiology of untreated and treated congenital hypothyroidism even in advanced stages of development.

This article has an associated First Person interview with the first author of the paper.

KEY WORDS: Congenital hypothyroidism, Growth retardation, Infertility, Thyroid

INTRODUCTION

Congenital hypothyroidism (CH) is an endocrine disorder that may result from disrupted thyroid hormone (TH) synthesis (15–20% of all cases) or impaired development of the thyroid gland [thyroid dysgenesis (TD)] (80% of all cases) (Kizys et al., 2017). CH is the most prevalent congenital endocrine disorder and is believed to be one of the most preventable causes of mental retardation (Chakera et al., 2012; Olivieri, 2015; Roberts and Ladenson, 2004). Indeed, in infants younger than 3 months of age, neurological damage progressively worsens with delay in starting treatment (Virtanen et al., 1983). Mutations in the NADPH oxidase *DUOX2* and, to a lesser extent, *DUOX1* have been associated with dyshormonogenesis in CH patients (Aycan et al., 2017; Moreno et al., 2002). DUOX1 and DUOX2 generate hydrogen peroxide (H_2O_2), which is a crucial electron acceptor during thyroid peroxidase-catalysed iodination and coupling reactions occurring while TH synthesis is underway (De Deken et al., 2000; Dupuy et al., 1999). H_2O_2 production is a limiting step in TH biosynthesis. The main source of H_2O_2 in the thyroid is DUOX2 in conjunction with its maturation factor DUOX2A, both of which are located at the apical surface of the thyroid follicular cells, thyrocytes. DUOX2-mediated H_2O_2 acts as a thyroperoxidase (TPO) co-substrate, rapidly oxidising iodine and resulting in its covalent binding to the tyrosine residues of thyroglobulin in the follicular lumen. This produces monoiodotyrosine (MIT) and diiodotyrosine (DIT), in the thyroglobulin molecule, which undergo coupling to give the THs triiodothyronine (T_3) and thyroxine (T_4) (Carvalho and Dupuy, 2013; Muzza and Fugazzola, 2017; Sugawara, 2014). A negative feedback loop is in charge of thyroid size and function. Thyrocytes secrete T_3 and T_4 and these inhibit the production of the thyroid-stimulating hormone (TSH) via the anterior pituitary thyrotropes (Dumont et al., 1992). Thyrocytes respond to limiting physiological stimuli by way of hypertrophy and proliferation. This is a direct response to compensate for diminishing THs in conditions including, but not limited to, iodine deficiency, exposure to anti-thyroid drugs and punctuated production of reactive oxygen species (ROS). It has been shown that early initiation of TH treatment (within 3 weeks post-partum) leads to normal IQ and physical growth and correlates with excellent prognoses (Aronson et al., 1990; Clause, 2013; Rahmani et al., 2016; Rovet et al., 1987). Expectedly then, if treatment is delayed beyond 4 weeks, individuals become increasingly prone to mental retardation and incomplete physical growth (Gilbert et al., 2012; Zimmermann, 2011). To date, various approaches have been adopted to induce hypothyroidism in animal models, including surgical removal of the thyroid gland, thyroid gland removal via radioactive iodine isotope (^{131}I), dietary restriction of iodine, and goitrogen administration (Argumedo et al., 2012). We present here a zebrafish model of CH, which exhibits several phenotypes associated with CH in humans, including growth retardation. Interestingly, while CH zebrafish display growth retardation initially, they are able to reach normal size eventually without the need for pharmacological intervention. The additional external and internal phenotypes associated with hypothyroidism are restored upon treatment with T_4, including restoration of reproductive function, even when treatment is applied during adulthood.

RESULTS

Molecular characterisation of *duox* mutant alleles

Duox is a member of the NADPH oxidase (NOX) family of enzymes. Seven NOX family members are present in the human

Division of Cell Matrix Biology & Regenerative Medicine, School of Biological Sciences, Faculty of Biology, Medicine and Health, University of Manchester, Manchester M13 9PT, UK.

*Author for correspondence (enrique.amaya@manchester.ac.uk)

E.A., 0000-0002-1805-8548

Received 9 August 2018; Accepted 17 January 2019

Biology Open (2019) 8, bio037655. doi:10.1242/bio.037655

genome: NOX1, NOX2, NOX3, NOX4, NOX5, DUOX1 and DUOX2, and their primary function is to produce reactive oxygen species (ROS). All NOX enzymes are transmembrane proteins, exhibiting structural and functional conservation. They participate in electron transport across biological membranes, effecting the reduction of molecular oxygen to superoxide (Bedard and Krause, 2007). All NOX enzymes share conserved structural domains, including intracellular C-terminal tails containing NADPH and FAD binding sites and six transmembrane domains anchoring four highly conserved heme-binding histidines. DUOXes have an additional transmembrane domain, an extracellular N-terminal domain with peroxidase homology and two EF Ca^{2+} binding hands within their first intracellular loop (Fig. 1A) (Rada and Leto, 2008). The zebrafish genome encodes a single *duox* gene, rather than two *DUOX* paralogues present in humans (*DUOX1* and *DUOX2*) and lacks a *NOX3* orthologue (Kawahara et al., 2007). In zebrafish *duox* is located on chromosome 25 and encodes a 1528 amino acid protein. In order to investigate the function of *duox* in zebrafish, we obtained two nonsense mutation alleles, which arose from a large-scale ENU mutagenesis screen (Kettleborough et al., 2013). One allele, *duox sa9892*, contains a nonsense mutation in exon 21, resulting in a C>T change (Fig. 1B) and a premature stop codon (TAG) after the 944th amino acid; the second allele, *duox sa13017*, contains a nonsense mutation in exon 23, resulting in a C>T change (Fig. 1C) creating a premature stop codon (TGA) after the 997th amino acid. Since both these premature codons result in truncations of the Duox protein, including the loss of the two critical C-terminal NADPH and FAD binding sites, they would be expected to be loss-of-function mutations. Genotyping of these alleles can be performed via genomic PCR followed by sequencing of these regions (Fig. 1B,C).

duox mutants are growth retarded

We in-crossed *duox sa9892*$^{+/-}$ and *duox sa13017*$^{+/-}$ sibling adults and inter-crossed *duox sa9892*$^{+/-}$ with *duox sa13017*$^{+/-}$ adults to produce a range of wild-type (WT), heterozygous, homozygous mutant and compound heterozygous mutant animals containing both alleles. While the WT, *duox sa9892*$^{+/-}$ and *duox sa13017*$^{+/-}$ animals were phenotypically indistinguishable, the homozygous mutants of both alleles, and the compound mutants (i.e. *duox sa9892/sa13017)* displayed a number of phenotypes that were distinct from those seen in the WT and heterozygous siblings. The first overtly apparent phenotype exhibited by the *duox sa9892*$^{-/-}$, the *duox sa13017*$^{-/-}$ and the trans-heterozygous *duox sa9892/sa13017* mutants was that they were growth retarded. At 3 months of age, the *sa9892*$^{-/-}$, *sa13017*$^{-/-}$ and *sa9892/sa13017* mutant fish were significantly shorter in terms of body length than their WT and heterozygous siblings (Fig. 2A–G). At 6 months of age, the *duox sa9892*$^{-/-}$ and *sa9892/sa13017* mutant animals caught up in size with their WT and heterozygous siblings. However, the *duox sa13017*$^{-/-}$ animals still remained stunted (Fig. 2H). Another phenotype suggestive of slowed growth was apparent in the growth and organogenesis of the swim bladder. The swim bladder is a hydrostatic organ, which becomes bi-lobed by 21 dpf (Winata et al., 2009). We found that the swim bladder in the *duox sa9892*$^{-/-}$ animals remained unilobed even at 54 dpf (n=9) (Fig. 2I,J). Homozygous *duox* mutants also exhibit a delay or absence of development of barbels, which are a set of anterior sensory appendages. Zebrafish develop a short pair of nasal barbels and a long trailing pair of maxillary barbels (Fig. 2K,N). These are normally visible by 1 month post-fertilisation and sustained throughout life (LeClair and Topczewski, 2010). In all cases, homozygous *duox* mutants lacked barbels at 3 months of age (Fig. 2L,O,P). However, between 6 and 10 months of age, maxillary barbels were seen in some older *duox sa9892*$^{-/-}$ (five out of 11; see Fig. 2M) and *sa9892/sa13017* (two out of 11) animals, but in none of the *sa13017*$^{-/-}$ animals (zero out of nine).

duox mutants have dark pigmentation, erythema and ragged fins

Zebrafish are recognisable by their eponymous pattern of five dark blue stripes alternating with four lighter yellow inter-stripes, covering the lateral flanks, and anal and caudal fins (Singh and Nüsslein-Volhard, 2015). The stripes are comprised of black melanophores with a few iridescent iridophores, while the inter-stripes are comprised of yellow and orange xanthophores and numerous iridophores (Hirata et al., 2003). We found that the homozygous *duox* mutants were darker than their WT and heterozygote siblings (Fig. 3A–C). The darker pigmentation was associated with the presence of approximately twice the number of melanophores in the homozygous *duox* mutants, relative to their heterozygous and WT siblings (Fig. 3D). Conveniently, we also found that the difference in pigmentation was sufficient to allow for phenotypic identification of homozygous *duox* mutants from their heterozygous and WT siblings, with 100% accuracy, as confirmed retrospectively via genotyping. In addition, homozygous *duox* mutants also showed stripe irregularities not seen in WT and heterozygous siblings, such as wavy stripes and stripe discontinuities (Fig. 3E,F). Thus, pigmentation differences can be used as a reliable identification method for distinguishing homozygous *duox* mutants from their heterozygous and WT siblings, as early as 60 dpf.

Less apparent but nevertheless significant were craniofacial anomalies among adult mutants. In particular, we found a significant shortening of the frontal height among the *duox sa9892*$^{-/-}$, *sa13017*$^{-/-}$ and *sa9892/sa13017* animals, when compared to their WT and heterozygous siblings (Fig. 3G–I). Adding further to the list of phenotypes, we noticed erythema (redness) in the opercular region of mutants (Fig. 3J–O). This was especially prominent in background strains that lack melanophores, such as *nacre* and *casper*. The redness was most apparent in juvenile fish.

Finally, the homozygous *duox* mutants often displayed misshapen or damaged fins (Fig. 3P–U). We found that the *duox sa9892*$^{-/-}$ (15 out of 15), *sa13017*$^{-/-}$ (seven out of seven) and *sa9892/sa13017* (19 out of 23) animals displayed damaged fins. In many cases this was manifested as vertical (dorsal and anal fin) or horizontal (caudal fin) tears in the fins. In other cases, there were spontaneous losses of portions of fins or ragged fin margins (Fig. 3S–U). Damaged fins were noticeable as early as 42 dpf.

Homozygous *duox* mutants are viable but are unable to breed

While we found that *duox sa9892*$^{-/-}$ and *sa13017*$^{-/-}$ mutants reached adulthood, unlike their heterozygous and WT siblings, they were unable to breed. Females, although gravid, were found not to lay eggs regardless of pairing with mutant, heterozygous or WT males. Similarly, mutant males failed to cross with females, regardless of genotype. Furthermore, we noticed that homozygous *duox* mutant females seemed egg-bound, suggesting that they were unable to lay eggs (Fig. 4A,B; left panels). We confirmed that females do contain eggs internally via histological sectioning (Fig. 4A,B; right panels) as well as via abdominal squeezing to release eggs. Similarly, compound heterozygotes of the two alleles were found to be viable but failed to breed, and the females also became egg bound.

Biology Open (2019) 8, bio037655. doi:10.1242/bio.037655

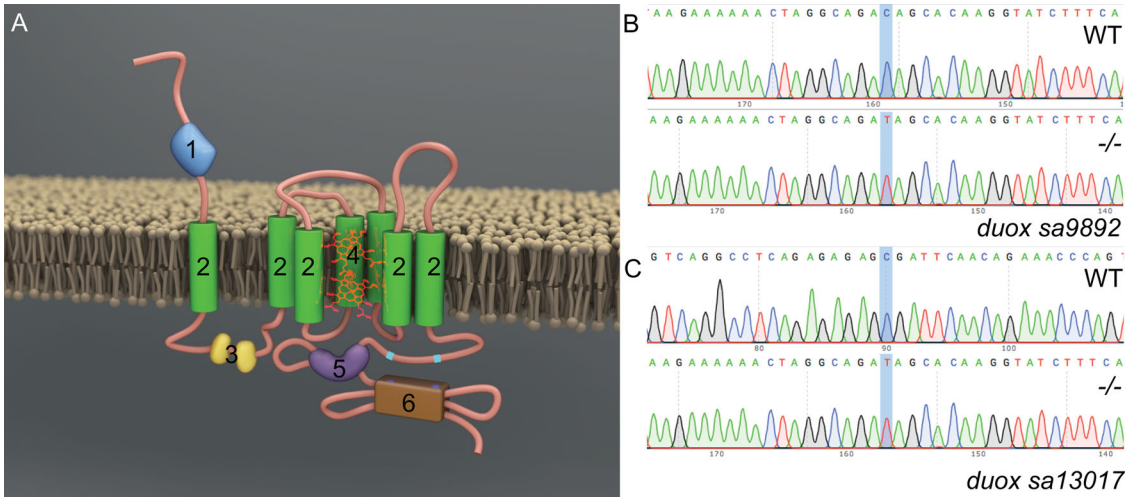

Fig. 1. Molecular characterisation of *duox* mutant alleles. Duox is a transmembrane protein belonging to the NADPH oxidase family of enzymes. Duox (A) consists of seven transmembrane domains (2), two EF hands (3), heme (4), FAD domain (5), an NADPH oxidase domain (6) at the C-terminus as well as a peroxidase homology domain (1), thus named Dual oxidase. Characterisation of *duox sa9892* (B) and *duox sa13017* (C), via Sanger sequencing, shows the single nucleotide change C>T in contrast to a WT reference sequence.

Homozygous *duox* mutants develop goitres

In addition to the phenotypes described above, we noted that some of the homozygous *duox* mutant adult animals displayed external goitre-like growths in the submandibular area (Fig. 5A,B). These external goitre-like growths were observed among adults older than 3 months of age, across all three mutant combinations – *duox sa9892*$^{-/-}$ (11 out of 18), *sa13017*$^{-/-}$ (six out of 11) and *sa9892/sa13017* (three out of 22). These richly vascularised growths were variously sized. Additionally, some of the animals also exhibited lateral flaring of opercular flaps (Fig. 5C). To confirm whether these goitre-like growths were indeed enlarged thyroids, we fixed and sectioned a subset of *sa9892*$^{-/-}$ and *sa9892/sa13017 duox* mutants, along with some of their WT and heterozygous mutant siblings, and performed *in situ* hybridization (ISH) analysis for the expression of *thyroglobulin*, a thyroid marker. The results confirmed that these growths were indeed of thyroid origin (Fig. 5D–L). Also, the thyroid hyperplasia was in striking contrast to the size of the thyroids in the WT and heterozygous siblings, where the extent of *thyroglobulin* staining was much smaller and more distinct, presenting as discreet rings confined to the ventral mid-pharyngeal region (Fig. 5E,F). Importantly, all mutants had internal thyroid hyperplasias, regardless of the presence or absence of external goiters (Fig. 5G–L).

duox mutants are in a state of hypothyroidism

The goitre-like growths, as well as the other phenotypes observed in the homozygous *duox* mutants suggested that the mutants might be exhibiting hypothyroidism. To test whether this might be the case, we assessed the presence of thyroxine (T_4) in the homozygous *duox* mutants and in their heterozygous and WT siblings via wholemount immunostaining. We found that, while the WT and heterozygous siblings exhibited robust T_4 staining (Fig. 6A–C), *duox sa9892*$^{-/-}$ and *sa13017*$^{-/-}$ larvae had no detectable T_4 staining in their thyroids (Fig. 6D,E). Consistent with the loss of T_4 being due to lack of NADPH oxidase activity in the homozygous *duox* mutants, we were able to phenocopy the loss of T_4 staining in the larvae by treating them with the NADPH oxidase inhibitor, diphenyleneiodonium (DPI) (Fig. 6F).

duox-mediated hypothyroidism is responsive to T_4 treatment

Among humans, CH responds very well to T_4 treatment, especially when treatment is initiated as soon as hypothyroidism is suspected (Rahmani et al., 2016). Here, we decided to ask whether supplementation of the aquarium water with T_4 could reverse some or all of the phenotypes observed in the homozygous *duox* mutants. We initiated T_4 (30 nM) treatment of the *duox sa9892*$^{-/-}$ and *sa9892*$^{+/-}$ animals starting at 11 months of age, when all of the phenotypes described previously were already apparent. We found that most of the phenotypes associated with loss of *duox* function could be reversed by treatment with T_4. Body pigmentation was the first phenotype to be reversed in the treated animals, such that by 2 weeks after the initiation of treatment the *duox sa9892*$^{-/-}$ animals became visibly paler than their untreated *duox sa9892*$^{-/-}$ siblings (Fig. 7A versus 7B). The difference in pigmentation was associated with a significant decrease in melanophore density in T_4-treated homozygous mutant animals when compared to the untreated homozygous mutant animals (Fig. 7C–G). Indeed, the density of melanophores in the treated mutants was similar to that seen in untreated or treated heterozygous mutant animals, suggesting a complete rescue (Fig. 7C–G). In addition, we found that fin quality improved markedly, with treated mutants showing fuller, unbroken fins compared to the ragged fins of the untreated controls (compare Fig. 7A and B). Furthermore, after 8 weeks of T_4 treatment we were able to rescue breeding behaviour in both sexes. Mutant males and females were able to spawn with WT animals or with each other. These mating episodes resulted in the production of four clutches of eggs in four consecutive weeks. Rescue of fertility was perhaps the most striking outcome of T_4 treatment.

Having observed a rescue of most of the phenotypes associated with the homozygous *duox* mutants, we wondered whether T_4 treatment also diminished the size of the thyroid gland in the *duox* mutants. Anecdotally, we had noted that one of the homozygous *duox sa9892*$^{-/-}$ mutant animals in the treated group had a small external goitre before treatment, but the goitre resorbed after 2 weeks of treatment. In comparison, a homozygous mutant sibling in the untreated group, that also had an external goitre, showed an increase in the size of the goitre during the course of the experiment (data not shown). This suggested that T_4 treatment might lead to a diminution in the size of the thyroid glands in the homozygous mutant animals. To confirm whether this was the case, we sectioned and performed ISH for *thyroglobulin* on some of the treated and untreated homozygous mutant animals. We found that treatment led

Biology Open (2019) 8, bio037655. doi:10.1242/bio.037655

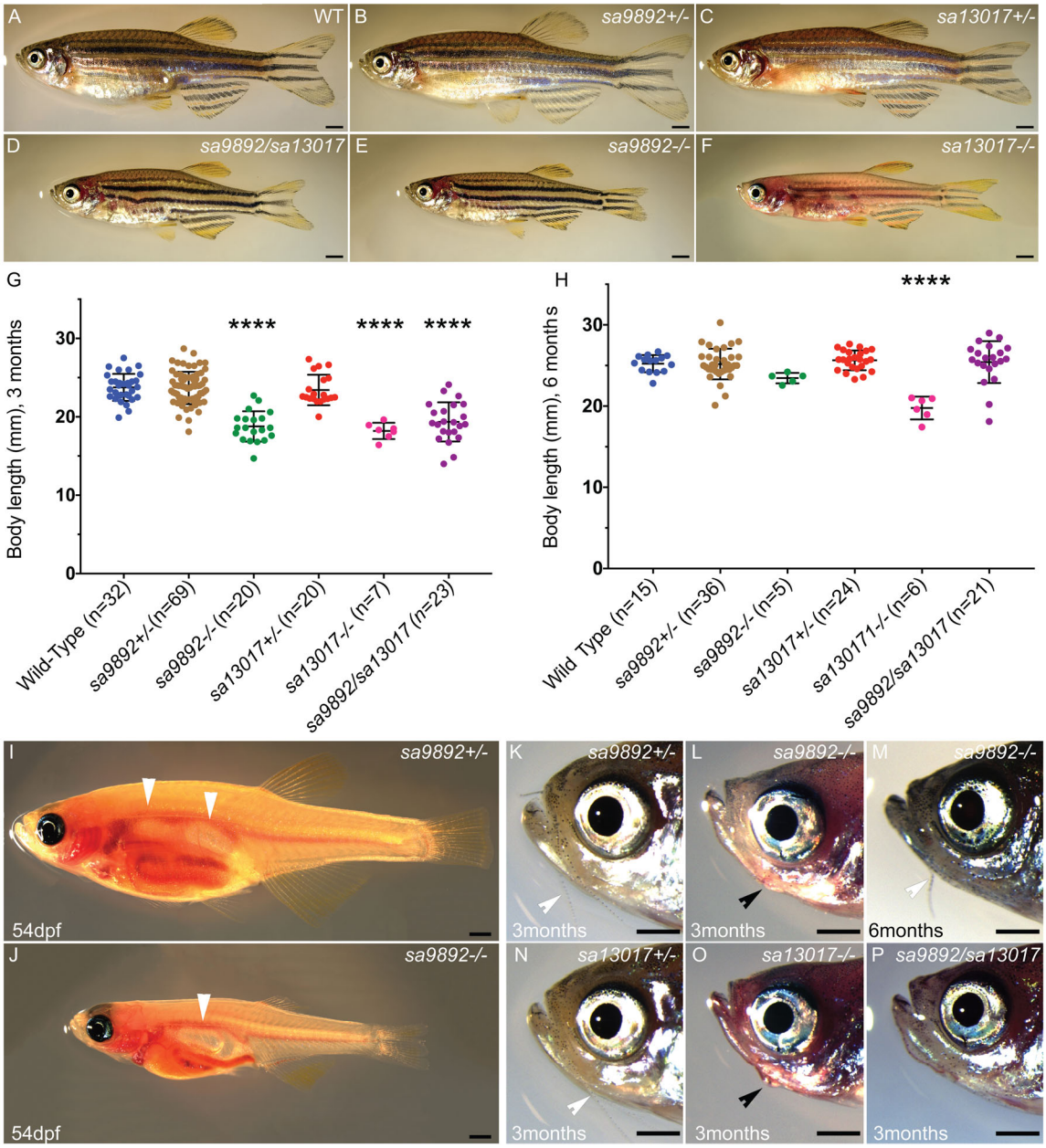

Fig. 2. *duox* mutants exhibit growth retardation. Mutants for both alleles as well as compound heterozygotes are shorter than their WT and heterozygous siblings at 3 months (A–G) but catch up by 6 months (H). *sa13017*$^{-/-}$ animals are trailing behind even at 6 months (H). Asterisks in G denote statistically significant differences (Bonferroni's multiple comparisons test, ****P<0.0001) *duox* mutants also have a delay in the inflation of the anterior lobe of the swim bladder (I,J) (white arrowheads indicate lobes). Adults at 3 months old also lack barbels (L–P), which are observed in heterozygous siblings (white arrowheads; K,N). Barbels emerge in some older animals (6 months and older) (white arrowhead, M). External goitres are often visible in young adults (black arrowheads; L,O). Scale bars: 1 mm.

to a dramatic decrease in the thyroid hyperplasia normally associated with the *duox* homozygous mutants. However, some of the treated animals did retain some small areas of ectopic *thyroglobulin* staining in the head not seen in WT animals, suggesting that these animals had extensive ectopic thyroid follicular tissue prior to treatment (Fig. 7H–J).

Methimazole phenocopies *duox* mutant phenotypes

For final confirmation that the phenotypes found in the homozygous *duox* mutants were due to hypothyroidism, we asked whether exposure of WT fish to the goitrogen methimazole (1 mM) phenocopied the homozygous mutant phenotypes. To counter the influence of already circulating THs, we exposed the adult fish over a 3-month period. Treated animals became darker, owing to an increase in the number of melanophores (Fig. 8A–C). In addition, adult fish treated with methimazole failed to breed, as observed among homozygous *duox* mutant animals. They also developed external goitres (three out of seven) (Fig. 8F) and, internally, their thyroid follicles spread dramatically in area (Fig. 8G,H). This was reminiscent of the observations made in homozygous *duox* mutants (Fig. 8I). Finally, WT larval zebrafish continuously treated with methimazole from between 3 hpf and 5 hpf onwards showed resistance to follicular T_4 immunostaining, similar to that found in *duox sa9892*$^{-/-}$ and *duox sa13017*$^{-/-}$ mutant larvae (Fig. 8D,E).

Biology Open (2019) 8, bio037655. doi:10.1242/bio.037655

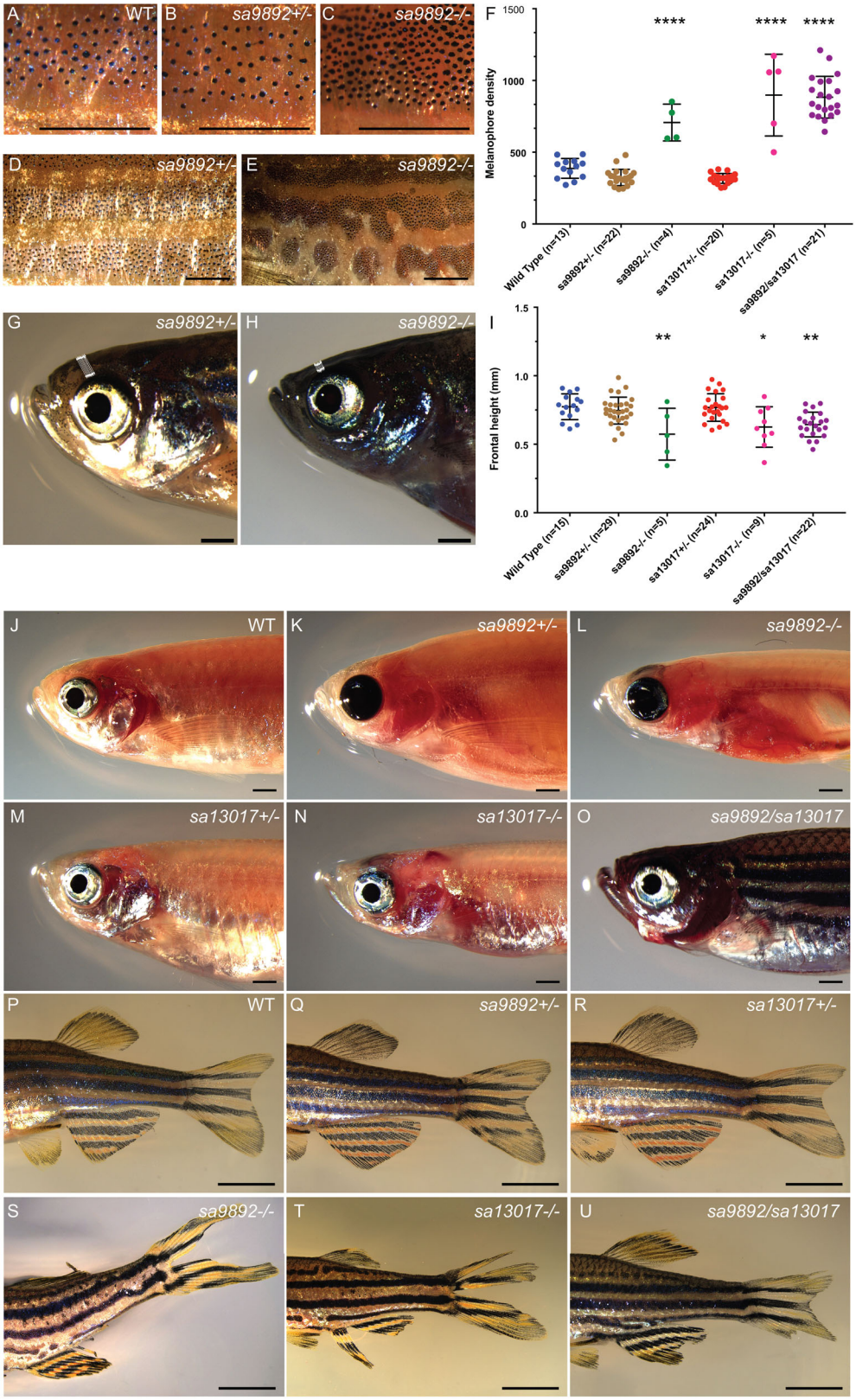

Fig. 3. Adult *duox* mutant zebrafish display an array of visible phenotypes. (A–C) 5× magnification of flank region showing the distribution of melanophores in WT, *sa9892*$^{+/-}$ and *sa989*$^{-/-}$ siblings. The apparent abundance of melanophores was statistically significant in *duox* mutants (D). Asterisks denote statistically significant differences (Bonferroni's multiple comparisons test, ****P<0.0001). *duox* mutants also showed irregularities in stripe pattern in contrast to heterozygous siblings, shown here in a 2× magnification of the flank in *sa9892* siblings (E,F). Craniofacial anomalies were evident among mutants, with frontal height significantly shorter among mutants (G–I) (Bonferroni's multiple comparisons test, *P<0.5, **P<0.01). Erythema in the thoracic region was prominent among mutants. This was especially noticeable in *nacre* backgrounds (L,N,O). *duox* mutants also suffered from perpetual fin damage, which manifest as ragged margins and tears (S–U). Scale bars: 1 mm.

Biology Open

Biology Open (2019) 8, bio037655. doi:10.1242/bio.037655

DISCUSSION

The zebrafish has recently emerged as a new, genetically tractable model for investigating the molecular mechanisms underpinning thyroid organogenesis and function (Alt et al., 2006; Elsalini and Rohr, 2003; Guillot et al., 2016; McMenamin et al., 2014; Trubiroha et al., 2018; Wendl et al., 2002). Although a recent report described the larval phenotype associated with CRISPR generated bi-allelic loss-of-function *duox* mutations in F0 zebrafish (Trubiroha et al., 2018), there have been no prior reports describing the phenotypic consequences of fully characterised *duox* alleles in adult zebrafish. This is despite the fact that mutations in *DUOX2* and *DUOX1* have been shown to be associated with congenital hypothyroidism in humans for more than a decade (Aycan et al., 2017; Donkó et al., 2014; Jin et al., 2014; Johnson et al., 2007; Kizys et al., 2017; Tonacchera et al., 2009; Vigone et al., 2005). Here, we describe a comprehensive assessment of the adult phenotypes associated with homozygosity of two loss-of-function alleles of zebrafish *duox* in adult fish. The additional round of genome duplication in teleost fish (Taylor et al., 2003) notwithstanding, there only exists a single orthologue of *duox* in zebrafish, instead of the two orthologues present in tetrapods (*DUOX1* and *DUOX2*) (Kawahara et al., 2007). Remarkably then, in this instance, zebrafish has less genetic redundancy for this gene than is commonly found in this system. Thus, assessing phenotypes associated with homozygosity of the single *duox* orthologue in zebrafish has allowed us to model the effect of losing the function of both *duox* orthologues in tetrapods. This is particularly important as mutations in both *DUOX1* and *DUOX2* in humans have been associated with a more severe form of CH (Aycan et al., 2017), suggesting that *DUOX1*, while normally playing a minor role in TH synthesis in humans, does partially compensate for the loss of *DUOX2* in humans.

Amongst the various adult phenotypes displayed by the homozygous *duox* mutants, most have been previously observed following pharmacological disruptions in thyroid hormone synthesis or in mutant strains where the hypothalamic–pituitary–thyroid (HPT) axis in zebrafish is affected. For example, goitrogen treatments, thyroid ablation and *tshr* mutant strains display alterations in pigmentation (McMenamin et al., 2014), similar to those we found in homozygous *duox* mutants. More specifically, thyroid ablated zebrafish have a darker striped pattern due to an increase in the density of melanophores within each stripe (McMenamin et al., 2014), akin to our homozygous *duox* mutants. Another notable phenotype in our homozygous mutants reminiscent of prior findings in goitrogen-treated zebrafish was erythema in the proximity of the operculum. Schmidt and Braunbeck (2011) came across a striking histopathological phenotype following treatment of WT zebrafish with the goitrogen, phenylthiouracil (PTU) (Elsalini and Rohr, 2003), wherein treatment resulted in excessive proliferation of blood vessels surrounding the thyroid follicles. This proliferation is attributed to hyperemia resulting from blood aggregation in proximally swollen blood vessels surrounding the thyroid follicles and is concentration-dependent, with the highest concentrations leading to hyperemia (Schmidt and Braunbeck, 2011). Macroscopically, this proliferation of vasculature manifests as erythema, giving a red colour to the entire opercular region. While we did not perform a histological examination of the vasculature, our macroscopic observations are consistent with these reported findings, with all our mutants displaying this conspicuous redness of the opercular region. The colouration was most notable amongst younger animals and especially apparent in backgrounds lacking melanophores. Space constraints together with follicular expansion and vascular proliferation in the pharyngeal region could also explain for the flaring opercula observed in some mutants, although this could also be due to thyroid hyperplasia, which was also noted by Schmidt and Braunbeck (2011) in their PTU-treated fish.

We were also able to induce this chronic hypothyroid/goitrogenic state in WT animals following treatment with methimazole, resulting in similar phenotypic outcomes. In our reverse experiment, however,

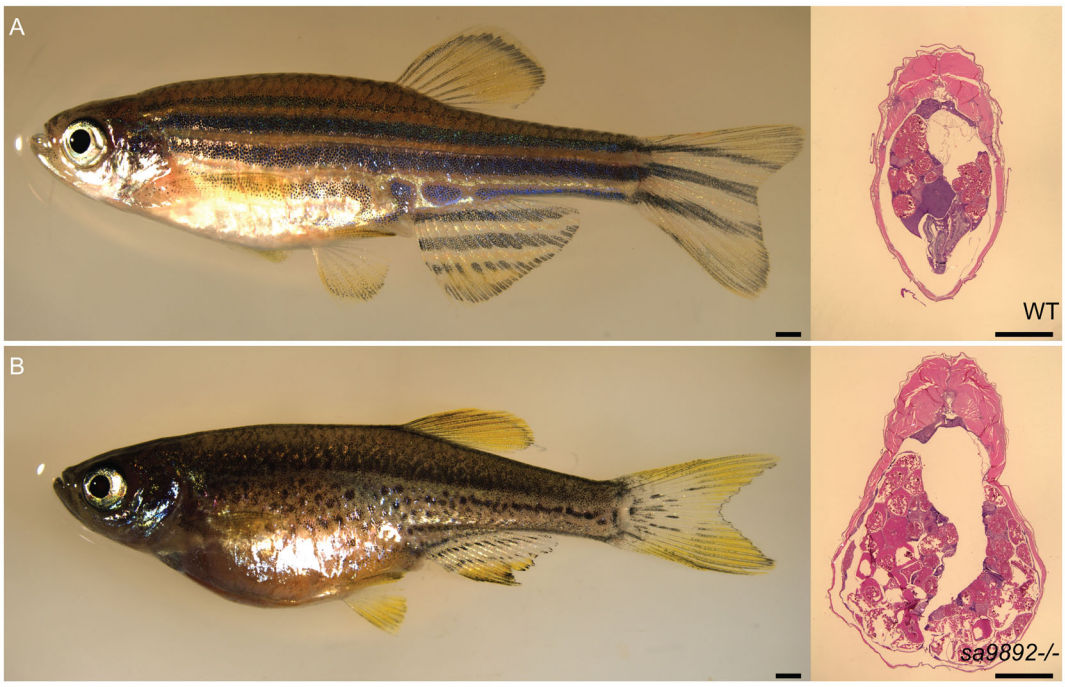

Fig. 4. *duox* mutant females are unable to ovulate and become egg bound. H&E staining of abdominal sections reveals oocytes (A,B). Scale bars: 1 mm.

Biology Open (2019) 8, bio037655. doi:10.1242/bio.037655

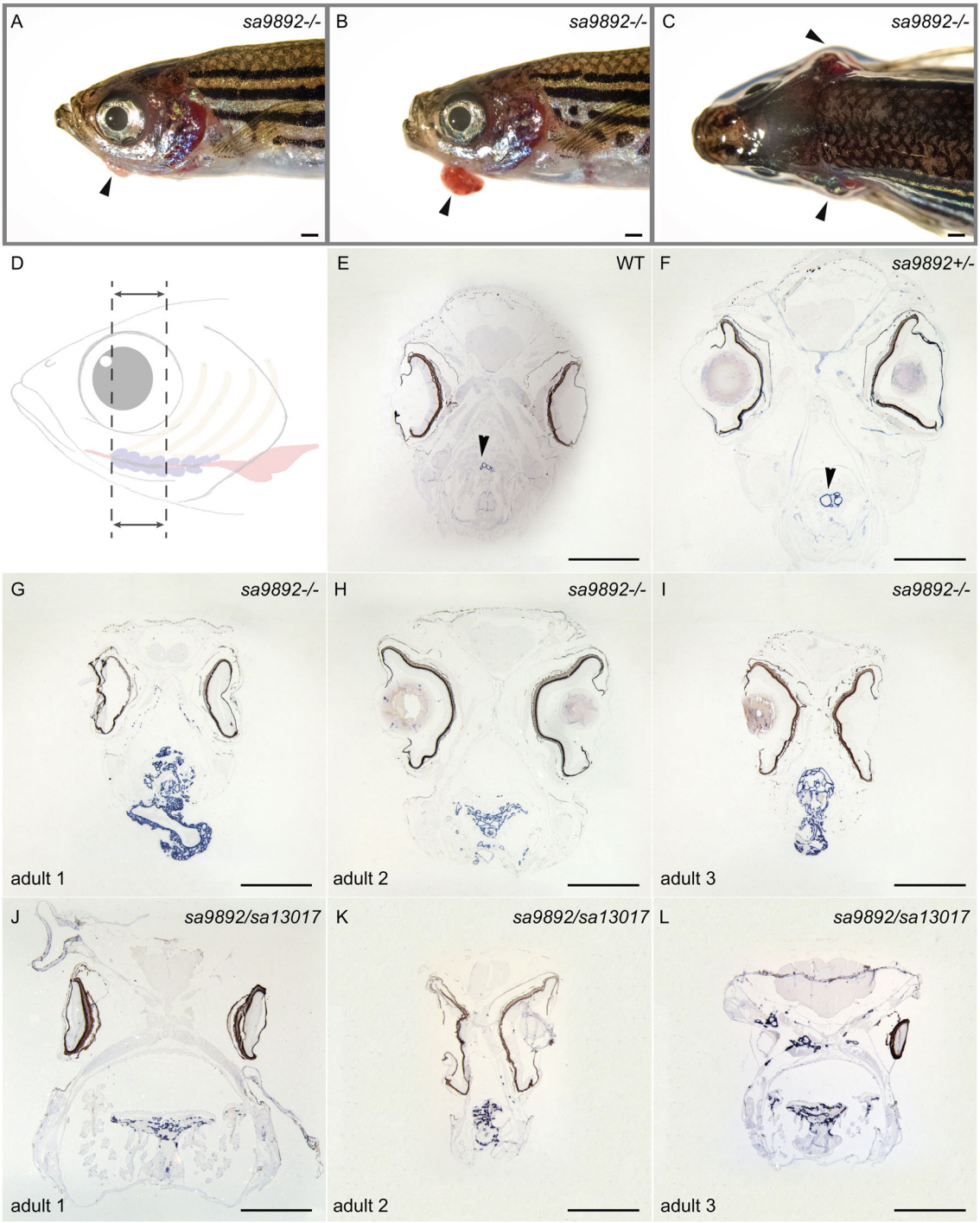

Fig. 5. Homozygous *duox* mutations lead to goitre. Adult mutant animals exhibit an array of variably sized external goitres (arrowheads; A,B), as well as lateral flaring of opercula (arrowheads; C). When sectioned along the length of the follicular region (dotted area, D) and subjected to ISH for *thyroglobulin*, mutants reveal extensive spread of and ectopic thyroid follicular tissue (G–L), in contrast to the localised, discreet distribution in WT and heterozygous siblings (arrowheads; E,F). Scale bars: 1 mm.

it was very interesting to note that while T_4 treatment of mutants resolved the goitres, some follicular staining remained in ectopic regions. Even so, the overall amount of thyroid tissue was largely diminished. It has been reported that at concentrations ≥25 mg/l of PTU, follicular encroachment is found in the gills of zebrafish, suggesting ectopic follicular expansion (Schmidt and Braunbeck, 2011). Follicular expansion following exposure to methimazole is attributed to thyroid hyperplasia, both, in zebrafish (Schmidt and Braunbeck, 2011) and in frog tadpoles (Hsü et al., 1974). This is regarded to be the first step in compensating for TH production via TSH (Schmidt and Braunbeck, 2011). Concentration dependent increases in the extent of follicular hypertrophy and hyperplasia have also been reported in the fathead minnow (*Pimephales promelas*), when exposed to the thyroid peroxidase inhibitor 2-mercaptobenzothiazole (Nelson et al., 2016). *duox* mutants and methimazole-treated WTs presented with amplified *thyroglobulin*

Biology Open (2019) 8, bio037655. doi:10.1242/bio.037655

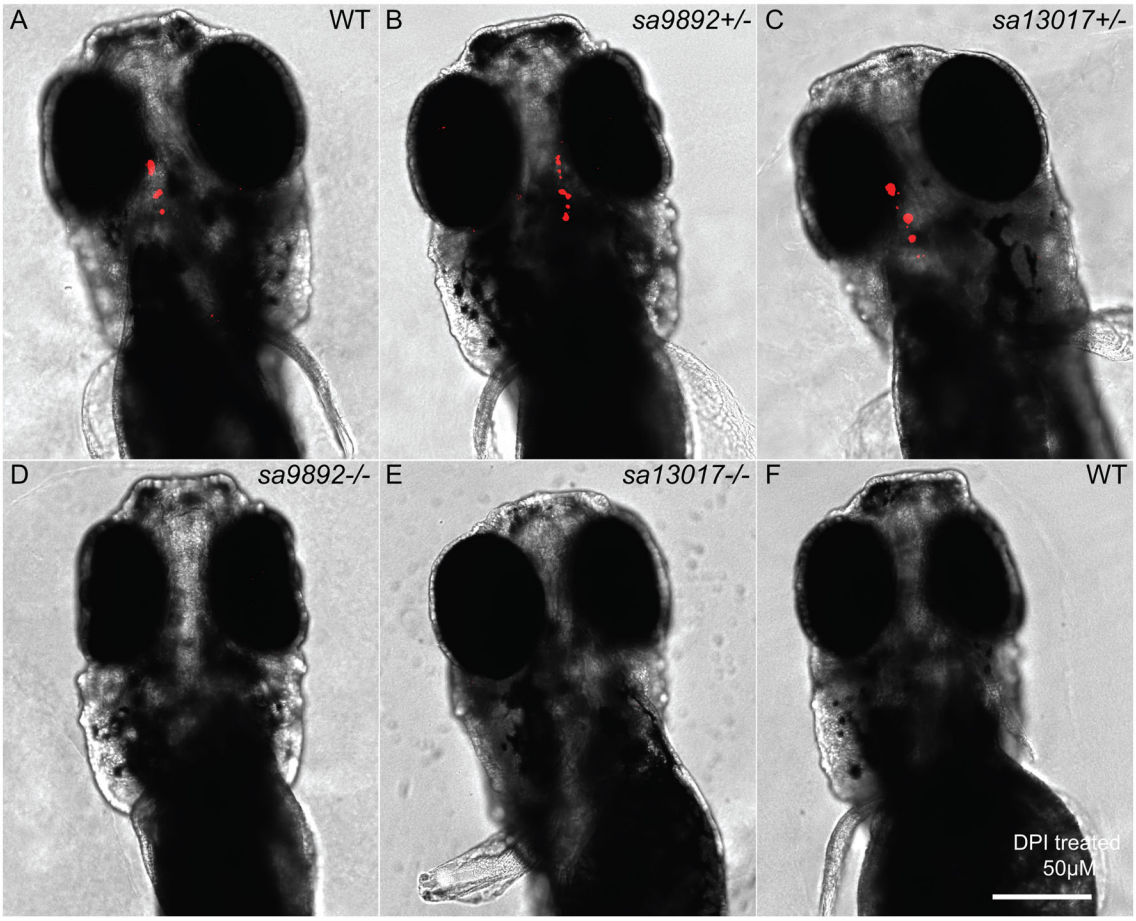

Fig. 6. Hypothyroidism is evident among *duox* mutants. At 5 dpf, homozygous mutant larvae lack staining for bound T_4 in the thyroid follicles, based on wholemount fluorescent immunohistochemistry (D,E). This is in sharp contrast to the robust staining observed in WT and heterozygous siblings (A–C). The NADPH oxidase inhibitor DPI successfully phenocopies *duox* mutations in WT larvae, resulting in an absence of T_4 detection (F). Scale bar: 50 µm.

expression that showed follicular crowding in the pharyngeal regions and invasion in other ectopic locations. Thyroid dyshormonogeneis (TD) is among the leading causes of CH, and ectopia (ectopic thyroid) is the commonest subtype of TD (De Felice and Di Lauro, 2004). Ectopic thyroid glands have recently been reported in human *DUOX2* mutations wherein scintigraphy revealed submandibular and sublingual thyroid ectopic locations (Kizys et al., 2017).

Teleost fins have garnered interest within the scientific community not only due to their extensive morphological diversity, but also due to their remarkable regenerative capacities (Johnson and Bennett, 1999; Nakatani et al., 2007). Fins are composed of multiple branched and multi-segmented rays covered in a thin layer of epidermal cells. Individual rays consist of a pair of hemirays. Mature hemirays, known as lepidotrichia, are surrounded by a monolayer of osteoblasts that synthesise the bone matrix. With no musculature present, the remainder is made up of mesenchymal cells with nerve fibres and vasculature running along and inside the fin rays. Because of the constant growth, renewal and maintenance of the fins, it is relatively uncommon to find animals in aquaria with damaged fins (Wills et al., 2008). Thus, the ragged fins in the *duox* mutants stand out. We have found that the presence of ragged fins is ameliorated, however, by treatment of the mutants with T_4. Our observations are in line with those in the medaka (*Oryzias latipes*) hypothyroidism mutant, $kmi^{-/-}$, which also frequently exhibit damaged or ragged fins (Sekimizu et al., 2007). Furthermore, $kmi^{-/-}$ animals have also been reported to show delayed regeneration, which can be rescued via exogenous T_4.

CH has been associated with cephalic and facial defects and developmental neurological abnormalities (Gamborino et al., 2001). Such defects have been attributed to improper development of the cranial neural crest (CNC), which is a transient population of migratory embryonic stem cells. Arising from the neural ectoderm, these cells contribute to a long list of cell types, including bone, cartilage, craniofacial connective tissue, corneal stroma and endothelium, iris stroma, ciliary body stroma and muscles, sclera and the trabecular meshwork of the eye (Barembaum and Bronner-Fraser, 2005; Minoux and Rijli, 2010). An investigation of craniofacial morphogenesis using rats exposed to methimazole revealed a 25% reduction in the overall head size throughout gestation (Gamborino et al., 2001). These findings are consistent with observations on craniofacial shape in zebrafish $manet^{wp.r23e1}$ mutants as well as metronidazole-mediated thyroid ablated transgenics $Tg(tg{:}nVenus\text{-}2a\text{-}nfnB)^{wp.rt8}$, which have narrower heads than controls (McMenamin et al., 2014). Further evidence on the role of THs has been gathered using pharmacological and morpholino-based approaches in zebrafish larvae. In one study, methimazole treatment resulted in reduced head depth and shorter jaw length (Liu and Chan, 2002). In another study, methimazole and PTU were found to inhibit pharyngeal arches and ceratohyal cartilage development, while knockdown of *thraa* (thyroid receptor α a) led to malformations in the Meckel's

Biology Open (2019) 8, bio037655. doi:10.1242/bio.037655

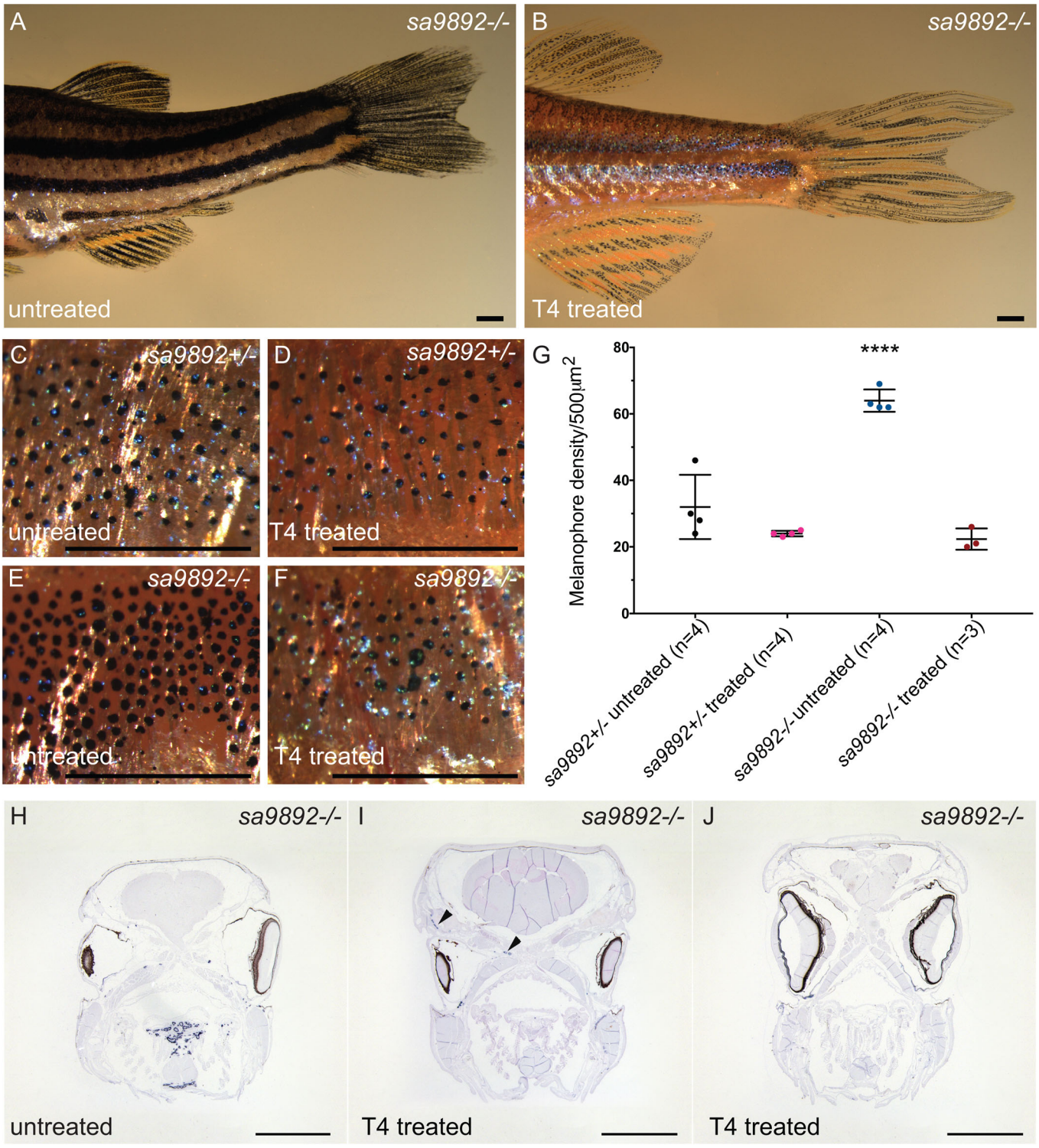

Fig. 7. T_4 treatment alleviates phenotypic anomalies in *duox* mutants. T_4-treated mutants show an improvement in fin health, compared to untreated mutants (A,B). Pigment changes are evident among T_4-treated mutants. C–F show a 5× magnification of the distribution of melanophores on the flank region of *sa9892*$^{+/-}$ and *sa989*$^{-/-}$ siblings, with a significant reduction in melanophore number (G). Asterisks denote statistically significant differences (Bonferroni's multiple comparisons test, ****P<0.0001). Goitres resolve following T_4 administration, but small ectopic thyroids are still evident (black arrowheads) (I,J). Scale bars: 1 mm.

and ceratohyal cartilages (Bohnsack and Kahana, 2013). Our observations of the shorter frontal height among *duox sa9892*$^{-/-}$, *sa13017*$^{-/-}$ and *sa9892/sa13017* animals are yet another indicator of TH deficiency.

Furthermore, *duox* mutants appear to experience several phenotypes associated with retarded growth and development. These include delayed growth rate, and delayed or incomplete swim bladder morphogenesis and barbel emergence. As development is

Biology Open (2019) 8, bio037655. doi:10.1242/bio.037655

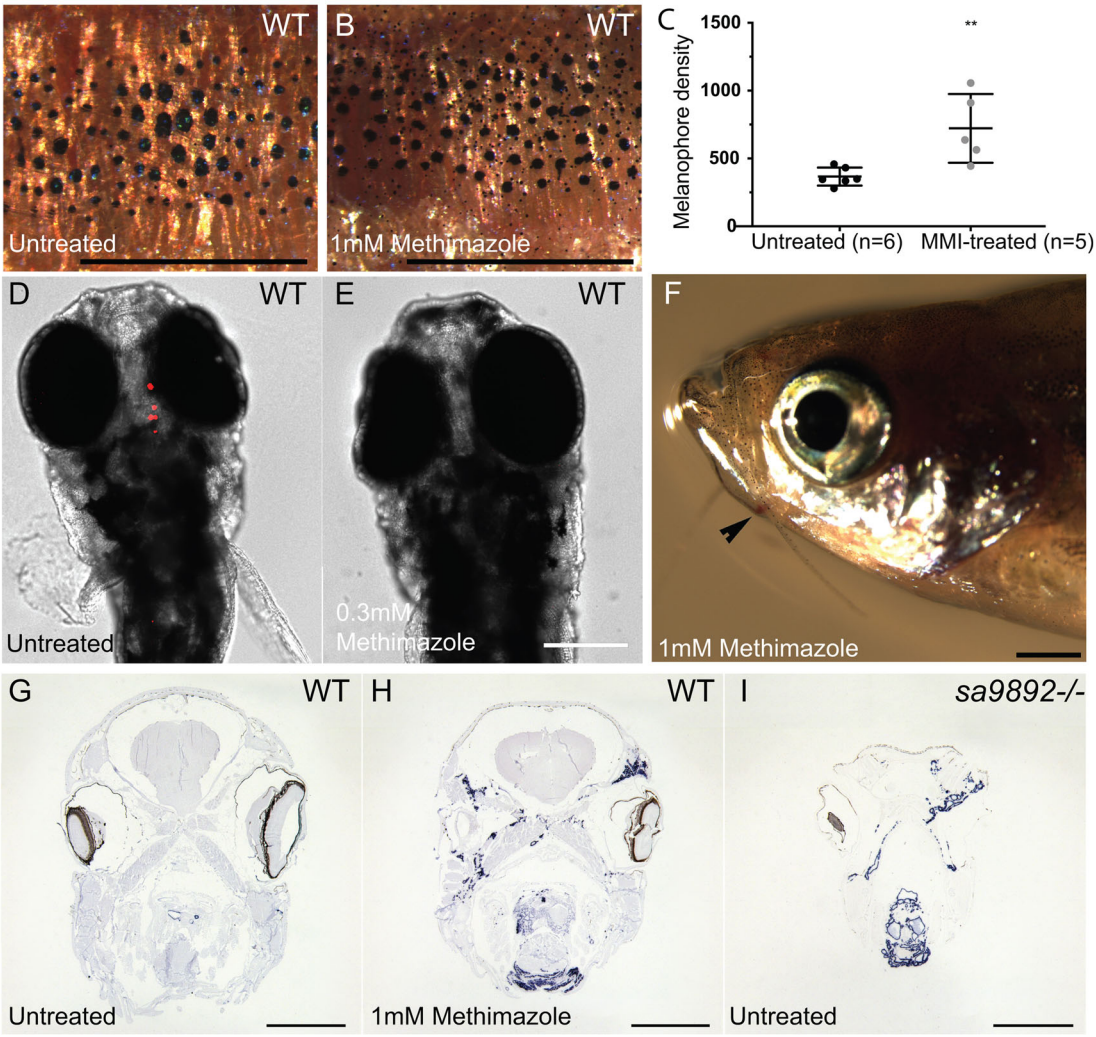

Fig. 8. The goitrogen methimazole (MMI) phenocopies *duox* mutations. A and B show a 5× magnification of the distribution of melanophores on the flank region among MMI-treated and untreated WT fish. Treated animals have at least two distinct populations of melanophores, based on size (A,B). Pigment change pertaining to melanophore numbers is significant following MMI treatment (C). (Bonferroni's multiple comparisons $^{**}P<0.01$). MMI leads to loss of bound T_4 in WT larvae (D,E) and induces external goitre (arrowhead; F). ISH for thyroglobulin reveals widespread follicular tissue, not limited to the mid-ventral region (H), similar to *duox* mutants (I). Scale bars: 1 mm.

underway, fish standard length (SL) is subject to both genetic and environmental factors, thus introducing variation amongst siblings. Indeed, environmental influences on SL is clearly apparent as larvae reared in groups show greater variation in SL than larvae raised individually (Parichy et al., 2009). SL is, thus, regarded as a more reliable measure of fish maturation than age (Parichy et al., 2009; Singleman and Holtzman, 2014). Considering the mean values for SL for our groups, it was clearly apparent that at 3 months of age all mutant groups were significantly shorter (i.e. less mature) than their heterozygous or WT siblings. Remarkably, by 6 months, however, the homozygous *duox* mutant fish caught up with the WT and heterozygotes siblings. This suggests that it is not growth per se, but the state of maturation, which is dependent on thyroid hormones. This finding is consistent with findings in non-metamorphosing *Xenopus laevis* tadpoles, which become giants and can live for years in an immature neotenic state (Rot-Nikcevic and Wassersug, 2004). This arrested development, associated with continued growth, has been attributed to a lack of thyroid glands in these animals (Rot-Nikcevic and Wassersug, 2004). In fish, definitive evidence of TH insufficiency causing metamorphic stasis is well appreciated from studies on flatfish. Larvae of the summer flounder (*Paralichthys dentatus*), when treated with thiourea, do not develop beyond early metamorphic climax (Schreiber and Specker, 1998). Likewise, olive flounder (*Paralichthys olivaceus*) larvae treated with the goitrogen, thiourea, enter metamorphic stasis and become giant larvae (Inui and Miwa, 1985). Although metamorphosis among the roundfish is less dramatic, several examples illustrate the dependence of metamorphosis on THs. Thiourea treatment was found to arrest metamorphosis in the coral trout grouper (*Plectropomus leopardus*) (Trijuno et al., 2002), orange-spotted grouper (*Epinephelus coioides*) (de Jesus et al., 1998) and the red sea bream (*Pagrus major*) (Hirata et al., 1989). Meanwhile, the pesticide chlorpyrifos, reported to cause reductions in serum concentrations of T_4 and T_3 (Slotkin et al., 2013), was recently found to prevent metamorphic completion in the convict surgeonfish (*Acanthurus triostegus*) (Holzer et al., 2017). In zebrafish, a 1 mM concentration of methimazole inhibited the larval to juvenile transition (Brown, 1997). However, larvae treated with a concentration of 0.3 mM eventually escaped the inhibition and continued development. While our *duox* mutants eventually reach normal adult size, this

Biology Open (2019) 8, bio037655. doi:10.1242/bio.037655

might be associated with an incomplete metamorphic or immature state. Alternatively, there may be some genetic redundancy present in zebrafish, whereby a different source of H_2O_2 in the thyroid follicles might be capable of partially compensating for the loss of *duox* function. Indeed, another NOX isoform, NOX4, has been described in human thyrocytes. Unlike Duox though, NOX4 generates H_2O_2 in the intracellular compartment (Weyemi et al., 2010). It may thus be important to generate double mutants for *duox* and *nox4* to determine the contribution of Nox4 in thyroid hormonogenesis.

In the zebrafish, swim bladder inflation is dependent on THs (Godfrey et al., 2017; Liu and Chan, 2002). The posterior chamber of the swim bladder inflates around 4.5 dpf while the anterior chamber inflates by 21 dpf (Winata et al., 2009). These events appear to coincide with peaks in whole body T_3 at 5 dpf and 10 dpf and T_4 at 21 dpf (Chang et al., 2012). Previously, it was found that swim bladder inflation was significantly delayed in thyroid-ablated zebrafish, where the anterior chamber of the bladder inflated ∼50 dpf, compared to ∼20 days in controls (McMenamin et al., 2014). Similar observations were also made in thyroid-ablated *Danio albolineatus* (McMenamin et al., 2014). There also exists sufficient evidence of how pharmacologically disrupted thyroid processes affect swim bladder inflation. Ecological assessments of aquatic pollutants often employ key morphological events during fish development as predictive approaches. 2-Mercaptobenzothiazole (MBT), commonly used for rubber vulcanization, is found to occur in environmental water bodies. MBT is a potent TPO inhibitor and its role was recently examined in swim bladder inflation in the fathead minnow (*Pimephales promelas*) (Nelson et al., 2016) and zebrafish (Stinckens et al., 2016). Among minnows, larvae continuously exposed to MBT showed a concentration-dependent decrease in anterior lobe size (Nelson et al., 2016). Meanwhile, MBT-treated zebrafish larvae were reported to fare worse than minnows, where 22% of larvae exposed to the highest concentration failed to inflate the anterior chamber (Stinckens et al., 2016). Interestingly, even though both species belong to the order Cypriniformes, a compensatory T_4 response has been reported in the fathead minnow at 21 dpf (Nelson et al., 2016) but not in the zebrafish (Stinckens et al., 2016), suggesting species-specific differences. Our homozygous *duox* mutant animals also displayed a significant delay in anterior chamber inflation, suggesting that Duox is essential for this process, likely through its role in thyroid hormone synthesis.

Barbels are yet another easily observable phenotypic trait influenced by thyroid hormones. In zebrafish, both pairs develop as epithelial buds around 30–40 dpf, following the emergence of pelvic fin rays (Hansen et al., 2002; Parichy et al., 2009). Thus far, only one study has reported barbel emergence to be influenced by THs. Thyroid ablation via Mtz of *Tg(tg:nVenus-2a-nfnB)* of *Danio rerio* and *D. albolineatus* resulted in the absence of sensory barbels (McMenamin et al., 2014). Similarly, *manet* mutants were also found to lack barbels (McMenamin et al., 2014). Our homozygous *duox* mutants also show impairment of barbel emergence, consistent with their hypothyroid state. However, it is notable that a subset of the *sa9892*$^{-/-}$ mutants eventually did grow barbels, similar to their body length catch-up phenotype.

In humans, thyroid dysfunction during pregnancy has been positively associated with adverse maternal/foetal outcomes, including infertility, miscarriage, pre-eclampsia, pre-term (before 37 weeks) birth and maternal thyroid dysfunction postpartum (Hernández et al., 2018; Stagnaro-Green et al., 2011; Velasco and Taylor, 2018). TH is essential for early development and maturation of the foetal brain and maternal transfer of TH is especially important during the first trimester (Cooper and Biondi, 2012) since the embryo does not begin synthesising THs until 12–13 weeks into gestation (Casey and Leveno, 2006). The British Thyroid Foundation suggests prescribing levothyroxine to hypothyroid women trying to conceive in order to address these negative consequences of hypothyroidism on fertility and pregnancy. Intriguingly, we also noted significant defects in fertility in both sexes in our homozygous *duox* mutants. Although we do not currently know the reason for infertility in the *duox* mutants, a potential cause may be due to failure in mating behaviour as a consequence of the observed effects on pigmentation in the mutants. It has previously been noted that, in zebrafish, both sexes experience diurnal changes in their stripes and interstripe colours, a process termed ephemeral sexual dichromatism, during mating and spawning (Hutter et al., 2012). Another study reported that females utilise yellow colouration for sex recognition (Hutter et al., 2011). This ties in well with xanthophore deficiency reported in thyroid ablated, hypothyroid zebrafish (McMenamin et al., 2014), and by extension, the *duox* mutants. However, it is notable that casper strains of zebrafish, which lack xanthophores altogether, can successfully breed (White et al., 2008). Thus, there may be additional factors that may be contributing to infertility in *duox* mutants.

Associations between thyroid status and reproduction in teleosts have been previously reviewed (Cyr and Eales, 1996). Four physiological pre-requisites have been recognised as essential to spawning behaviour and fertility in fish: (1) the completion of vitellogenesis in the ovaries, (2) maturation and ovulation of oocytes stimulated by pituitary luteinizing hormone (LH), (3) completion of spermatogenesis, and (4) sufficient production and storage of milt (seminal plasma and mature sperm) in the sperm duct. These are largely regulated by the endocrine system (Kobayashi et al., 2002). T_3 enhances the response of the ovarian follicles to gonadotropins, thus facilitating secretion of 17β estradiol (Cyr and Eales, 1988). This regulates the production of vitellogenin by the liver, and in studies on Great Lakes salmonids it has been suggested that lowered T_3 levels may impair oocyte production (Leatherland and Barrett, 1993). In the fathead minnow (*Pimephales promelas*), Methimazole treatment led to a reduction of the cortical alveolus oocytes, relative to control females. Meanwhile, in post-spawning males, control animals showed an increase in the number of spermatozoa and a decrease in the number of spermatogonia. This increase in spermatozoa was not observed in methimazole-treated cohorts, suggesting that hypothyroidism affects spermatogenesis (Lema et al., 2009). Among the African sharptooth catfish (*Clarias gariepinus*), pre-spawning males treated with thiourea were shown to have narrower seminiferous tubules and fewer spermatozoa (Swapna et al., 2006). Intriguingly, hypothyroidism in humans has also been associated with impaired spermatogenesis and sperm abnormalities (La Vignera and Vita, 2018). We have found that fertility in our homozygous *duox* mutants can be restored in both sexes and we can successfully raise offspring to adulthood from a cross between a mutant male and WT female. This is in line with previous observations on growth-retarded (*grt*) mice. *grt* mice have autosomal recessive hypothyroidism, with females suffering lifelong infertility and males gradually acquiring fertility. When treated with THs, *grt* females showed an increase in the size of their uteri and ovaries, which was comparable with heterozygous and WTs. Furthermore, they engaged in copulatory behaviour and were able to conceive and deliver pups (Hosoda et al., 2008). Zebrafish *duox* mutants thus provide an excellent model to investigate the consequences of human CH associated with mutations in *DUOX1* and *DUOX2*, and the mechanisms by which treatment with THs, even in adults, can

Biology Open (2019) 8, bio037655. doi:10.1242/bio.037655

restore many of the defects caused by chronic hypothyroidism, including restoration of fertility in both males and females.

Conclusion

Overall, we found that homozygous mutants display a number of phenotypes, which can be ascribed to hypothyroidism, including growth retardation, pigmentation defects, ragged fins, thyroid hyperplasia and external goitre. By and large, the growth retardation defect is not permanent, as fish continue to grow despite being chronically hypothyroid, and ultimately catch up with their euthyroid heterozygous and WT siblings. This contrasts with findings in humans suffering from hypothyroidism, who remain growth retarded unless T_4 treatment is initiated within weeks after birth. Most other phenotypes associated with chronic hypothyroidism in the *duox* mutant fish were rescued by T_4 treatment, even if supplementation was not initiated until adulthood. These include recovery of fertility, return to normal pigmentation, improvement in fin morphology and return to normal size thyroid glands. In summary, *duox* mutant zebrafish provide a new and potentially powerful system to understand the consequences of chronic congenital hypothyroidism on growth and maintenance of body physiology, as well as the mechanisms of recovery of normal physiology following thyroid hormone supplementation. Thus, our *duox* mutant fish appear to be in a chronic hypothyroid/goitrogenic state, as indicated by their external goitres as well as internal expansion of *thyroglobulin* expressing tissue.

MATERIAL AND METHODS

Ethics statement

All experiments involving animals were approved by the local ethics committee and the Home Office.

Animals and husbandry

Adults and larvae were used in this study. The zebrafish (*D. rerio*) WT line used was AB. Mutant lines used were *duox sa9892* and *duox sa13017* (Kettleborough et al., 2013) and were obtained from the European Zebrafish Resource Center (EZRC). Compound heterozygotes for these mutant alleles were generated in-house. Both *duox* alleles were also crossed into *nacre* (*nac*^{w2}) (Lister et al., 1999) and *casper* (White et al., 2008) strains for visualising larval thyroid follicles, swim bladder and adult erythema. In all cases, embryos were raised in sea salts (Sigma-Aldrich, S9883) medium containing 0.0001% Methylene Blue until 5 days post-fertilisation (dpf) and then transferred to the system where they were maintained at a temperature of 28°C, pH 7.4, constant salinity and a 14:10 photoperiod.

PCR and genotyping

Genomic DNA was extracted from caudal fin clips or whole larvae using lysis buffer, in a thermal cycler. The conditions for this procedure were 2 h at 55°C, 10 min at 95°C and a hold (if necessary) at 12°C. PCR was performed using ExTaq DNA polymerase (TaKaRa RR001A) with the following primer pairs: for the *duox sa9892* allele, forward 5′-ACGAGGTACACAACTCAAGCTG-3′ and reverse 5′-GACGTTCAAAGCGAAACCTGAC-3′; for the *duox sa13017* allele, forward 5′-TGGTACACCATTTGAGGATGTGA-3′ and reverse 5′-ACACCCACCATAGAGGTCTCT-3′. PCR conditions were as follows: 36 cycles at 94°C for 30 s, 55°C for 30 s and 72°C for 30 s. Samples were subject to Sanger sequencing (GATC Biotech). Sequencing primers used were 5′-CTTGGTCTGCCTTTGACGAAGT-3′ for the *duox sa9892* allele and 5′-GTGACTCAAGTCAGAACAGGTC-3′ for the *duox sa13017* allele. Siblings were stage-matched, phenotypically WT, heterozygous and homozygous animals obtained by crossing heterozygous carriers.

Whole mount immunofluorescence

Zebrafish larvae, at 5 dpf, were fixed overnight in 4% phosphate-buffered paraformaldehyde (PFA) (Sigma-Aldrich), at 4°C. This was followed by 15 min of dehydration in 100% methanol. Larvae were then transferred to fresh 100% methanol and stored at −20°C until usage. Larvae were gradually rehydrated to PBST, treated with 10 µg/ml proteinase K (Roche) for 30 min, briefly rinsed in PBST, and postfixed in 4% PFA for 20 min. Following further rinsing in PBST, larvae were immersed in blocking buffer (PBST containing 1% dimethylsulfoxide, 1% BSA, 5% horse serum and 0.8% Triton X-100) for 2 h. This was followed by overnight incubation, at 4°C, in blocking buffer containing the primary antibody (1:1000) against thyroxine (T_4) (Biorbyt orb11479). Overnight incubation was followed by several wash steps in PBST containing 1% BSA. Larvae were then incubated overnight, at 4°C, in blocking buffer containing the secondary antibody (1:250) Alexa Fluor 568 (Invitrogen A11057) (Opitz et al., 2011). Stained larvae were washed in PBST, imaged and then subject to genotyping.

Histology and ISH

In situ hybridization on sections of adult zebrafish was performed essentially as described (Paul et al., 2016). Briefly, adult zebrafish were fixed whole in 4% PFA for 1 week followed by a decalcification step in 20% EDTA, for 10 days. Animals were then cut at the operculum and mid trunk level and processed in a Leica TP1050 tissue processor in preparation for paraffin embedding. The embedding station used was a Leica EG1150H. The cut face of the tissue was oriented towards the leading edge of the paraffin block and sectioned at 5 µm thicknesses on a LeicaRM2255 microtome. Sections were arranged and held on Superfrost Plus™ slides (Thermo Fisher Scientific). Alternating sections were then taken forward for Haematoxylin and Eosin (H&E) staining and ISH. Sections were put through H&E staining via a Varistain 24-4 carousel (Thermo Fisher Scientific, Shandon). *Thyroglobulin* (*tg*) cDNA used for riboprobe synthesis was amplified using forward 5′-AGGTGGAGAATGTTGGTGTG-3′ and reverse 5′-CTCCAACTCTGGC-AATGACT-3′ primers. Digoxigenin-labelled probes were synthesised *in vitro* using a MEGAscript®T7 kit (Ambion).

Body length and melanophore counts

For measuring body length, all fish were briefly anaesthetised in 0.02% MS 222 (tricaine) (Sigma-Aldrich). They were then transferred onto an agarose bed in a petri dish and imaged at 0.73× magnification. For each fish two or three images were captured in order to include the entire length including the caudal fin. These part images were stitched together in Adobe® Photoshop to obtain a single image. The 'ruler' tool and 'analyse measurement' command in Photoshop CS5 were used on these images to calculate the length from the tip of the mandible to the caudal peduncle.

For determining melanophore density, all fish were treated with epinephrine to contract pigment granules. To obtain a 1 mg/ml working solution, 0.1 g of epinephrine was dissolved into 100 ml of a 0.01% tricaine solution. Epinephrine is only partially soluble in water and thus, the solution was filtered to obtain a clear filtrate. The solution turns pink-orange during filtration. Fish were treated for 5 min in this working solution. They were then transferred onto an agarose bed in a petri dish and imaged at two locations on the lowermost continuous stripe extending from the operculum to the trunk. A 5× magnification was used. The 'multi-point' tool on FIJI was used to manually count all melanophores contained within a stripe, in the field of view, for each image. All images were acquired on a Leica MZ16FA fluorescence stereomicroscope with a DC490 camera.

Pharmacological treatments

For rescuing mutant phenotypes, a 12-week treatment with T_4 (Sigma-Aldrich) was sustained in a closed system that closely resembled aquarium conditions. Four groups- *sa9892*$^{+/-}$ untreated, *sa9892*$^{+/-}$ treated, *sa9892*$^{-/-}$ untreated and *sa9892*$^{-/-}$ treated were subject to this regime, with each group comprised of four adult fish. T_4 was added tri-weekly, at a concentration of 30 nM. Water was changed three times each week.

For phenocopy experiments, a 12-week treatment with methimazole (Sigma-Aldrich) was administered, once again, in a closed system simulating aquarium conditions. This regime was applied to six WT adult fish, while six untreated WT animals comprised the control group. Methimazole was added tri-weekly, at a concentration of 1 mM. Water was changed three times each week.

For immunostaining, WT larvae were treated with methimazole (0.3 mM) from 0 dpf. Animals were then fixed at 5 dpf and stained for T_4 as described above.

Statistical analyses

GraphPad Prism 7 was used for statistical testing. Column statistics and analyses of variance were implemented for all data sets. For column statistics, we calculated median, s.d., s.e.m., confidence intervals and Gaussian distribution. The D'Agostino and Pearson test was used to check for Gaussian distribution. One-way ordinary ANOVA was used to analyse variance. Differences were considered significant at $P<0.0001$. Bonferroni's multiple comparisons test was used to compare means between groups.

Acknowledgements

We would like to thank Peter Walker, Grace Bako and Natalie Partington, at the Core Histology Facility, for their help with histological sectioning and staining. We would also like to thank the aquarium staff in the BSF unit for their care and support of the fish. We also extend our gratitude to Simone Schindler, University of Exeter, for her guidance on performing ISH on tissue sections. We would like to thank Kalin Narov, (www.embryosafari.com) for his contribution to Fig. 1. Finally, we thank Sabine Costagliola and Pierre Gillotay, Université Libre de Bruxelles, Belgium, for their advice with the T_4 antibody protocols in larvae.

Competing interests

The authors declare no competing or financial interests.

Author contributions

Conceptualisation: K.C., S.I., E.A.; Methodology: K.C., S.I.; Validation: K.C.; Formal analysis: K.C.; Investigation: K.C., S.I.; Writing - original draft: K.C.; Writing - review & editing: E.A.; Visualisation: E.A.; Supervision: E.A.; Project administration: E.A.; Funding acquisition: E.A.

Funding

This work was supported by a PhD studentship from The Scar Free Foundation to K.C., and a Medical Research Council Research Project Grant [MR/L007525/1] to S.I., E.A.

References

Alt, B., Reibe, S., Feitosa, N. M., Elsalini, O. A., Wendl, T. and Rohr, K. B. (2006). Analysis of origin and growth of the thyroid gland in zebrafish. *Dev. Dyn.* **235**, 1872-1883.

Argumedo, G. S., Sanz, C. R. and Olguín, H. J. (2012). Experimental models of developmental hypothyroidism. *Horm. Metab. Res.* **44**, 79-85.

Aronson, R., Ehrlich, R. M., Bailey, J. D. and Rovef, J. F. (1990). Growth in children with congenital hypothyroidism detected by neonatal screening. *J. Pediatr.* **116**, 33-37.

Aycan, Z., Cangul, H., Muzza, M., Bas, V. N., Fugazzola, L., Chatterjee, V. K., Persani, L. and Schoenmakers, N. (2017). Digenic DUOX1 and DUOX2 mutations in cases with congenital hypothyroidism. *J. Clin. Endocrinol. Metab.* **102**, 3085-3090.

Barembaum, M. and Bronner-Fraser, M. (2005). Early steps in neural crest specification. *Semin. Cell Dev. Biol.* **16**, 642-646.

Bedard, K. and Krause, K.-H. (2007). The NOX family of ROS-generating NADPH oxidases: physiology and pathophysiology. *Physiol. Rev.* **87**, 245-313.

Bohnsack, B. L. and Kahana, A. (2013). Thyroid hormone and retinoic acid interact to regulate zebrafish craniofacial neural crest development. *Dev. Biol.* **373**, 300-309.

Brown, D. D. (1997). The role of thyroid hormone in zebrafish and axolotl development. *Proc. Natl. Acad. Sci. USA* **94**, 13011-13016.

Carvalho, D. P. and Dupuy, C. (2013). Role of the NADPH oxidases DUOX and NOX4 in thyroid oxidative stress. *Eur Thyroid J* **2**, 160-167.

Casey, B. M. and Leveno, K. J. (2006). Thyroid disease in pregnancy. *Obstet. Gynecol.* **108**, 1283-1292.

Chakera, A. J., Pearce, S. H. S. and Vaidya, B. (2012). Treatment for primary hypothyroidism: current approaches and future possibilities. *Drug Des. Dev. Ther.* **6**, 1-11.

Chang, J., Wang, M., Gui, W., Zhao, Y., Yu, L. and Zhu, G. (2012). Changes in thyroid hormone levels during zebrafish development. *Zool. Sci.* **29**, 181-184.

Clause, M. (2013). Newborn screening for congenital hypothyroidism. *J. Pediatr. Nurs.* **28**, 603-608.

Cooper, D. S. and Biondi, B. (2012). Subclinical thyroid disease. *Lancet* **379**, 1142-1154.

Cyr, D. G. and Eales, J. G. (1988). *In vitro* effects of thyroid hormones on gonadotropin-induced estradiol-17 beta secretion by ovarian follicles of rainbow trout, *Salmo gairdneri*. *Gen. Comp. Endocrinol.* **69**, 80-87.

Cyr, D. G. and Eales, J. G. (1996). Interrelationships between thyroidal and reproductive endocrine systems in fish. *Rev. Fish Biol. Fish.* **6**, 165-200.

De Deken, X., Wang, D., Many, M.-C., Costagliola, S., Libert, F., Vassart, G., Dumont, J. E. and Miot, F. (2000). Cloning of two human thyroid cDNAs encoding new members of the NADPH oxidase family. *J. Biol. Chem.* **275**, 23227-23233.

De Felice, M. and Di Lauro, R. (2004). Thyroid development and its disorders: genetics and molecular mechanisms. *Endocr. Rev.* **25**, 722-746.

de Jesus, E. G. T., Toledo, J. D. and Simpas, M. S. (1998). Thyroid hormones promote early metamorphosis in grouper (Epinephelus coioides) larvae. *Gen. Comp. Endocrinol.* **112**, 10-16.

Donkó, Á., Morand, S., Korzeniowska, A., Boudreau, H. E., Zana, M., Hunyady, L., Geiszt, M. and Leto, T. L. (2014). Hypothyroidism-associated missense mutation impairs NADPH oxidase activity and intracellular trafficking of Duox2. *Free Radic. Biol. Med.* **73**, 190-200.

Dumont, J. E., Lamy, F., Roger, P. and Maenhaut, C. (1992). Physiological and pathological regulation of thyroid cell proliferation and differentiation by thyrotropin and other factors. *Physiol. Rev.* **72**, 667-697.

Dupuy, C., Ohayon, R., Valent, A., Noël-Hudson, M. S., Dème, D. and Virion, A. (1999). Purification of a novel flavoprotein involved in the thyroid NADPH oxidase. Cloning of the porcine and human cDNAs. *J. Biol. Chem.* **274**, 37265-37269.

Elsalini, O. A. and Rohr, K. B. (2003). Phenylthiourea disrupts thyroid function in developing zebrafish. *Dev. Genes Evol.* **212**, 593-598.

Gamborino, M. J., Sevilla-Romero, E., Muñoz, A., Hernández-Yago, J., Renau-Piqueras, J. and Pinazo-Durán, M. D. (2001). Role of thyroid hormone in craniofacial and eye development using a rat model. *Ophthalmic Res.* **33**, 283-291.

Gilbert, M. E., Rovet, J., Chen, Z. and Koibuchi, N. (2012). Developmental thyroid hormone disruption: prevalence, environmental contaminants and neurodevelopmental consequences. *Neurotoxicology* **33**, 842-852.

Godfrey, A., Hooser, B., Abdelmoneim, A., Horzmann, K. A., Freemanc, J. L. and Sepúlveda, M. S. (2017). Thyroid disrupting effects of halogenated and next generation chemicals on the swim bladder development of zebrafish. *Aquat. Toxicol.* **193**, 228-235.

Guillot, R., Muriach, B., Rocha, A., Rotllant, J., Kelsh, R. N. and Cerdá-Reverter, J. M. (2016). Thyroid hormones regulate zebrafish melanogenesis in a gender-specific manner. *PLoS ONE* **11**, e0166152.

Hansen, A., Reutter, K. and Zeiske, E. (2002). Taste bud development in the zebrafish, Danio rerio. *Dev. Dyn.* **223**, 483-496.

Hernández, M., López, C., Soldevila, B., Cecenarro, L., Martínez-Barahona, M., Palomera, E., Rius, F., Lecube, A., Pelegay, M. J., García, J. et al. (2018). Impact of TSH during the first trimester of pregnancy on obstetric and foetal complications: usefulness of 2.5 mIU/l cut-off value. *Clin. Endocrinol. (Oxf)* **88**, 728-734.

Hirata, Y., Kurokura, H. and Kasahara, S. (1989). Effects of thyroxine and thiourea on the development of larval Red sea bream *Pagrus major*. *Nippon Suisan Gakkaishi* **55**, 1189-1195.

Hirata, M., Nakamura, K.-I., Kanemaru, T., Shibata, Y. and Kondo, S. (2003). Pigment cell organization in the hypodermis of zebrafish. *Dev. Dyn.* **227**, 497-503.

Holzer, G., Besson, M., Lambert, A., François, L., Barth, P., Gillet, B., Hughes, S., Piganeau, G., Leulier, F., Viriot, L. et al. (2017). Fish larval recruitment to reefs is a thyroid hormone-mediated metamorphosis sensitive to the pesticide chlorpyrifos. *eLife* **6**, 742.

Hosoda, Y., Sasaki, N. and Agui, T. (2008). Female infertility in GRT mice is caused by thyroid hormone deficiency, not by insufficient TPST2 activity in the reproductive organs. *J. Vet. Med. Sci.* **70**, 1043-1049.

Hsü, C.-Y., Huang, H.-C., Chang, C.-H. and Liang, H.-M. (1974). Independence of ovarian masculinization and hypothyroidism in frog tadpoles after methimazole treatment. *J. Exp. Zool.* **189**, 235-241.

Hutter, S., Zala, S. M. and Penn, D. J. (2011). Sex recognition in zebrafish (*Danio rerio*). *J. Ethol.* **29**, 55-61.

Hutter, S., Hettyey, A., Penn, D. J. and Zala, S. M. (2012). Ephemeral Sexual Dichromatism in Zebrafish (Danio rerio). *Ethology* **118**, 1208-1218.

Inui, Y. and Miwa, S. (1985). Thyroid hormone induces metamorphosis of flounder larvae. *Gen. Comp. Endocrinol.* **60**, 450-454.

Jin, H. Y., Heo, S.-H., Kim, Y.-M., Kim, G.-H., Choi, J.-H., Lee, B.-H. and Yoo, H.-W. (2014). High frequency of *DUOX2* mutations in transient or permanent congenital hypothyroidism with eutopic thyroid glands. *Hormone Res. Paediatr.* **82**, 252-260.

Johnson, S. L. and Bennett, P. (1999). Growth control in the ontogenetic and regenerating zebrafish fin. *Methods Cell Biol.* **59**, 301-311.

Johnson, K. R., Marden, C. C., Ward-Bailey, P., Gagnon, L. H., Bronson, R. T. and Donahue, L. R. (2007). Congenital hypothyroidism, dwarfism, and hearing impairment caused by a missense mutation in the mouse dual Oxidase 2 gene, Duox2. *Mol. Endocrinol.* **21**, 1593-1602.

Kawahara, T., Quinn, M. T. and Lambeth, J. D. (2007). Molecular evolution of the reactive oxygen-generating NADPH oxidase (Nox/Duox) family of enzymes. *BMC Evol. Biol.* **7**, 109-121.
Kettleborough, R. N. W., Busch-Nentwich, E. M., Harvey, S. A., Dooley, C. M., de Bruijn, E., van Eeden, F., Sealy, I., White, R. J., Herd, C., Nijman, I. J. et al. (2013). A systematic genome-wide analysis of zebrafish protein-coding gene function. *Nature* **496**, 494-497.
Kizys, M. M. L., Louzada, R. A., Mitne-Neto, M., Jara, J. R., Furuzawa, G. K., de Carvalho, D. P., Dias-da-Silva, M. R., Nesi-França, S., Dupuy, C. and Maciel, R. M. B. (2017). DUOX2 mutations are associated with congenital hypothyroidism with ectopic thyroid gland. *J. Clin. Endocrinol. Metab.* **102**, 4060-4071.
Kobayashi, M., Sorensen, P. W. and Stacey, N. E. (2002). Hormonal and pheromonal control of spawning behavior in the goldfish. *Fish Physiol. Biochem.* **26**, 71-84.
La Vignera, S. and Vita, R. (2018). Thyroid dysfunction and semen quality. *Int. J. Immunopathol. Pharmacol.* **32**, 2058738418775241.
Leatherland, J. F. and Barrett, S. B. (1993). Investigations into the development of the pituitary gland-thyroid tissue axis and distribution of tissue thyroid hormone content in embryonic coho salmon (Oncorhynchus kisutch) from Lake Ontario. *Fish Physiol. Biochem.* **12**, 149-159.
LeClair, E. E. and Topczewski, J. (2010). Development and regeneration of the zebrafish maxillary barbel: a novel study system for vertebrate tissue growth and repair. *PLoS ONE* **5**, e8737.
Lema, S. C., Dickey, J. T., Schultz, I. R. and Swanson, P. (2009). Thyroid hormone regulation of mRNAs encoding thyrotropin beta-subunit, glycoprotein alpha-subunit, and thyroid hormone receptors alpha and beta in brain, pituitary gland, liver, and gonads of an adult teleost, Pimephales promelas. *J. Endocrinol.* **202**, 43-54.
Lister, J. A., Robertson, C. P., Lepage, T., Johnson, S. L. and Raible, D. W. (1999). nacre encodes a zebrafish microphthalmia-related protein that regulates neural-crest-derived pigment cell fate. *Development* **126**, 3757-3767.
Liu, Y.-W. and Chan, W.-K. (2002). Thyroid hormones are important for embryonic to larval transitory phase in zebrafish. *Differentiation* **70**, 36-45.
McMenamin, S. K., Bain, E. J., McCann, A. E., Patterson, L. B., Eom, D. S., Waller, Z. P., Hamill, J. C., Kuhlman, J. A., Eisen, J. S. and Parichy, D. M. (2014). Thyroid hormone-dependent adult pigment cell lineage and pattern in zebrafish. *Science* **345**, 1358-1361.
Minoux, M. and Rijli, F. M. (2010). Molecular mechanisms of cranial neural crest cell migration and patterning in craniofacial development. *Development* **137**, 2605-2621.
Moreno, J. C., Bikker, H., Kempers, M. J. E., van Trotsenburg, A. S. P., Baas, F., de Vijlder, J. J. M., Vulsma, T. and Ris-Stalpers, C. (2002). Inactivating mutations in the gene for thyroid oxidase 2 (THOX2) and congenital hypothyroidism. *N. Engl. J. Med.* **347**, 95-102.
Muzza, M. and Fugazzola, L. (2017). Disorders of H2O2 generation. *Best Pract. Res. Clin. Endocrinol. Metab.* **31**, 225-240.
Nakatani, Y., Kawakami, A. and Kudo, A. (2007). Cellular and molecular processes of regeneration, with special emphasis on fish fins. *Dev. Growth Differ.* **49**, 145-154.
Nelson, K. R., Schroeder, A. L., Ankley, G. T., Blackwell, B. R., Blanksma, C., Degitz, S. J., Flynn, K. M., Jensen, K. M., Johnson, R. D., Kahl, M. D. et al. (2016). Impaired anterior swim bladder inflation following exposure to the thyroid peroxidase inhibitor 2-mercaptobenzothiazole part I: fathead minnow. *Aquat. Toxicol.* **173**, 192-203.
Olivieri, A. (2015). Epidemiology of congenital hypothyroidism. In *Thyroid Diseases in Childhood* (ed. G. Bona, F. De Luca and A. Monzani), pp. 53-63. Springer International Publishing.
Opitz, R., Maquet, E., Zoenen, M., Dadhich, R. and Costagliola, S. (2011). TSH receptor function is required for normal thyroid differentiation in zebrafish. *Mol. Endocrinol.* **25**, 1579-1599.
Parichy, D. M., Elizondo, M. R., Mills, M. G., Gordon, T. N. and Engeszer, R. E. (2009). Normal table of postembryonic zebrafish development: staging by externally visible anatomy of the living fish. *Dev. Dyn.* **238**, 2975-3015.
Paul, S., Schindler, S., Giovannone, D., de Millo Terrazzani, A., Mariani, F. V. and Crump, J. G. (2016). Ihha induces hybrid cartilage-bone cells during zebrafish jawbone regeneration. *Development* **143**, 2066-2076.
Rada, B. and Leto, T. L. (2008). Oxidative innate immune defenses by Nox/Duox family NADPH oxidases. *Contrib. Microbiol.* **15**, 164-187.
Rahmani, K., Yarahmadi, S., Etemad, K., Koosha, A., Mehrabi, Y., Aghang, N. and Soori, H. (2016). Congenital hypothyroidism: optimal initial dosage and time of initiation of treatment: a systematic review. *Int. J. Endocrinol. Metab.* **14**, e36080.
Roberts, C. G. P. and Ladenson, P. W. (2004). Hypothyroidism. *The Lancet* **363**, 793-803.
Rot-Nikcevic, I. and Wassersug, R. J. (2004). Arrested development in Xenopus laevis tadpoles: how size constrains metamorphosis. *J. Exp. Biol.* **207**, 2133-2145.
Rovet, J., Ehrlich, R. and Sorbara, D. (1987). Intellectual outcome in children with fetal hypothyroidism. *J. Pediatr.* **110**, 700-704.
Schmidt, F. and Braunbeck, T. (2011). Alterations along the hypothalamic-pituitary-thyroid axis of the zebrafish (Danio rerio) after exposure to propylthiouracil. *J. Thyroid Res.* **2011**, 376243-376217.
Schreiber, A. M. and Specker, J. L. (1998). Metamorphosis in the summer flounder (Paralichthys dentatus): stage-specific developmental response to altered thyroid status. *Gen. Comp. Endocrinol.* **111**, 156-166.
Sekimizu, K., Tagawa, M. and Takeda, H. (2007). Defective fin regeneration in medaka fish (Oryzias latipes) with hypothyroidism. *Zool. Sci.* **24**, 693-699.
Singh, A. P. and Nüsslein-Volhard, C. (2015). Zebrafish stripes as a model for vertebrate colour pattern formation. *Curr. Biol.* **25**, R81-R92.
Singleman, C. and Holtzman, N. G. (2014). Growth and maturation in the zebrafish, Danio rerio: a staging tool for teaching and research. *Zebrafish* **11**, 396-406.
Slotkin, T. A., Cooper, E. M., Stapleton, H. M. and Seidler, F. J. (2013). Does thyroid disruption contribute to the developmental neurotoxicity of chlorpyrifos? *Environ. Toxicol. Pharmacol.* **36**, 284-287.
Stagnaro-Green, A., Abalovich, M., Alexander, E., Azizi, F., Mestman, J., Negro, R., Nixon, A., Pearce, E. N., Soldin, O. P., Sullivan, S. et al. (2011). Guidelines of the American Thyroid Association for the diagnosis and management of thyroid disease during pregnancy and postpartum. *Thyroid* **21**, 1081-1125.
Stinckens, E., Vergauwen, L., Schroeder, A. L., Maho, W., Blackwell, B. R., Witters, H., Blust, R., Ankley, G. T., Covaci, A., Villeneuve, D. L. et al. (2016). Impaired anterior swim bladder inflation following exposure to the thyroid peroxidase inhibitor 2-mercaptobenzothiazole part II: Zebrafish. *Aquat. Toxicol.* **173**, 204-217.
Sugawara, M. (2014). Reactive oxygen species and thyroid diseases. In *Systems Biology of Free Radicals and Antioxidants* (ed. I. Laher), pp. 3521-3538. Berlin, Heidelberg: Springer Berlin Heidelberg.
Swapna, I., Rajasekhar, M., Supriya, A., Raghuveer, K., Sreenivasulu, G., Rasheeda, M. K., Majumdar, K. C., Kagawa, H., Tanaka, H., Dutta-Gupta, A. et al. (2006). Thiourea-induced thyroid hormone depletion impairs testicular recrudescence in the air-breathing catfish, Clarias gariepinus. *Comp. Biochem. Physiol. A Mol. Integr. Physiol.* **144**, 1-10.
Taylor, J. S., Braasch, I., Frickey, T., Meyer, A. and Van de Peer, Y. (2003). Genome duplication, a trait shared by 22,000 species of ray-finned fish. *Genome Res.* **13**, 382-390.
Tonacchera, M., De Marco, G., Agretti, P., Montanelli, L., Di Cosmo, C., Freitas Ferreira, A. C., Dimida, A., Ferrarini, E., Ramos, H. E., Ceccarelli, C. et al. (2009). Identification and functional studies of two new dual-oxidase 2 (DUOX2) mutations in a child with congenital hypothyroidism and a eutopic normal-size thyroid gland. *J. Clin. Endocrinol. Metab.* **94**, 4309-4314.
Trijuno, D. D., Yoseda, K., Hirokawa, J., Tagawa, M. and Tanaka, M. (2002). Effects of thyroxine and thiourea on the metamorphosis of coral trout grouper Plectropomus leopardus. *Fish. Sci.* **68**, 282-289.
Trubiroha, A., Gillotay, P., Giusti, N., Gacquer, D., Libert, F., Lefort, A., Haerlingen, B., De Deken, X., Opitz, R. and Costagliola, S. (2018). A rapid CRISPR/Cas-based mutagenesis assay in zebrafish for identification of genes involved in thyroid morphogenesis and function. *Sci. Rep.* **8**, 5647.
Velasco, I. and Taylor, P. (2018). Identifying and treating subclinical thyroid dysfunction in pregnancy: emerging controversies. *Eur. J. Endocrinol.* **178**, D1-D12.
Vigone, M. C., Fugazzola, L., Zamproni, I., Passoni, A., Di Candia, S., Chiumello, G., Persani, L. and Weber, G. (2005). Persistent mild hypothyroidism associated with novel sequence variants of the DUOX2 gene in two siblings. *Hum. Mutat.* **26**, 395-395.
Virtanen, M., Mäenpää, J., Santavuori, P., Hirvonen, E. and Perheentupa, J. (1983). Congenital hypothyroidism: age at start of treatment versus outcome. *Acta Pædiatr.* **72**, 197-201.
Wendl, T., Lun, K., Mione, M., Favor, J., Brand, M., Wilson, S. W. and Rohr, K. B. (2002). Pax2.1 is required for the development of thyroid follicles in zebrafish. *Development* **129**, 3751-3760.
Weyemi, U., Caillou, B., Talbot, M., Ameziane-El-Hassani, R., Lacroix, L., Lagent-Chevallier, O., Al Ghuzlan, A., Roos, D., Bidart, J.-M., Virion, A. et al. (2010). Intracellular expression of reactive oxygen species-generating NADPH oxidase NOX4 in normal and cancer thyroid tissues. *Endocr. Relat. Cancer* **17**, 27-37.
White, R. M., Sessa, A., Burke, C., Bowman, T., LeBlanc, J., Ceol, C., Bourque, C., Dovey, M., Goessling, W., Burns, C. E. et al. (2008). Transparent adult zebrafish as a tool for in vivo transplantation analysis. *Cell Stem Cell* **2**, 183-189.
Wills, A. A., Kidd, A. R., Lepilina, A. and Poss, K. D. (2008). Fgfs control homeostatic regeneration in adult zebrafish fins. *Development* **135**, 3063-3070.
Winata, C. L., Korzh, S., Kondrychyn, I., Zheng, W., Korzh, V. and Gong, Z. (2009). Development of zebrafish swimbladder: the requirement of Hedgehog signaling in specification and organization of the three tissue layers. *Dev. Biol.* **331**, 222-236.
Zimmermann, M. B. (2011). The role of iodine in human growth and development. *Semin. Cell Dev. Biol.* **22**, 645-652.

Manuscript #3 - Letter

Zebrafish *nox5* mutations: A brief description of an anaesthesia-resistance phenotype

Zebrafish *nox5* mutations: A brief description of an anaesthesia-resistance phenotype

Kunal Chopra[1], Enrique Amaya[1ʃʃ]

[1]Division of Cell Matrix Biology & Regenerative Medicine, Michael Smith Building, School of Biological Sciences, Faculty of Biology, Medicine and Health, University of Manchester, Oxford Road, Manchester, United Kingdom

[ʃʃ]Corresponding author

Email addresses:

KC: kunal.chopra@postgrad.manchester.ac.uk

EA: Enrique.amaya@manchester.ac.uk

Zebrafish *nox5* mutations: A brief description of an anaesthesia-resistance phenotype

A summary of ROS-producing enzymes

ROS include superoxide anion ($O_2^{\bullet -}$), hydrogen peroxide (H_2O_2), hydroxyl radicals and an assortment of their reaction products (Lambeth 2004; Nathan and Ding 2010). While, the mitochondrion is a major production centre of ROS (Moldovan and Moldovan 2004), enzymatic production of ROS via the transmembrane NOXes has been a major focus of investigations on pathologies (Buvelot et al. 2016; Muzza and Fugazzola 2017) and regeneration (Gauron et al. 2013; Zhang et al. 2016).

Seven NOX isoforms are presently recognised, viz. NOX1, 2, 3, 4, 5, and DUOX1 and 2. Zebrafish, the model described in this essay, lacks Nox3 and has a single Duox (Kawahara, Quinn, and Lambeth 2007). All NOXes produce H_2O_2, either via the dismutation of superoxide (NOX 1-5) mediated by superoxide dismutase (SOD), or, directly (DUOX1-2) (Ameziane-el-hassani et al. 2005). In line with this preserved function, all NOXes share structural homology including an NADPH-binding site at the intracellular C-terminus, a FAD-binding region in the proximity of the most C-terminal transmembrane domain, six conserved transmembrane domains, and four highly conserved heme-binding histidines (Bedard and Krause 2007). Their biochemical function is tightly regulated by additional subunits, regulatory proteins and ions. These include $P22^{phox}$ (CYBA), $P47^{phox}$ and $P67^{phox}$ (Bedard and Krause 2007). While NOX3 and 4 are believed to be constitutively active, NOX5, DUOX1, and DUOX2 are activated by Ca^{2+} and do not appear to require subunits (Bedard and Krause 2007). With the discovery of the NOXes and their regulated production of ROS, the negative reputation of ROS has somewhat given way to an appreciation of their functions in signalling, innate immunity but also possible roles in disease.

Having only being discovered in 2001 (Bánfi et al. 2001; Cheng et al. 2001), Nox5 is the most recently characterised NOX. Structural peculiarities of NOX5 include a

unique N-terminal extension called the EF hand, which features Ca^{2+} binding domains. NOX5 activation is entirely Ca^{2+} dependent. It is unusual in that it is missing in rodents, yet is found in other mammals and non-mammalian vertebrates (Touyz et al. 2019). Clinical significance for NOX5 comes from its implications in neurodegenerative disease (Tarafdar and Pula 2018) and pulmonary arterial hypertension (Peng et al. 2017). Also, using mice expressing NOX5 in a muscle-specific manner, and the triatomine bug *Rhodnius prolixus*, NOX5 has recently been shown to regulate vascular contraction and smooth muscle contraction (Montezano et al. 2018).

As an enzymatic source of ROS, Nox5 was one of our targets for investigating its role in regeneration of the zebrafish caudal fin, post amputation. *nox5* was successfully targeted via CRISPR/Cas9, but adult animals did not display any noticeable phenotypes. Thus, the question emerged as to whether the mutation led to a functional defect. Indeed, a phenotype was uncovered when animals were exposed to the anaesthetic MS-222. We hypothesised that *nox5* mutants experience increased resistance to anaesthesia.

Materials and Methods

Zebrafish husbandry

Zebrafish (*Danio rerio*) husbandry was undertaken in a re-circulating system maintained at 28.5°C, with a 14h photoperiod. These conditions are uniform for wild type and all GM strains. Embryos were obtained by marbling tanks, or by isolating pairs in breeding chambers. All animal work was performed under a Home Office Licence.

Genomic Extraction

Fish were anaesthetised using 0.4 mg/mL (0.04%) MS-222 (Sigma Aldrich). Fin clips from caudal or anal fins of individual adults were added to a mixture of lysis Buffer (10mM Tris-HCL, pH 8.0, 1mM EDTA, 0.3% Tween-20, 0.3% NP40), and proteinase K (20-25mg/ml), 1ul/50ul lysis buffer. This was incubated in a thermal cycler programmed to 55°C (2hours), 95°C (10 minutes) and a 12°C hold.

sgRNA design and production of CRISPR mutants

Single guide RNAs (sgRNAs) were designed for targeting exon exon 4 of *nox5*, using the online tool CRISPRscan. Entering the Ensemble ID for each gene automatically listed multiple gRNAs against coding exons. gRNAs were then chosen based on rank, location within the first 50% of the ORF, and

distance from the initiation codon. A sgRNA template requires a 52nt oligo (sgRNA primer) 5' TAATACGACTCACTATAGG(N=18)GTTTTAGAGCTAGAA, containing the T7 promoter, the 20nt specific DNA-binding sequence [GG(N=18)] and a constant 15nt tail annealing sequence. This was annealed to an 80nt reverse oligo AAAAGCACCGACTCGGTGCCACTTTTTCAAGTTGATAACGGACTAGCCTTATTTTAACTTGCTATTTCTAGCTC TAAAAC invariant 3' end (tail primer) to generate a 117bp PCR product. Oligos were obtained from Sigma-Aldrich®. The PCR cycler settings for this primer extension were 3 min at 95°C; 30 cycles of 30s at 95°C, 30s at 45°C and 30s at 72°C; and a final step at 72°C for 7 min. PCR products were purified using Qiaquick (Qiagen) columns, and approximately 120–150ng of DNA were used as a template for a T7 *in vitro* transcription reaction. *In vitro* transcribed sgRNAs were treated with DNase and precipitated using sodium acetate and ethanol (Moreno-mateos et al. 2015). Purified sgRNA and Cas9-NLS protein (New England Biolabs® Inc.) were diluted to 300ng/ul. Equal volumes of Cas9-NLS protein, sgRNA and Phenol Red (Sigma-Aldrich®) were mixed to obtain the final injection mix. Injection drop size was adjusted to 1nl using a graticule scale. All embryos were injected at the one-cell stage. F_1 heterozygous animals were identified via restriction digest with HaeIII, and indels were characterised using Sanger sequencing.

Polymerase Chain Reaction

PCRs for were undertaken using ExTaq DNA Polymerase (TaKaRa). Primers used are listed below**.** The T_M for the primer pair was 55C.

nox5 F	GCTCAAGGGCTTACATGATCC	Genomic PCR for CRISPR mutants
nox 5 R	GCCTCAACATCAGCACCTAC	Genomic PCR for CRISPR mutants
M13 Reverse	GTAAAACGACGGCCAGTG	For identifying indels

Statistical analyses

Comparisons were made via an unpaired t-test using Prism 8.1 (GraphPad Software, Inc.). Significance was assumed at $P<0.05$.

Results

Generation and molecular characterisation of a *nox5* mutant allele

Zebrafish *nox5* is mapped to chromosome 25: 7,927,349-7,946,732, on the reverse strand. It has 2 splice variants, both of which are protein coding (Ensemble 84 Mar 2016). In the zebrafish, *nox5* has 16 exons. To achieve early protein truncation, we targeted two sequences on exon 4 (which is shared by both variants). A single mutation was identified among individual F_1 animals, which were obtained by crossing F_0 adults to WTs. This was found to be a 4bp indel (2novel BPs and 2 deleted

BPs) leading to a frameshift mutation. Incrossing F_1 heterozygotes led to the establishment of a stable mutant line harbouring this indel (**Fig. 1**), hereafter referred to as *nox*$^{ex4.4bp-/-}$. The CRISPR-targeted region of exon 4 includes a diagnostic HaeIII restriction site, which enabled easy identification of mutants from WT animals. Mutants are viable and fertile.

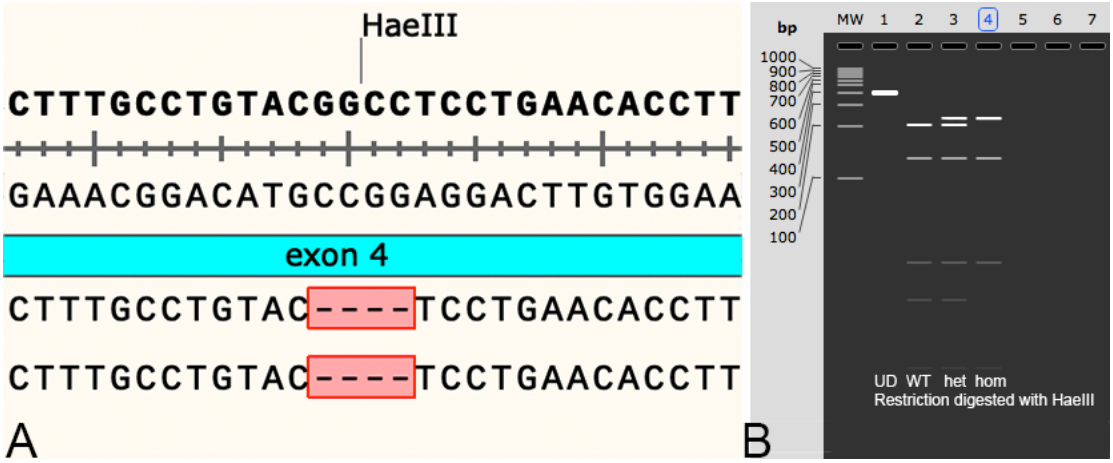

Fig. 1. CRISPR/Cas9-mediated mutation of exon 4 in zebrafish *nox5*. A. 4bp indel leads to the loss of a restriction site for HaeIII. B. Electrophoresis gel showing the identification of mutants via restriction digest.

nox5 mutants display resistance to MS-222

While anaesthetising animals for a caudal fin amputation experiment, most mutants appeared to take longer than usual to respond to the anaesthetic tricaine methanesulfonate (MS-222). After the animals had made a full recovery of the amputated fin, we decided to investigate further the response to anaesthetic. As per standard protocol, MS-222 was freshly prepared. *nox*$^{ex4.4bp-/-}$ adults (n=22) and WT adults (n=23) were individually immersed in anaesthetic, in a beaker. Two attributes were measured: 1) righting reflex, and 2) cessation of opercular movement. The righting reflex serves to resume orientation when the body loses its upright orientation. All WT animals lost the righting reflex in under 30s following immersion. A simple tapping of the surface on which the beaker was placed elicited no response from the WTs. Meanwhile, *nox*$^{ex4.4bp-/-}$ took upto 360s to achieve loss of the righting reflex (**Fig. 2**). Even though they stopped swimming, mutants remained responsive to the tapping by responding with jerky, erratic movements. Loss of opercular movement in WTs took upto 200s, while in the mutants this took as long as 382s

(**Fig. 2**). Interestingly, most mutants appeared to lose the righting reflex very close to cessation of opercular movement. Overall, we found that *nox5* mutants show a prolonged resistance to a commonly used anaesthetic.

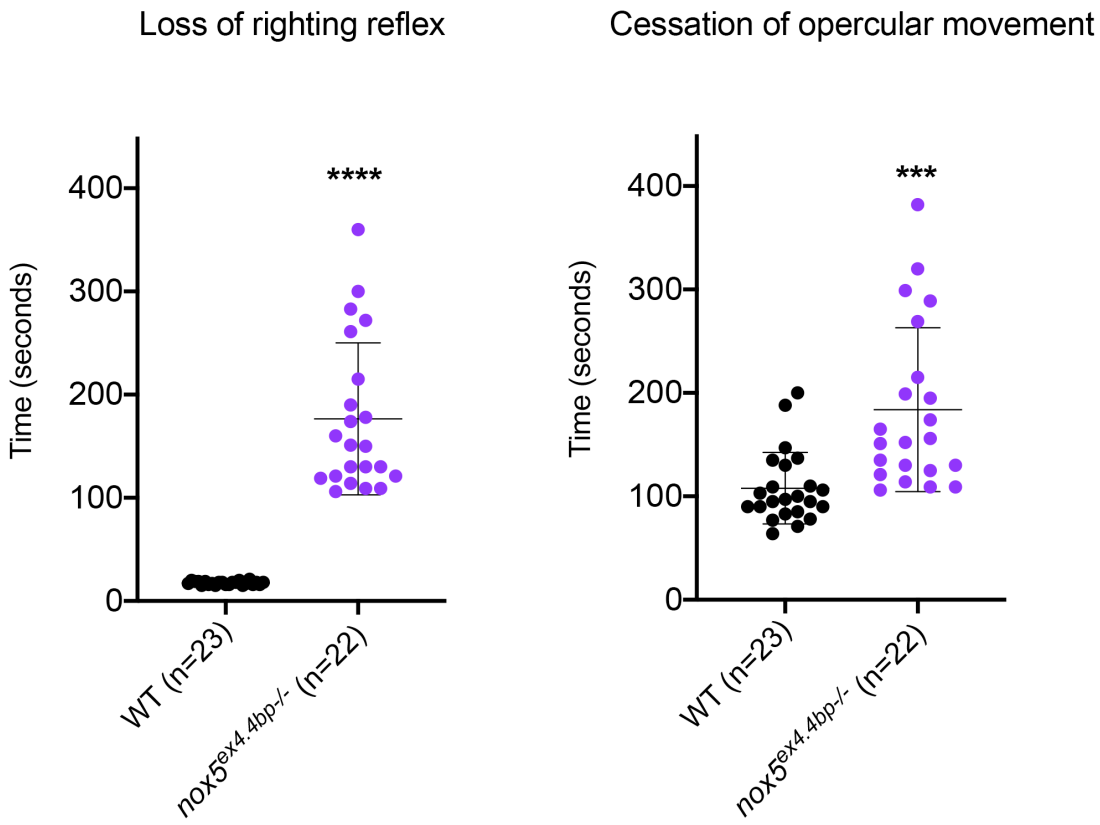

Fig. 2. *nox5* mutants show increased resistance to MS-222. Unpaired t test **** P< 0.0001, *** P 0.0001.

Discussion

In this brief correspondence we describe a phenotype for anaesthesia resistance in *nox5* mutant zebrafish. As the newest nox to be discovered, and being absent in rodents, characterisation of *nox5* mutations is still nascent. The idea for generating a *nox5* mutant came from a need to investigate whether nox5-mediated ROS influences regeneration in the zebrafish caudal fin. A prior consideration to targeting genome sequences in fish is the complete genome duplication event that occurred after the divergence of the ray-finned and lobe-finned fishes, in the common ancestor of zebrafish and 22,000 other ray-finned species (Taylor et al. 2003). A nucleotide BLAST of PCR primers for *nox5*, as well as a protein BLAST for Nox5 did

not reveal any additional paralogues. Then, using CRISPR/Cas9, we successfully targeted *nox5* to establish a loss of function allele for the gene.

nox$^{ex4.4bp-/-}$ mutants have no phenotypic distinctions from WT fish, and thus, the revelation of a phenotype was serendipitous, yet inevitable given that anaesthesia is applied to adults while performing fin amputation. MS-222 is by far the commonest anaesthetic for fish (Harper and Lawrence 2011) and amphibians (Dodelet-devillers, Roy, and Vachon 2016). It acts by depolarising Na^+ channels, leading to unconsciousness, immobility, and ultimately vascular collapse. Death occurs due to hypoxia (Matthews and Varga 2012). Studies on MS-222 tolerance have mainly centred around identifying optimum anaesthetising (Dodelet-devillers, Roy, and Vachon 2016), or euthanising concentrations (Collymore, Banks, and Turner 2016; Wallace et al. 2018), rather than in the context of mutation-related resistance. However, there are two pieces of work that focus on anaesthesia, ROS and regeneration. According to one report, the inhibition of Na^+ channels achieved by MS-222 application deters regeneration in *Xenopus laevis* tadpoles, thus highlighting the importance of these channels during regeneration (Tseng et al. 2010). In a second interesting example, anaesthetic preconditioning (APC) of rat cardiomyocytes with the anaesthetics desflurane and sevoflurane has been shown to correlate with the magnitude of mitochondrial ROS production (Sedlic et al. 2009). APC is a method that can be used to elicit the innate defence cardiac mechanisms that are only triggered during ischemic injury.

A very quick method of corroborating our findings would be treating WT fish with Nox-specific inhibitors, such as VAS2870, which has previously been shown to interfere with regeneration of the zebrafish caudal fin (Gauron et al. 2013). Equally, to determine if the mutation specifically affects the effect of MS-222, it would be interesting to look at the action of other anaesthetics. For zebrafish, evaluated protocols exist for gradual cooling, lidocaine hydrochloride, metomidate hydrochloride, and isoflurane (Collymore et al. 2014), and etomidate, propofol and ketamine (Martins et al. 2018). From the perspective of animal licensing conditions, any anaesthetic aside from MS-222 would require approval, given their chemical

natures. However, gradual cooling (Collymore et al. 2014) may be a straightforward option as it only involves water. Gradual cooling slowed opercular movement at 10.3 °C. Average recovery time was also reported to be significantly ($P \leq 0.001$) less for gradual cooling (0s), compared to that for MS222 (140s). Importantly, fish exposed to gradual cooling achieved a surgical plane of anaesthesia, similar to the effects of exposure to MS-222 (Collymore et al. 2014).

nox5 mutations have very recently been generated in zebrafish, and these were examined in the context of optical tectum development. Mutants were observed to suffer from decreased innervation of the tectum. However, these were reported to be embryonic lethal (Weaver et al. 2018). Given that our mutants are not embryonic lethal, it may be possible to investigate this further. Finally, cues may be taken from other *nox* mutants for identifying other phenotypes. *duox* mutants exhibit unmistakable external and physiological phenotypes (Chopra, Ishibashi, and Amaya 2019) none of which were evident in $nox^{ex4.4bp-/-}$ animals. cyba mutants, however, appear healthy unless exposed to *Aspergillus sps*., which produces significant mortality in comparison to WT siblings. It would be interesting to expose $nox^{ex4.4bp-/-}$ animals and compare their susceptibility to infection.

While an in-depth knowledge of the pharmacodynamics of anaesthetics and the workings of ion channels would be instrumental in further explaining our observations, we find that a *nox5* mutant of zebrafish demonstrates resistance to anaesthesia, and maybe a useful model to uncover new interactions of the NOXes.

References

1. Ameziane-el-hassani, Rabii, Stanislas Morand, Jean-luc Boucher, Yves-michel Frapart, Diane Agnandji, Marie-sophie Noe, Jacques Francon, Khalid Lalaoui, Alain Virion, and Corinne Dupuy. 2005. "Dual Oxidase-2 Has an Intrinsic Ca 2 -Dependent H 2 O 2 -Generating Activity *" 280 (34): 30046–54. https://doi.org/10.1074/jbc.M500516200.
2. Bánfi, Botond, Gergely Molnár, Andres Maturana, Klaus Steger, Balázs Hegedûs, Nicolas Demaurex, and Karl-Heinz Krause. 2001. "A Ca2+-Activated NADPH Oxidase in Testis, Spleen, and Lymph Nodes ." *Journal of Biological Chemistry* 276 (40): 37594–601. https://doi.org/10.1074/jbc.M103034200.
3. Bedard, Karen, and Karl-Heinz Heinz Krause. 2007. "The NOX Family of ROS-Generating NADPH Oxidases: Physiology and Pathophysiology." *Physiological Reviews* 87 (1): 245–313. https://doi.org/10.1152/physrev.00044.2005.
4. Buvelot, Helene, Klara M Posfay-Barbe, Patrick Linder, Jacques Schrenzel, and Karl-Heinz Krause. 2016. "Staphylococcus Aureus, Phagocyte NADPH Oxidase and Chronic Granulomatous Disease." *FEMS Microbiology Reviews* 41 (2): 139–57. https://doi.org/10.1093/femsre/fuw042.
5. Cheng, Guangjie, Zehong Cao, Xiangxi Xu, Erwin G.Van Meir, and J.David Lambeth. 2001. "Homologs of Gp91phox: Cloning and Tissue Expression of Nox3, Nox4, and Nox5." *Gene* 269 (1): 131–40. https://doi.org/https://doi.org/10.1016/S0378-1119(01)00449-8.
6. Chopra, Kunal, Shoko Ishibashi, and Enrique Amaya. 2019. " Zebrafish Duox Mutations Provide a Model for Human

Congenital Hypothyroidism .” *Biology Open* 8 (2): bio037655. https://doi.org/10.1242/bio.037655.
7. Collymore, Chereen, E Kate Banks, and Patricia V Turner. 2016. “Lidocaine Hydrochloride Compared with MS222 for the Euthanasia of Zebrafish (Danio Rerio).” *Journal of the American Association for Laboratory Animal Science : JAALAS* 55 (6): 816–20. https://www.ncbi.nlm.nih.gov/pubmed/27931323.
8. Collymore, Chereen, Angela Tolwani, Christine Lieggi, and Skye Rasmussen. 2014. “Efficacy and Safety of 5 Anesthetics in Adult Zebrafish (Danio Rerio).” *Journal of the American Association for Laboratory Animal Science : JAALAS* 53 (2): 198–203. https://pubmed.ncbi.nlm.nih.gov/24602548.
9. Dodelet-devillers, Aurore, Stéphane Roy, and Pascal Vachon. 2016. “Evaluation of the Anesthetic Effects of MS222 in the Adult Mexican Axolotl (Ambystoma Mexicanum),” 1–7.
10. Gauron, Carole, Christine Rampon, Mohamed Bouzaffour, Eliane Ipendey, Jeremie Teillon, Michel Volovitch, and Sophie Vriz. 2013. “Sustained Production of ROS Triggers Compensatory Proliferation and Is Required for Regeneration to Proceed.” *Scientific Reports* 3: 1–9. https://doi.org/10.1038/srep02084.
11. Kawahara, By Tsukasa, Mark T. Quinn, and J. David Lambeth. 2007. “Molecular Evolution of the Reactive Oxygen-Generating NADPH Oxidase (Nox/Duox) Family of Enzymes.” *BMC Evolutionary Biology* 7: 1–21. https://doi.org/10.1186/1471-2148-7-109.
12. Lambeth, J. David. 2004. “NOX Enzymes and the Biology of Reactive Oxygen.” *Nature Reviews Immunology* 4 (3): 181–89. https://doi.org/10.1038/nri1312.
13. Martins, Tânia, Enoque Diniz, Luís M Félix, and Luís Antunes. 2018. “Evaluation of Anaesthetic Protocols for Laboratory Adult Zebrafish (Danio Rerio).” *PloS One* 13 (5): e0197846–e0197846. https://doi.org/10.1371/journal.pone.0197846.
14. Matthews, Monte, and Zoltán M Varga. 2012. “Anesthesia and Euthanasia in Zebrafish.” *ILAR Journal* 53 (2): 192–204. https://doi.org/10.1093/ilar.53.2.192.
15. Moldovan, Leni, and Nicanor I. Moldovan. 2004. “Oxygen Free Radicals and Redox Biology of Organelles.” *Histochemistry and Cell Biology* 122 (4): 395–412. https://doi.org/10.1007/s00418-004-0676-y.
16. Montezano, Augusto C, Livia De Lucca Camargo, Patrik Persson, Francisco J Rios, Adam P Harvey, Aikaterini Anagnostopoulou, Roberto Palacios, et al. 2018. “NADPH Oxidase 5 Is a Pro-Contractile Nox Isoform and a Point of Cross-Talk for Calcium and Redox Signaling-Implications in Vascular Function.” *Journal of the American Heart Association* 7 (12): e009388. https://doi.org/10.1161/JAHA.118.009388.
17. Moreno-mateos, Miguel A, Charles E Vejnar, Jean-denis Beaudoin, Juan P Fernandez, Emily K Mis, Mustafa K Khokha, and Antonio J Giraldez. 2015. “CRISPRscan : Designing Highly Efficient SgRNAs for CRISPR-Cas9 Targeting in Vivo” 12 (10). https://doi.org/10.1038/nmeth.3543.
18. Muzza, Marina, and Laura Fugazzola. 2017. “Disorders of H2O2 Generation.” *Best Practice and Research: Clinical Endocrinology and Metabolism* 31 (2): 225–40. https://doi.org/10.1016/j.beem.2017.04.006.
19. Nathan, Carl, and Aihao Ding. 2010. “SnapShot : Reactive Oxygen Intermediates (ROI),” 8–10. https://doi.org/10.1016/j.cell.2010.03.008.
20. Peng, Jing-Jie, Bin Liu, Jin-Yun Xu, Jun Peng, and Xiu-Ju Luo. 2017. “NADPH Oxidase: Its Potential Role in Promotion of Pulmonary Arterial Hypertension.” *Naunyn-Schmiedeberg’s Archives of Pharmacology* 390 (4): 331–38. https://doi.org/10.1007/s00210-017-1359-2.
21. Sedlic, Filip, Danijel Pravdic, Marko Ljubkovic, Jasna Marinovic, Anna Stadnicka, and Zeljko J Bosnjak. 2009. “Differences in Production of Reactive Oxygen Species and Mitochondrial Uncoupling as Events in the Preconditioning Signaling Cascade between Desflurane and Sevoflurane.” *Anesthesia and Analgesia* 109 (2): 405–11. https://doi.org/10.1213/ane.0b013e3181a93ad9.
22. Tarafdar, Anuradha, and Giordano Pula. 2018. “The Role of NADPH Oxidases and Oxidative Stress in Neurodegenerative Disorders.” https://doi.org/10.3390/ijms19123824.
23. Taylor, Js, Ingo Braasch, Tancred Frickey, and Axel Meyer. 2003. “Genome Duplication, a Trait Shared by 22 000 Species of Ray-FInned FIsh.” *Genome Research*, 382–90. https://doi.org/10.1101/gr.640303.1.
24. Touyz, Rhian M, Aikaterini Anagnostopoulou, Francisco Rios, Augusto C Montezano, and Livia L Camargo. 2019. “NOX5: Molecular Biology and Pathophysiology.” *Experimental Physiology* 104 (5): 605–16. https://doi.org/10.1113/EP086204.
25. Tseng, Ai-Sun, Wendy S Beane, Joan M Lemire, Alessio Masi, and Michael Levin. 2010. “Induction of Vertebrate Regeneration by a Transient Sodium Current.” *The Journal of Neuroscience : The Official Journal of the Society for Neuroscience* 30 (39): 13192–200. https://doi.org/10.1523/JNEUROSCI.3315-10.2010.
26. Wallace, Chelsea K, Lauren A Bright, James O Marx, Robert P Andersen, Mary C Mullins, and Anthony J Carty. 2018. “Effectiveness of Rapid Cooling as a Method of Euthanasia for Young Zebrafish (Danio Rerio).” *Journal of the American Association for Laboratory Animal Science : JAALAS* 57 (1): 58–63. https://www.ncbi.nlm.nih.gov/pubmed/29402353.
27. Weaver, Cory J, Aslihan Terzi, Haley Roeder, Theodore Gurol, Qing Deng, Yuk Fai Leung, and Daniel M Suter. 2018. “Nox2/Cybb Deficiency Affects Zebrafish Retinotectal Connectivity.” *The Journal of Neuroscience* 38 (26): 5854 LP – 5871. https://doi.org/10.1523/JNEUROSCI.1483-16.2018.
28. Zhang, Qing, Yongjun Yingjie Wang, Lili Man, Ziwen Zhu, Xue Bai, Sumei Wei, Yan Liu, et al. 2016. “Reactive Oxygen Species Generated from Skeletal Muscles Are Required for Gecko Tail Regeneration.” *Scientific Reports* 6 (February): 20752. https://doi.org/10.1038/srep20752.

Manuscript #4

Zebrafish *nox* mutations reveal an oscillatory pattern of ROS production during regeneration

Zebrafish *nox* mutations reveal an oscillatory pattern of ROS production during regeneration

Kunal Chopra[1], Milda Folkmanaite[2], Shoko Ishibashi[1], Enrique Amaya[1ʃʃ]

[1]Division of Cell Matrix Biology & Regenerative Medicine, Michael Smith Building, School of Biological Sciences, Faculty of Biology, Medicine and Health, University of Manchester, Oxford Road, Manchester, United Kingdom

[2] Division of Medicine, University College London, Gower Street, London, United Kingdom

[ʃʃ]Corresponding author

Email addresses:

KC: kunal.chopra@postgrad.manchester.ac.uk

EA: Enrique.amaya@manchester.ac.uk

Zebrafish *nox* mutations reveal an oscillatory pattern of ROS production during regeneration

Abstract

A sustained increase in ROS is essential for regeneration to occur in various models systems ranging from the fin in zebrafish, to the tail in frogs, salamanders and geckos. This effect of ROS has been, so far, demonstrated using pharmacological compounds such as diphenyleneiodonium and apocynin, which target various sources of ROS including the transmembrane NADPH oxidases (NOXes). We wanted to focus on the role of NOXes in regeneration, and so we generated *nox* mutants by targeting *duox*, *nox5* and *cyba* (a key subunit of NOXes 1-4). Further, to estimate their individual contribution to ROS production these mutants were generated in a transgenic background, *HyPer*, which specifically helps visualise H_2O_2 flux. We found that ROS levels remain elevated for up to two weeks post-amputation in wild type animals, but only a week among *nox* mutants. While regeneration did not cease, a consequence of this reduced ROS flux was a significantly reduced rate of caudal fin regeneration among *cyba* and *duox* mutants. We also provide clues into the possible temporal distribution of Nox activity post-amputation. Finally, we show that ROS levels, both in the amputated and unamputated state, oscillate during the day.

INTRODUCTION

The presence of a H_2O_2 gradient, akin to a paracrine signal, attracting leukocytes to a wound was first demonstrated in the zebrafish larval tail (Niethammer et al. 2009). Pioneering work then in *Xenopus* (Love et al. 2013) and zebrafish (Gauron et al. 2013) established that amputation-induced ROS were vital for caudal regeneration. These reports collectively indicated that epidermal wounding prompted an increase in the levels of intracellular H_2O_2, which were sustained until the completion of healing. Post-wounding gene expression assays in *Xenopus tropicalis* revealed a number of genes involved in the production of ROS to exhibit "significant modulation" (Love et al. 2011).

ROS and its manufacturing enzymes

ROS are a family of chemically reactive, oxygen-containing biomolecules that includes singlet oxyradical, superoxide anion ($O_2^{\bullet -}$), hydroxyl radical ($OH^{\bullet}$), peroxyl

($RO_2^{\bullet}$), & alkoxyl (RO^{-}) and non-radicals such as hydrogen peroxide (H_2O_2) (Mailloux 2015). Exhaustive literature ascribes the production and roles of ROS varying from being the by-products of aerobic respiration causing oxidative stress to regulated products of enzymatic activity participating in signalling. A major source of physiological H_2O_2 is believed to be a series of enzymes, namely the NADPH oxidases (NOXes). Seven NOX isoforms are presently recognised. These are NOX1, NOX2, NOX3, NOX4, NOX5, DUOX1 and DUOX2. The zebrafish does not have Nox3 and has a single Duox instead of DUOX1 and DUOX2 (Kawahara, Quinn, and Lambeth 2007). While Nox1–5 generate superoxide, which requires dismutation into H_2O_2 by a separate superoxide dismutase (SOD), DUOXes generate H_2O_2 without requiring a separate SOD (Ameziane-el-hassani et al. 2005). In line with their preserved function, all NOX enzymes exhibit structural and functional conservation. Common structural attributes include 1) an NADPH-binding site at the COOH terminus, 2) a FAD-binding region in the proximity of the most COOH-terminal transmembrane domain, 3) six conserved transmembrane domains, and 4) four highly conserved heme-binding histidines (Bedard and Krause 2007) (**Fig. 1**). Localisation of NOXes is reported on the plasma membrane (Bedard and Krause 2007), nuclear membrane (Hilenski et al. 2004), and the mitochondria (Ameziane-el-hassani et al. 2005). For their biochemical function the NOX enzymes feature additional subunits, regulatory proteins and ions. Among these, $P22^{phox}$ (CYBA) plays an essential role in the maturation and structural integrity of NOXes 1-4 (Bedard and Krause 2007). For example, phagocytes from cyba-deficient patients have no detectable NOX2 protein (Dinauer et al. 1990; Stasia et al. 2002) and *cyba* mutant mice suffer from vestibular defects brought on by NOX3 instability (Nakano et al. 2008). At least NOX3 and 4 are believed to be constitutively active. NOX5, DUOX1, and DUOX2 are activated by Ca^{2+} and do not appear to require subunits. For their activity DUOX 1 and 2 require the maturation factors DUOXA1 and DUOXA2, respectively (Bedard and Krause 2007) (**Fig. 1**). Interestingly, in zebrafish, the maturation factor for Duox is perplexingly called Duox2.

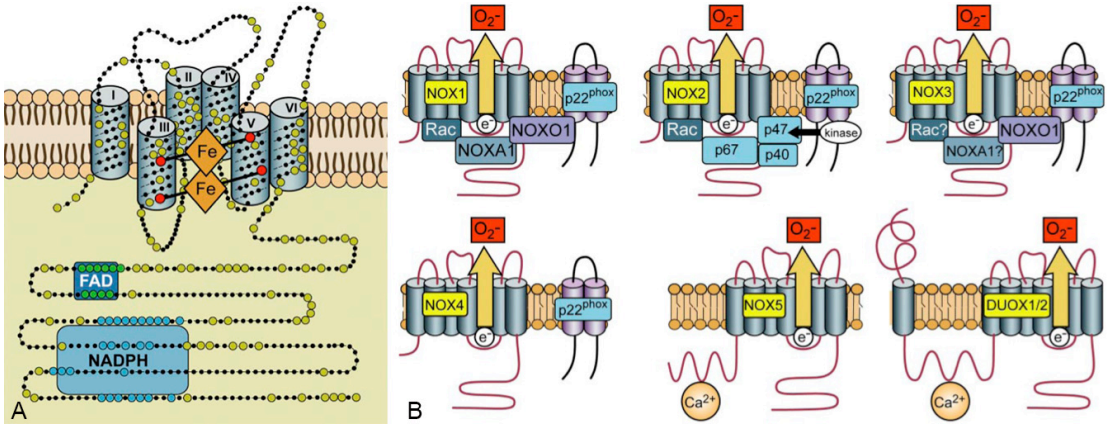

Fig. 1. The NOX enzymes. A. Consensus structure of a NOX enzyme. As single electron transporters, NOX enzymes pass electrons from NADPH to the electron acceptor oxygen, on the other side of the membrane. B. Activation of NOX isoforms. Regardless of their structural similarities, NOX enzymes differ in their activation, requiring various subunits, regulatory proteins and ions (Adapted from Bedard and Krause, 2007).

The suitability of ROS as signalling molecules is contingent on their reactivity. •OH is believed to be the most toxic ROS since it indiscriminately reacts with most biomolecules that it encounters. Meanwhile $O_2•^-$ and H_2O_2 are less reactive and have longer half-lives. H_2O_2 acts as a signalling molecule via the oxidation of protein cysteine thiols (Moldovan and Moldovan 2004). Relative chemical stability and diffusibility across cell membranes qualify it as a paracrine signalling molecule.

Defining regeneration

Regeneration is defined as a process that permits organisms to regain the functionality of organs or structures following injury or disease (Stoick-Cooper, Moon, and Weidinger 2007), a process that likely involves common mechanistic principles operating regardless of the extent of damage, tissue, age and maybe conserved across species (Yoshinari et al. 2009). Caudal fin regeneration in the zebrafish fin is described as epimorphic. In the words of T H Morgan (1901) this refers to "*the case of regeneration in which a proliferation of material precedes the development of the new part*". The proliferative tissue that forms at the amputation margin is the blastema, and in the zebrafish it is now established that blastema formation results from migrating fibroblasts and dedifferentiating osteoblasts (Knopf et al. 2011; Pfefferli and Jaźwińska 2015).

Gene expression changes during regeneration

Gene expression changes during tadpole tail regeneration have been measured in *Xenopus tropicalis* (Love et al. 2011) and *Xenopus laevis* (Tazaki et al. 2005). Data were categorised into functional categories including inflammation response, wound healing, cell proliferation, cell signalling, cell differentiation, cell structure and unclassified. In *Xenopus tropicalis*, a surprising find of this microarray was that **"**H_2O_2 metabolic process**"**, **"**superoxide metabolic process**"**, **"**NADP metabolic process**"**, **"**nicotinamide metabolic process**"** and **"**oxygen and ROS metabolic process**"** came up amongst the top ten most upregulated processes in the first 24hpa, when compared to levels immediately after amputation. The modulation of these NADP/H related genes suggested a role for NADPH-dependent metabolic processes during tail regeneration (Love et al. 2011). Similarly, the most abundantly modulated functional groups during zebrafish larval fin fold and adult fin regeneration included molecules related to metabolism (40%), followed by signalling proteins (16.0%), transcription factors (15.2%), and cell cycle regulators (7.2%) (Yoshinari et al. 2009).

Early injury signals during regeneration

At the onset of injury, highly conserved immediate damage signals are triggered at the cellular level. These signals mediate early, transcription-independent wound responses and contribute to the activation of various ligands and receptors to activate signalling pathways and gene transcription. Even though wound-healing processes are multifactorial complex molecular mechanisms, consensus points to the common importance of three inter-related diffusible molecular mechanisms as the earliest responses to wounding (Cordeiro and Jacinto 2013). The first of these is Ca^{2+}, which is kept at very low steady-state cytosolic levels (**<**100 nM) compared to mM extracellular concentrations, thus creating a steep Ca^{2+} gradient across the plasma membrane. Zebrafish models of tail fin injury have demonstrated that rapid Ca^{2+} flashes in response to injury are directly responsible for early H_2O_2 production mediated by duox (Razzell et al. 2013). Purinergic molecules such as ATP are the second highly conserved danger signal. These are abundant intracellularly in healthy cells (estimated to be **~**100mM in case of ATP) compared to dramatically lower extracellular concentrations. For example, bronchial epithelial cells when subject to

wounding stimuli exhibit rapid wound-induced H_2O_2 production due to the activation of DUOX1, in response to ATP-dependent signalling through P2Y purinoceptors (Van Der Vliet and Janssen-Heininger 2014). Thus, Ca^{2+} and ATP-dependent signalling come together to mediate the cellular production of ROS, which can be regarded as the third early damage signal.

ROS and appendage regeneration

The role of ROS in appendage regeneration was uncovered around the same time in *Xenopus* tadpole tail regeneration (Love et al. 2013) and in the adult zebrafish caudal fin (Gauron et al. 2013). The key observation was the sustained production of ROS up until regeneration concluded. Additionally, the role of cyba attracted interest, as *cyba* morphant *Xenopus* tadpoles showed a 33% reduction in amputation-induced ROS (Love et al. 2013). Meanwhile, employing a pharmacological inhibitor of the NOXes led to a reduction in the blastema size post caudal fin amputation, in the zebrafish (Gauron et al. 2013). More recently, ROS was shown to be essential during the regeneration of the gecko tail, with particular focus on NOX2 (Q. Zhang et al. 2016). The newest report is a description of how ROS initiates regeneration in the axolotl tail (Al Haj Baddar, Chithrala, and Voss 2019). Also, the estimation of ROS necessitates a suitable method, one that is not transient and can regulate itself specifically in response to a dynamic H_2O_2 flux. These criteria were met with the generation of a genetically encoded, H_2O_2-specific, ratiometric sensor called HyPer. HyPer derives its specificity from the regulatory domain of *E. coli* Oxy R, a protein specifically sensitive to H_2O_2. Wild-type OxyR also contains a DNA-binding domain. In the presence of H_2O_2 the reduced form of OxyR converts into its oxidized, DNA-binding form (Zheng, Åslund, and Storz 1998). HyPer features a YFP inserted into the Oxy R, and two excitation peaks at 420 and 500 nm and one emission peak at 516 nm. Upon exposure to H_2O_2, the excitation peak at 420 nm decreases proportionally to the increase in the peak at 500 nm. Upon encountering the antioxidant catalase, HyPer is restored to the initial level several minutes after the H_2O_2 burst. Thus, HyPer reports H_2O_2 as a spectral shift in fluorescence, and also has the added virtue of being reversible in its action, allowing real time estimation of ROS flux (**Fig. 2**) (Belousov et al. 2006).

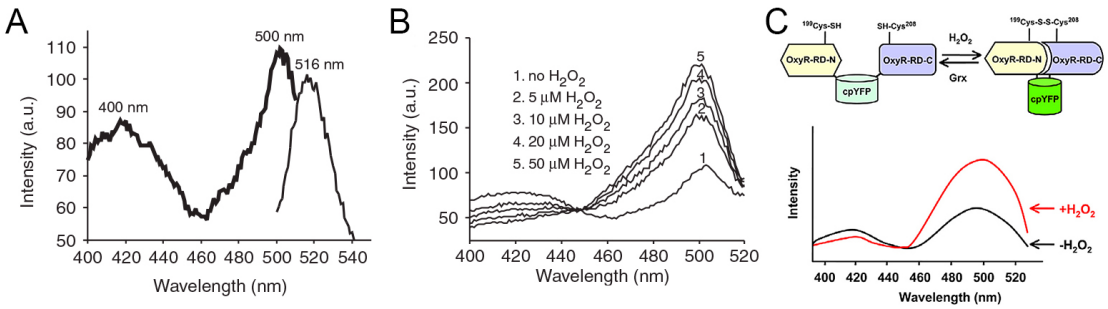

Fig. 2. HyPer is a specific reporter of H_2O_2 flux. **A.** HyPer features two excitation and one emission peak. **B.** A proportional increase of the 500nm peak in relation to the decrease in the 420nm peak occurs when H_2O_2 is encountered. **C.** A schematic showing the reversible property of HyPer. Adapted from Belousov et al. 2006.

ROS and thyroid hormone synthesis

The functional unit of the thyroid gland is the thyroid follicle. It is comprised of thyrocytes, which are polarised cells responsible for TH biosynthesis, storage and secretion. Follicles specialise in the production of thyroxine (T_4) and 3,3',5-triiodothyronine (T_3). THs are synthesised while bound to thyroglobulin, a high molecular weight, thyroid-specific protein. Fundamental chemical reactions for TH synthesis include: (1) iodide oxidation, (2) tyrosyl radical oxidation, (3) iodine organification, and (4) coupling of iodotyrosines to form the iodothyronines, mainly T_4 and T_3 (Carvalho and Dupuy 2013) (**Fig. 3**). Enzymatic reactions involving the oxidation of substrates during this process depend on the presence of H_2O_2 (the oxidant substance) and a catalyst, thyroperoxidase (TPO). H_2O_2 necessary for hormone biosynthesis is generated at the apical surface of the thyrocyte, its main source being DUOX2 (Carvalho and Dupuy 2013), and its usage is rate limited (Gillam and Kopp 2001). Mutations in both, *DUOX1* and *DUOX2* have been reported in human congenital hypothyroidism, indicating their importance for TH biosynthesis (Moreno et al. 2002; Aycan et al. 2017; Kizys et al. 2017; Liu et al. 2019).

A lacuna still remains to be filled about how critical pan nox-mediated ROS really are in the wake of appendage amputation. Specifically, the questions to ask are: 1) Do they work in concert? 2) Is there a critical nox? 3) How long does the ROS flux sustain post-amputation? When discussing regeneration, it is also essential to consider the contribution of growth to the regenerating fin. We begin by showing that growth has a non-significant addition to the regenerating tissue. Then, using CRISPR/Cas9 and

ENU mutants for the *nox*es generated in the lab, we report for the first time the contribution of these NOXes during caudal fin regeneration. Previously, our lab generated transgenic *(HyPer) Xenopus laevis* as a tool for investigating regeneration (Love et al. 2013) and the cell cycle during early development (Han et al. 2018). Here, we describe the successful establishment of a stable transgenic *Tg(HyPEr)* zebrafish reporter line, which we use as a background strain for *nox* mutations. Using *Tg(HyPEr)* animals we estimate the post-amputation ROS flux in various *nox* mutants, while also observing how this flux follows an oscillatory trend. We have recently shown how *duox* mutations in zebrafish recapitulate clinical phenotypes of congenital hypothyroidism (Chopra, Ishibashi, and Amaya 2019), and here arguments are presented for the role of thyroid hormones during regeneration.

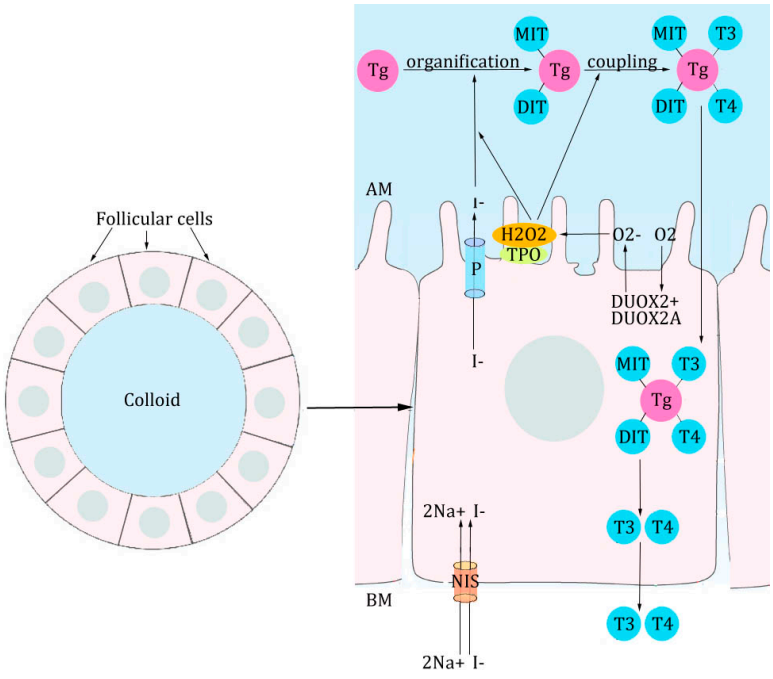

Fig. 3. Thyroid hormone synthesis requires ROS. DUOX generates H_2O_2 at the apical surface. MIT- monoiodotyrosine, DIT- diiodotyrosine, T_4- thyroxine, T_3- triiodotyrosine, Tg- thyroglobulin, TPO- thyroid peroxidase, P- pendrin, NIS- natrium iodide symporter, AM- apical membrane, BM- basal membrane

Materials and Methods

Zebrafish husbandry

Zebrafish (*Danio rerio*) husbandry was undertaken in a re-circulating system maintained at 28.5°C, with a 14h photoperiod. These conditions are uniform for wild type and all GM strains. Embryos were

obtained by marbling tanks, or by isolating pairs in breeding chambers. All animal work was overseen by a Home Office Licence.

Genomic Extraction

Fin clips from caudal or anal fins of individual adults were added to a mixture of lysis Buffer (10mM Tris-HCL, pH 8.0, 1mM EDTA, 0.3% Tween-20, 0.3% NP40), and proteinase K (20-25mg/ml), 1ul/50ul lysis buffer. This was incubated in a thermal cycler programmed to 55°C (2hours), 95°C (10 minutes) and a 12°C hold.

sgRNA design and production of CRISPR mutants

Single guide RNAs (sgRNAs) were designed for targeting exon 1 of *cyba*, and exon 4 of *nox5*, as previously described (Moreno-mateos et al. 2015). Briefly, the Ensemble ID for each gene when entered online on CRISPRscan generated multiple gRNAs. Exon-targeting gRNAs were then chosen based on rank, location within the first 50% of the ORF, and distance from the initiation codon. A sgRNA template requires a 52nt oligo (sgRNA primer) 5' TAATACGACTCACTATAGG(N=18)GTTTTAGAGCTAGAA, containing the T7 promoter, the 20nt specific DNA-binding sequence [GG(N=18)] and a constant 15nt tail annealing sequence. This was annealed to an 80nt reverse oligo AAAAGCACCGACTCGGTGCCACTTTTTCAAGTTGATAACGGACTAGCCTTATTTTAACTTGCTATTTCTAGCTCTAAAAC invariant 3' end (tail primer), generating a 117bp PCR product. Oligos were obtained from Sigma-Aldrich®. The PCR cycler settings for this primer extension were 3 min at 95°C; 30 cycles of 30s at 95°C, 30s at 45°C and 30s at 72°C; and a final step at 72°C for 7 min. PCR products were purified using Qiaquick (Qiagen) columns. Approximately 120–150ng of DNA were used as a template for a T7 *in vitro* transcription reaction. *In vitro* transcribed sgRNAs were treated with DNase and precipitated using sodium acetate and ethanol. Purified sgRNA and Cas9-NLS protein (New England Biolabs® Inc.) were diluted to 300ng/ul. Equal volumes of Cas9-NLS protein, sgRNA and Phenol Red (Sigma-Aldrich®) were mixed to obtain the final injection mix. Injection drop size was adjusted to 1nl using a graticule scale. All embryos were injected at the one-cell stage. F_1 heterozygous animals were identified via restriction digest, and indels were characterised using Sanger sequencing.

ENU mutant strains and transgenic strains

ENU mutants for *cyba* (*sa11798*) and *duox* (*sa9892* and *sa13717*) were discovered during the Zebrafish Mutation Project (Kettleborough *et al*., 2013). These fish were sourced from the European Zebrafish Resource Centre (EZRC). *manet* mutants were sourced from laboratory of David Parichy (McMenamin et al. 2014). *cyba* and *duox* mutants were identified via Sanger sequencing. *manet* mutants were identified via restriction digest. The *Tg(HyPer)* reporter line was generated in the lab using Tol2 transgenesis. The expression of *HyPer* was driven by the ubiquitous promoter *ubb* (Shoko Ishibashi, unpublished).

Polymerase Chain Reaction

PCRs for were undertaken using ExTaq DNA Polymerase (TaKaRa). Primers used are listed below**.**

cyba F1	AGTTTATTTGCCAGTGACAGCA	Genomic PCR for CRISPR mutants
cyba R1	CTCAAGCAGCCTACCAAACC	Genomic PCR for CRISPR mutants
duox sa9892 F	ACGAGGTACACAACTCAAGCTG	Genomic PCR for *sa9892* mutants
duox sa9892 R	GACGTTCAAAGCGAAACCTGAC	Genomic PCR for *sa9892* mutants
sa9892 seq	CTTGGTCTGCCTTTGACGAAGT	Sequencing of *sa9892* mutants
duox sa13017 F	TGGTACACCATTTGAGGATGTGA	Genomic PCR for *sa13017* mutants
duox sa13017 R	TCTCTCTGCACATGGTGATCAG	Genomic PCR for *sa13017* mutants
sa13017 seq	GTGACTCAAGTCAGAACAGGTC	Sequencing of *sa13017* mutants
manet F	TGCAAATTTCGATAAATTGTAATAA	Genomic PCR for *manet* mutants
manet R	GGTGAGGCTGCTTCATTTTC	Genomic PCR for *manet* mutants
nox5 F	GCTCAAGGGCTTACATGATCC	Genomic PCR for CRISPR mutants
nox 5 R	GCCTCAACATCAGCACCTAC	Genomic PCR for CRISPR mutants
M13 Reverse	GTAAAACGACGGCCAGTG	For identifying indels

Caudal fin amputation and regeneration

Fish were anaesthetised using 0.4 mg/mL (0.04%) MS-222 (Sigma Aldrich). Animals were imaged prior to amputation, T0, 1, 2, 3, and 4weeks amputation (wpa), on a Leica M165 FC (Leica Microsystems). Using Photoshop CS5 (Adobe®), images were cropped at the level of the caudal peduncle, and fins were outlined using the brush tool. The "Record Measurements" command was used to obtain the total area of the outlined fin. Regeneration was calculated as a weekly increase, relative to the unamputated state, where the unamputated state was regarded as 100%. This is formulated as:

$$\frac{\text{weekly fin size}}{\text{unamputated fin size}} \times 100$$

H_2O_2 detection

For visualising H_2O_2 levels in the caudal fin, excitation wavelengths of 500nm and 420nm and an emission wavelength of 530nm were used. Fish were imaged on a high-end widefield microscope (Decon Vision) using a 4X objective. Animals were imaged before and after amputation, over a series of time points. To calculate the HyPer ratio, YFP emission was divided by CFP emission, generating the new image showing the ratio. The average H_2O_2 over the area captured in the image was then calculated and visualised using Prism 8.1 (GraphPad Software, Inc.).

Statistical analyses

Comparisons were made using ANOVA (repeated measures and one-way) or t-test. Linear regressions were performed without interpolation, with a 95% significance level. The strength of the correlation was assessed by the correlation coefficient, adjusted R square. Where applicable, Pearson's

correlation coefficient and Spearman's rank correlation coefficient was reported. For the unamputated fin, distribution was used for explaining the relationship between age and fin size. The Wald–Wolfowitz run test was used to assess the correlation between age and fin size. Oscillations were tested using power spectrum analysis based on Fourier transform as well as autocorrelation. MATLAB (MathWorks) was used to perform power spectrum analysis and SSPS (IBM Corporation) was used for autocorrelations.

Results

The zebrafish caudal fin is in a state of continuous growth

Zebrafish possibly retain a lifelong potential for growth, evidence for which is glimpsed by the permanent patency of cranial sutures (Topczewska et al. 2016), as well as observations on other teleosts (Dutta 1994). This may obscure the contribution of regenerative growth following amputation. Therefore, to assess fin growth trends during their adult lifespan, we compared the total caudal fin size among adult WT animals. Adulthood is characterised by the attainment of sexual maturity, and this usually correlates with a standard length (SL) of 17.5±0.6mm for males and 18.3±0.7mm for females (Parichy et al. 2009). All adults used for this experiment exceeded SL 20mm, and ranged from three months to twenty-two months of age. For contrast, I also included juveniles, at one and two months of age. All the animals came from tanks maintained at optimum stocking density and none of these animals had ever experienced caudal fin amputation. Here, no significant difference in fin size was apparent between any two consecutive months (except between 1, 2 and 3 month old animals). Instead, significant differences in fin size were only apparent among age groups 2 months apart, up until 18 months. From 18 through 22 months no significant difference in fin size was recorded. Interestingly though, the preceding increase segues into a slight, non-significant decline. The overall fin size correlated well with age across the entire age range (linear regression, adjusted R square =0.83). The data fit a distribution curve well, with Wald–Wolfowitz runs test insignificant for all time points. Even so, the there was prominent intra-group variability in fin size across the entire age range (**Fig. 4**).

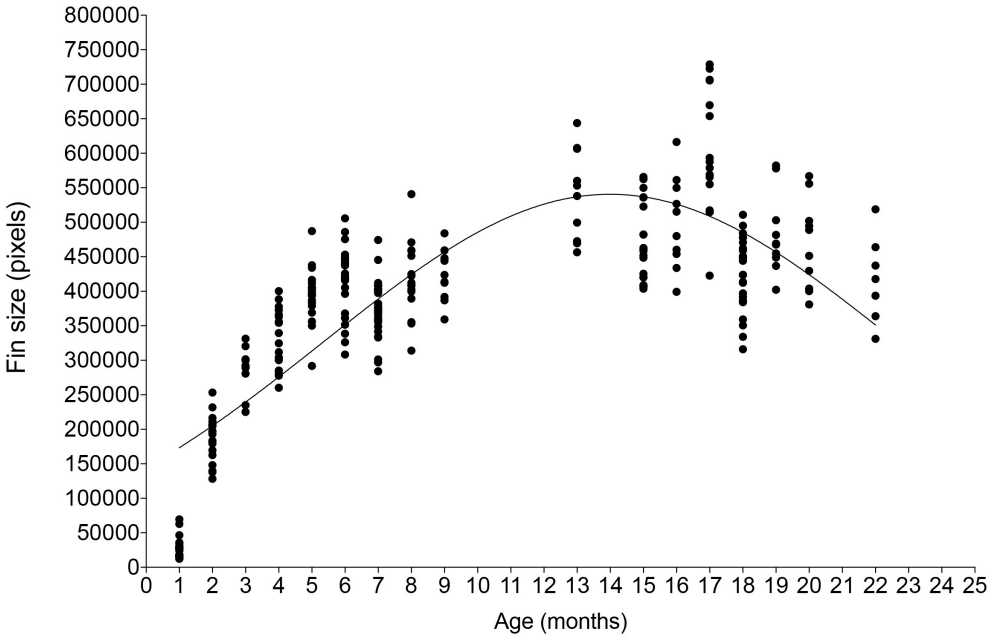

Fig. 4. Zebrafish of different ages differ in their fin sizes. Fin sizes increase linearly with age up until 18 months of age. Wald–Wolfowitz runs test is insignificant at all time points.

Post-amputation caudal fin outgrowth is due to regeneration

Given the observations above, it is reasonable to assume that growth-related processes would be concurrent to regeneration. This would be especially noticeable in younger animals. To examine the effect of growth, as well as age on regeneration, WT animals at 3, 4, 5, 6, 8, 13, 16, 19 and 22 months of age were chosen for caudal fin amputation. Images were recorded before, immediately after (t0), 1, 2, 3 and 4 weeks post amputation (wpa) (**Fig. 5**) to monitor the re-emergence of the lost portion. The rate of regeneration was determined by calculating the slopes of linear regressions. A linear model was applied to the raw as well as to the percentage data (data was normalised and unamputated fin size was taken as a 100%).

To assess how much growth was occurring weekly, the size of the fin stump immediately post-amputation was compared with its size (after subtracting area of new fin) during successive weeks in the regenerative period. Growth of the stump ranged from 0.9%-1.4%, over 4 weeks, across all examined age groups (**Fig. 6**). It is interesting to note that the significant differences within this narrow range, between young and older animals, align quite well with the data on overall fin growth. Thus, only a minor percentage of the regenerated fin may be accounted for by growth.

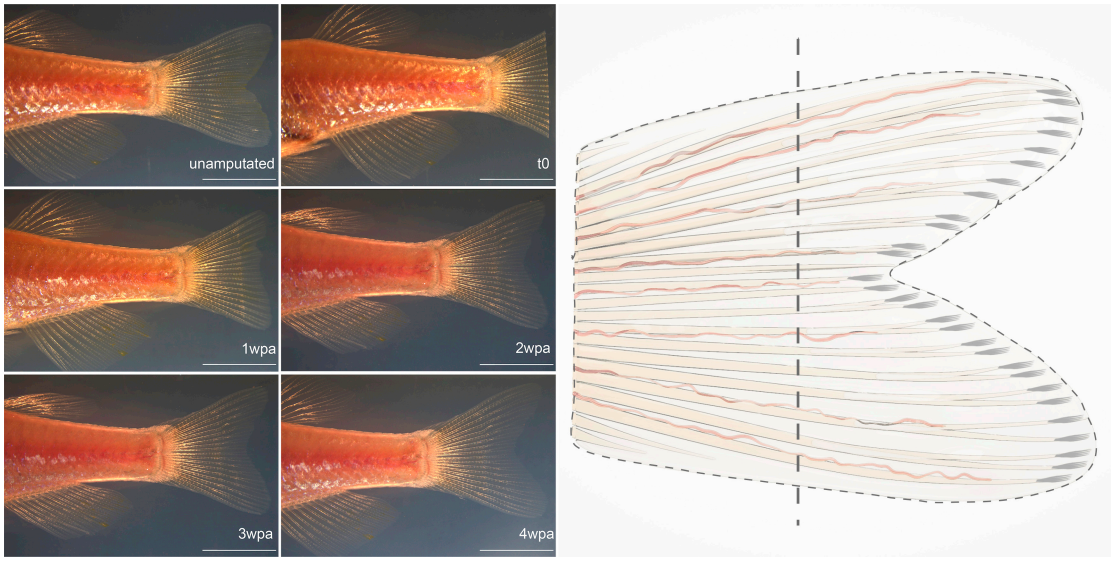

Fig. 5. Left. Caudal fin regeneration in the WT adult zebrafish completes over 4 weeks post amputation. The plane of amputation is evident for most of the process. Scale bar=5mm. **Right.** Schematic diagram of caudal fin showing the plane of amputation (dashed vertical line). The entire fin proximal to the caudal peduncle (dashed margin) is treated as the reference from which percentage values of the regenerating fin are derived weekly.

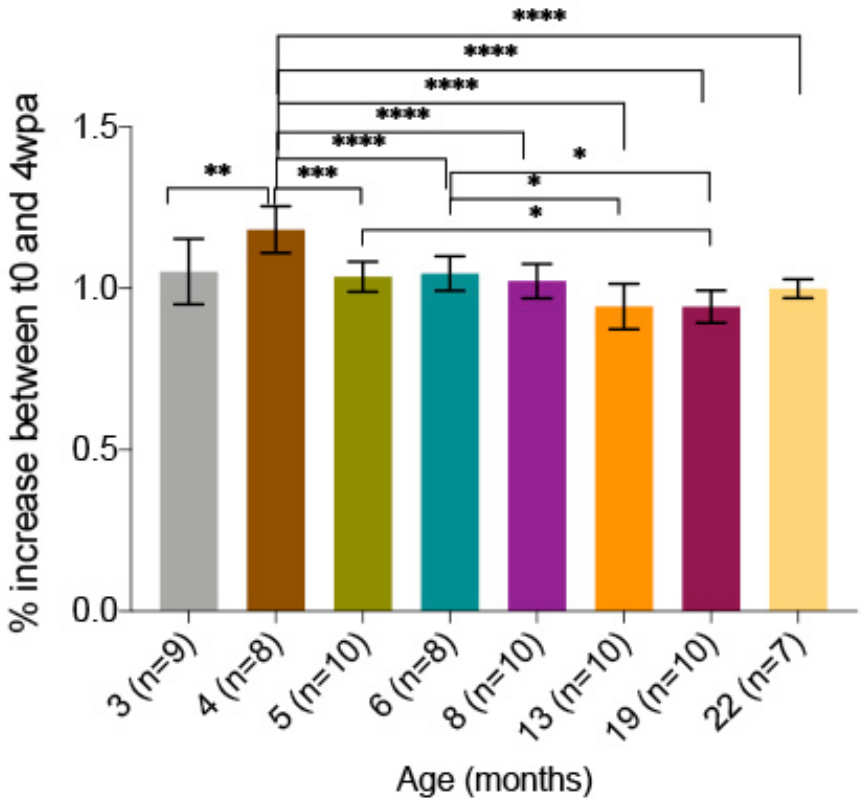

Fig. 6. Percent growth over 4wpa, across various age groups. Even within a narrow range of 0-1.5%, significant differences are evident across younger and older groups. The lack of significance between 3months and 13, 19 and 22 months is interesting, and may possibly be extrapolated to suggest similar fin size, which in turn may suggest age-related reduction (Ordinary one-way ANOVA **** P<0.0001).

Caudal fin regeneration in zebrafish may be influenced by age

While zebrafish retain a lifelong ability for caudal fin regeneration (Itou et al. 2012), the related cyprinid, killifish (*Nothobranchius furzeri*), is reported to show age-related decline for the same. This led us to check for caudal fin regeneration across the abovementioned age groups. With a maximum lifespan of 43.5 months (Carneiro et al. 2016), zebrafish adults may be categorised into young (8-12 months), middle-aged (15-20 months) and old (25-30 months) (Gilbert, Zerulla, and Tierney 2013).

Following amputation, increase in fin size negatively correlated with time (adjusted R square values for different groups range from 0.88 to 0.98). Linear regression on raw as well as normalised data yielded similar results. The average slopes of linear regression were then compared across the age groups. Strikingly, it was observed that younger animals regenerated their fins to their unamputated levels within 2 weeks whereas older animals achieved the same over 4 weeks, with some animals falling short even at 4 weeks (**Fig. 6, and 7**). Even so, we found that while younger animals have steeper slopes than older animals, mean slopes did not differ significantly, suggesting a similar rate of increase over the 4-week regeneration period (**Fig. 8C**). These findings indicate that zebrafish retain the ability to regenerate their fins, at least until considered as old.

The rate of regeneration (normalised slopes) correlated well with the age of the fish (Spearman's r=-0.929; Pearson's r=-0.731). The differential rate of regeneration among young and older adults led us to estimate weekly rates of regeneration in this 4-week span. It was found that the rate of regeneration was proportional to time elapsed since amputation, across all groups ($p<0.0001$, $X^2=43628$, 150 d.f.). In all cases, there was a significant difference between the rates of regeneration in consecutive weeks (RM-ANOVA, $p<0.0001$). In other words, the amount of regeneration significantly differed between 1 and 3, 1 and 4, 2 and 3, and 2 and 4wpa. Regeneration was the fastest during the first week post amputation (**Fig. 8A**). Taken together, these results are indicative of the regenerative success that zebrafish of all ages appear to demonstrate, with a statistically non-significant decline revealed among older animals.

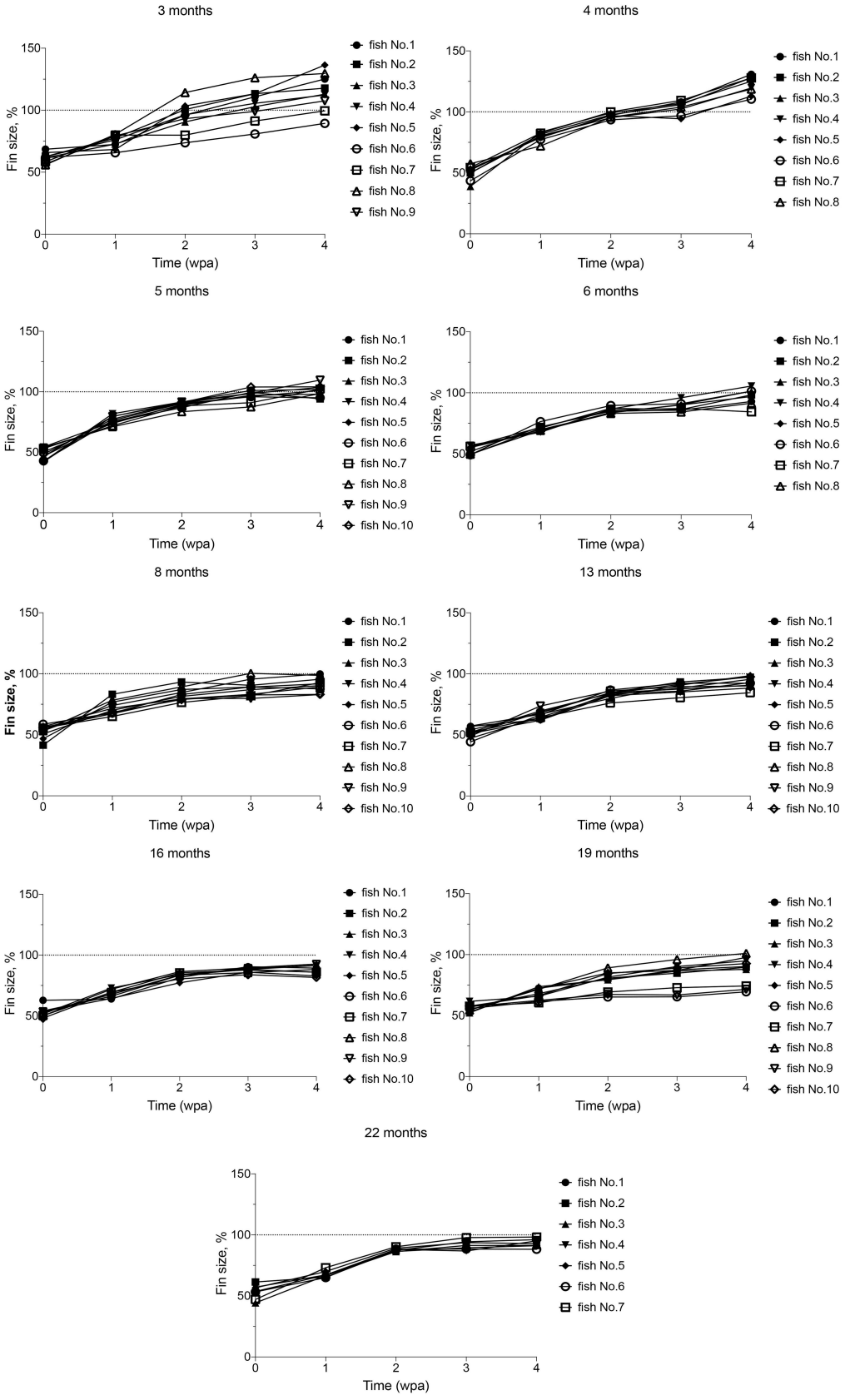

Fig. 7. Regeneration of the caudal fin among adults of various ages is represented using linear regression modelling. Younger animals exceed the original unamputated area by 4wpa, while 8months onwards groups trail short of 100% in the same time span. Within each group, individual slopes were not significantly different.

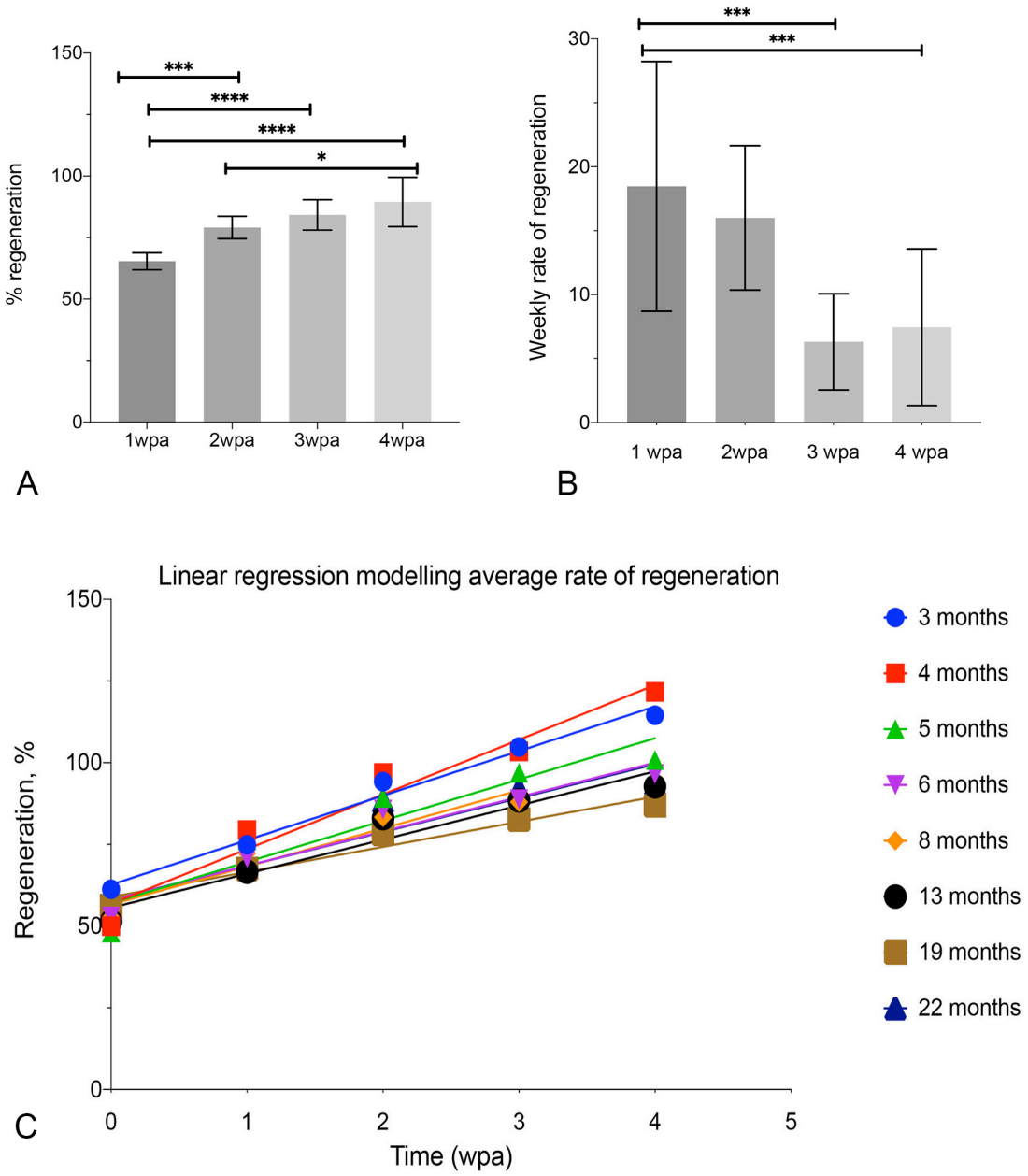

Fig. 8. A. Percentage rate of regeneration. Data from animals across all age groups was pooled week-wise. Majority of the recovery is indicated to occur within 1wpa (Ordinary one-way ANOVA. P value <0.0001). **B.** Rate of regeneration during different weeks post amputation. Regeneration is fastest during the first week and significantly slows down by the third week (t-test, p<0.0001). **C.** Linear regression models for the average normalised fin sizes of WTs of different ages. Within each age group, shown in Fig. 5, individual slopes were not significantly different, and since the slopes are not significantly different, it is possible to calculate one slope for all the data. These unified slopes from each group were then compared. (Ordinary one-way ANOVA. P value <0.0001; t-test, p<0.0001).

cyba and *duox* mutations affect caudal fin regeneration

Having identified regeneration trends in WT animals, we proceeded to investigate the rate of regeneration in the *nox* mutants. Previously described *cyba*$^{5bp.ex1-/-}$ (n=13), *duox* (n=6) and *nox5*$^{4bp.ex4-/-}$ (n=6) fish were subject to caudal fin amputation and

followed to 4wpa. As earlier, the rate of regeneration was determined by calculating the slopes of linear regression (**Fig. 9**). t-test indicated significant differences between *cyba*$^{5bp.ex1-/-}$ and WT (P=0.0069), *duox* and WT (P=0.0048), *cyba*$^{5bp.ex1-/-}$ and *duox* (P=0.0001), *cyba*$^{5bp.ex1-/-}$ and *nox5*$^{4bp.ex4-/-}$ (P=0.0324), and *nox5*$^{4bp.ex4-/-}$ and *duox* (P=0.0274). Meanwhile, no significance was found between WT and *nox5*$^{1bp.ex4-/-}$ (P=0.8466). Comparison of the four groups via ANOVA confirmed the significance between *duox* and the other three groups. A reflection of these differences is evident among *cyba* and *duox* mutants, many of which did not reach the original fin size by 4wpa (**Fig. 9**).

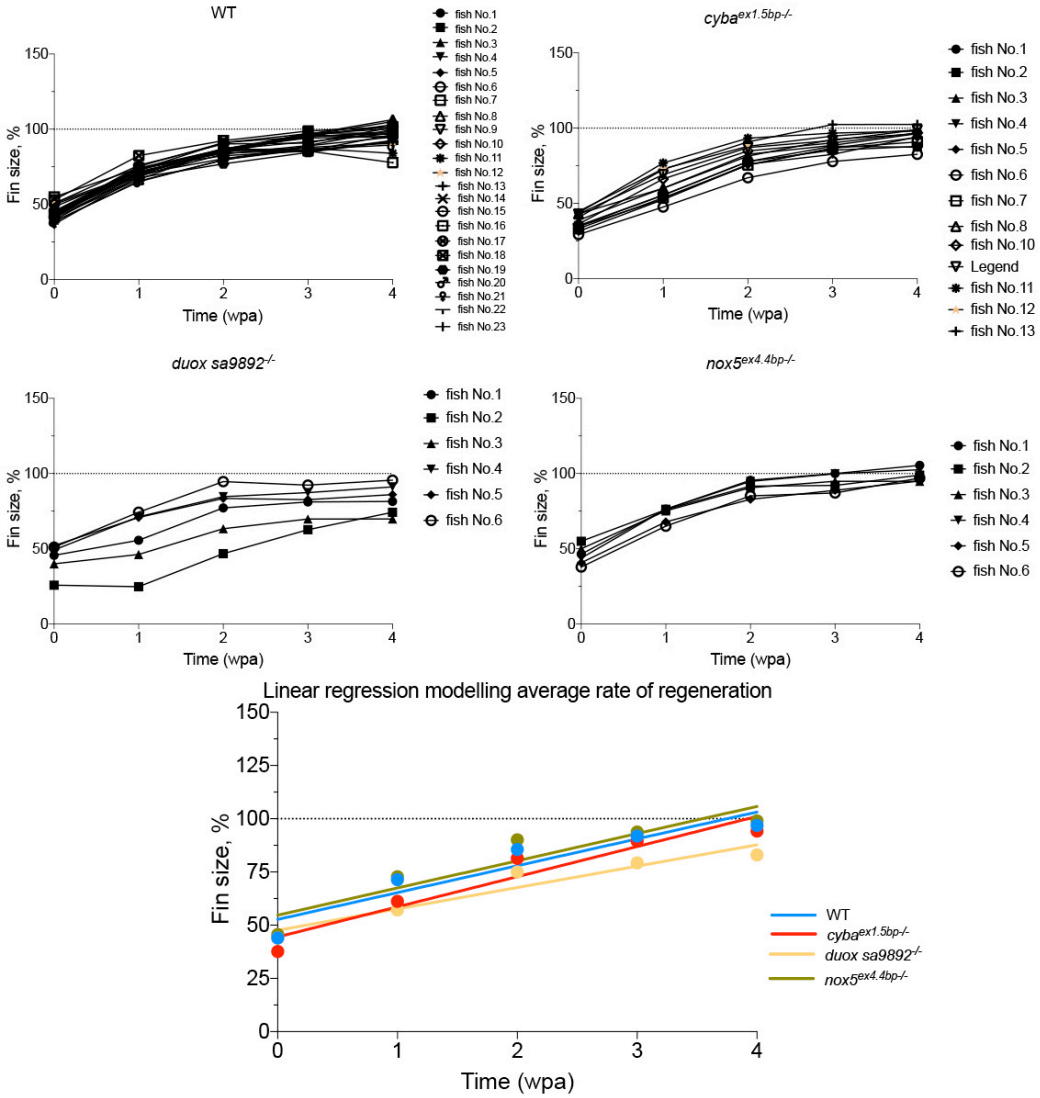

Fig. 9. *cyba* and *duox* mutations slow down regeneration. Most *cyba* and all *duox* mutants failed to reach the original fin size by 4wpa. Using linear regression modelling, graphs show normalised change of fin size, with the unamputated fin being 100% (not shown on graph). Within each group, individual slopes were not significantly different, and since the slopes are not significantly different, it is possible to calculate one slope for all the data. These unified slopes from each group were then compared. (Ordinary one-way ANOVA. P value <0.0001; t-test, p<0.0001).

An important consideration among *duox* mutants was the hypothyroidism. We have previously reported that mutants display ragged fins, and as we found, some suffered from spontaneous loss of fin fragments at various stages of regeneration (Chopra, Ishibashi, and Amaya 2019). Such animals were excluded from analysis, as they would have required extrapolation of the missing fragments.

Thyroid hormones may affect the rate of regeneration

duox is very well documented to be implicit in thyroid hormone (TH) maturation (Dupuy et al. 2002; Carvalho and Dupuy 2013; Muzza and Fugazzola 2017; Aycan et al. 2017). Recently, we reported the first piscine model of congenital hypothyroidism, including the resolution of phenotypes upon continued application of T_4 (Chopra, Ishibashi, and Amaya 2019). Since this TH deficient state affects fin health, we were curious whether the reduced rate of regeneration among *duox* mutants was influenced by hypothyroidism. We applied a two-pronged approach in trying to determine the influence of THs. We continuously treated *duox sa9892*$^{-/-}$ and WT siblings with 0.3nM of T_4, for a period of three weeks (with the first week reserved for conditioning), during which we performed caudal fin amputation and allowed regeneration to continue concurrent to treatment. Untreated counterpart groups served as controls. The second strategy saw WT animals being continuously treated with the goitrogen methimazole (MMI), for a period of twelve weeks (with the first four weeks reserved for conditioning. The concentration used was 1mM, and untreated animals served as controls. No significant differences were found between treated and untreated *duox sa9892*$^{-/-}$ animals, over 2wpa. Also, MMI did not decelerate regeneration as no significant difference was found between treated and untreated WTs by 2wpa (**Fig. 10**). Both observations suggested that THs do not affect regeneration. The effect of T_4 treatment on WTs could not be pursued owing to technical challenges that caused mortality in the group.

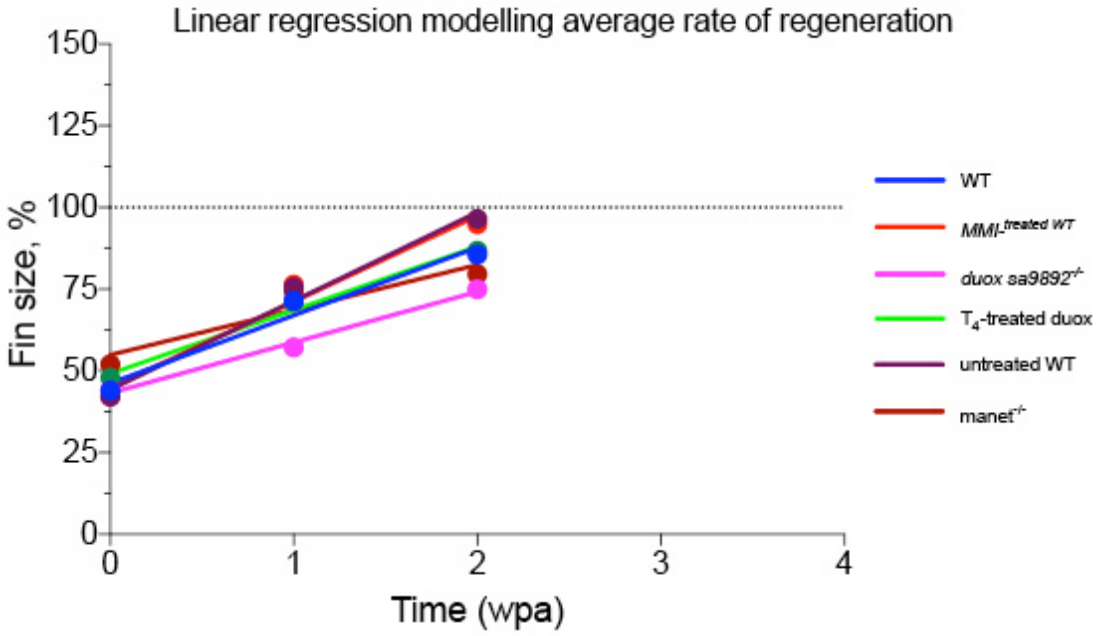

Fig. 10. Linear regression modelling regeneration upto 2wpa. T4 treatment had no effect on regeneration in *duox* mutants. MMI did not appear to slow down regeneration among WTs. Surprisingly, no significant differences were found between regenerating *duox* and *manet* mutants (Ordinary one-way ANOVA. P value <0.0001).

To arrive at a more definitive view of the role of THs in regeneration, we again turned to a genetic model that did not have confounding *duox* mutations. The *manet* strain of zebrafish harbours a nonsense mutation in exon 2 of *tshr*, which results in congenital hypothyroidism. This strain has been characterised at length (McMenamin et al. 2014), and we have reported phenotypic concordance between *manet* and *duox* mutants (Chopra, Ishibashi, and Amaya 2019). Conveniently, the mutation causes destruction of the HpyCH4V restriction site, providing a straightforward diagnostic. The effect of the *tshr* mutation on body length has not been reported, and so, WT, *manet*$^{+/-}$ and *manet*$^{-/-}$ siblings were measured at 3 months of age, yet again mirroring *duox* mutants. Mutants were significantly shorter (**Fig. 11**). We amputated the caudal fin in *manet* animals and intriguingly, found a significant difference between regenerating mutants and WTs (**Figs. 10 and 12**). Further, no significant difference was observed between regenerating *duox*$^{-/-}$ and *manet*$^{-/-}$ animals, suggesting that THs may be playing a role during regeneration, after all. The sample size for *manet* was small (n=3) and calls for further repeats to derive a more meaningful conclusion.

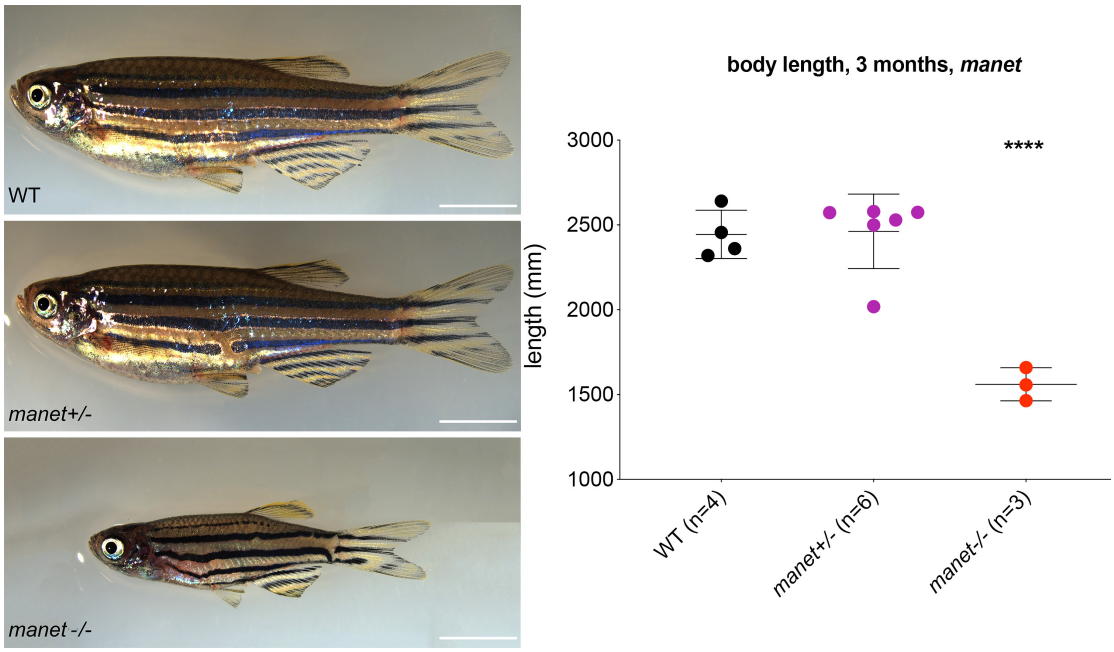

Fig. 11. Body length of *manet* siblings, at 3months of age. Scale bar=5mm. (Ordinary one-way ANOVA, **** P<0.0001)

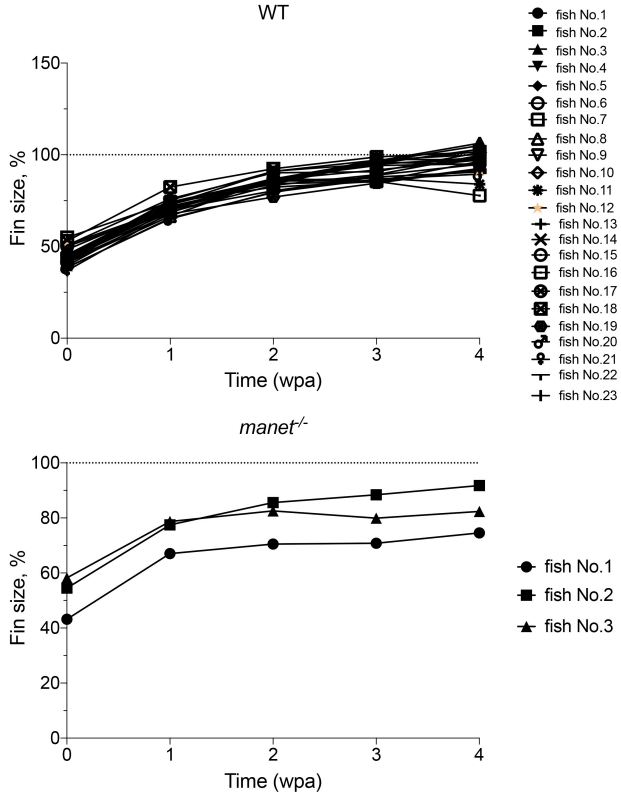

Fig. 12. Regeneration in *manet* mutants over a 4-week period. Graphs show normalised change of fin size, with the unamputated fin being 100% (not shown on graph). Within each group, individual slopes were not significantly different. Mutants did not achieve full regeneration by 4wpa.

Something that we did not observe previously was the fact that *duox sa9892*$^{-/-}$ animals did not develop a blastema, even by 48hpa. This only became apparent

while using mutants for HyPer imaging (described below). Thus, we initiated another long-term T_4 treatment regime. Amputation and regeneration in the midst of this continuous treatment rescued blastema formation (n=13) (**Fig. 13**). Owing to time constraints these animals were not followed for regeneration. Overall, the role of T_4 calls for further investigation, with a possibility that it may be acting during regeneration.

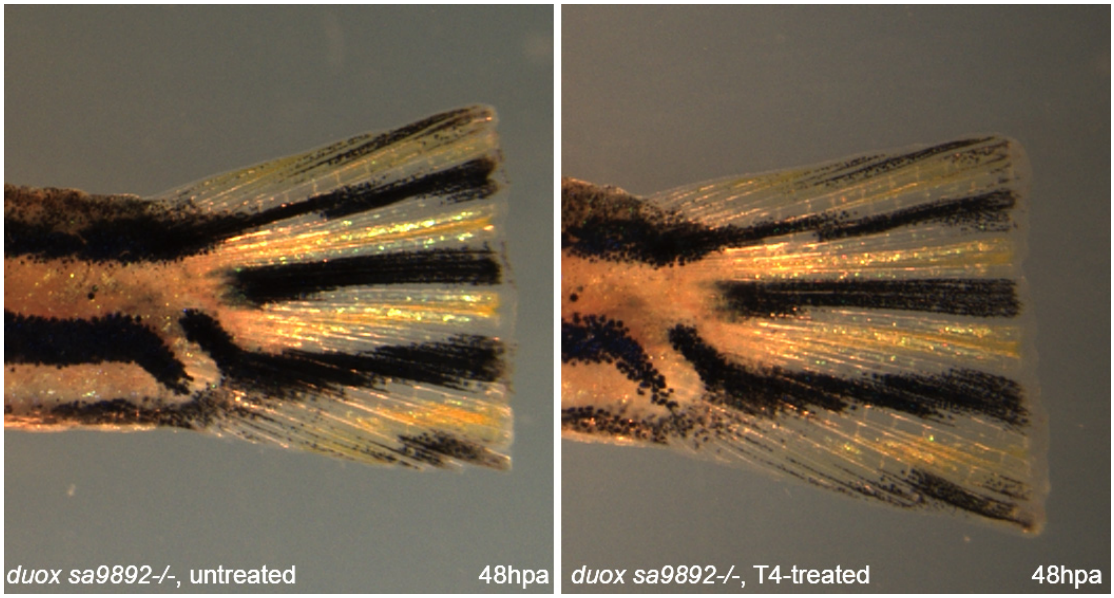

Fig. 13. T_4-treatment rescues blastema formation in *duox* mutants. Shown here is the same animal, following recovery from amputation (left), and amputated again in the midst of continuous treatment (right). The blastema is distinctive following treatment.

ubb:HyPer is an effective reporter of sustained, amputation-induced ROS

Amputation induces a ROS flux, and the next step was to visualise this ROS post-amputation. Previously, the H_2O_2-specific reporter, HyPer (Belousov et al. 2006) has been used for generating transgenic *Xenopus laevis* to visualise the sustained production of ROS during tadpole tail regeneration (Love et al. 2013). We generated zebrafish transgenic for *ubb:HyPer* and used 7month old F_4 adults (n=8, **Group A**) for analysing ROS dynamics post-amputation. Unlike transmitted light images that allow easy identification of individual fish, HyPer imaging can obscure individual recognition especially if the imaged area across the sample set is uniform. I devised a simple strategy for following individual animals by using scale morphology. Scale morphology is distinctive and amply apparent under fluorescent channels. Given that the lowest optical zoom on our widefield microscope was 4X, the caudal fin was

amputated closer to the caudal peduncle in anticipation of keeping the regenerating portion as well as terminal scales in the frame of view for all image captures. Animals were amputated a little after midday. Concurrently, we followed a set of unamputated controls (n=7, **Group B**), which were recorded between the same time intervals. At t0, H_2O_2 levels were slightly elevated, followed by a significant increase (paired t-test, p=0.0009) above the unamputated level, at 2hpa (3PM). By 6hpa and 10hpa, this increase was steadily sustaining. The most surprising observation though was recorded between the early hours of the following day (between 7AM and 8AM), when we saw a peak in the ROS flux. The flux dipped to its lowest between 3PM and 4PM, although remaining significantly above the unamputated levels. Between 10PM and 11PM, the flux was recorded as higher than that in the afternoon but lower than early in the day. We continued to see this rise and fall of ROS flux and recorded these three time points for three consecutive days. After three days, recording was narrowed down to once daily, between 3PM and 4PM. After another three consecutive days of doing this, imaging was further narrowed down to once every two days, between 3PM and 4PM, while continuing to see ROS flux still being sustained significantly above the baseline. The final recording was made between 3PM and 4PM, at 2wpa. By this time the ROS levels had returned to pre-amputation levels. Among unamputated controls, H_2O_2 levels seemed to be significantly higher between 7AM and 8AM before exposure to light compared to between 3PM and 4PM (paired t-test, p=0.03). However, the set of recordings between 7AM and 8AM were not significantly different from those between 3PM and 4PM. Following these recordings, an oscillating trend line emerged with distinctive peaks at 7AM for three subsequent days (18, 42 and 66 hpa). In summary, we found that elevated ROS levels sustained up until 2wpa (**Fig. 14**). These findings are especially exciting, seeing as 2wpa is the time point when we see the rate of regeneration slowing down in WTs.

Amputation-induced ROS follows a daytime-dependent oscillatory trend

Having observed oscillating ROS in the wake of caudal fin resection, we were curious whether the timing of these oscillations is set by the amputation itself, or whether amputation exaggerates a naturally existing trend. Logically then, we decided to

perform amputations at a different time of the day. 5 month old non-mutant *Tg(HyPer)* animals (n=8, **group C**) were transported to the microscopy facility under

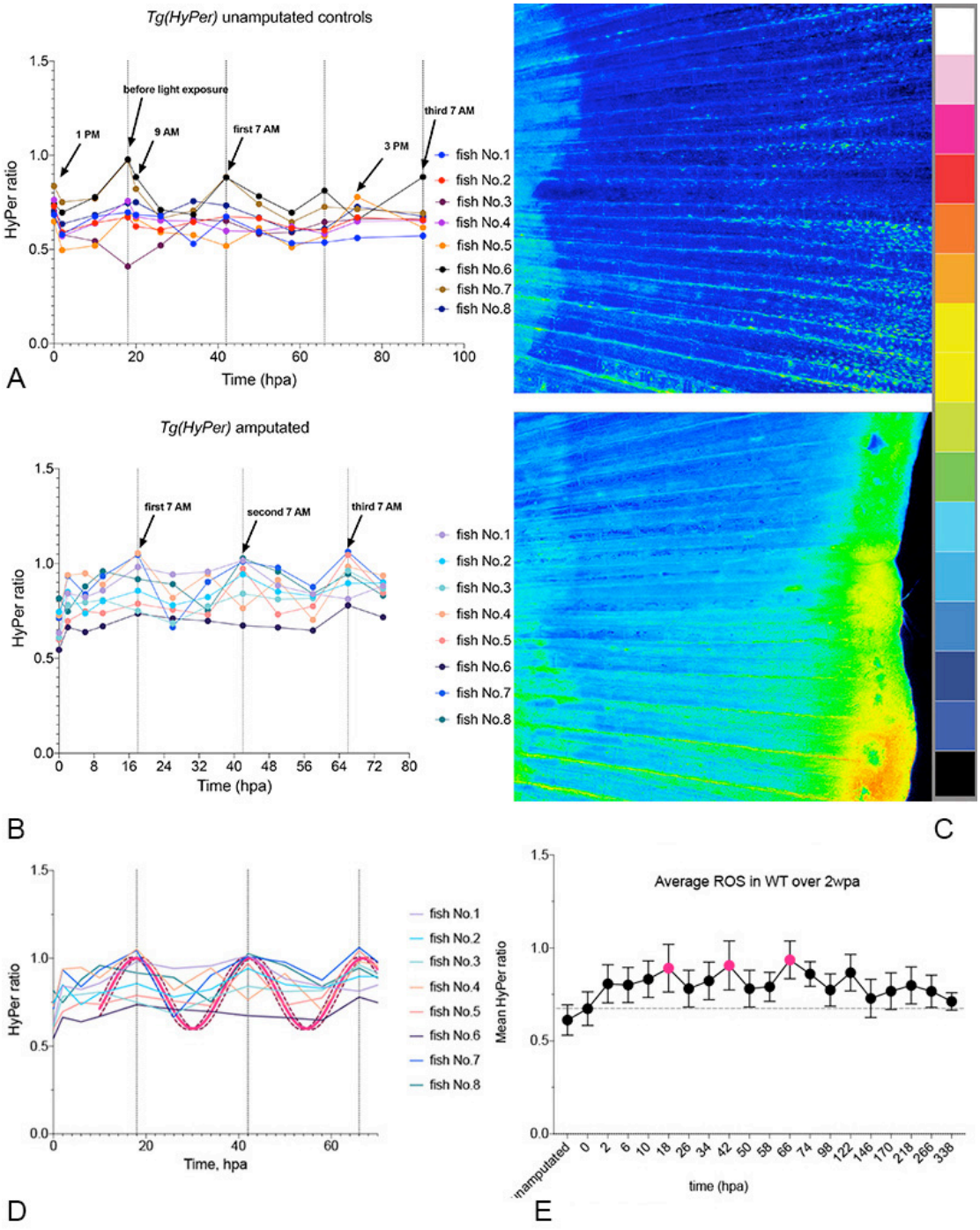

Fig. 14. ROS levels elevate and sustain in an elevated state for 2wpa in an amputated fin. **A.** Caudal fin in unamputated controls (group B). H_2O_2 levels oscillate by the time of day with highest levels at 7AM. **B.** Distinct oscillations ensure caudal fin amputation (group A). **C.** Visual scale of ROS flux, with black being lowest and white being highest. **D.** H_2O_2 levels rise sharply immediately after amputation and continue to oscillate for at least 3 days. H_2O_2 levels at 7AM for three consecutive days were significantly higher than at 3PM and 11PM (repeated measures ANOVA, p=0.0008, 23 d.f.). Vertical dotted lines represent 7AM values. Sinusoidal curve fitted to the data (RMSE=0.1455) **E.** Average H_2O_2 levels in group A animals over 2wpa.

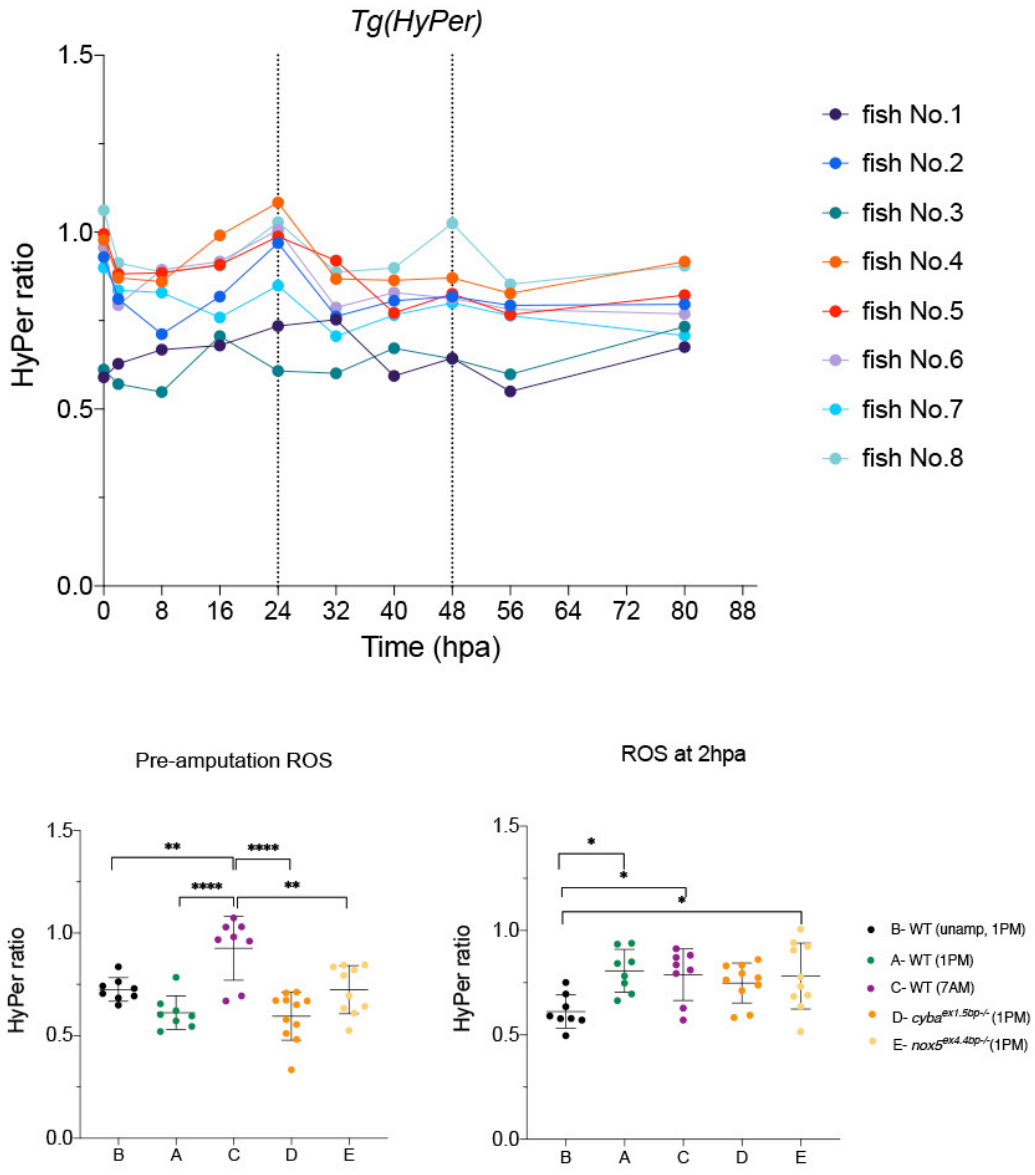

Fig. 15. Top. H_2O_2 levels in *Tg(Hyper)* group C animals amputated at 7AM follow the same oscillation trend as group A, exhibiting highest H_2O_2 levels at 7AM. **Bottom** H_2O_2 levels before amputation are significantly higher in group C compared to other groups (Bonferroni correction for multiple comparisons, one-way ANOVA, 0.04>p-value>0.0001). Shown here are H_2O_2 levels in *Tg(HyPer)* amputated at 1PM (A), *Tg(HyPer)* unamputated controls at 1PM (B), *Tg(HyPer)* animals amputated at 7AM (C), *cyba*$^{ex1.5bp-/-}$ at 1PM (D), and *nox5*$^{ex4.4bp-/-}$ animals at 1PM (E). H_2O_2 levels at 2hpa reach the same values in all fish regardless of the time of amputation (group A, D and E amputated at 1PM, group C at 7AM). Unamputated *Tg(HyPer)* controls measured at 3PM show the same H_2O_2 levels as group D, but differ from Group A (p=0.0075), C (p=0.018) and E (p=0.017).

cloak. Their caudal fins were amputated under a halogen lamp at the lowest setting. The idea was to resect fins while the animals had not yet perceived the first light of day (between 7AM and 8AM). ROS flux was imaged at the same time intervals as group A. In sharp contrast to afternoon amputations, these animals had significantly

higher H_2O_2 levels (t-test, p=0.0001) preceding amputation than at 2hpa i.e. 'basal' H_2O_2 levels of these zebrafish were significantly higher than other groups (**Fig. 15**).

When further analysing results, it became clear that H_2O_2 levels were dependent on the time of day in all *Tg(HyPer)* animals observed (χ^2 test, p<0.0001 for all groups; χ^2 =415.3 for group A, χ^2 =299.4 for group B and χ^2 =394.8 for group C). To confirm oscillations weren't noise, a power spectrum analysis based on Fourier transform was performed. This showed a high peak in all ROS levels in all fish from group A at frequency 0.04. Oscillations were 'noisier' in the unamputated group as only two fish exhibited clear peaks indicating 24hour periods of oscillations. Periodicity in group C was similar to that in group A (**Fig. 16**).

Post-amputation oscillations are affected by *nox* mutations

Having determined post-amputation ROS production trends in non-mutants, we were keen to find out how these oscillations were affected by *nox* mutations. *cyba*$^{5bp.ex1-/-}$ animals (n=10) provided the first surprising result in this series of experiments. There was an increase post-amputation (t-test, p=0.0004) only to decrease later. It did not manifest as markedly dynamic until 24hpa. In other words, H_2O_2 levels did not peak at the first 7AM (18hpa) time point, but significant increases were recorded at subsequent 7AM time points (42hpa, t-test, p=0.04; 66hpa, t-test, p=0.01, and 90hpa, t-test, p=0.01). Most surprisingly, *cyba* mutants 'baselined' by 1wpa (**Fig. 17A**). Also, the oscillations exhibited peaks of smaller amplitudes and had a lower H_2O_2 increase overall. Interestingly, H_2O_2 levels in *cyba* mutants were the same as in WTs at 2hpa, but failed to match up with values at other times (**Fig. 18A**).

Difficulties were encountered while applying HyPer imaging to *duox* mutants. Very early on, three animals died. Further on, one animal lost a significant portion of the fin, reducing the ample size to 4. Statistically, the animals fell into 2 markedly distinct and spaced out compartments, which is reflected in the wide error bars (**Fig. 17B**).

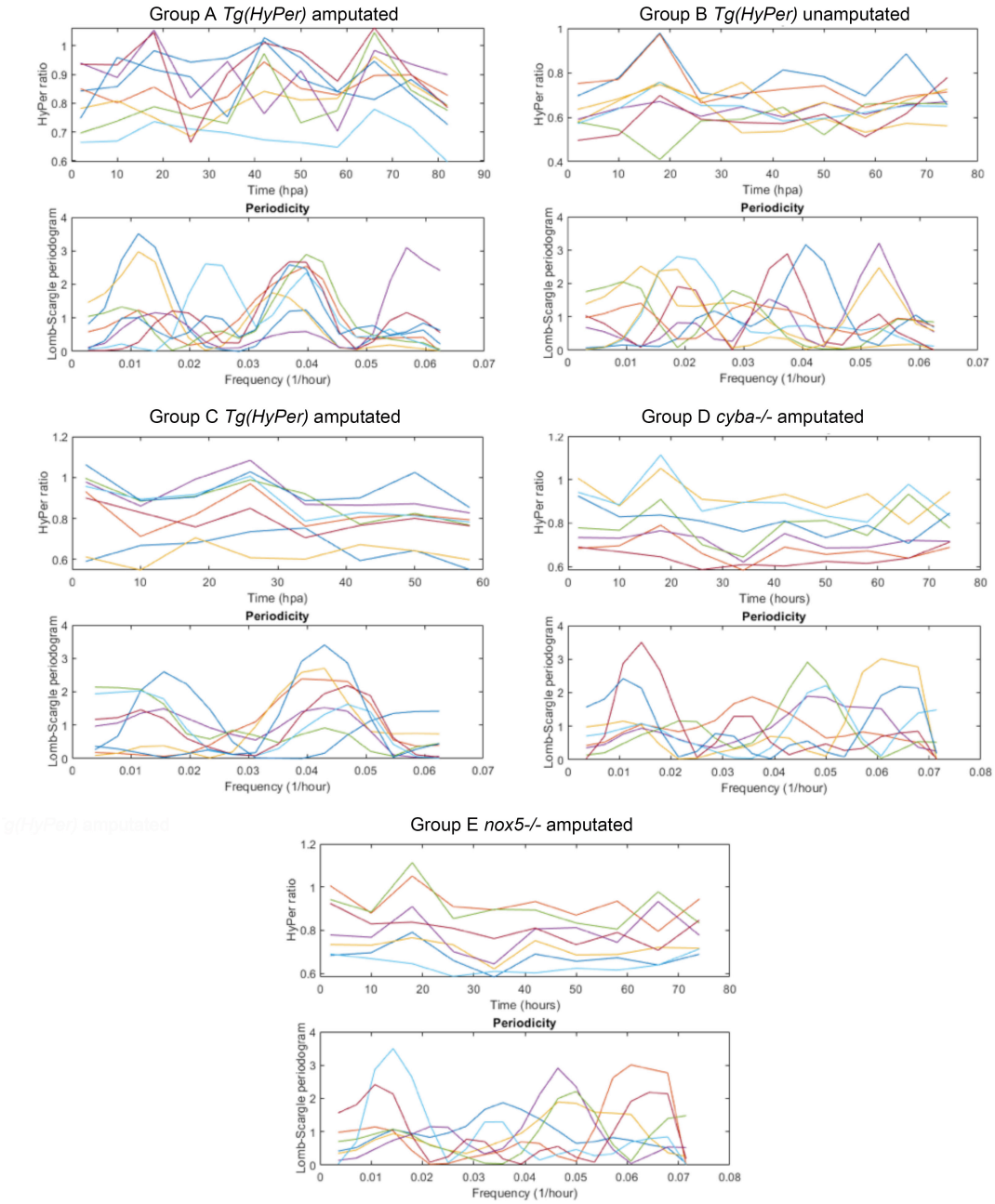

Fig. 16. Estimating periodicity of ROS oscillations. H_2O_2 oscillations follow a daytime-dependent trend. Periodograms for groups A, B, and C reveal a periodicity around 0.4, indicative of a ~24 hour phase. While oscillations are distinctive post-amputation, unamputated animals also show this trend, suggestive of ROS inherently oscillating. *cyba* and *nox5* mutants showed a periodicity around 0.06, indicative of a ~17 hours phase.

A quick analysis using these data revealed the ROS levels to be significantly low, to the extent that it was even lower than those seen in unamputated controls. As previously stated, another major revelation was the delayed blastema formation (**Fig. 13**). While the disparity among individuals requires addressing via future repeats, the indication is that *duox* mutations have a significant impact on ROS production, post-amputation, perhaps explaining, in part, for the blastema delay and the reduced rate of regeneration described earlier (**Fig. 9**).

Nox5 is the least physiologically characterised Nox. To examine its contribution, *nox5*$^{ex4.4bp-/-}$ animals (n=8) were taken through the same protocol. A significant increase was observed at 2hpa (3PM) (t-test, p=0.04), which peaked at 7AM (18hpa) the next day (t-test, p=0.036) (**Fig. 17C**), and rapidly 'baselined' thereafter, showing no further significant increase.

Overall, the results suggest that nox5 might be responsible for producing H_2O_2 later during the post-amputation period, whereas partner NOXes of cyba predominantly produce H_2O_2 immediately post-amputation. Results from *duox* mutants though inconclusive, suggest its requirement throughout the observed time period but the extent remains to determined. Overall, H_2O_2 levels in *cyba* and *nox5* mutants seemed to be dependent on time (χ^2 test, p<0.0001 for both) based on the first three days of observations. Despite that, periodograms highlight less clear oscillations and noisier signal. Interestingly, after Fourier Transform, quite a few peaks can be noticed at the frequency around 0.06 (equating to a periodicity of ~17 hours) in group D and E animals (**Fig. 16**). Average H_2O_2 levels recorded over 2wpa were compared between different groups (**Fig. 18**). Significant differences were detected between *nox* mutants and WTs (amputated), as well as between all amputated groups and the unamputated group (ANOVA, p<0.0001, Bonferroni test correction for multiple comparisons).

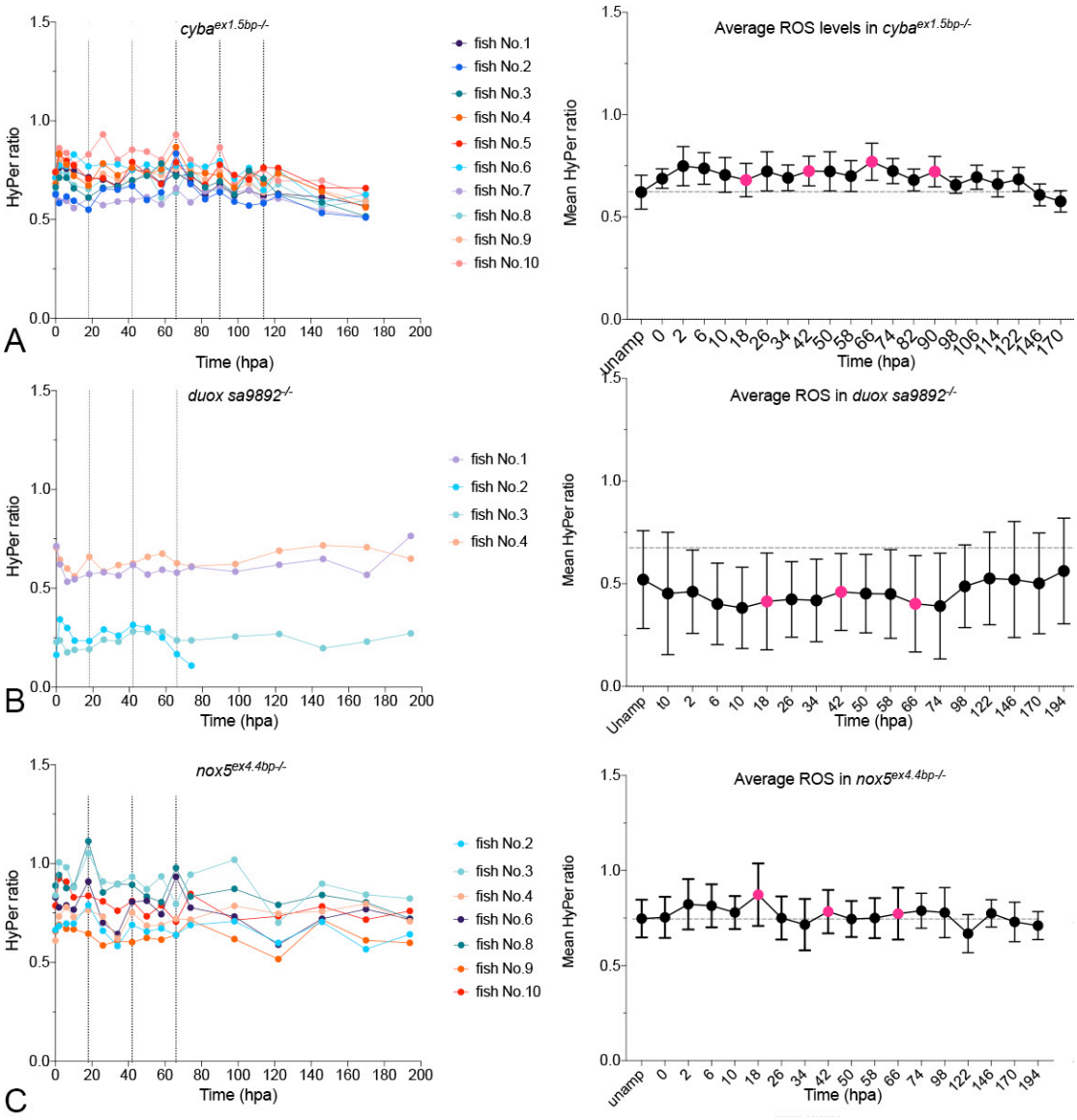

Fig. 17. A. H_2O_2 levels in *cyba* mutants begin oscillating later than those in WTs. H_2O_2 levels also reach pre-amputation levels by 1wpa. Vertical dotted lines represent 7AM values. **B.** *duox* mutants yielded a distinct variation, making it challenging to arrive at an average. **C**. *nox5* mutants show typical H_2O_2 oscillations initially with a significant peak at 7AM (18hpa) (t-test, p=0.036) but decline rapidly.

Discussion

Here, we describe how ROS-producing enzymes affect caudal fin regeneration, in an adult zebrafish model. We begin our investigation not by directly fast forwarding to ROS, but by first observing growth trends in our model. Like most teleosts, zebrafish continue to grow throughout their lifetime, a process known as indeterminate growth (Dutta 1994; Iovine and Johnson 2000). Further, the fin adheres to isometry i.e. it grows in proportion to the animal's body size, and it is synchronous i.e. all fin rays grow simultaneously (Iovine and Johnson 2000; Goldsmith et al. 2003). This

coupled with the anatomical and histological simplicity of the fin makes it desirable for investigating regeneration.

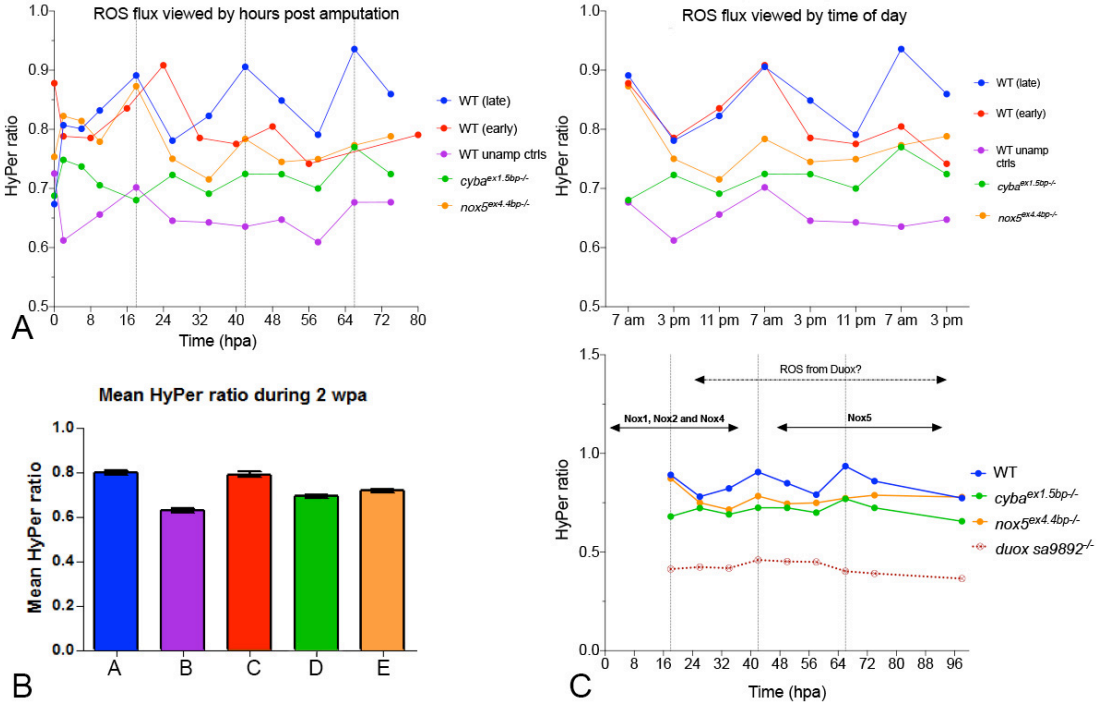

Fig. 18. Average H_2O_2 levels change over time in a different manner in different groups. **A.** When matched by the time post amputation, both WT groups (early amputation and late amputation, A and C, respectively) exhibit oscillations. Unamputated animals (group B) oscillate as well but their amplitudes are lower and oscillations less pronounced. The Y axes have been altered to better visualise changes. Groups A and C match well in the manner of their oscillation manner suggesting H_2O_2 changes are daytime dependent. *nox5* mutants appear to follow the same pattern as the WTs, but does not sustain the oscillations for long. In contrast, *cyba* mutants attempt keeping up H_2O_2 production after an initial hiatus. **B.** Average H_2O_2 levels over 2wpa in different groups. **C.** Patterns allow estimating the time of activation and the amount of H_2O_2 produced by different NADPH oxidases, as well as speculate about H_2O_2 production by Duox. The representation of *duox* is only advisory as more repeats are necessary.

Fin growth occurs by the addition of bone fragments to the distal end of the fin rays (Santamaría and Becerra 1991; Goldsmith et al. 2006). This addition of segments is followed by a period of stasis, thus giving rise to a saltatory mechanism of growth. Proportionality is maintained by regulating segment addition with varying lengths of stasis. Previously, *in situ* hybridisation (ISH) for the surrogate growth marker *fa93e10* in the caudal fin revealed a decreasing trend with increasing age, with 100% fins being *fa93e10*-positive in 8 week old fish to 0% in 35 week old animals (Goldsmith et al. 2003). Our observations tend to be a reflection of this, as we find a significant difference in size monthly, during the first three months. This is succeeded by a more

steady increase wherein significance is spaced out. Of course, what is also apparent is the variation in fin size within each age group. This variation among members of the same cohort, however, has also been previously acknowledged as growth rate varies markedly among larvae from the same clutch (Parichy et al. 2009).

Blastema formation in the adult zebrafish fin is complete by 48hpa (Gauron et al. 2013) and regeneration eventually lays out the original structure. It is interesting to note here that the regenerative capacity of the fin is unaffected by repeated amputation. Even after 10 consecutive episodes of resection, the fin has been shown to retain its regenerative potential (Azevedo et al. 2011). The importance of the blastema may be noted in runt animals that may occasionally be found alongside their siblings. These animals are outcompeted for food and are smaller than their peers. We have noticed on more than one occasion that these animals also fail to regenerate. The amputation margin never develops a blastema (**Fig. 19**). Supplementing these prior findings related to the blastema is our observation that there is minimal fin growth taking place during the regenerative period, even among the youngest adults (3months).

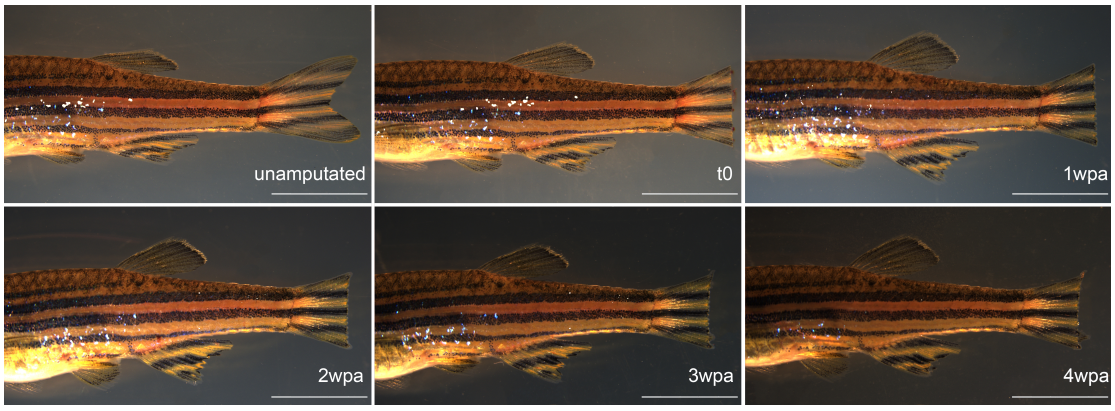

Fig. 19. Runt animals do not recover from caudal fin amputation. Scale bar=5mm.

The influence of advancing age on regenerative decline is known among fish. In a zebrafish model of axonal regeneration, the latency between resection and reinnervation increases with the age of the animals, even though regeneration is achieved at all examined ages (Graciarena, Dambly-Chaudière, and Ghysen 2014). Caudal fin regeneration in the killifish (*Nothobranchius furzeri*) also appears to

strongly correlate with age. While 8week old killifish achieve complete regeneration, animals over a year old were only found to achieve ~46% regeneration (Wendler et al. 2015). A more direct comparison is available from previous work on zebrafish caudal fin regeneration that revealed comparable results among young and old zebrafish, up to 13dpa (Itou et al. 2012). Meanwhile, a longer monitoring of the regenerative period revealed a significant difference between older and younger animals, with the former showing ~90% regeneration and the latter achieving 90%-98% regeneration by 30dpa. Our results on animals from different age groups appear to reconcile with both these findings, translating into steeper slopes of linear regression for younger animals and older animals just falling short of 100% regeneration. However, our data did not report the shortfall as significant. It is possible that older animals may need to be tracked for a longer length of time to fully determine the extent of regeneration. Alternatively, it might mean that regeneration is already complete, and the smaller fin is an outcome of age-related senescence. The latter suggestion may be supported by a recent investigation on telomere behaviour during aging in zebrafish. Here, a 58% telomerase upregulation among 3month old animals contrasted with an 18% upregulation among 24month old animals, at 5dpa (Anchelin et al. 2011). This study, however, broadly declared regeneration among older animals as not “normal”, based on irregular fin margins. This is an excessive generalisation and is not universally applicable as is evident from our data.

Pharmacological arrest of the noxes has been shown to be critical for blastema formation during caudal fin regeneration, in zebrafish. Briefly, JNK signalling is essential during early fin regeneration (Ishida et al. 2010). The MAP kinase phosphatases (MKPs) that inactivate JNK are critical targets of ROS in that their oxidation serves to sustain JNK activity. The nox-specific inhibitor, VAS2870, is able to sustain the inactivity of JNK and cause a reduction in blastema size (Gauron et al. 2013). This pharmacological targeting of the noxes is highly indicative of verifying their roles in mutant backgrounds. With the exception of *duox* mutants characterised by us (Chopra, Ishibashi, and Amaya 2019), there are no accounts of *nox* mutant teleost models, at the present time. After successfully targeting *cyba* and

nox5 using CRISPR/Cas9, these mutants were characterised to varying extents, as detailed in previous chapters. Briefly, we found that 1) *cyba* mutants do not display any apparent phenotypes but succumb to aspergillosis while their WT siblings successfully mount a defence; 2) *duox* mutants display a host of phenotypes in line with their congenital hypothyroidism; 3) *nox5* mutants also lack phenotypic peculiarities but are significantly resistant to anaesthesia.

The rationale behind targeting *cyba* was its essential partnering with noxes 1, 2 and 4. This was further propped up by microarray data from *Xenopus tropicalis*, which have shown that expression levels of *cyba* more than treble following amputation and remain upregulated throughout regeneration (Love et al. 2011). Moreover, post-amputation HyPer imaging showed *cyba* morphant *Xenopus* tadpoles had a ~33% reduction in amputation-induced ROS (Love et al. 2013). Surprisingly, a reduction in caudal fin regeneration was evident among our $cyba^{ex1.5bp-/-}$ adults, who failed to achieve 100% regeneration. These similar outcomes between *cyba* morphants in one species and *cyba* mutants in another was especially remarkable, and might be considered as a commentary on the functional conservation of cyba. In recent times, concerns have been raised about the virtues of using morpholinos for simulating loss-of-function. Equally, mutants have revealed mechanisms for countering deleterious effects, which have not been observed following transcriptional or translational knockdown, resulting in poor correlation between the two (Kok et al. 2015; Blum et al. 2015; Rossi et al. 2015; El-Brolosy and Stainier 2017). At least in this regard, it would appear that our *cyba* mutants have failed to deploy a compensatory mechanism to rescue regeneration.

nox5 mutations have very recently been generated in zebrafish, and examined in the context of optical tectum development, where mutants were observed to suffer from decreased innervation of the tectum. However, the mutants were reported to be embryonic lethal (Weaver et al. 2018), which is in sharp contrast to our findings. Thus, no other accounts exist of *nox5* and its influence on regeneration, outside of our findings.

The *duox* mutations, however, are a different story. Its relevance for regeneration may already be glimpsed from the animals' behaviour. As a shoaling species, zebrafish demonstrate social hierarchies, allied aggression and dominance behaviours (Nunes et al. 2017). Biting is one such behaviour where animals dart towards each other, attacking the gill region and fins (Zabegalov et al. 2019). Even so, it is unusual to see adult WT zebrafish with missing fin fragments, a likely outcome of continuous "microregeneration". *duox* mutants, however, persistently display ragged fins, an outcome of their underlying hypothyroidism (Chopra, Ishibashi, and Amaya 2019). Now, T_4 treatment will resolve the ragged fin phenotype. This observation is supported by findings in the medaka hypothyroid mutant *kamaitachi* (*kmi*), where T_4 treatment improves fin health. Also, the reduced rate of regeneration in *duox*$^{-/-}$ animals is similar to that in *kmi*$^{-/-}$ animals, which show a small but significant reduction. Further, induced hypothyroidism in WT medaka via thiourea also slowed the rate of regeneration (Sekimizu, Tagawa, and Takeda 2007). It came as no surprise then when zebrafish *manet* mutants also showed retardation in regeneration. Intriguingly though, WT zebrafish with goitrogen-induced hypothyroidism did not experience retardation in regeneration. This is, however, in line with previous reports wherein MMI treatment did not alter regeneration of the zebrafish fin (Bouzaffour et al. 2010). Further, while T_4 treatment rescues hypothyroidism-related phenotypes (Chopra, Ishibashi, and Amaya 2019), it does not rescue regeneration. An important revelation emerged while doing HyPer imaging on *duox* mutants. The HyPer imaging protocol enables a daily monitoring of animals, which revealed that the blastema was not forming in mutants even by 48hpa. We had previously missed this since our regeneration protocol only calls for a weekly observation. Furthermore, amputation in the midst of continuous long-term T_4 treatment of *duox* mutants resulted in the blastema forming within the expected time frame. While this may suggest, broadly, that T_4 treatment is able to rescue the reduced rate of regeneration, this observation is in opposition to existing reports. mRNA for deiodinase 3 (D3), the enzyme responsible for locally inactivating T_3, is reported to be upregulated in the regenerating fin, indicating that THs are dispensable for blastema formation. Furthermore, inhibiting D3 with iopanoic acid led to a reduction in the size of the blastema (Bouzaffour et al. 2010). Therefore, In

the midst of these conflicting observations, the role of THs in fin regeneration seems murky. Our observations on *manet* mutants would suggest that there is some importance of the THs, and *manet* mutants crossed into a *Tg(HyPer)* background may shed further light in the future.

The use of dichlorofluorescein (DCF) derivatives remains a popular approach for estimating post-amputation ROS production (Gauron et al. 2013; Q. Zhang et al. 2016; Al Haj Baddar, Chithrala, and Voss 2019). However, these are sensitive to more than one type of ROS (Crow 1997), and can also produce ROS upon exposure to light, thus resulting in artifact ROS (Rota, Fann, and Mason 1999). Using a stable *Tg(Hyper)* strain allowed us to bypass these disadvantages, as well as record flux for an extended length of time. Indeed, this is the USP of a transgenic reporter, and in this instance it revealed the duration of sustained ROS following amputation, similar to previous findings from our lab (Love et al. 2013). ROS 'baselined' prior to the completion of regeneration, instead of sustaining throughout. The mutants were worse off, experiencing an even briefer period. Nevertheless, the mutants gave us clues as to the temporal contribution of each. The fact that ROS levels sustain, regardless of length of time, reinforces the fact that regeneration proceeds in *nox* mutants, instead of ceasing, thus suggesting compensation. Thus, a future direction that we are planning to take is to use the mutations in combinations, hopefully obtaining a strain with all *noxes* mutated.

The most surprising observation perhaps was the circadian trend of ROS oscillations. From a biochemical point of view, it does make sense, as perpetually high ROS could be injurious to tissues. In relation to circadian rhythms, a trend must meet the following five criteria: (i) the ability to become entrained (synchronised), (ii) the persistence of the cycle after the removal of external stimuli, (iii) the ability to shift the phase of the cycle, (iv) a period of around 24 h, and (v) the ability to maintain its period independent of temperature (Golombek and Rosenstein 2010).

The vertebrate circadian clock is a transcription-translation feedback loop repeating every ~24h (Reppert and Weaver 2002). In a vertebrate system, products of the

master regulator genes *Clock* and *Bmal1*, heterodimerise and bind to enhancer E-box regions, promoting the transcription of the negative master regulators, Period (*Per*) and Cryptochrome (*Cry*). Per/Cry heterodimerise, translocate to the nucleus and bind to the Clock/Bmal1 complex, inhibiting their own transcription, as well the transcription of other Clock/Bmal1 targets (Lowrey and Takahashi 2011). Eventual ubiquitination and degradation of the Per/Cry complex resets the cycle (Busino et al. 2007). Upto 43% protein encoding genes show circadian oscillation in their expression in at least one organ (R. Zhang et al. 2014) and this cyclic expression follows external cues (zeitgebers) such as light exposure and feeding (Golombek and Rosenstein 2010; Refinetti 2015).

As it has done in other fields of enquiry, the zebrafish has established a presence in the study of circadian rhythms. In the zebrafish, traditional views of the pineal gland being a central pacemaker of circadian rhythm (Vatine et al. 2011) have been demolished and given way to a decentralised model stating that independent, light-sensitive pacemakers exist in all cells and tissues (Steindal and Whitmore 2019). This view is applicable to other teleosts as well, including the Senegalese sole (*Solea senegalesnsis*) (Martín-Robles et al. 2011, 2012), Mexican blind cavefish (*Astyanax mexicanus*) (Beale et al. 2013), and medaka (*Oryzia latipes*) (Cuesta et al. 2014). Zebrafish are receptive to light-dark cycles as early as the blastula stage, before any classical photoreceptor organs have even come into inception (Ziv and Gothilf 2006). Light exposure is essential to development, as embryos reared in dark incubators experience developmental defects and lower survival rates (Tamai et al. 2004). We found that even in an unamputated state, ROS undergoes oscillations, and that these are more marked prior to exposure to the first light of day. Therefore, use of the terms ‘basal’ or ‘baseline levels’ is very much context-dependent.

Evidence is now available for regenerative processes coordinating with circadian rhythms during skin, intestinal and hematopoietic stem cell (HSC) regeneration. Mouse skin explants heal faster when harvested and wounded nocturnally (active phase for mice) (Hoyle et al. 2017). In another mouse model, *Per* knockout mice showed decreased proliferation of the intestinal epithelium following the ingestion

of dextran-sodium sulphate, a drug used for simulating gastrointestinal diseases (Pagel et al. 2017). In the case of HSCs, regeneration has a different dynamic, that of continuous replenishment. Differential expression of circadian regulators has been reported in murine HSCs, depending on the state of differentiation. *Per1* mRNA levels were three times higher and *Cry1* levels were lower among long-term HSCs when compared to whole bone marrow cells, suggesting (Tsinkalovsky et al. 2005). No studies have been documented in relation to regeneration among fish and circadian rhythm. However, seeing as the role of ROS in regeneration is now established, the preamble to ROS and circadian rhythm becomes pertinent. Cellular defences, such as antioxidant mechanisms, which keep ROS in check appear to be regulated in rhythmic fashion, suggesting that ROS and circadian rhythm are intertwined (Martín et al. 2003; Wilking, Ndiaye, and Mukhtar 2013). In investigating the role of Noxes, this work has also drawn a connection between circadian rhythms and elevated ROS levels post-amputation as regeneration commences.

References

1. Ameziane-el-hassani, Rabii, Stanislas Morand, Jean-luc Boucher, Yves-michel Frapart, Diane Agnandji, Marie-sophie Noe, Jacques Francon, Khalid Lalaoui, Alain Virion, and Corinne Dupuy. 2005. "Dual Oxidase-2 Has an Intrinsic Ca 2 -Dependent H 2 O 2 -Generating Activity *" 280 (34): 30046–54. https://doi.org/10.1074/jbc.M500516200.
2. Anchelin, Monique, Laura Murcia, Francisca Alcaraz-Pérez, Esther M García-Navarro, and María L Cayuela. 2011. "Behaviour of Telomere and Telomerase during Aging and Regeneration in Zebrafish." *PLOS ONE* 6 (2): e16955. https://doi.org/10.1371/journal.pone.0016955.
3. Aycan, Zehra, Hakan Cangul, Marina Muzza, Veysel N. Bas, Laura Fugazzola, V. Krishna Chatterjee, Luca Persani, and Nadia Schoenmakers. 2017. "Digenic DUOX1 and DUOX2 Mutations in Cases with Congenital Hypothyroidism." *Journal of Clinical Endocrinology and Metabolism* 102 (9): 3085–90. https://doi.org/10.1210/jc.2017-00529.
4. Azevedo, Ana Sofia, Bartholomäus Grotek, António Jacinto, Gilbert Weidinger, and Leonor Saúde. 2011. "The Regenerative Capacity of the Zebrafish Caudal Fin Is Not Affected by Repeated Amputations." *PLOS ONE* 6 (7): e22820. https://doi.org/10.1371/journal.pone.0022820.
5. Beale, Andrew, Christophe Guibal, T Katherine Tamai, Linda Klotz, Sophie Cowen, Elodie Peyric, Víctor H Reynoso, Yoshiyuki Yamamoto, and David Whitmore. 2013. "Circadian Rhythms in Mexican Blind Cavefish Astyanax Mexicanus in the Lab and in the Field." *Nature Communications* 4 (1): 2769. https://doi.org/10.1038/ncomms3769.
6. Bedard, Karen, and Karl-Heinz Heinz Krause. 2007. "The NOX Family of ROS-Generating NADPH Oxidases: Physiology and Pathophysiology." *Physiological Reviews* 87 (1): 245–313. https://doi.org/10.1152/physrev.00044.2005.
7. Belousov, Vsevolod V., Arkady F. Fradkov, Konstantin A. Lukyanov, Dmitry B. Staroverov, Konstantin S. Shakhbazov, Alexey V. Terskikh, and Sergey Lukyanov. 2006. "Genetically Encoded Fluorescent Indicator for Intracellular Hydrogen Peroxide." *Nature Methods* 3 (4): 281–86. https://doi.org/10.1038/nmeth866.
8. Blum, Martin, Edward M. De Robertis, John B. Wallingford, and Christof Niehrs. 2015. "Morpholinos: Antisense and Sensibility." *Developmental Cell* 35 (2): 145–49. https://doi.org/10.1016/j.devcel.2015.09.017.
9. Bouzaffour, Mohamed, Christine Rampon, Martine Ramaugé, Françoise Courtin, and Sophie Vriz. 2010. "Implication of Type 3 Deiodinase Induction in Zebrafish Fin Regeneration." *General and Comparative Endocrinology* 168 (1): 88–94. https://doi.org/10.1016/j.ygcen.2010.04.006.
10. Busino, Luca, Florian Bassermann, Alessio Maiolica, Choogon Lee, Patrick M Nolan, Sofia I H Godinho, Giulio F Draetta, and Michele Pagano. 2007. "SCFFbxl3 Controls the Oscillation of the Circadian Clock by Directing the Degradation of Cryptochrome Proteins." *Science* 316 (5826): 900 LP – 904. https://doi.org/10.1126/science.1141194.
11. Carneiro, Madalena C., Catarina M. Henriques, Joana Nabais, Tânia Ferreira, Tânia Carvalho, and Miguel Godinho Ferreira. 2016. "Short Telomeres in Key Tissues Initiate Local and Systemic Aging in Zebrafish." *PLoS Genetics* 12 (1): 1–31. https://doi.org/10.1371/journal.pgen.1005798.
12. Carvalho, Denise P., and Corinne Dupuy. 2013. "Role of the NADPH Oxidases DUOX and NOX4 in Thyroid Oxidative Stress." *European Thyroid Journal* 2 (3): 160–67. https://doi.org/10.1159/000354745.

13. Chopra, Kunal, Shoko Ishibashi, and Enrique Amaya. 2019. " Zebrafish Duox Mutations Provide a Model for Human Congenital Hypothyroidism ." *Biology Open* 8 (2): bio037655. https://doi.org/10.1242/bio.037655.
14. Cordeiro, João V, and António Jacinto. 2013. "The Role of Transcription-Independent Damage Signals in the Initiation of Epithelial Wound Healing." *Nature Reviews Molecular Cell Biology* 14 (4): 249–62. https://doi.org/10.1038/nrm3541.
15. Crow, John P. 1997. "Dichlorodihydrofluorescein and Dihydrorhodamine 123 Are Sensitive Indicators of Peroxynitritein Vitro:Implications for Intracellular Measurement of Reactive Nitrogen and Oxygen Species." *Nitric Oxide* 1 (2): 145–57. https://doi.org/https://doi.org/10.1006/niox.1996.0113.
16. Cuesta, Ines H, Kajori Lahiri, Jose Fernando Lopez-Olmeda, Felix Loosli, Nicholas S Foulkes, and Daniela Vallone. 2014. "Differential Maturation of Rhythmic Clock Gene Expression during Early Development in Medaka (Oryzias Latipes)." *Chronobiology International* 31 (4): 468–78. https://doi.org/10.3109/07420528.2013.856316.
17. Dinauer, M C, E A Pierce, G A Bruns, J T Curnutte, and S H Orkin. 1990. "Human Neutrophil Cytochrome b Light Chain (P22-Phox). Gene Structure, Chromosomal Location, and Mutations in Cytochrome-Negative Autosomal Recessive Chronic Granulomatous Disease." *The Journal of Clinical Investigation* 86 (5): 1729–37. https://doi.org/10.1172/JCI114898.
18. Dupuy, Corinne, Renée Ohayon, Alexander Valent, Marie-Sophie Noël-Hudson, Danielle Dème, and Alain Virion. 2002. "Purification of a Novel Flavoprotein Involved in the Thyroid NADPH Oxidase." *Journal of Biological Chemistry* 274 (52): 37265–69. https://doi.org/10.1074/jbc.274.52.37265.
19. Dutta, H. 1994. "Growth in Fishes." *Gerontology* 40 (2–4): 97–112. https://doi.org/10.1159/000213581.
20. El-Brolosy, Mohamed A., and Didier Y.R. Stainier. 2017. "Genetic Compensation: A Phenomenon in Search of Mechanisms." *PLoS Genetics* 13 (7): 1–17. https://doi.org/10.1371/journal.pgen.1006780.
21. Gauron, Carole, Christine Rampon, Mohamed Bouzaffour, Eliane Ipendey, Jeremie Teillon, Michel Volovitch, and Sophie Vriz. 2013. "Sustained Production of ROS Triggers Compensatory Proliferation and Is Required for Regeneration to Proceed." *Scientific Reports* 3: 1–9. https://doi.org/10.1038/srep02084.
22. Gilbert, Matthew J H, Tanja C. Zerulla, and Keith B. Tierney. 2013. "Zebrafish (Danio Rerio) as a Model for the Study of Aging and Exercise: Physical Ability and Trainability Decrease with Age." *Experimental Gerontology* 50 (1): 106–13. https://doi.org/10.1016/j.exger.2013.11.013.
23. Gillam, Mary P, and Peter Kopp. 2001. "Genetic Defects in Thyroid Hormone Synthesis." *Current Opinion in Pediatrics* 13 (4). https://journals.lww.com/co-pediatrics/Fulltext/2001/08000/Genetic_defects_in_thyroid_hormone_synthesis.14.aspx.
24. Goldsmith, Matthew I, Shannon Fisher, Rick Waterman, and Stephen L Johnson. 2003. "Saltatory Control of Isometric Growth in the Zebrafish Caudal Fin Is Disrupted in Long Fin and Rapunzel Mutants." *Developmental Biology* 259 (2): 303–17. https://doi.org/https://doi.org/10.1016/S0012-1606(03)00186-6.
25. Goldsmith, Matthew I, M Kathryn Iovine, Thomas O'Reilly-Pol, and Stephen L Johnson. 2006. "A Developmental Transition in Growth Control during Zebrafish Caudal Fin Development." *Developmental Biology* 296 (2): 450–57. https://doi.org/https://doi.org/10.1016/j.ydbio.2006.06.010.
26. Golombek, Diego A, and Ruth E Rosenstein. 2010. "Physiology of Circadian Entrainment." *Physiological Reviews* 90 (3): 1063–1102. https://doi.org/10.1152/physrev.00009.2009.
27. Graciarena, Mariana, Christine Dambly-Chaudière, and Alain Ghysen. 2014. "Dynamics of Axonal Regeneration in Adult and Aging Zebrafish Reveal the Promoting Effect of a First Lesion." *Proceedings of the National Academy of Sciences* 111 (4): 1610 LP – 1615. https://doi.org/10.1073/pnas.1319405111.
28. Haj Baddar, Nour W Al, Adarsh Chithrala, and S Randal Voss. 2019. "Amputation-Induced Reactive Oxygen Species Signaling Is Required for Axolotl Tail Regeneration." *Developmental Dynamics* 248 (2): 189–96. https://doi.org/10.1002/dvdy.5.
29. Han, Yue, Shoko Ishibashi, Javier Iglesias-Gonzalez, Yaoyao Chen, Nick R Love, and Enrique Amaya. 2018. "Ca^{2+}-Induced Mitochondrial ROS Regulate the Early Embryonic Cell Cycle." *Cell Reports* 22 (1): 218–31. https://doi.org/10.1016/j.celrep.2017.12.042.
30. Hilenski, Lula L, Roza E Clempus, Mark T Quinn, J David Lambeth, and Kathy K Griendling. 2004. "Vascular Smooth Muscle Cells," 677–83. https://doi.org/10.1161/01.ATV.0000112024.13727.2c.
31. Hoyle, Nathaniel P, Estere Seinkmane, Marrit Putker, Kevin A Feeney, Toke P Krogager, Johanna E Chesham, Liam K Bray, et al. 2017. "Circadian Actin Dynamics Drive Rhythmic Fibroblast Mobilization during Wound Healing." *Science Translational Medicine* 9 (415): eaal2774. https://doi.org/10.1126/scitranslmed.aal2774.
32. Iovine, M K, and S L Johnson. 2000. "Genetic Analysis of Isometric Growth Control Mechanisms in the Zebrafish Caudal Fin." *Genetics* 155 (3): 1321–29. https://www.ncbi.nlm.nih.gov/pubmed/10880491.
33. Ishida, Takashi, Teruhiro Nakajima, Akira Kudo, and Atsushi Kawakami. 2010. "Phosphorylation of Junb Family Proteins by the Jun N-Terminal Kinase Supports Tissue Regeneration in Zebrafish." *Developmental Biology* 340 (2): 468–79. https://doi.org/https://doi.org/10.1016/j.ydbio.2010.01.036.
34. Itou, J., H. Kawakami, T. Burgoyne, and Y. Kawakami. 2012. "Life-Long Preservation of the Regenerative Capacity in the Fin and Heart in Zebrafish." *Biology Open* 1 (8): 739–46. https://doi.org/10.1242/bio.20121057.
35. Kawahara, By Tsukasa, Mark T. Quinn, and J. David Lambeth. 2007. "Molecular Evolution of the Reactive Oxygen-Generating NADPH Oxidase (Nox/Duox) Family of Enzymes." *BMC Evolutionary Biology* 7: 1–21. https://doi.org/10.1186/1471-2148-7-109.
36. Kizys, Marina M.L., Ruy A. Louzada, Miguel Mitne-Neto, Jessica R. Jara, Gilberto K. Furuzawa, Denise P. De Carvalho, Magnus R. Dias-Da-Silva, Suzana Nesi-França, Corinne Dupuy, and Rui M.B. Maciel. 2017. "DUOX2 Mutations Are Associated with Congenital Hypothyroidism with Ectopic Thyroid Gland." *Journal of Clinical Endocrinology and Metabolism* 102 (11): 4060–71. https://doi.org/10.1210/jc.2017-00832.
37. Knopf, Franziska, Christina Hammond, Avinash Chekuru, Thomas Kurth, Stefan Hans, Christopher W. Weber, Gina Mahatma, et al. 2011. "Bone Regenerates via Dedifferentiation of Osteoblasts in the Zebrafish Fin." *Developmental Cell* 20 (5): 713–24. https://doi.org/https://doi.org/10.1016/j.devcel.2011.04.014.
38. Kok, Fatma O., Masahiro Shin, Chih Wen Ni, Ankit Gupta, Ann S. Grosse, Andreas vanImpel, Bettina C. Kirchmaier, et al. 2015. "Reverse Genetic Screening Reveals Poor Correlation between Morpholino-Induced and Mutant

Phenotypes in Zebrafish." *Developmental Cell* 32 (1): 97–108. https://doi.org/10.1016/j.devcel.2014.11.018.
39. Liu, Shiguo, Wenxiu Han, Yucui Zang, Hongwei Zang, Fang Wang, Pei Jiang, Hongwei Wei, et al. 2019. "Identification of Two Missense Mutations in DUOX1 (p.R1307Q) and DUOXA1 (p.R56W) That Can Cause Congenital Hypothyroidism Through Impairing H2O2 Generation ." *Frontiers in Endocrinology* . https://www.frontiersin.org/article/10.3389/fendo.2019.00526.
40. Love, Nick R., Yaoyao Chen, Boyan Bonev, Michael J. Gilchrist, Lynne Fairclough, Robert Lea, Timothy J. Mohun, Roberto Paredes, Leo Ah Zeef, and Enrique Amaya. 2011. "Genome-Wide Analysis of Gene Expression during Xenopus Tropicalis Tadpole Tail Regeneration." *BMC Developmental Biology* 11 (1): 70. https://doi.org/10.1186/1471-213X-11-70.
41. Love, Nick R., Yaoyao Chen, Shoko Ishibashi, Paraskevi Kritsiligkou, Robert Lea, Yvette Koh, Jennifer L. Gallop, Karel Dorey, and Enrique Amaya. 2013. "Amputation-Induced Reactive Oxygen Species Are Required for Successful Xenopus Tadpole Tail Regeneration." *Nature Cell Biology* 15 (2): 222–28. https://doi.org/10.1038/ncb2659.
42. Lowrey, Phillip L, and Joseph S Takahashi. 2011. "Chapter 6 - Genetics of Circadian Rhythms in Mammalian Model Organisms." In *The Genetics of Circadian Rhythms*, edited by Stuart B T - Advances in Genetics Brody, 74:175–230. Academic Press. https://doi.org/https://doi.org/10.1016/B978-0-12-387690-4.00006-4.
43. Mailloux, Ryan J. 2015. "Teaching the Fundamentals of Electron Transfer Reactions in Mitochondria and the Production and Detection of Reactive Oxygen Species." *Redox Biology* 4: 381–98. https://doi.org/10.1016/j.redox.2015.02.001.
44. Martín-Robles, Águeda J, Esther Isorna, David Whitmore, José A Muñoz-Cueto, and Carlos Pendón. 2011. "The Clock Gene Period3 in the Nocturnal Flatfish Solea Senegalensis: Molecular Cloning, Tissue Expression and Daily Rhythms in Central Areas." *Comparative Biochemistry and Physiology Part A: Molecular & Integrative Physiology* 159 (1): 7–15. https://doi.org/https://doi.org/10.1016/j.cbpa.2011.01.015.
45. Martín-Robles, Águeda J, David Whitmore, Francisco Javier Sánchez-Vázquez, Carlos Pendón, and José A Muñoz-Cueto. 2012. "Cloning, Tissue Expression Pattern and Daily Rhythms of Period1, Period2, and Clock Transcripts in the Flatfish Senegalese Sole, Solea Senegalensis." *Journal of Comparative Physiology B* 182 (5): 673–85. https://doi.org/10.1007/s00360-012-0653-z.
46. Martín, Vanesa, Rosa María Sainz, Juan Carlos Mayo, Isaac Antolín, Federico Herrera, and Carmen Rodríguez. 2003. "Daily Rhythm of Gene Expression in Rat Superoxide Dismutases." *Endocrine Research* 29 (1): 83–95. https://doi.org/10.1081/ERC-120018679.
47. McMenamin, Sarah K., Emily J. Bain, Anna E. McCann, Larissa B. Patterson, Dae Seok Eom, Zachary P. Waller, James C. Hamill, Julie A. Kuhlman, Judith S. Eisen, and David M. Parichy. 2014. "Thyroid Hormone-Dependent Adult Pigment Cell Lineage and Pattern Inzebrafish." *Science* 345 (6202): 1358–61. https://doi.org/10.1126/science.1256251.
48. Moldovan, Leni, and Nicanor I. Moldovan. 2004. "Oxygen Free Radicals and Redox Biology of Organelles." *Histochemistry and Cell Biology* 122 (4): 395–412. https://doi.org/10.1007/s00418-004-0676-y.
49. Moreno-mateos, Miguel A, Charles E Vejnar, Jean-denis Beaudoin, Juan P Fernandez, Emily K Mis, Mustafa K Khokha, and Antonio J Giraldez. 2015. "CRISPRscan : Designing Highly Efficient SgRNAs for CRISPR-Cas9 Targeting in Vivo" 12 (10). https://doi.org/10.1038/nmeth.3543.
50. Moreno, José C, Hennie Bikker, Marlies J E Kempers, A S Paul van Trotsenburg, Frank Baas, Jan J M de Vijlder, Thomas Vulsma, and C Ris-Stalpers. 2002. "Inactivating Mutations in the Gene for Thyroid Oxidase 2 (THOX2) and Congenital Hypothyroidism." *New England Journal of Medicine* 347 (2): 95–102. https://doi.org/10.1056/NEJMoa012752.
51. Muzza, Marina, and Laura Fugazzola. 2017. "Disorders of H2O2 Generation." *Best Practice and Research: Clinical Endocrinology and Metabolism* 31 (2): 225–40. https://doi.org/10.1016/j.beem.2017.04.006.
52. Nakano, Yoko, Chantal M Longo-guess, David E Bergstrom, William M Nauseef, Sherri M Jones, and Botond Bánfi. 2008. "Mutation of the CYBA Gene Encoding P22 Phox Causes Vestibular and Immune Defects in Mice." *The Journal of Clinical Investigation* 118 (3): 1176–85. https://doi.org/10.1172/JCI33835.1176.
53. Niethammer, Philipp, Clemens Grabher, A. Thomas Look, and Timothy J. Mitchison. 2009. "A Tissue-Scale Gradient of Hydrogen Peroxide Mediates Rapid Wound Detection in Zebrafish." *Nature* 459 (7249): 996–99. https://doi.org/10.1038/nature08119.
54. Nunes, Ana Rita, Nathan Ruhl, Svante Winberg, and Rui F Oliveira. 2017. "Social Phenotypes in Zebrafish." In *The Rights and Wrongs of Zebrafish: Behavioral Phenotyping of Zebrafish*, edited by Allan V Kalueff, 95–130. Cham: Springer International Publishing. https://doi.org/10.1007/978-3-319-33774-6_5.
55. Pagel, René, Florian Bär, Torsten Schröder, Annika Sünderhauf, Axel Künstner, Saleh M Ibrahim, Stella E Autenrieth, et al. 2017. "Circadian Rhythm Disruption Impairs Tissue Homeostasis and Exacerbates Chronic Inflammation in the Intestine." *The FASEB Journal* 31 (11): 4707–19. https://doi.org/10.1096/fj.201700141RR.
56. Parichy, David M., Michael R. Elizondo, Margaret G. Mills, Tiffany N. Gordon, and Raymond E. Engeszer. 2009. "Normal Table of Postembryonic Zebrafish Development: Staging by Externally Visible Anatomy of the Living Fish." *Developmental Dynamics* 238 (12): 2975–3015. https://doi.org/10.1002/dvdy.22113.
57. Pfefferli, Catherine, and Anna Jaźwińska. 2015. "The Art of Fin Regeneration in Zebrafish." *Regeneration (Oxford, England)* 2 (2): 72–83. https://doi.org/10.1002/reg2.33.
58. Razzell, William, Iwan Robert Evans, Paul Martin, and Will Wood. 2013. "Calcium Flashes Orchestrate the Wound Inflammatory Response through DUOX Activation and Hydrogen Peroxide Release." *Current Biology : CB* 23 (5): 424–29. https://doi.org/10.1016/j.cub.2013.01.058.
59. Refinetti, Roberto. 2015. "Comparison of Light, Food, and Temperature as Environmental Synchronizers of the Circadian Rhythm of Activity in Mice." *The Journal of Physiological Sciences* 65 (4): 359–66. https://doi.org/10.1007/s12576-015-0374-7.
60. Reppert, Steven M, and David R Weaver. 2002. "Coordination of Circadian Timing in Mammals." *Nature* 418 (6901): 935–41. https://doi.org/10.1038/nature00965.
61. Rossi, Andrea, Zacharias Kontarakis, Claudia Gerri, Hendrik Nolte, Soraya Hölper, Marcus Krüger, and Didier Y.R. Stainier. 2015. "Genetic Compensation Induced by Deleterious Mutations but Not Gene Knockdowns." *Nature* 524

(7564): 230–33. https://doi.org/10.1038/nature14580.
62. Rota, Cristina, Yang C. Fann, and Ronald P. Mason. 1999. “Phenoxyl Free Radical Formation during the Oxidation of the Fluorescent Dye 2’,7’-Dichlorofluorescein by Horseradish Peroxidase. Possible Consequences for Oxidative Stress Measurements.” *Journal of Biological Chemistry* 274 (40): 28161–68. https://doi.org/10.1074/jbc.274.40.28161.
63. Santamaría, J A, and J Becerra. 1991. “Tail Fin Regeneration in Teleosts: Cell-Extracellular Matrix Interaction in Blastemal Differentiation.” *Journal of Anatomy* 176 (June): 9–21. https://www.ncbi.nlm.nih.gov/pubmed/1917678.
64. Sekimizu, Koshin, Masatomo Tagawa, and Hiroyuki Takeda. 2007. “Defective Fin Regeneration in Medaka Fish (Oryzias Latipes) with Hypothyroidism.” *Zoological Science* 24 (7): 693–99. https://doi.org/10.2108/zsj.24.693.
65. Stasia, Marie, Pierre Bordigoni, Cécile Martel, and Françoise Morel. 2002. “A Novel and Unusual Case of Chronic Granulomatous Disease in a Child with a Homozygous 36-Bp Deletion in the CYBA Gene (A220) Leading to the Activation of a Cryptic Splice Site in Intron 4.” *Human Genetics* 110 (5): 444–50. https://doi.org/10.1007/s00439-002-0720-8.
66. Steindal, Inga A Frøland, and David Whitmore. 2019. “Circadian Clocks in Fish — What Have We Learned so Far ?” https://doi.org/10.3390/biology8010017.
67. Stoick-Cooper, Cristi L, Randall T Moon, and Gilbert Weidinger. 2007. “Advances in Signaling in Vertebrate Regeneration as a Prelude to Regenerative Medicine.” *Genes & Development* 21 (11): 1292–1315. https://doi.org/10.1101/gad.1540507.
68. Tamai, T.Katherine, Varut Vardhanabhuti, Nicholas S Foulkes, and David Whitmore. 2004. “Early Embryonic Light Detection Improves Survival.” *Current Biology* 14 (5): 446. https://doi.org/10.1016/j.cub.2004.02.040.
69. Tazaki, Akira, Atsushi Kitayama, Chie Terasaka, Kenji Watanabe, Naoto Ueno, and Makoto Mochii. 2005. “Macroarray-Based Analysis of Tail Regeneration in Xenopus Laevis Larvae.” *Developmental Dynamics* 233 (4): 1394–1404. https://doi.org/10.1002/dvdy.20472.
70. Topczewska, Jolanta M., Ramy A. Shoela, Joanna P. Tomaszewski, Rupa B. Mirmira, and Arun K. Gosain. 2016. “The Morphogenesis of Cranial Sutures in Zebrafish.” *PLoS ONE* 11 (11): 1–23. https://doi.org/10.1371/journal.pone.0165775.
71. Tsinkalovsky, Oleg, Benedikte Rosenlund, Ole Didrik Laerum, and Hans Geir Eiken. 2005. “Clock Gene Expression in Purified Mouse Hematopoietic Stem Cells.” *Experimental Hematology* 33 (1): 100–107. https://doi.org/10.1016/j.exphem.2004.09.007.
72. Vatine, Gad, Daniela Vallone, Yoav Gothilf, and Nicholas S Foulkes. 2011. “It’s Time to Swim! Zebrafish and the Circadian Clock.” *FEBS Letters* 585 (10): 1485–94. https://doi.org/https://doi.org/10.1016/j.febslet.2011.04.007.
73. Vliet, Albert Van Der, and Yvonne M.W. Janssen-Heininger. 2014. “Hydrogen Peroxide as a Damage Signal in Tissue Injury and Inflammation: Murderer, Mediator, or Messenger?” *Journal of Cellular Biochemistry* 115 (3): 427–35. https://doi.org/10.1002/jcb.24683.
74. Weaver, Cory J, Aslihan Terzi, Haley Roeder, Theodore Gurol, Qing Deng, Yuk Fai Leung, and Daniel M Suter. 2018. “Nox2/Cybb Deficiency Affects Zebrafish Retinotectal Connectivity.” *The Journal of Neuroscience* 38 (26): 5854 LP – 5871. https://doi.org/10.1523/JNEUROSCI.1483-16.2018.
75. Wendler, Sebastian, Nils Hartmann, Beate Hoppe, and Christoph Englert. 2015. “Age-Dependent Decline in Fin Regenerative Capacity in the Short-Lived Fish Nothobranchius Furzeri.” *Aging Cell* 14 (5): 857–66. https://doi.org/10.1111/acel.12367.
76. Wilking, Melissa, Mary Ndiaye, and Hasan Mukhtar. 2013. “Circadian Rhythm Connections to Oxidative Stress : Implications for Human Health” 19 (2): 192–208. https://doi.org/10.1089/ars.2012.4889.
77. Yoshinari, Nozomi, Takashi Ishida, Akira Kudo, and Atsushi Kawakami. 2009. “Gene Expression and Functional Analysis of Zebrafish Larval Fin Fold Regeneration.” *Developmental Biology* 325 (1): 71–81. https://doi.org/https://doi.org/10.1016/j.ydbio.2008.09.028.
78. Zabegalov, Konstantin N., Tatiana O. Kolesnikova, Sergey L. Khatsko, Andrey D. Volgin, Oleg A. Yakovlev, Tamara G. Amstislavskaya, Ashton J. Friend, et al. 2019. “Understanding Zebrafish Aggressive Behavior.” *Behavioural Processes* 158 (April 2018): 200–210. https://doi.org/10.1016/j.beproc.2018.11.010.
79. Zhang, Qing, Yongjun Yingjie Wang, Lili Man, Ziwen Zhu, Xue Bai, Sumei Wei, Yan Liu, et al. 2016. “Reactive Oxygen Species Generated from Skeletal Muscles Are Required for Gecko Tail Regeneration.” *Scientific Reports* 6 (February): 20752. https://doi.org/10.1038/srep20752.
80. Zhang, Ray, Nicholas F Lahens, Heather I Ballance, Michael E Hughes, and John B Hogenesch. 2014. “A Circadian Gene Expression Atlas in Mammals: Implications for Biology and Medicine.” *Proceedings of the National Academy of Sciences* 111 (45): 16219 LP – 16224. https://doi.org/10.1073/pnas.1408886111.
81. Zheng, Ming, Fredrik Åslund, and Gisela Storz. 1998. “Activation of the OxyR Transcription Factor by Reversible Disulfide Bond Formation.” *Science* 279 (5357): 1718 LP – 1722. https://doi.org/10.1126/science.279.5357.1718.
82. Ziv, Limor, and Yoav Gothilf. 2006. “Circadian Time-Keeping during Early Stages of Development.” *Proceedings of the National Academy of Sciences of the United States of America* 103 (11): 4146 LP – 4151. https://doi.org/10.1073/pnas.0600571103.

Future Directions

Investigating the role of Nox-mediated ROS in caudal fin regeneration follows from numerous pharmacological and knockdown studies (Al Haj Baddar, Chithrala, & Voss, 2019; Gauron et al., 2013; Love et al., 2013; Zhang et al., 2016). In the zebrafish, the ease of generating CRISPR mutants, and the availability of a library of ENU mutations for protein coding genes allow to apply a genetic approach to prior findings. Using CRISPR, we targeted *cyba* and *nox5*, while for duox we used ENU mutants. Regeneration was scored using two methods: increasing area of the regenerating fin, and the underlying ROS flux. The latter was achieved using a transgenic reporter, *Tg(HyPer)*, and all mutants were either crossed into or generated in this transgenic background. Now, both, *cyba* and *duox* mutations are well known to cause pathologies, and so, exploring the role of *nox* mutations in fin regeneration led us to concurrently characterising phenotypes associated with these mutations. To publish these findings, further experimental enquiries are indicated. The following descriptions refer to these future experiments.

Manuscript #1

We described a new piscine model for CGD, from its generation to its partial functional characterisation. These findings will be deemed more roust if they can be replicated in another *cyba* mutant. While it has not been reported in this work, we have obtained a second mutant allele, known as *cyba sa11798.* This an ENU mutant, with a nonsense mutation in exon 4 (Kettleborough et al., 2013). Like the CRISPR mutants, we found that *cyba sa11798*$^{-/-}$ larvae also succumb to aspergillosis. Fully characterising the mutants will require determining whether they are knockouts or not. This will be addressed via western blotting.

In the case of CGD, innate phagocytes extend differential responses during infection, based on fungal morphology (Knox, Deng, Rood, Eickhoff, & Keller, 2014). Macrophages pursue non-oxidative mechanisms, phagocytosing conidia (Sprenkeler, Gresnigt, & van de Veerdonk, 2016). The hyphae are resistant to phagocytosis and

are countered by neutrophils via ROS generation and neutrophil extracellular traps (NETs). The latter are an assembly of a DNA scaffold and cytoplasmic and granular proteins, which can trap and eliminate microbes (McCormick et al., 2010). In line with this, investigating *in vitro* and *in vivo* interactions between neutrophils and *A. fumigatus* is indicated. Previously, we crossed transgenic reporters for neutrophils (*mpx*:GFP - myeloperoxidase promoter driving GFP expression) (Renshaw *et al*., 2006) and macrophages (*mpeg*:mCherry- *mpeg1* promoter driving mCherry) (Ellet *et al*., 2011) to generate *Tg(mpeg:mCherry)(mpx:GFP)* (**Fig. 1**). This has now been crossed with both *cyba* mutants. The aim will be to compare the killing activity of WT neutrophils with those of *cyba* mutants. The fluorescent protein tags on these leukocytes will enable FAC sorting, thus ruling out the need for cumbersome techniques to isolate cells for *in vitro* assays. The combating efficiency of neutrophils has recently been investigated using fast (CEA10) and slow (Af293) germinating strains of *Aspergillus fumigatus*. In neutrophil-deficient animals CEA10 infection is lethal (Rosowski et al., 2018). It would thus be interesting to note how variable fungal strains fare in CGD hosts. Assuming that ROS generation confers hyphal killing abilities on neutrophils, and the fact that neutrophils from CGD are deficient in NET formation (Segal, Veys, Malech, & Cowan, 2011), would it encourage alternative defence mechanisms? This is especially relevant given that our *cyba* mutants remain healthy while murine models and patients develop clinically apparent symptoms. It would also be interesting to note what phenotypes heterozygotes present with, if any. At least, human female carriers of X-CGD have not been known to have a predisposition to infection (Windhorst, Holmes, & Good, 1967).

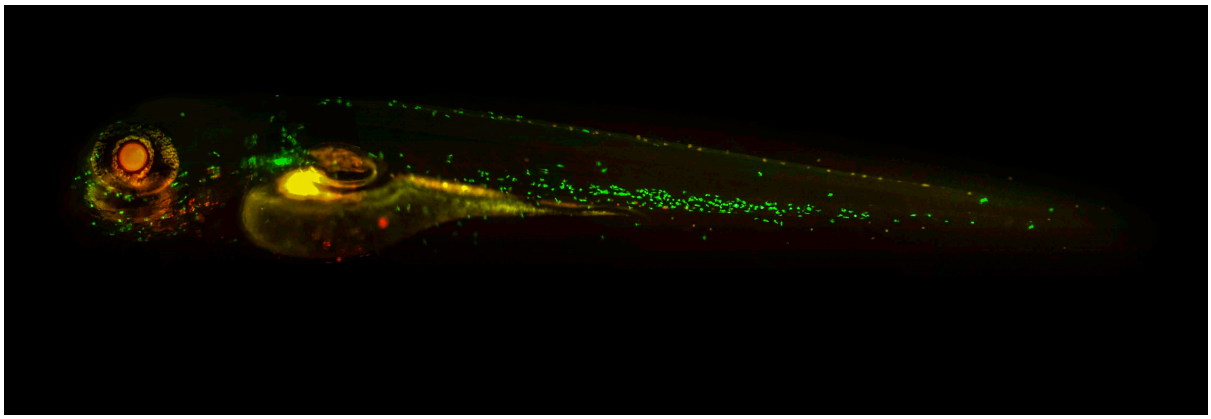

Fig. 1. *Tg(mpeg:mCherry)(mpx:GFP)* larva, at 5dpf, showing GFP-tagged neutrophils and mCherry-tagged macrophages.

Interestingly, oxidative mechanisms for countering catalase-positive pathogens are still not fully understood. A case in point is *Staphylococcus aureus* infection, a classical CGD complication. The hypothesis supporting oxidative killing suggests that H_2O_2 produced by catalase-negative pathogens accumulates in the phagosome and antagonises the very pathogens that produced it. This removes dependency on NOX-generated ROS. Thus, catalase-positive pathogens are able to counter their own destruction by way of antioxidant production (Holmes and Good, 1972). Even so, there is little evidence in support of the antioxidant enzymes contributing to defence in *Staphylococcus aureus* (Buvelot, Posfay-Barbe, Linder, Schrenzel, & Krause, 2016). While elevated ROS levels poison bacteria (Imlay, 2013), *Staphylococcus aureus* has mechanisms for evading neutrophil-mediated collapse (Buvelot et al., 2016). By employing *cyba* mutants, the extent to which ROS is important can be determined, thus providing a CGD model for *Staphylococcus aureus* infection. This may also be applied to *Aspergillus* and may help understand reasons for variable prognoses in CGD patients.

Finally, rescue experiments are also indicated, and this may be achieved by co-injecting mutant larvae with WT *cyba* mRNA and *A. fumigatus*.

Manuscript #3

Nox5 remains the most intriguing of the NOXes, and its observed role in anaesthesia resistance is certainly the first report of a phenotype in an adult model organism. To substantiate this we plan to employ a second mutant, *nox5 sa10707*. This mutation affects an essential splice site on exon 10 (Kettleborough et al., 2013). Concordance between the two mutants would then call for testing various anaesthetics to check for specificity of nox5. Considering the ethical guidelines, cold water (Collymore, Tolwani, Lieggi, & Rasmussen, 2014) would be a suitable choice as it excludes the need to try different chemicals.

Manuscript #4

In manuscript #4, we examined the roles of NOXes in an adult zebrafish model of caudal fin regeneration. We found that zebrafish retain the ability to regenerate their fins even among older animals, and this rate of regeneration is not affected by age. Following this, we achieved our aim to successfully target/acquire *nox* mutants. It was then essential to confirm that the effects of these mutations aligned with described pathologies. Having functional mutants added confidence in reconciling any effect on regeneration with the mutations, instead of being due to off-target effects or idiosyncrasies. While all mutants were in the *Tg(HyPer)* background, we were unable to suitably apply HyPer imaging on *duox*$^{-/-}$ animals. This was partly due to their solid stripes and partly due to the fish not doing well with repeated anaesthesia demanded by the protocol. This will be mitigated by outcrossing these into a *nacre*$^{-/-}$ or *casper*$^{-/-}$ pigment background and then incrossing the progeny. We would also need to start with a greater number of animals to balance out any mortality occurring downstream during the procedure. Seeing as slowed caudal fin regeneration was most apparent in *duox*$^{-/-}$ animals, HyPer imaging on these would be an especially exciting investigation.

Given that regeneration did not cease in any of the mutants, there remains the need to further examine ROS signalling using combinatorial mutants. This may be a challenge as animals that are mutants for all *nox*es may not be viable. Yet, we are now attempting to rear double mutants, having already identified some double homozygotes for *cyba* and *duox*.

Further, while it is evident that ROS oscillations depend on the time of day, we did notice noise. This may be because we only recorded ROS at three times points during the day. Therefore, recording additional time points, as well as considering a larger sample size may be considered as reasonable measures to address this.

We were also left intrigued by the role of thyroid hormones in regeneration. While

untreated and T_4-treated *duox*$^{-/-}$ animals showed no difference in the rate of regeneration, the *tshr* mutant, *manet*$^{-/-}$, showed a reduction when compared to their WT siblings. Following the experiments already attempted, the next step would be to cross *manet* mutants into a *Tg(HyPer)* background and proceed with HyPer imaging post amputation.

In conclusion, we have generated and characterised (to varying extents) zebrafish *nox* mutants. Functional mutations in these animals appeared to have an effect on caudal fin regeneration. In conjunction with their H_2O_2 reporting transgenic background, these strains are stable models that allow for studying regeneration and visualising the underlying ROS flux, without the need for pharmacologically demonstrating the same. Their fertility also means that in the future these could be crossed with other mutants to study the impact of other genes involved in regeneration.

References

1. Al Haj Baddar, N. W., Chithrala, A., & Voss, S. R. (2019). Amputation-induced reactive oxygen species signaling is required for axolotl tail regeneration. *Developmental Dynamics*, *248*(2), 189–196. https://doi.org/10.1002/dvdy.5
2. Buvelot, H., Posfay-Barbe, K. M., Linder, P., Schrenzel, J., & Krause, K.-H. (2016). Staphylococcus aureus, phagocyte NADPH oxidase and chronic granulomatous disease. *FEMS Microbiology Reviews*, *41*(2), 139–157. https://doi.org/10.1093/femsre/fuw042
3. Collymore, C., Tolwani, A., Lieggi, C., & Rasmussen, S. (2014). Efficacy and safety of 5 anesthetics in adult zebrafish (Danio rerio). *Journal of the American Association for Laboratory Animal Science : JAALAS*, *53*(2), 198–203. Retrieved from https://pubmed.ncbi.nlm.nih.gov/24602548
4. Gauron, C., Rampon, C., Bouzaffour, M., Ipendey, E., Teillon, J., Volovitch, M., & Vriz, S. (2013). Sustained production of ROS triggers compensatory proliferation and is required for regeneration to proceed. *Scientific Reports*, *3*, 1–9. https://doi.org/10.1038/srep02084
5. Imlay, J. A. (2013). The molecular mechanisms and physiological consequences of oxidative stress: lessons from a model bacterium. *Nature Reviews Microbiology*, *11*, 443. Retrieved from https://doi.org/10.1038/nrmicro3032
6. Kettleborough, R. N. W., Busch-Nentwich, E. M., Harvey, S. A., Dooley, C. M., De Bruijn, E., Van Eeden, F., … Stemple, D. L. (2013). A systematic genome-wide analysis of zebrafish protein-coding gene function. *Nature*, *496*(7446), 494–497. https://doi.org/10.1038/nature11992
7. Knox, B. P., Deng, Q., Rood, M., Eickhoff, J. C., & Keller, N. P. (2014). *Distinct Innate Immune Phagocyte Responses to Aspergillus fumigatus Conidia and Hyphae in Zebrafish Larvae*. *13*(10), 1266–1277. https://doi.org/10.1128/EC.00080-14
8. Love, N. R., Chen, Y., Ishibashi, S., Kritsiligkou, P., Lea, R., Koh, Y., … Amaya, E. (2013). Amputation-induced reactive oxygen species are required for successful Xenopus tadpole tail regeneration. *Nature Cell Biology*, *15*(2), 222–228. https://doi.org/10.1038/ncb2659
9. McCormick, A., Heesemann, L., Wagener, J., Marcos, V., Hartl, D., Loeffler, J., … Ebel, F. (2010). NETs formed by human neutrophils inhibit growth of the pathogenic mold Aspergillus fumigatus. *Microbes and Infection*, *12*(12), 928–936. https://doi.org/https://doi.org/10.1016/j.micinf.2010.06.009
10. Rosowski, E. E., Raffa, N., Knox, B. P., Golenberg, N., Keller, N. P., & Huttenlocher, A. (2018). Macrophages inhibit Aspergillus fumigatus germination and neutrophil-mediated fungal killing. *PLoS Pathogens*, *14*(8), 1–28. https://doi.org/10.1371/journal.ppat.1007229
11. Segal, B. H., Veys, P., Malech, H., & Cowan, M. J. (2011). Chronic Granulomatous Disease: Lessons from a Rare Disorder. *Biology of Blood and Marrow Transplantation*, *17*(1 SUPPL), S123–S131. https://doi.org/10.1016/j.bbmt.2010.09.008
12. Sprenkeler, E. G. G., Gresnigt, M. S., & van de Veerdonk, F. L. (2016). LC3-associated phagocytosis: a crucial

mechanism for antifungal host defence against Aspergillus fumigatus. *Cellular Microbiology*, *18*(9), 1208–1216. https://doi.org/10.1111/cmi.12616

13. Windhorst, D., Holmes, B., & Good, R. (1967). A NEWLY DEFINED X-LINKED TRAIT IN MAN WITH DEMONSTRATION OF THE LYON EFFECT IN CARRIER FEMALES. *The Lancet*, *289*(7493), 737–739. https://doi.org/https://doi.org/10.1016/S0140-6736(67)91360-8
14. Zhang, Q., Wang, Y. Y., Man, L., Zhu, Z., Bai, X., Wei, S., … Wang, Y. Y. (2016). Reactive oxygen species generated from skeletal muscles are required for gecko tail regeneration. *Scientific Reports*, *6*, 20752. https://doi.org/10.1038/srep20752